Dissertation zur Erlangung des Doktorgrades der
Fakultät für Chemie und Pharmazie der
Ludwig-Maximilians-Universität München

Analysis of Adenovirus-Host Interactions to Improve Recombinant Adenoviral Vectors for Gene Therapy

Christina Theresa Rauschhuber

aus Eggenfelden

2011

Diese Dissertation wurde im Sinne von § 13 Abs. 3 bzw. 4 der Promotionsordnung vom 29. Januar 1998 (in der Fassung der vierten Änderungssatzung vom 26. November 2004) von Frau PD Dr. Anja Ehrhardt betreut und von Herrn Prof. Dr. Ernst Wagner von der Fakultät für Chemie und Pharmazie vertreten

Ehrenwörtliche Versicherung

Die vorliegende Dissertation mit dem Titel:

„ Analysis of Adenovirus-Host Interactions to Improve Recombinant Adenoviral Vectors for Gene Therapy „

wurde selbstständig verfasst und alle benutzten Hilfsmittel vollständig angegeben.

Die Dissertation wurde nicht schon in einer anderen Doktorarbeit verwendet.

München, den 18.01.2011

Christina Rauschhuber

Dissertation eingereicht am   18.01.2011

1. Gutachter: Prof. Dr. Ernst Wagner

2. Gutachterin   PD Dr. Anja Ehrhardt

Mündliche Prüfung am   03.03.2011

Table of contents

Zusammenfassung

Rekombinante Adenoviren zählen zu den am häufigsten verwendeten Vektoren in der Gentherapie. Die replikationsdefizienten rekombinanten Adenoviren umfassen Vektoren der frühen Generation mit Deletionen von wenigen adenoviralen Genen und als modernste Form Gen-deletierte Adenoviren (HC-AdVs), denen alle virale Gene fehlen. Das Genom von HC-AdVs besitzt als virale Bestandteile lediglich die beiden invertierten Wiederholungssequenzen (ITRs) und das Verpackungssignal, wodurch bis zu 36 Kilobasen an fremder DNA eingebaut und in die Zielzelle eingeschleust werden können. Die Effizienz dieser Vektoren konnte in mehreren Tiermodellen gezeigt werden. So konnte nach einer einmaligen Injektion eines HC-AdVs bis zu drei Jahre Transgenexpression nachgewiesen werden. Dennoch gibt es in Bezug auf rekombinante Adenoviren inklusive den HC-AdVs limitierende Faktoren, die im Zuge dieser Arbeit verbessert werden sollten.

Ein bekannter limitierender Faktor ist die ineffiziente Produktion von HC-AdVs, da sie einen zeitintensiven Prozess darstellt und eine fundierte, experimentelle Erfahrung voraussetzt. Daher wurde im Rahmen dieser Arbeit zunächst ein vereinfachtes Protokoll entwickelt, das die effiziente Generierung dieser Viren von Beginn der Klonierung bis hin zur Titration der aufgereinigten Partikel detailliert beschreibt. Als Anwendungsbeispiel dieses Protokolls konnte daraufhin im Rahmen dieser Studie die Fähigkeit von HC-AdVs für den Transport von haarnadelförmigen RNAs (shRNAs) gezeigt werden. Eine spezifische shRNA gerichtet gegen Hepatitis B RNA Moleküle erzielte dabei eine signifikante Verbesserung der Hepatitis B Infektionsparameter *in vitro* und *in vivo*.

Derzeit basieren die meisten HC-AdVs auf dem humanen Serotypen 5 (Ad5). In vergangenen Studien zeigte sich jedoch, dass die verbleibenden viralen Sequenzen von Ad5 (ITR und Verpackungssignal) die Dauer und die Stabilität der Transgenexpression entscheidend beeinflussen, was für einen gentherapeutischen Ansatz von Nachteil sein kann. In der vorliegenden Studie ergab die Analyse der ITRs verschiedener adenoviraler Serotypen sowohl nach innen und außen gerichtete transkriptionelle Aktivität als auch eine inhibierende Funktion einiger ITRs. Zudem konnte der negative Einfluss der ITRs auf nahegelegene Promotoren gezeigt werden. In der Zukunft ist es daher zu empfehlen, die Transgenexpressionskassette im HC-AdV Genom mit insulierenden Sequenzen zu flankieren, um eine unerwünschte Beeinflussung der Genexpression zu verhindern. Des weiteren zeigte diese Arbeit, dass vor allem Adenovirus des Serotyps 7 eine mögliche Alternative zu Ad5 darstellt, da dieser nur moderate transkriptionelle Aktivität besitzt und nahegelegene Promotoren nur geringfügig beeinflusst.

Zusammmenfassung

Wie in Lebertransferstudien gezeigt wurde, beruht die Effizienz von HC-AdV vor allem auf der Stabilität der Vektorgenome in ruhenden Zellen. In teilenden Zellen hingegen führt eine stetige Reduktion der viralen DNA aufgrund fehlender Retentionsmechanismen zum Verlust des therapeutischen Effekts. Daher wurden virale Hybridsysteme entwickelt, die mittels nichtviraler Rekombinasen eine dauerhafte somatische Integration der therapeutischen DNA vom HC-AdV Genom in die chromosomale DNA vermitteln. Prominentester Vertreter der nichtviralen Integrationssysteme stellt die *Sleeping Beauty* (SB) Transposase dar. Obwohl die Funktion und Effektivität dieser Transposase mittels HC-AdV Gentransfer bereits gezeigt wurde, stellte sich heraus, dass nach SB vermittelter Transposition eine Inhibition der Transgenexpression den therapeutischen Effekt vermindert. In dieser Arbeit zeigte die Untersuchung der Transposition in Zellen mit unterdrücktem RNAi Weg eine verbesserte Transpositionsrate durch erhöhte Transgenexpression. Dies bestätigte erstmals ein Model, dem zufolge durch konvergente Transkription, ausgehend von dem Transposon, doppelsträngige RNAs (dsRNAs) und somit Substrate für den RNAi Mechanismus gebildet werden, die für die Inhibierung der Genexpression verantwortlich sind. Die daraus gewonnenen Erkenntnisse können in der Zukunft dafür genutzt werden, die Transposon Technologie entscheidend zu verbessern.

Weiterhin wurde in dieser Arbeit der Einfluss des RNAi Mechanismus auf den adenoviralen Lebenszyklus untersucht. Es konnte dabei gezeigt werden, dass sowohl die Replikation also auch die Virusproduktion von Adenoviren durch ein RNAi Inhibitorprotein um das 10- bis 100-fache verbessert werden konnte. Zudem steigerte die Bindung von doppelsträngigen siRNAs an dieses Inhibitorprotein die Produktion von HC-AdVs um das 6-fache. Es wurde in dieser Arbeit bereits begonnen den Mechanismus, der die erhöhte Replikation bedingt, zu untersuchen. Die vorliegenden Ergebnisse weisen darauf hin, dass vor allem die erhöhte Expression viraler, regulatorischer Proteine sowie die Unterdrückung kleiner adenoviraler RNAs (virus-assoziierte RNAs), den Effekt verursachen.

Zusammenfassend eröffnet diese Arbeit verschiedene Optimierungsstrategien, um den therapeutischen Erfolg von rekombinanten Adenoviren zu verbessern. Vor allem der Einfluss des RNA Interferenz Signalwegs auf die Replikation von Adenoviren konnte in dieser Arbeit zum ersten Mal demonstriert werden. Die erworbenen Erkenntnisse können zur Verbesserung der Virusproduktion und der Weiterentwicklung von onkolytischen Adenoviren von Nutzen sein. Zudem verdeutlicht diese Arbeit mit ihren verschiedenen Angriffspunkten, dass eine sorgfältige biologische Charakterisierung der Gen-therapeutischen Vektoren notwendig ist, um das Potential der Vektoren für therapeutische Ansätze entscheidend zu erweitern.

Abstract

Recombinant adenoviral vectors are among the most commonly used vehicles in gene therapy. Replication-deficient adenoviruses include early generation adenoviruses, which are deleted in less than three adenoviral genes, and the high-capacity adenoviruses (HC-AdV) as the most advanced form. HC-AdVs are deleted for all viral sequences leaving only the two inverted terminal repeat sequences (ITRs) and the packaging signal from the original viral genome. Therefore, up to 36 kilobases of foreign DNA can be packaged by HC-AdV particles and transduced into the desired target cell. Efficacy of these vectors was shown in several animal models, in which a single injected virus dose resulted in up to 3 years of transgene expression. However, also for recombinant adenoviruses including HC-AdVs limiting factors remain, which were investigated and improved in the course of this work.

The production of HC-AdV represents one limiting factor because it is a labour intensive and sophisticated process that requires some experience. Therefore, in this study, a protocol was developed that simplifies the generation of these viruses starting with an improved cloning procedure and ending with precise titration of the purified particles. In addition, this improved virus production procedure was used to demonstrate the feasibility of HC-AdV to delivery short-hairpin RNAs, thus reducing hepatitis B RNA molecules *in vitro* and *in vivo*.

The majority of HC-AdVs are currently based on the adenovirus serotype 5 (Ad5). However, DNA sequences inserted into the HC-AdV genome and remaining viral sequences were shown to influence duration and stability of transgene expression, which can negatively influence the outcome of a therapeutic approach. By analyzing viral ITR sequences derived from different adenoviral serotypes, this work demonstrated that ITR-driven transcriptional activity from several serotypes but also inhibiting functions occur leading to reduced transgene expression. Furthermore, a negative impact of ITR sequences on nearby promoters could be observed. The data obtained in this work suggest that it could be beneficial to introduce shielding sequences into the HC-AdV genome, which flank the transgene expression cassettes and therefore, prevent undesired side effects. Moreover, the results indicated, that pursuing ITRs from adenovirus serotype 7 in the context of an adenoviral vector could be advantageous, as it demonstrated most suitable features regarding transcriptional activation and influence on promoter performance.

The efficiency of HC-AdV in terms of long-term expression of foreign DNA sequences is mainly based on the stability of vector genomes in quiescent cells. In dividing cells, however, a continuous reduction of the viral DNA reduces the therapeutic effect. Thus, integration

systems on the basis of viral hybrid vectors were developed, which result into recombinase-mediated somatic integration of the therapeutic DNA from the HC-AdV genome into the chromosomal DNA. The most prominent representative of non-viral integration systems is the Sleeping Beauty (SB) transposase. Although function and efficacy of this transposase was shown in the context of an HC-AdV, it turned out, that transgene expression is decreased after Sleeping Beauty mediated transposition. Herein, analysis of transposition in cells with suppressed RNA interference pathway, showed a higher transposition rate in RNA interference knockdown cells compared to control cells, which was mainly based on an increased transgene expression. Therefore, this work shows for the first time that due to convergent transcription, originated from the two SB recognition sequences (IRs) flanking the transposon, formation of double-stranded RNAs (dsRNAs) can occur. These dsRNAs can be substrates for the RNAi mechanism and contribute to the silencing of gene expression. In the future this finding can be used to significantly improve the SB transposon technology.

Moreover the influence of the RNAi mechanism on the adenovirus life cycle could be demonstrated within this project. By the suppression of the RNAi pathway using an RNAi suppressor protein we could improve recombinant adenovirus replication and viral particle production, up to 100-fold. In addition, this RNAi suppressor protein increased production of HC-AdV up to 6-fold. This upregulation was mainly based on the increased expression of viral regulatory proteins as well as the suppression of small adenoviral RNAs.

In conclusion, this work provides different strategies to improve HC-AdVs for gene therapeutic purposes. Furthermore, it investigated mechanisms that negatively interfere with the therapeutic outcome, which need to be considered in future work. In particular, the influence of the RNA interference pathway on the replication profile of recombinant adenoviruses could be demonstrated for the first time essentially broadening the potential of these vectors with respect to viral production and design of oncolytic adenoviruses. In summary, this study emphasizes the importance of understanding the biology of viral vectors systems, which then can be translated into the development of optimized vectors for gene therapeutic applications.

1   Introduction

Gene therapy is a young, emerging field of molecular medicine. It is based on the administration of therapeutic DNA sequences into the target cell to repair genetic defects. In 1990 the first gene therapy treatment utilizing a viral vector was performed in a SCID (severe combined immunodeficiency) patient with adenosine deaminase deficiency. This novel approach caused worldwide attention and a boost for gene therapy. Until 1999, the database "Gene Therapy Clinical Trials World Wide" recorded more than 400 clinical trials (Wiley 2010). However, the death of Jesse Gelsinger in 1999 after being given a high dose of adenoviral particles meant a drawback for the popularity of gene therapy (Raper *et al.,* 2003). Furthermore an additional phase 2 study treating 27 SCID-X1 patients with a retrovirus based vector could indeed achieve a significant improvement of the disease, but 5 patients developed leukemias after several years, which was due to insertional mutagenesis after provirus integration. Both studies emphasize the importance of a detailed characterization and continuous improvement of gene therapy vehicles to prevent negative side effects. Since 1990 until to date more than 1,500 clinical trials with various viral and non-viral vectors have been performed with adenovirus, retrovirus and plasmid DNA being the predominantly used vector types (**Figure 1.1**) and especially over the past few years, very promising results were obtained. The treatment of patients suffering from liver congenital amaurosis with an adeno-associated virus could partially restore the ability to see in nearly blind patients without inducing toxicity (Bainbridge *et al.,* 2008; Cideciyan *et al.,* 2009; Wright *et al.,* 2010). Furthermore a phenotypic correction of up to 30 month in two X-linked adrenoleukodystrophie patients could be demonstrated after ex-vivo administration of a lentiviral vector encoding for the defective ABCD1 gene (Cartier *et al.,* 2009). Last but not least in a very recent publication the phenotypic correction of a ß-thallasemia patient for 22 month after treatment with a lentiviral vector was reported (Cavazzana-Calvo *et al.,* 2010).

Adenovirus 23.8% (n=400)
Retrovirus 20.5% (n=344)
Naked/ Plasmid DNA 17.7% (n=304)
Vaccinia virus 7.9% (n=133)
Lipofection 6.5% (n=109)
Poxvirus 5.5% (n=93)
Adeno-associated virus 4.5% (n=75)
Herpes simplex virus 3.3% (n=56)
Lentivirus 1.7% (n=29)
Other categories 4.9% (n=82)
Unknown 3.3% (n=55)
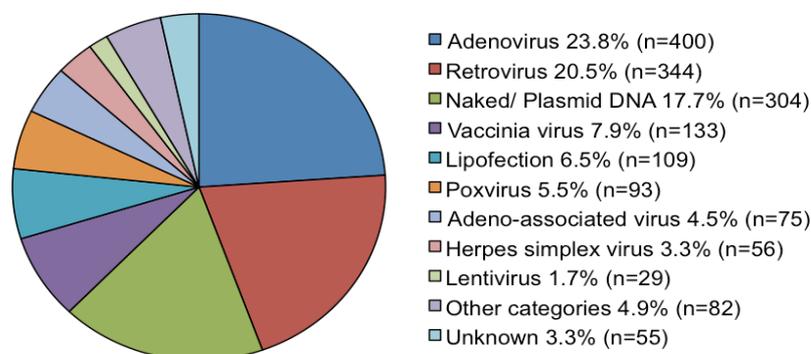
Figure   1.1:   Vectors   used   for   clinical   trials.   Modified   from   the   source: *www.abedia.com/wiley/vectors.php* (Wiley 2010).

1.1 Adenoviral Vectors

Adenoviral vectors (AdV) are among the most commonly used vectors in gene therapy (**Figure 1.1**). The structure of their capsid, the composition of the genome and the replication cycle of adenoviruses provide ideal conditions for use as a gene therapeutic vector. Furthermore, they offer the opportunity of a wide range of possible modifications to improve vector properties. As most of the biological information exists from the two human serotypes 2 and 5 (Ad2 and Ad5), therapeutic approaches are mainly based on these two species.

1.1.1 Adenovirus taxonomy and virus particle composition

To date, there are 53 known adenoviral serotypes, which are assigned to seven subgroups (A, B1, B2, C, D, E, F). The classification is based on their genetic variability, the oncogenic potential and the tropism of each species (**Table 1.1**). According to the tropism Ads infect a wide host cell range, which defines the diversity of diseases. Therefore, Ads can cause acute respiratory, gastro-intestinal and ocular infections, which are usually self-limiting, however, in immuno-compromised patients they can cause serious illness.

In 1991, the first intact adenoviral particle was visualized by cryo-electron microscopy, to which today's morphological knowledge is based on (Stewart *et al.,* 1991). A schematic representation of the viral capsid is shown in **Figure 1.2**.

Adenoviruses are non-enveloped, icosahedral particles with 70-100 nm in diameter. Dependent on the serotype, they harbour an 25-45 kilo basepair (kb) long double-stranded DNA genome which, together with four structural proteins, build up the core. The viral capsid consists of 252 subunits (240 hexons and 12 pentons) and seven structural proteins (II, III, IIIa, IV, VI, VIII, IX). In addition, in each viral capsid, 10 copies of the adenoviral protease are packaged. On the viral surface and connected to the penton the fiber protein appears whose C-terminal knob domain mediates the contact to the cellular receptors.
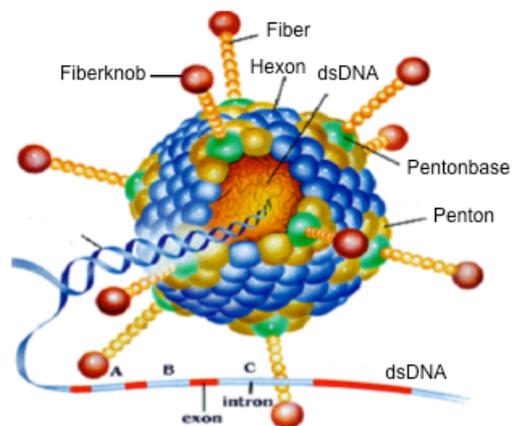
Figure 1.2: Composition of the adenoviral particle. Modified from http://nobelprize.org/nobel_prizes/medicine/laureates/1993/illpres/genes-in-pieces.html.

Table 1.1: Classification and tropism of human adenoviruses. Serotypes, with known receptor are labeled: [b]coxsackie and adenovirus-receptor (CAR); [c]CD46; [d]Sialin acid (SA); [e]CD80/86; [f]Heparinsulfat; [g]Desmoglein 2 (Wang *et al.,* 2010); [h]GD1a (Nilsson *et al.,* 2010). Modified from Zhang and Bergelson (Zhang and Bergelson 2005).

Subgroup	Serotype	Tropism
A	12^b, 18, 31^b	intestinal, respiratory
B1	$3^{c,e,g}$, 7^g, 16^c, 21^c, 50^c	respiratory, ocular
B2	$11^{c,g}$, $14^{c,g}$, 34, 35^c	renal, respiratory, ocular
C	1, $2^{b,f}$, $5^{b,f}$, 6	respiratory, ocular, lymphoid
D	8^d, 9, 10, 13, 15^b, 17, $19p^b$, $19a^d$, 20, 22, 23, 24, 25, 26, 27, 28, 29, 30, 32, 33, 36, $37^{c,d,h}$, 38, 39, 42, 43, 44, 45, 46, 47, 48, 49, 51	ocular, respiratory
E	4^b	respiratory, ocular
F	40, 41^b	intestinal

The adenoviral DNA genome within the virion contains overlapping transcription units, which are located on both strands of the DNA and in case of Ad5 encode for round 38 genes and 50 proteins (**Figure 1.3**). All viral coding regions are transcribed by the cellular RNA polymerase II. Only the two non-coding virus-associated RNAs I and II (VAI, VAII) are read from the RNA polymerase III. The transcription is divided into three phases, the expression of early genes (E1A, E1B, E2, E3, E4), the delayed transcription of proteins IX and IVA2 and the expression of the late transcription unit from the major late promoter (MLP). From the latter 5 mRNAs are generated by alternative splicing processes, which code for structural proteins forming the viral capsid. The packaging of the viral genome is mediated by the
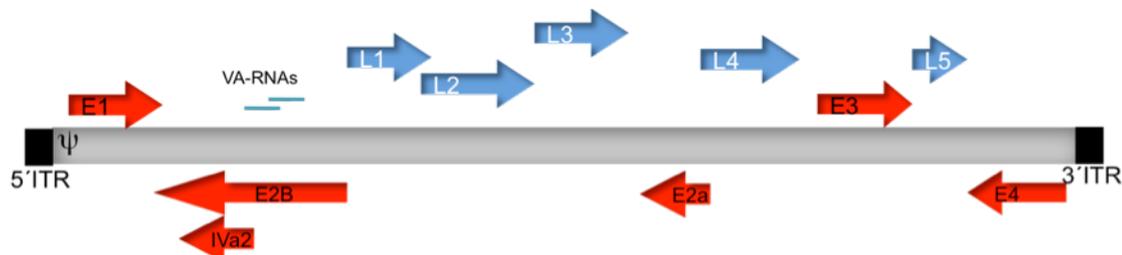
Figure 1.3: Composition of the adenoviral genome and location of coding regions of human serotype 2 from subgroup C. The double-stranded DNA genome is colored in grey, the 2 inverted terminal repeats (ITRs) in black. The arrows determine the transcriptional direction of the different early (red) and late (blue) gene coding regions. Ψ: packaging signal; VA-RNAs: Virus-associated RNAs.

3

packaging signal Ψ, which is located on the left end of the genome in close proximity to the 5´inverted terminal repeat (ITR). Within the viral capsid the terminal protein (TP) is covalently attached to the 110-160 nt long 5´- and 3´ ITRs (the length is determined by the serotype) flanking the whole Ad genome. TP in concert with the adenoviral polymerase and cellular factors such as NFI / CTF, and NFII NFIII / OctI (nuclear factors), are essential proteins for viral replication (Curiel and Douglas 2002).

1.1.2 Infection and replication cycle of adenoviruses

The first contact of Ad2 / 5 with the host cell is mediated by the interaction of the fiber knob domaine with cellular receptors (Bergelson *et al.,* 1997; Tomko *et al.,* 1997; Freimuth *et al.,* 1999). Nearly all Ad serotypes, except subgroup B Ads, use the cellular coxsackie and adenovirus receptor (CAR) for cellular uptake of the virus (Arnberg 2009). Besides this specific interaction also other capsid components bind to cellular surface receptors, such as the fibershaft of type C Ads to heparan sulfates and penton base proteins to members of the integrin family. In contrast the group B Ads use CD46, CD80, CD86 and Desmoglein 2 for entry into the cell, thus enabling transduction of hematopoietic stem cells and also a variety of cancer cells (Arnberg 2009; Wang *et al.,* 2010). Other co-receptors that are recognized by the surface proteins of different serotypes are shown in **Table 1.1**.

CAR alone is not sufficient to mediate uptake of the viral particle. The binding of penton base within the capsid to the two co-receptors αvβ3 and αvβ5, both members of the integrin family, induces endocytosis via clathrin-coated pits and initiates the formation of the endosome (Wickham *et al.,* 1993; Davison *et al.,* 1997). In the endosome the slight acidic pH induces the destruction of capsid proteins and subsequently the activation of the viral cysteine protease. This protease then initiates the degradation of the endosome. In the cytoplasm, the particles are transported along the microtubules to the nucleus. The inward transfer of the viral DNA into the nucleus is mediated by the nuclear pore complexes and the replication starts (Saphire *et al.,* 2000). The entire process, from initial contact with the cellular surface until viral DNA appears in the nucleus takes about 30-60 minutes.

E1A is the first viral protein that is produced after introduction of the DNA into the nucleus. As a transcription factor it activates the expression of early viral genes (E1B-E4). The function of the early viral gene products is comprised by the manipulation of the cell cycle and the modification of the cellular metabolism in favor of viral replication. Two proteins encoded by E1A (12S and 13S) drive the host cell from the inactive G1/GO phase in the active S-phase by inactivation of cellular factors such as the tumor suppressor retinoblastoma (pRb) protein, CBP or p300. The E1B encoded products modulate the host

cell environment by inhibition of p53 and tumor necrosis factor induced apoptosis. Together with the E4Orf6 protein, E1B55K stabilizes the transport of viral mRNAs out of the nucleus, thus forcing the viral protein synthesis and simultaneously inhibiting the production of cellular proteins. In addition, other early phase proteins encoded by the E2 transcription unit are involved in viral replication, such as the viral polymerase or the 72 kilo Dalton (kDa) major DNA-binding protein (DBP), which binds to single-stranded DNA during replication, unwindes the DNA and protects it against degradation. The transcripts of the E3 region are mainly required for the modulation of the host immune response, because they prevent the expression of MHC class I molecules on the cellular surface, but are not essential for replication *in vitro*. In contrast, E4 is essential for replication because it was shown that a deletion of the complete E4 region reduced viral replication by approximately 5-log levels compared to wild type adenovirus. E4 encodes for six different open reading frames. The respective proteins have a variety of features which are important for viral replication, like the inhibition of apoptosis, mRNA transport and stability. However, in this context it is worth mentioning that only one protein either E4Orf3 or E4Orf6 is necessary to restore virus growth up to 10-fold of wild type. Both factors bind the DNA protein kinase, and thereby block DNA repair mechanisms such as the double strand break repair (DSBR). This process prevents the formation of long concatemers from the viral genomes that can not be packaged into the capsid. E4Orf6 alone binds and inhibits p53 wheras the interaction with the E1B55K protein mediates its proteasome-dependent degradation (Curiel and Douglas 2002). Futhermore, the transforming properties of E4Orf6 are enhanced by E1A, probably also by binding to p53.

The expression of late proteins is initiated by the MLP promoter. The activation of this promoter requires cellular transcription factors such as TBP / TF-IID, as well as viral proteins and a change in genome structure. First, a long transcript of about 30.000 nt is generated, which is then cut by a number of splicing processes into 5 groups. The late transcripts encode almost exclusively for structural proteins, such as hexon, penton and fiber proteins. The assembly of the capsid takes lace in the nucleus but it is not yet known in detail which factors initiate the subsequent lysis of the cells.

The entire replication cycle takes about 24 hours resulting in the release of about 10 000 viral particles per cell (Curiel and Douglas 2002).

1.1.3 Types of recombinant adenoviral vectors and their application in gene therapy

Gene therapy encompasses a wide range of applications. Historically, the term gene therapy

has been characterized by the use of vectors in gene-replacement therapy for the treatment of genetic disorders. However, in today's modern medicine, this term includes many other applications, as demonstrated by a statistics from "Gene Therapy Clinical Trials World Wide" (Wiley 2010). According to this database the vast majority of clinical trials aim at the treatment of tumors, followed by treatment of cardiovascular and monogenic diseases (**Figure 1.4**). In addition, viral vectors are also used for vaccination. Each of these indications has specific demands on the vector used, and only a few systems can be applied to all areas. Adenoviral vectors, however, find success in almost all fields of gene therapeutic applications.

Monogenic diseases are based on the mutation or disregulation of only one protein and are therefore particularly accessible to gene therapy treatment. A successful gene substitution requires efficient transduction of specific target cells with a sufficient amount of therapeutic DNA without inducing toxicity.

In the early 90s adenoviral vectors have been used mainly because of their high transduction efficiency. Within the adenoviral vectors of the first generation, only the E1 region was deleted (**Figure 1.5A**), whereas in some cases also the E1- and E3-deleted Ads are refered to as first generation (Berkner 1988). This created space for therapeutic DNA of about 7.6 kb. In order to ensure the production of these replication-defective vectors, the recombinant viruses were amplified in specific producer cell lines (eg HEK293 cells, human embryonic kidney cells), in which the left arm of Ad5 was stably integrated into the genome. Because most natural adenoviral infections affecting the respiratory tract, these vectors were especially used for the treatment of cystic fibrosis as a monogenetic model disease (Brody *et al.,* 1994). The deletion of the E1 transcription factor should prevent the expression of further viral genes and therefore viral replication. But it became quickly clear that even in the

Cancer diseases 64.5% (n=1060)
Cardiovascular diseases 8.7% (n=143)
Monogenic diseases 8.2% (n= 134)
Infectious diseases 8% (n= 131)
Neurological diseases 1.8% (n=30)
Ocular diseases 1.1% (n=18)
Other diseases 2.4% (n= 40)
Gene marking 3% (n= 50)
Healthy volunteers 2.3% (n= 38)
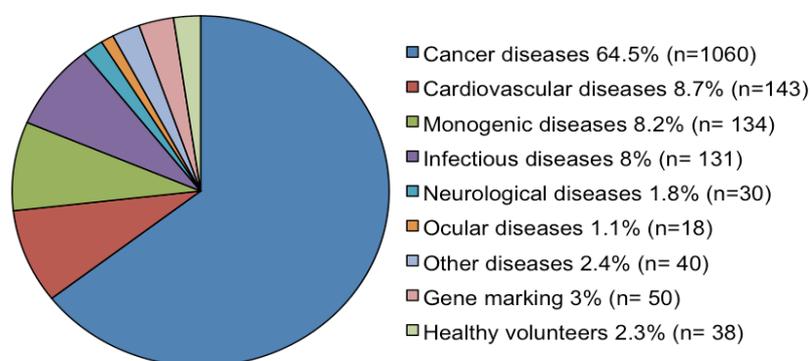
Figure 1.4: Indications of all gene therapeutic trials reported in 2010. Modified from the source: *www.abedia.com/wiley/indications.php* (Wiley 2010).

absence of the E1 proteins low- level transcription of the remaining viral genes occurred, resulting in activation of a rapid innate and adaptive immune response and subsequently to antibody-mediated destruction of the transduced cells (Yang *et al.,* 1994; Yang *et al.,* 1995a; Yang *et al.,* 1995b; Kay *et al.,* 2001; Thomas *et al.,* 2003). Thus, the therapeutic effect is drastically reduced.

Consequently, second-generation adenoviral vectors were developed in which E1 and E2 or E3 and / or the E4 region were deleted (**Figure 1.5B**). Although these vehicles showed a better toxicity profile, the administration of a high dose of an E1/E4 deleted adenovirus in the artery of a young man with ornithintranscarbamylase-deficiency was responsible for the first death in a gene therapy trial (Gao *et al.,* 1996; Gorziglia *et al.,* 1996; Lusky *et al.,* 1998; O'Neal *et al.,* 1998) Due to the uncontrolled immune response triggered by viral components multi-organ failure was induced, which subsequently caused the death of the patient (Raper *et al.,* 2003). As a consequence within the next years reduction of toxicity directed against adenoviral incoming particles and de novo synthesized viral proteins was an important research priority.

The most advanced generation of adenoviral vectors, the so-called high-capacity adenoviral vectors (HC-AdV), consists of the two adenoviral ITRs and the packaging signal, but lacking all viral coding sequences (**Figure 1.5C**)(Parks *et al.,* 1996; Palmer and Ng 2003). Thus, the capacity for therapeutic DNA, in contrast to earlier generations rises up to 36 kb and toxicity due to de novo synthesized viral proteins can be excluded. The production of these viruses is based on a "two-vector" system consisting of the high-capacity adenoviral construct that contains the transgene expression cassette and a helper virus, providing all viral proteins for packaging *in trans*. All production protocols are based on the publication of Parks *et al.* in 1996 (Parks *et al.,* 1996). However, many labs are still restricted in generating these viruses due to lack of experience in this sophisticated procedure.

The long-term therapeutic effect after systemic administration of the HC-AdV was demonstrated in both small and large animal models. A study in mice showed the expression of the human coagulation Factor IX for 54 weeks after a single injection (Ehrhardt and Kay 2002). This effect is independent of the species, since hemophilia B dogs as well as baboons demonstrated transgene expression for up to 964 days (Brunetti-Pierri *et al.,* 2004; Brunetti-Pierri *et al.,* 2005; Brunetti-Pierri *et al.,* 2007; Brunetti-Pierri *et al.,* 2009; Hausl *et al.,* 2010). Furthermore in a rat model for the Crigler-Najjar syndrome life-long phenotypic correction of the bilirubin metabolism was shown (Toietta *et al.,* 2005). Therefore, HC-AdVs were used for the treatment of numerous monogenic diseases such as Duchenne muscular dystrophy, cystic fibrosis, haemophilia A and B or

hypoalphalipoproteinemia (Ehrhardt and Kay 2002; Ehrhardt *et al.,* 2003; Gilbert *et al.,* 2003; Brown *et al.,* 2004; Brunetti-Pierri *et al.,* 2005; McCormack *et al.,* 2006; Cerullo *et al.,* 2007; Deol *et al.,* 2007; Oka *et al.,* 2007; Kawano *et al.,* 2008). Nevertheless, there are also limitations of the HC-AdV system. The episomal status of the adenoviral genome in the nucleus allows the sufficient production of the transgene, but over time a constant decrease of the therapeutic effect could be observed (Morral *et al.,* 1998; Ehrhardt and Kay 2002; Jager and Ehrhardt 2007). Also the loss of viral genomes in rapidly dividing cells remains a challenge to be overcome (Ehrhardt and Kay 2002; Yant *et al.,* 2002). Moreover, the immune response against the incoming viral capsid or the introduced transgene must be considered. Further modifications for achieving stable expression of the therapeutic gene and reduced toxicity of the capsid are therefore the focus of prospective vector modifications.
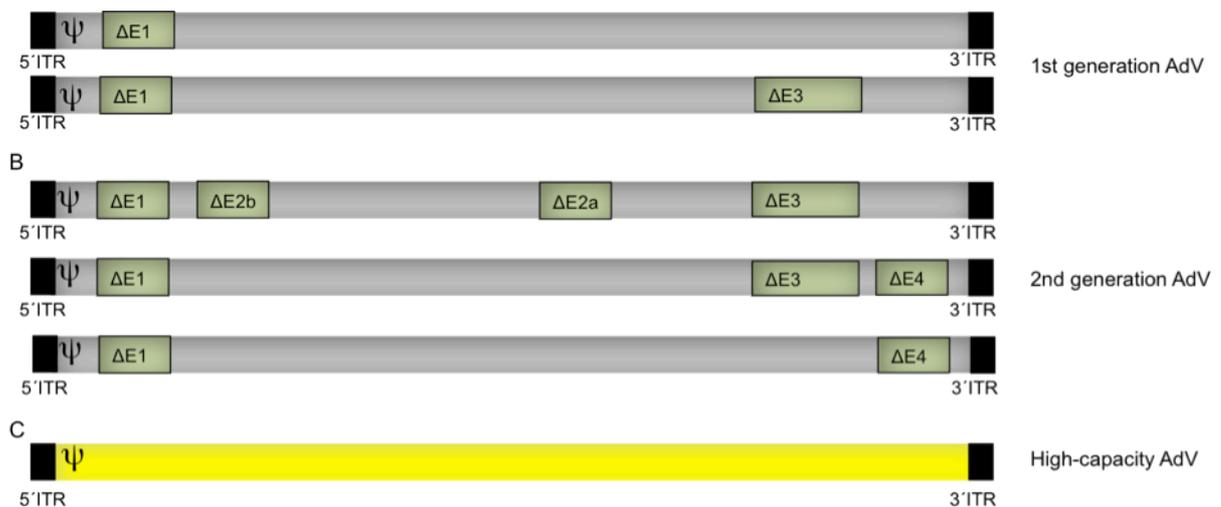
Figure 1.5: Summary of recombinant adenoviral vectors used in gene therapy. A) The genome of first generation adenoviral vectors. This vector is lacking the early E1 coding region or E1 in concert with an E3 deletion. B) Adenoviral vector genomes of the second generation. This vectors are deleted in several coding regions, e.g. E1, E3 and additionaly E2 (upper panel) or E4 (middle panel) or only E1 and E4 (lower panel). C) High-capacity adenoviral vector genome. The vector genome is deleted in all viral coding sequences only the inverted terminal repeats (ITRs) and the packaging signal (Ψ) are left.

In contrast to the studies aiming at gene correction or gene-replacement therapy a high immunogenic potential of adenoviruses can also be advantageous for instance in tumor therapy. Currently several adenoviral mutants are being applied in the clinic for the treatment of cancer patients. In 2004, the first gene therapeutic application based on a replication deficient adenovirus was approved in China, which is now, in combination with conventional chemotherapy, routinely used for the treatment of head and neck tumors (Peng 2005; Garber 2006; Yu and Fang 2007). The adenoviral genome of this mutant contains the

wildtype human p53 gene instead of the E1 region, thus substituting the p53 defect of most tumors (Peng 2005). Another approach for tumor therapy was introduced by Fueyo and his colleagues in 2000, who generated the first conditional replicating adenovirus (CRA) also called, oncolytic adenovirus (Delta24) (Fueyo *et al.,* 2000). Compared to the replication deficient virus (see above), which usually infiltrate and lyse only the outer regions of tumors, CRA have a higher transduction rate, better penetration into the tumor tissue and could be classified as safe in several studies (Hemminki and Alvarez 2002; Lichtenstein and Wold 2004). By the deletion of a 24 bp region in the E1A gene, Fueyo limited the replication of adenovirus specifically to tumor cells because this deletion removes the Retinoblastom (pRB) binding site and therefore leads to the inhibition of viral replication in normal cells by RB-mediated apoptosis. The productive replication of these viruses in pRB-lacking tumor cells thereby results in lysis of aberrant cells and subsequently to regression of the tumor (Sherr 1996; Hernando *et al.,* 2004). Another CRA, Onyx-015, has a deletion in the E1B55KDa protein, thus it replicates only in cells with p53 deregulation and is currently being tested in over 15 clinical trials (Bischoff *et al.,* 1996; Heise *et al.,* 2000; Ries and Brandts 2004; Liu *et al.,* 2007). One injection of the virus directly into the tumor *in vivo* confirmed a transient anti-tumor activity (Heise *et al.,* 2000). Nevertheless, the low replication rate of these oncolytic viruses in the tumor still remains an obstacle (Pesonen *et al.,* 2010).

Another field, in which adenoviral vectors are being extensivley studied is vaccination. The activation of a strong immune response against the adenovirus mediated by T and B cells, the high transduction efficiency in mammalian cells and the ease of modifications and production are excellent pre-conditions for the use of adenovirus in this area. Adenoviral vaccination strategies in the field of HIV, HCV and malaria control are currently being investigated in phase I and II clinical trials (Priddy *et al.,* 2008; Wiley 2010).

1.1.4   Adenoviral vector modifications

Adenoviral vectors offer many opportunities for optimization of their gene therapeutic profile. In general, one can distinguish between two levels of vector modifications: (1) the modulation on the genome level and (2) the change in the capsid composition.

With respect to vector modifications on the genome level the introduction of HC-AdVs was an important milestone in vector development, as the deletion of all viral coding sequences could greatly reduce the immunogenic potential and simultaneously increase the packaging capacity of foreign DNA up to 36 kb. To ensure packaging of the adenoviral genome, stuffer DNA was incorporated into the HC-AdV genome in addition to the therapeutic DNA for

achieving the smallest possible packaging size of 27.7 kb (Sandig *et al.,* 2000). Notably, it turned out that these additional sequences significantly influence the maintanance of the viral vector genomes and stability of transgene expression (Parks *et al.,* 1999). For instance, bacterial DNA, extensivley shorten the duration of protein expression *in vivo* due to the high GC content and destabilizes the whole genome (Parks *et al.,* 1999). Several versions of HC-AdV genomes with varying genomic composition were developed. The vector used in our laboratory contains, a 16 kbp long DNA fragment of the centromeric region of human chromosome 17 and a matrix attachment region of the murine immunoglobulin kappa locus (Ehrhardt and Kay 2002; Taylor *et al.,* 2002; Yant *et al.,* 2002).

Besides the stuffer DNA also the DNA composition of the expression cassette plays a crucial role in robustness of transgene expression. For instance, Schiedner and colleagues used the liver-specific hAAT (human α1-antitrypsin) promoter together with parts of the first intron of the human coagulation factor IX (FIX). In comparison to the viral cytomegalovirus promoter this approach significantly improved the expression profile in liver cells (Schiedner *et al.,* 1998). The construct was also used in hemophilia B dogs and could demonstrate for the first time partial phenotypic correction of the FIX gene deficiency for up to 4.5 months with negligible toxicity (Ehrhardt *et al.,* 2003). This demonstrated that the use of tissue-specific promoters in the context of Ad vectors clearly improves the outcome of the gene therapeutic approach. Also for targeted expression of transgenes in lung, skeletal and smooth muscle cells tissue-specific promoters could be used successfully. A disadvantage of cell-specific promoters is their relatively low expression rate compared to virus-derived promoters. The incorporation of regulatory elements such as woodchuck hepatitis virus post-transcriptional regulatory element (WPRE) or the before mentioned intron of the FIX gene, also have a positive effect on the expression profile of the transgene and can increase the transgene expression up to 50-fold *in vivo* (Xu *et al.,* 2003b). Also inducible promoters such as the Tet system (Invitrogen) offer advantages for certain indications (Xu *et al.,* 2003a). Especially in systems requiring short-term expression of a toxic transgene, negative side effects directed against these factors can be reduced.

The remaining, virus-derived DNA sequences within the HC-AdV are the two ITRs on both ends of the adenovirus DNA molecule and the packaging signal near the 5 'end. An investigation showed that cis-activating elements, which are located next to the 5' ITR along with the ITRs exhibit transcriptional activity and affect nearby expression cassettes (Hearing *et al.,* 1987; Shi *et al.,* 1997; Rubinchik *et al.,* 2001; Yamamoto *et al.,* 2003; Xing and Tikoo 2004; Xing and Tikoo 2005). Therefore, it is not surprising that two groups demonstrated that tissue specific promoters could be both inhibited and activated by these viral sequences,

and thus lose their specific properties (Shi *et al.,* 1997; Hoffmann *et al.,* 2005). One may speculate that these elements are also able to modulate transgene expression over long distances. Hence, the location of the therapeutic DNA within the HC-AdV genome is important, but an in depth study analyzing transcriptional activity of solely the left and right arm of the HC-AdV genome is still lacking.

With respect to vector modifications and the capsid composition several different approaches can be followed to improve the viral vector and its biological properties.

The limiting factor covering all areas of gene therapeutic use of adenoviruses are developing or pre-existing anti-adenoviral neutralizing antibodies, leading to a rapid elimination of the particles after systemic administration (Raper *et al.,* 2003). For instance, in the case of repeated administration of vectors, which are often required for vaccination regimen. In primates it was shown that a pre-immunization with Ad5 can strongly decrease the T-and B-cell response, thus reducing the success of a vaccination (Barouch and Nabel 2005). Moreover, within the most commonly used serotypes 2 and 5, a high serum prevalence in the human population can be observed, for instance in about 40-90% of the Caucasian population neutralizing antibodies (NAs) are detected (Schmitz *et al.,* 1983; Chirmule *et al.,* 1999; Arnberg 2009). Another limitation of commonly used Ads is represented by the strong tropism for liver cells when injected systemically into the bloodstream. The group led by Andrew Baker was able to uncover the mechanism in 2008. The binding of coagulation factor X to hyper variable regions of the hexon in the viral capsid mediates liver transduction independent of the interaction between fiber and CAR receptor (Waddington *et al.,* 2008). Since most of the negative effects listed above are mediated by viral surface proteins, capsid modifications to improve vector properties in favour of a lower immune response and a transport into specific target cells is of great interest to the research community. Both fiber and hexon modifications, which are mainly based on serotype switch, could reduce toxicity; significantly improve the tropism and the biological vector properties (Havenga *et al.,* 1996; Roy *et al.,* 1998).

In addition to the replacement of individual capsid components, one can also perform a complete serotype switch. There are 53 human serotypes with varying biological features available (**Table 1**) and therefore this can alter the specific tropism to another cell type and may probably reduce clearance by pre-existing antibodies. The serum prevalence of Ad35 and 11 for example is in contrast to Ad5 (40-90%) very low (5-18%) (Arnberg 2009).

Another strategy to reduce the innate immune response is to improve the administration technique. It could be demonstrated in mouse experiments and in baboons that a (pseudo-)

hydrodynamic injection of an HC-AdV increases transduction of the liver by 4-fold without inducing cytotoxic side effects. Furthermore one could circumvent the innate immune response by *ex vivo* administration of the viral vector into the liver, but this implies at least a certain risk as an invasive surgery is needed (Brunetti-Pierri *et al.,* 2007). Moreover, targeted administration to the desired tissue, such as an intra-muscular injection or aerosol catheter administration into the lung significantly decreased organ toxicity, while increasing transduction efficiency (Gilbert *et al.,* 2003; Koehler *et al.,* 2005).

Upon infection adenoviruses persist as episomal DNA molecules within the nucleus (Jager and Ehrhardt 2007). In resting cells, thus an expression of up to two years can be achieved in dogs and chimpanzees. However, in rapidly dividing cells a much faster clearance of the transgene could be observed because the episomal genome is lost during cell devision due to lacking retention mechanisms (Ehrhardt and Kay 2002; Ehrhardt *et al.,* 2003; Brunetti-Pierri *et al.,* 2005; Brunetti-Pierri *et al.,* 2007). For most gene therapeutic purposes in humans a longer therapeutic time span is needed. Hence, there is accumulating interest in developing hybrid vectors, which combine the advantages of the transduction efficiency of Ads with the potential of other viral and non-viral integration systems. Adenovirus / retrovirus or Ad / Foamy virus hybrids utilizing the integration machinery of retroviruses allow stable expression in transduced cells; however, always include the risk of insertional mutagenesis, since retroviruses preferentially insert in gene regions (Zheng *et al.,* 2000; Murphy *et al.,* 2002; Picard-Maureau *et al.,* 2004). To reduce the oncogenic potential of hybrid vectors, non-viral integration systems have been explored. Both the Sleeping Beauty (SB) transposase and the PhiC31 integrase proved to be an adequate system for stable integration of the transgene cassette into the host genome (Kuhstoss and Rao 1991; Ivics *et al.,* 1997; Groth *et al.,* 2000; Ivics *et al.,* 2007). Both mechanisms have already demonstrated their effectiveness in *in vivo* experiments in small and large animal models (Babiss *et al.,* 1986b; Olivares *et al.,* 2002; Yant *et al.,* 2002; Yant and Kay 2003; Ehrhardt *et al.,* 2007; Hausl *et al.,* 2010). Also the Rep protein derived from the adeno-associated virus mediates integration into the genomic DNA from the AdV, uses in 25% of all cases the AAVS1 locus on chromosome 19 (Wang and Lieber 2006), is speculated as a safe "harbor". Quite new is the use of a non-viral plasmid replicon called pEPito in the context of AdV, which examines autonomously replication in cells in association with AdVs (Haase *et al.,* 2010). This would exclude the risk of insertional mutagenesis and simultaneously ensure long-term transgene expression.

1.2 RNA interference

Since the discovery of RNA interference (RNAi) in 1998 by Fire and Mello, research in the field of double-stranded RNA (dsRNA) was revolutionized, which resulted in 2006 by the awarding of the Nobel Prize in medicine for both investigators (Fire *et al.,* 1998).

In the nematode *Caenorhabditis elegans* (*C. elegans*), Fire and Mello made the pivotal observation that dsRNA can inhibit the expression of homologous endogenous genes. This discovery could be confirmed in *Drosophila melanogaster* and also in *Xenopus laevis* (Fire *et al.,* 1998; Caplen 2000; Nakano *et al.,* 2000).

The breakthrough of the RNAi mechanism in the field of genetic engineering was achieved by Tom Tuschl in 2001, as he demonstrated for the first time the function of small synthetic interfering RNAs (siRNAs) in mammalian cells (Elbashir *et al.,* 2001a).

Nowadays it is known that RNAi is a highly conserved mechanism, as it could be found in many living organisms such as plants, protozoa, eukaryotes and viruses. Up to now 1100 human miRNAs and 45 000 potential targets have been discussed and function range from gene regulation, disease and cancer development, immune activation, DNA methylation to the morphogenesis and differentiation of cells, and one can expect that more new functions will be identified (www.microrna.org; Kloosterman and Plasterk 2006; Krutzfeldt and Stoffel 2006; Skalsky and Cullen 2010).

1.2.1 The RNA interference mechanism

The RNA interference pathway, which results in the post-transcriptional silencing of a specific gene, takes place in the cytosol (**Figure 1.6**). In vertebrates, this step is initiated by a group of molecules, called micro-RNAs (miRNAs) (Lagos-Quintana 2001).

MiRNAs are non-coding RNA molecules that are basically transcribed by RNA polymerase II. It is estimated that approximately 75% of the miRNA sequences are located in independent, non-coding regions or intron sequences of genes (Lagos-Quintana 2001; Cai 2004; Lee *et al.,* 2004). Moreover, they are often produced in a tissue specific manner or dependent on the developmental stage. In *C. elegans*, they were first described and their particiation at key developmental processes recognized (Pasquinelli and Ruvkun 2002). The transcription first leads to about 160 nucleotide (nt) long primary RNAs (pri-RNAs), which are processed in the nucleus by the RNase III enzyme Drosha in cooperation with the RNA-binding enzyme DGCR8 (DiGeorge critical region 8) in 60 nt pre-miRNA precursors (Pasquinelli and Ruvkun 2002; Han 2004; Lee *et al.,* 2004; Zeng and Cullen 2004; Kim *et*

al., 2005; Zeng and Cullen 2005). The transport into the cytoplasm is regulated via the energy-dependent Exportin-5/RanGTP pathway that is also used by cellular mRNAs (Yi 2003; Zeng and Cullen 2004). In the cytosol the pre-miRNA binds to the RNase III Dicer, which generates an imperfect 21-25 nt long double-stranded RNA (Hutvagner *et al.,* 2001; Ketting 2001). Characteristic for these dsRNAs are the 2 nt long, overhanging 3' OH ends and 5' phosphat residues. One strand, the so-called "guide" strand is then incorporated into a complex containing ribonucleoproteins (miRNP, microRNA-containing ribonucleoproteins). This multimeric complex greatly resembles the RNA induced silencing complex RISC in composition as well as in function (Mourelatos 2002; Hutvagner 2005). A thermodynamically
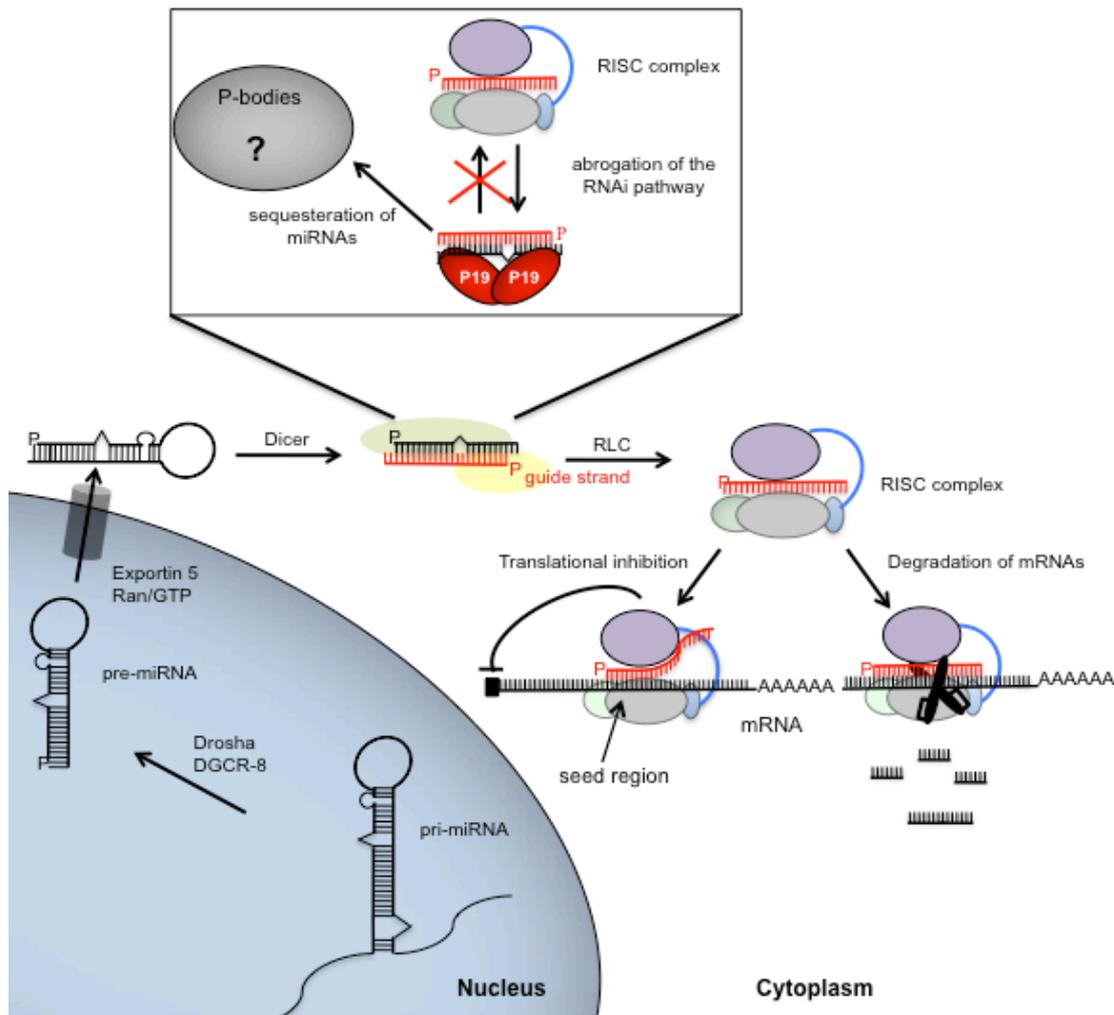
Figure 1.6: Schematic overview of the RNA interference pathway mediated by miRNAs and its inhibition by the RNAi supressor protein P19. The primary micro RNA (pri-miRNA) is generated from RNA polymerase II transcription of the chromosomal DNA. In the nucleus the pri-miRNA is processed by Drosha and DGCR-8 into 60 nt long pre-miRNAs, which are transported out of the nucleus through the Exportin5 pathway. The pre-miRNA is then cut by the cytoplasmatic protein Dicer in 21-23 nt long dsRNAs. One strand, the so-called guide strand (red) is then loaded into the RNA induced silencing complex (RISC), which subsequently initiates sequence-dependent mRNA degradation or translational inhibition. The framed picture shows the function of the RNAi suppressor protein P19. P19 binds to ds miRNAs after Dicer processing and is able to destroy RISC-miRNAs complexes. Upon binding, P19 sequesters the miRNA either in processing bodies (p-bodies).

unstable 5' end determines the strand that is loaded into the miRNP complex by the RISC loading complex (RLC). At the same time the complementary strand is degraded. In general, functional ribonucleoprotein particles that are associated with miRNAs are referred to as miRNPs, complexes associated with synthetic small interfering RNAs (siRNAs) are determined as RISC (Meister 2004). The single-stranded RNA is now opening and sequence-specific post-transcriptional inhibition of a complementary mRNA by cleavage of the mRNA or termination of translation is initiated. The destruction of the mRNA only occurs with full (100%) complementarity between miRNA and the respective mRNA. In mammalian cells this is a relatively rare event, thus usually the inhibition of translation rather than mRNA destruction occurs. During the blockade of translation the miRNA seed region between nucleotides 2-8 (viewed from the 5 'end) is crucial as it determines the contact to the mRNA (Chiu and Rana 2003; Haley and Zamore 2004). Recent studies showed that following this principle one miRNA can regulate up to 200 different transcripts (Lindow and Gorodkin 2007). Notably, there are also other gene silencing mechanisms mediated by dsRNAs and enzymes of the RNAi pathway, like the dsRNA-mediated DNA methylation. This mechanism leads to methylation of cystein residues predominantly in promoter regions and subsequently to transcriptional silencing of the transgene (Kawasaki and Taira 2004a).

1.2.2 Viral miRNAs and RNAi suppressor proteins

In 2004, three years after the discovery of the first siRNAs it was shown that viruses also express miRNA sequences within their genome (Pfeffer 2004). In general, viruses can be divided into three categories: 1) Members of the herpes viruses like Epstein-Barr virus and Kaposi sarcoma virus, which transcribe for a number of miRNAs, 2) nuclear viruses, like polyomavirus, which express only a few miRNAs and 3) RNA or cytoplasmatic DNA viruses that contain no miRNA coding sequences (Cullen 2010). Up to now over 200 viral miRNAs have been identified so far (Skalsky and Cullen 2010).

The target mRNAs of the viral miRNAs and therefore their biological function are largely unknown, but it is believed, that two basic mechanisms are affected. First, the miRNAs probably inhibit cellular immune responses. For instance, the polyomavirus SV40 expresses a miRNA that inhibits the viral T-antigen, thus preventing the destruction of the infected cells by cytotoxic T lymphocytes (Sullivan *et al.,* 2005). Secondly, viral miRNAs may affect the stabilization of the latent infection status, a mechanism that primarily plays a role in the replication cycle of herpes viruses. In herpes simplex virus for example, latency associated miRNAs are generated that deregulate the trans-activators ICP0 and ICP4. These are only expressed during latency and the effect of the miRNAs probable delays the entry into the lytic life cycle (Cullen 2010).

Simultanousley to the expression of viral miRNAs different mechanisms evolved that causes the inhibition of cellular and viral miRNAs. Lecellier *et al*. first reported a cellular miRNA inhibiting the replication of the primate foamy virus (Lecellier *et al.,* 2005). Especially in plants, this strategy based on endogenous generated miRNAs is widespread, as plants only rely on the RNAi interference pathway to protect themselfes from the attack of viruses (Baulcombe 1999; Voinnet 2001). Plant viruses usually have an RNA genome and are therefore accessible for degradation by host miRNAs (Vargason *et al.,* 2003). As a counterdefensive mechanism plant viruses express so-called RNAi suppressor proteins that inhibit miRNA-mediated destruction. One of the best-studied RNAi suppressors is the 19 kilodalton P19 protein, which is expressed by the tomato bushy stunt virus and other related viruses. The efficacy of this protein has already been demonstrated in several model organisms, including mammalian cells (Qu 2002; Voinnet 2003; Lakatos *et al.,* 2004; Lecellier *et al.,* 2005). P19 acts as a dimeric protein in the cytoplasm. The tryptophan residues at the N-terminal ends of both monomers and the basic, polar amino acids on the surface of the protein are responsible for the binding of specific 21-23 nt long dsRNA molecules. Presumably, the P19 molecule sequesters one miRNA and initiates the destruction of the dsRNAs. Because miRNAs are suggested to be translocated to cellular processing bodies (P-bodies), it is assumed that also P19 bound miRNAs are transported to this cytoplasmatic foci (Beckham and Parker 2008; Eulalio *et al.,* 2008). In general, this mechanism inhibits the activation of the RISC complex and finally the post-transcriptional silencing (Scholthof 2006). A schematic representation of the P19-mediated inhibition of the RNAi pathway is shown in **Figure 1.6**. As a crucial factor it was shown, that the amount of P19 in the cell seems to be important (Qiu *et al.,* 2002; Szittya *et al.,* 2002). It was assumed that this is due to the interaction of P19 with the miRNAs which follows a 1:1 stoichiometry, which limits the downregulation of all miRNAs (Scholthof 2006). However, there is a second controversy model available, explaining the mechanism of P19 binding. Rawlings disapproved the accepted hypothesis of Scholthof and showed, that the P19-miRNA interaction is a sub-stoichiometry event and subsequently relies on fast association and dissociation of the complex. Thus, concluding binding is a reversible mechanism (Scholthof 2006; Rawlings 2010). Furthermore it was demonstrated that there is an over 20-fold bias for siRNA-P19 complexes in comparison to siRNA-Dicer and in addition also mature RISC complexes are targeted, emphasizing the high efficieny of P19. Importantly, in her study, the dosage effect was confirmed, too. It is of note that also in other organisms RNAi inhibitors exists (Rawlings 2010). Examples are the HIV TAT, the vaccinia virus E3L protein, the Ebola virus derived protein VP35 and virus-associated RNAs (VA-RNAs) of adenovirus (Li *et al.,* 2004; Andersson *et al.,* 2005; Bennasser *et al.,* 2005; Haasnoot *et al.,* 2007).

1.2.3   Adenovirus associated RNAs (VA-RNAs)

Computational programs postulated that the Ad genome has a probability of 60% to contain miRNA sequences (Pfeffer 2004). Until now only the two non-coding virus-associated RNAs I and II (VAI- and VAII-RNA) are known to interfere with the RNAi pathway (Aparicio *et al.,* 2006; Sano *et al.,* 2006). VAI- and VAII-RNA and are 160 nt long, hairpin-shaped molecules that are transcribed by the cellular RNA polymerase III (Thimmappaya 1982; Liao *et al.,* 1998; Aparicio *et al.,* 2006). During a normal infection cycle, approximately 10^8 VA-RNA molecules are formed, which are transported across the cellular Exportin-5/RanGTP pathway into the cytoplasm (Ma 1996). The main function of VAI-RNA is the blockade of protein kinase R (PKR), a serine-threonine protein kinase that is activated upon infection by long dsRNAs resulting in the abrogation of the viral and cellular protein translation (O'Malley 1986; Akusjarvi *et al.,* 1987).

Mellitis and colleagues demonstrated by mutational studies, the binding of the apical domain of the VAI-RNA to PKR, wheras the central domain is responsible for its inhibition (Mellits and Mathews 1988; Mellits *et al.,* 1990). The terminal stem of the VA-RNA however, is the effector for the RNAi pathway. The interaction of VA-RNAs with the RNAi pathway starts with the export from the nucleus, since these export proteins are shared with the endogenous miRNAs and mRNAs and are therefore blocked for cellular molecules (Yi 2003; Aparicio *et al.,* 2006). In the cytoplasm, both Dicer and the RISC complex are inhibited probably also by competitive inhibition of VA-RNAs with these components of the RNAi machinery (Lu and Cullen 2004). This was confirmed by studies of Sano and Aparicio, where they showed that VA-RNAs are substrates of the cytoplasmic RNase III Dicer. Dicer cuts the terminal end of the VAI and VAII-RNA into small 21-29 nt long virus-associated RNAs (svaRNAs) that can be loaded into the RISC complex and thereby inhibit complementary RNA fragments (Aparicio *et al.,* 2006; Sano *et al.,* 2006). Although the VAI-RNA is quantitatively superior to the VAII-RNA, it was shown that the sva-RNAs of VAII-RNA are preferably incorporated into the RISC complex (Xu *et al.,* 2007). In the beginning, the function of the svaRNAs was not completley understood, as no target mRNA sequences could be identified. The inhibition of the sva-RNAs originated from VAI-RNA by antagomir RNAs (2'O Methyl oligonucleotides) demonstrated a significant attenuation of virus replication (Aparicio *et al.,* 2006). Recent *in silico* studies, together with conventional methods have now identified the protein TIA-1 as a cellular target protein. TIA-1 is an RNA-binding protein located within processing bodies that was associated with splicing and translation and it is a known apoptosis-inducing factor (Beckham and Parker 2008; Aparicio *et al.,* 2010). Probably thereby, adenoviruses regulate their RNA metabolism in the cell and manipulate the cellular antiviral mechanisms. Other proteins that have been shown to play

an important role in cellular signaling pathways, transcription, DNA repair mechanisms and RNA metabolism were also recognized as potential target proteins, but must be validated by molecular biological methods (Aparicio *et al.,* 2010). The precise mechanism of how the two functions are regulated, the inhibitory effect on the RNAi mechanism and the blockade of gene expression through the sva-RNAs remains unknown. There is speculation, however, that in the early infection period, the inhibition of gene expression takes place, whereas the blockade of RNA interference occurs more in the late phase to protect own viral gene expression.

1.3 RNAi in gene therapeutic applications

In modern molecular medicine miRNAs are widely explored for therapeutic purposes. SiRNA-based therapies mainly include the treatment of tumors and anti-viral strategies. In addition, with respect to vector development persistence and transduction properties can be improved and the immune response reduced utilizing miRNAs. However, not only the efficient and sequence specific degradation of mRNA target molecules plays a key role but also the restoration of degenerate expression profiles of proteins and miRNAs.

Most therapeutic approaches are based on the targeted application of small inhibitory dsRNAs. Two systems are currently being explored. On the one hand modified, synthetic RNAs are transfected into cells. This represents a very effective method because these RNAs can be easily produced in large quantities, there is no need to be processed by the endogenous miRNA pathway and it was shown that the inhibitory effect can be maintained approximately for up to one week in dividing tissues (Bartlett and Davis 2006). The most medical approaches, however, require a more sustained therapeutic effect. Towards this end, viral vectors were constructed that express short-hairpin RNAs (shRNA) mostly from RNA polymerase III promoters (Paddison *et al.,* 2002). These shRNAs are produced in sufficient quantities and can stably block transgene expression over a long period of time (Grimm *et al.,* 2006). In addition, viral vectors infect both primary and embryonic stem cells, thus widening the range of applications (Stewart *et al.,* 2003; Hoelters *et al.,* 2005). In contrast to siRNAs, the generation of shRNA sequences is very complex, since these molecules have to be recognized and processed by enzymes of the endogenous RNAi pathway. Moreover, the therapeutic window of the shRNA seems very small because with low quantities only insufficient effects could be observed but a high dose may induce toxicity (Grimm *et al.,* 2006). In general, the design of the dsRNA molecules is critical regardless of their origin and only a detailed characterization of different siRNAs prevents undesired "off-target" effects.

Besides the use of small inhibitory RNAs in anti-tumor approaches, siRNAs are appropriate to treat viral infection. The fight against viral infection by siRNAs is usually based on the inhibition of viral gene expression. Especially for chronic infections, this technology offers an attractive alternative to conventional therapies. For instance, during chronic infection with Hepatitis B virus (HBV) lifelong infections occur that are associated with a high incidence of liver cirrhosis and cancer (Rehermann and Nascimbeni 2005). Current strategies for the treatment of HBV reduce the disease symptoms in the liver but could not eliminate the infection itself. It was already demonstrated that upon introduction of small hairpin RNAs (shRNAs) directed against HBV proteins, infection parameters could be improved (Uprichard *et al.,* 2005; Grimm *et al.,* 2006).

Several vector models for effective transport of shRNA to hepatocytes have been evaluated. Grimm and colleagues developed an adeno-associated virus vector (AAV) for the delivery of a very potent shRNA, the HBVU6no.2, and demonstrated reduction of HBV-specific antigens, although toxic effects occurred due to saturation of the miRNA pathway (Grimm *et al.,* 2006). Also in 2004, the group of Susan Uprichard published the use of a first-generation AdV delivering a shRNA cassette (shHBV765) in mouse hepatocytes, which were chronically infected with HBV. Already 4 days after administration, a 5.5-fold reduction of HBV-specific antigens could be observed and further 13 days later barely any HBV RNA-based molecules could be detected (Uprichard *et al.,* 2005).

Besides these therapeutic approaches the presence of conserved, endogenous and tissue-specific miRNAs can be used for the modification of vector systems. For instance one limiting factor in many gene therapy trials is an immune response against the therapeutic protein when expressed in antigen-presenting cells (APCs). Based on the miRNA expression pattern of hematopoietic cells Brown and colleagues generated a lentiviral vector that expressed four miRNA target sequences in the 3´UTR of the reporter gene GFP recognized by the miRNA miR-142-3p, which is exclusively expressed in hematopoetic stem cells. By integrating these miR-142-3p target sequences into the lentiviral vector they could reduce transgene expression in hematopoetic stem cells below one percent after systemic administration of the vector into mice. Importantly, with this approach they maintained long-term expression of the transgene in normal cells (Brown *et al.,* 2007). Also in development of conditional replicating adenoviruses, this system has already been applied. The miRNA target sequence of liver-specific miR-122 was introduced into the 3'UTR of the E1A gene (with a 24bp deletion) and led to a drastically reduced viral replication in hepatocytes. This allowed a greatly enhanced toxicity profile for tumor therapy (Ylosmaki *et al.,* 2008).

In addition to viral vectors also non-viral vector systems may benefit from the RNAi pathway.

Evolutionarily determined, it is assumed that the RNAi mechanism primarily pursues the goal of protecting cells from jumping elements (transposons), and all kinds of foreign nucleic acids. Yang and Kazazian (2006) demonstrated that L1 retrotransposition is inhibited by endogenous siRNAs (Yang and Kazazian 2006). In gene therapy systems, the transposon-mediated integration of the transgene, based on the Sleeping Beauty transposon (SB), Piggy Bac or Tol 2, is an efficient mechanism to achieve stable long-term expression (Ivics *et al.,* 2009). Also AdVs systems in concert with non-viral integration systems such as SB transposase have been explored, resulting into high transduction efficiency and SB-mediated integration into the host genomic DNA of the target cell. Nevertheless, it was found that after SB-mediated transposition, transgene expression is reduced or completely disappears (Garrison *et al.,* 2007). With respect to that, the composition of the system and the integration mechanism seem to be a critical factor. A schematic overview of the SB-mediated integration mechanism is shown in **Figure 1.7**. The transposon containing the transgene cassette is flanked by two oppositely directed repeat sequences (IRs; inverted repeats). The SB uses a so-called "cut and paste" principle. It binds in a dimeric form to the IR cuts out the transgene flanked by the IRs, from the circular plasmid and integrates the transposon into the genomic DNA. The genome target site of SB is composed of a dinucleotide containing a tyrosine and an adenosine (TA) (Ivics *et al.,* 1997). Notably, Mikkelsen and colleagues showed that the two flanking IRs exhibit inward transcriptional activity (Moldt *et al.,* 2007). Presumably by the convergent transcription of the IRs, double-stranded RNA molecules are being generated, which are potential substrates for the cellular miRNA pathway, and thereby block transposon based gene expression. The exact involvement of the RNAi pathway has yet to be confirmed. Nevertheless, for the development of therapeutic vectors that are based on SB-mediated transposition the
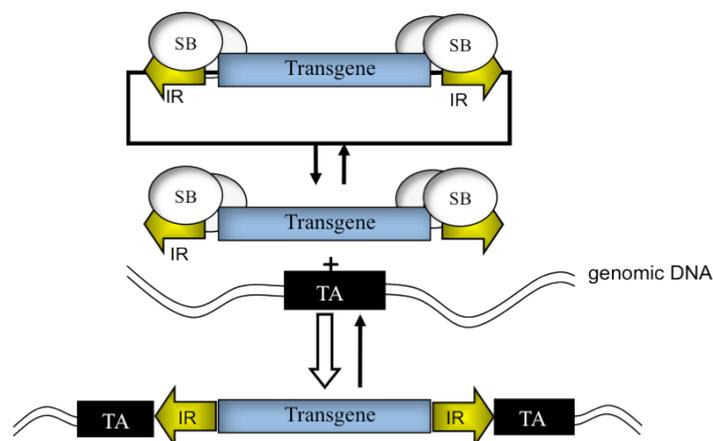
Figure 1.8: Mechanism of Sleeping Beauty mediated transposition. Sleeping Beauty (SB, white) binds in a dimeric form to the inverted repeats (IR, yellow) flanking the transgene (blue). By a cut and paste mechanism SB cuts out the transgene cassette and integrates it into a TA site (black; site composed of a tyrosin and an adenosin) in the chromosomal DNA.

introduction of insulators that inhibit a transcription seems to be advisable. With that respect it has been shown that such insulating elements significantly prolonged transposon-derived reporter gene expression.

1.4 Aims of the project

Adenoviral vectors are one of the most prominent gene therapeutic vehicles to date. Different generations of adenoviral vectors were produced and the most advanced version is represented by the high-capacity adenoviral vectors (HC-AdV). These vectors are deleted for all viral coding sequences, display a low toxicity profile and it was shown that they result into long-term transgene expression in quiescent cells *in vivo*. Nevertheless, also for HC-AdVs there are still limitations and therefore, in the present study we aimed at improving the features of the HC-AdV in several directions.

1. The first aim was the generation of a detailed protocol for large-scale production and precise titration of HC-AdVs. In addition, the plan was to evalute the feasibility of HC-AdV not only for the transfer of transgenes but also to deliver short-hairpin RNAs (shRNAs). In order to demonstrate efficacy for delivery of shRNAs, the aim was to treat a mouse model of medical relevance, the hepatitis B virus infection, aiming at downregulation of infection parameters *in vitro* and *in vivo*.

2. Since it was demonstrated that transcriptional activity of the ITRs strongly influences transgene expression from the Ad5 vector, other adenovirus serotypes gained more importance for gene transfer. Therefore, the goal was to investigate the potential of other than Ad5 ITRs to drive transcription and to discover potential candidates with less impact on transgene expression. Results of this study can be used for improved design of recombinant HC-AdVs.

3. Ad5 based HC-AdVs predominantly target the liver and persist in the nucleus as episomal and linear DNA monomers. Upon cell cycling, however, viral genomes are lost by cellular degradation processes and lacking retention mechanisms. Thus, for the treatment of cycling cells, adenovirus hybrid vectors were developed, which utilize Sleeping Beauty (SB) transposase for somatic integration of foreign DNA from the HC-AdV genome into host chromosomes at high efficiency. Nevertheless, it was demonstrated that silencing of the transgene takes place upon transposition. In this work it was hypothesized that convergent transcription initiated by the SB inverted repeats, flanking the transgene, could lead to the formation of double-stranded RNAs (dsRNAs). These dsRNAs may be incorporated into the RNA induced silencing complex (RISC) and guide silencing of the transgene after

transposition. Hence, the plan was to analyze transposition efficiencies and transgene expression after transposition in RNAi knockdown cells, which could have important implications for improving SB-based systems in the future.

4. In order to generate more advanced recombinant adenoviral vectors for gene therapy, the knowledge about basic virus-host interactions is essential. Especially, the RNA interference mechanism became of major interest within the last years as it was shown to regulate several viral pathways. Thus, the goal was to investigate whether the RNAi pathway plays a role in the adenoviral life cycle, with a special interest in virus replication and particle production. The hypothesis was that if one can get further insights into the interaction between the virus and the RNAi pathway, this knowledge can be used to further improve the production of recombinant adenovirus vectors including HC-AdVs or the fate of the vector during infection.

In general, this work is going to provide novel insights into adenovirus host-interactions, especially the impact of the RNAi pathway, and paves the way towards innovative strategies to further improve adenovirus vector properties for gene therapy.

.

2 Treatment of HBV infections by shRNAs delivered by an high-capacity adenoviral vector

The enveloped hepatitis B virus (HBV), a member of the hepadnavirus family, can cause lifelong infection, cirrhosis of the liver, acute and chronic hepatitis, and liver cancer (Rehermann and Nascimbeni 2005). Worldwide, two billion people have been infected with hepatitis B virus (HBV), 350 million have chronic infection (Wright 2006). Current therapeutic strategies against HBV infection reduce symptoms of liver disease but complete eradication of the infection is one of the major challenges of our time. Therapeutic options include therapy with lamivudine and/or interferon (IFN) alpha, Adefovir, and Entecavir treatment (Zoulim 2006), but resistance to these drugs due to the relatively high mutation rate of HBV genomes remains a problem (Tillmann 2007). Gene therapy approaches for the treatment of HBV infection based on introduction of gene drugs into hepatocytes by various viral and non-viral gene transfer systems may represent an attractive alternative to conventional treatment strategies. In previous studies gene drugs included antisense RNA and DNA approaches (Madon and Blum 1996; Wu and Gerber 1997), ribozymes (Beck and Nassal 1995; Welch *et al.,* 1997), dominant negative HBV antigen mutants (Scaglioni *et al.,* 1996), single chain antibodies (Ogata *et al.,* 1993), gene products for enhancement of anti-HBV immunity and small hairpin RNAs (shRNA). It was demonstrated that expression of shRNAs expressed from a non-viral (McCaffrey *et al.,* 2003) or a viral vector, including first generation adenoviral vectors (fgAd) (McCaffrey *et al.,* 2003; Moore *et al.,* 2005; Uprichard *et al.,* 2005; Carmona *et al.,* 2006; Grimm *et al.,* 2006; Chen *et al.,* 2007), leads to RNA interference mediated post-transcriptional reduction of HBV target transcripts. Our study focused on recombinant adenoviral vectors for shRNA delivery against HBV, but also prototype foamy virus (Moore *et al.,* 2005) and adeno-associated viruses (AAV) (Grimm *et al.,* 2006; Chen *et al.,* 2007) were evaluated in the past.

To date adenoviral vectors are the most frequently used vectors for clinical applications as a statistic from "Gene Therapy Clinical Trials World Wide" demonstrated (**Figure 1.1**) (Wiley 2010). The majority of adenovirus gene transfer is based on first- and second-generation adenoviral vectors, deleted in several viral coding genes including E1 and E3 or E1, E3 and E4, respectively. These vectors can be easily produced to very high titers by using different producer cell lines, all based on HEK293 cells complementing the respective defect (Weinberg and Ketner 1983; Luo *et al.,* 2007). Furthermore, commercial kits for production and purification of adenovirus 5 (Ad5) derived vectors are available (Sartorius). However, a major hurdle in gene therapy using these vectors is the strong immune response activated by leaky expression of viral proteins (Yang *et al.,* 1994; Yang *et al.,* 1995a; Yang *et al.,*

23

1995b; Kay *et al.,* 2001). Thus, the most advanced generation of adenoviral vectors, the high-capacity adenoviral vectors (HC-AdV) were generated, lacking all viral coding sequences, just containing the 5´and 3´ inverted terminal repeats (ITRs) and the packaging signal (Parks *et al.,* 1996; Hardy *et al.,* 1997) as remaining viral sequences. This design allows the transfer of foreign DNA up to 35 kb. Various studies showed efficacy of these vectors and *in vitro* and *in vivo* long-term transgene expression in rodents and non-human
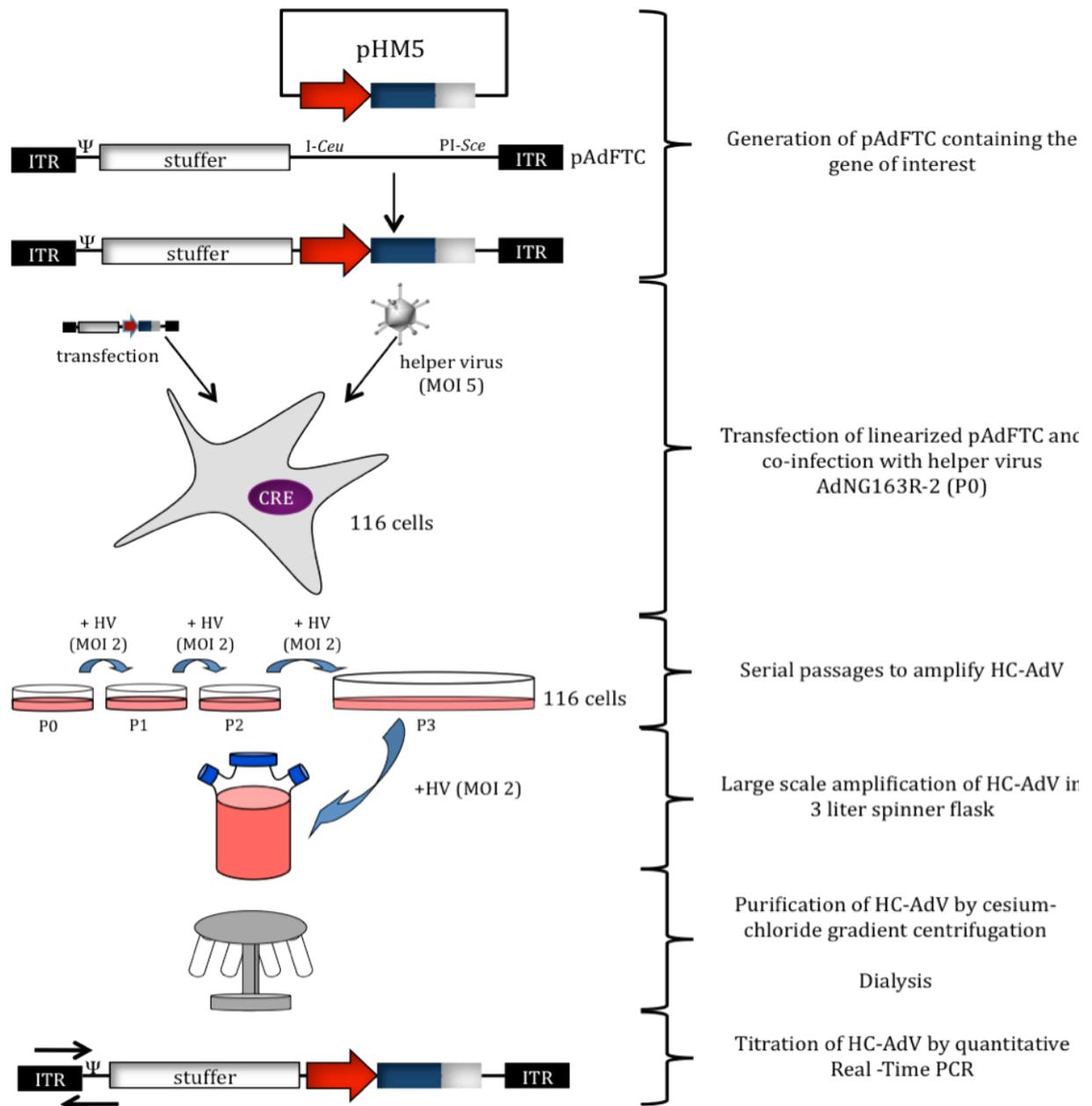
Figure 2.1: Schematic overview of the entire HC-AdV large-scale production procedure. After direct cloning of the gene of interest (red arrow: promoter; blue bar: gene of interest; white bar: polyadenylation signal) into pAdFTC, the linearized plasmid is transfected into 116 cells and cells were co-infected with helper virus AdNG163R-2 at a mulitplicity of infection (MOI) of 5. Three serial passages are used to amplify HC-AdV in adherent cells and then the 116 cells were cultivated in a 3 liter spinner flask. HC-AdV is purified by cesium chloride centrifugation, dialysed and quantitative Real-Time PCR with primers located in the ITR and the packaging signal (black arrows) are used to titrate the virus. ITR: Inverted terminal repeat; HV: helper virus; HC-AdV: High-capacity adenoviral vector.

primates for up to 3 years with a significantly reduced cytotoxic response was observed (Toietta *et al.,* 2005; Brunetti-Pierri *et al.,* 2009). Hence, HC-AdVs were already used for several therapeutic applications with a focus on monogenetic diseases such as Duchenne muscular dystrophy (Gilbert *et al.,* 2003), hemophilia A (Brown *et al.,* 2004) and B (Ehrhardt *et al.,* 2003) and hyperbilirubinemia (Toietta *et al.,* 2005).

For *in vivo* experiments and clinical applications large-scale production of HC-AdVs is necessary. The principle of all currently used systems is based on a pivotal study by Parks *et al*. (Parks *et al.,* 1996). Herein, HC-AdV production is dependent on a two-vector system, which encompasses the HC-AdV genome and a helper virus deleted in E1 and E3 (Parks *et al.,* 1996). This helper virus provides all essential proteins for amplification, generation and packaging of viral genomes *in trans*. In order to prevent undesirable helper virus contamination, its packaging signal is flanked by loxP sites and is excised upon infection by Cre-recombinase expression in the adenovirus producer cell line. By this mechanism helper virus contamination can be reduced to less than 1% in the final vector preparation.

However, the complex, sophisticated and time consuming cloning and production procedure of HC-AdV was a major limitation to many laboratories. Therefore, we aimed at developing a detailed protocol including all steps from the HC-AdV cloning to the amplification, purification and titration of the HC-AdV. A schematic overview is shown in **Figure 2.1**. Furthermore we evaluated HC-AdV produced with our improved protocol, for the delivery of short hairpin RNAs. To test efficacy of HC-AdV in a therapeutic setting, we aimed at suppressing HBV transcripts using a previously published shRNA coding sequence against HBV (HBVU6no.2) (McCaffrey *et al.,* 2003). HBVU6no.2 was demonstrated to be highly efficient for RNA interference mediated knockdown of HBV transcription products using a non-viral approach (McCaffrey *et al.,* 2003) and AAV vectors (Grimm *et al.,* 2006). However, after systemic administration of an AAV2/8 vector-encoding HBVU6no.2 at high dose lethality was observed in mice.

2.1 Materials and Methods

2.1.1   DNA constructs and enzymes

For HC-AdV production the shuttle vector pHM5 and the pAdFTC were used (Ehrhardt and Kay 2002). The nucleotide shRNA expression cassettes against luciferase and HBV (HBVU6no.2) were described elsewhere (McCaffrey *et al.,* 2002; McCaffrey *et al.,* 2003; Grimm *et al.,* 2006). Throughout the study the plasmid, encoding shRNA against HBV, will be referred to as pHBVU6no.2. All shRNAs were transcribed under the control of the U6

promoter. High-capacity adenoviral vectors (HC-AdV) with shRNA expression cassettes (FTC/lucRNAi and FTC/HBVU6no.2) and the vectors FTC-hFIX-attB-(FRT)2 and AdFTC/cFIX/ChMAR without shRNA expression cassette were based on the adenoviral backbone pAdFTC. As additional stuffer DNA FTC/lucRNAi and FTC/HBVU6no.2 comprised a transgene expression cassette encoding the human coagulation factor IX (hFIX) (Ehrhardt and Kay 2002). For the construction of the vector pFTC/lucRNAi, the bacteriophage integrase PhiC31 recognition site attB and the inverted repeats (IR) for *Sleeping Beauty* transposase mediated somatic integration were flanked by the Flp recognition sites (FRT). FTC-hFIX-attB-(FRT)2, a HC-AdV with a split hFIX expression cassette, and AdFTC/cFIX/ChMAR containing the canine FIX expression cassette, were used as control vectors and were described elsewhere (Ehrhardt *et al.,* 2003; Ehrhardt *et al.,* 2007). The plasmids pTHBV2 with the complete HBV genome and the plasmid pRSV.hAAT.bpA (phAAT) expressed the human α1-antitrypsin (hAAT) coding sequence transcribed under the control of the rous sarcoma virus (RSV) promoter were described previously (Yang *et al.,* 2002; Chen *et al.,* 2007). All enzymes for cloning were obtained from NEB and used as recommended by the manufacturer. Molecular biological methods were performed following the instructions from Sambrook and Russel (Sambrook 2001). Cloning of the viral constructs was performed by Anja Ehrhardt.

2.1.2 Cell lines and viruses

HEK293 and HeLa cells were obtained from ATCC and cultivated in DMEM supplemented with 10% FBS and 1% penicillin/streptomycin (P/S). 116 cells were kindly provided by Philip Ng and cultivated in MEM with the addition of 10% FBS, 1% P/S and 100 μg/ml hygromycin if not stated otherwise. Selection medium was used during amplification, hygromycin was not added during the infection procedure as this can interfere with efficient virus production. Huh7 cells and 2.2.15 cells were cultivated in DMEM with 10%FBS, 1% P/S and 1% non-essential amino acids. All cell lines were grown at 37°C in a 100% humidity atmosphere and 5% CO_2. Cell culture reagents were obtained from PAA.

The helper virus AdNg163R-2 was a kind gift from Philip Ng. The fg adenoviral vector fgAdluc was based on the adenoviral plasmid pAdHM4 (Mizuguchi and Kay 1998). The luciferase expression cassette contained in fgAdluc encodes luciferase under the control of Simian Virus 40 (SV40) promoter and was based on the pGL3-Control vector (Promega).

2.1.3   *In vitro* studies to characterize efficacy of HC-AdV mediated delivery of short-hairpin RNAs to reduce hepatitis B virus infection

For *in vitro* assays using adenovirus in HeLa cells, cells were co-infected with the fg adenoviral vector fgAdluc using an MOI of 10 and the HC-AdV FTC/lucRNAi expressing shRNA against luciferase at an MOI 10, 50, 100, and 500, respectively. To infect all cells with the identical total amount of virus, groups were spiked with an irrelevant HC-AdV (AdFTC/cFIX/ChMAR) (Ehrhardt *et al.,* 2003). Luciferase levels were measured three days post infection using a luciferase reporter assay system (Promega).

For plasmid based assays in Huh7 cells, either 0.67 µg of the plasmid pFTC/HBVU6no.2 (used for production of the HC-AdV FTC/HBVU6no.2) or 0.67 µg of pHBVRNAno.2 were co-transfected with 0.67 µg pTHBV2 into a well of a 6-well plate. Control groups received stuffer DNA, respectively. As an internal control and for normalization, all groups received the plasmid pRSV.hAAT.bpA. Hepatitis B virus antigen (HBsAg) levels in the supernatant were measured 3 days post-transfection by enzyme immunoassay (Abbott Laboratories, Abbott Park, IL, USA).

For studies in Huh7 cells using adenoviral vectors, cells were transfected with the plasmid pTHBV2. Twenty-four hours post transfection cells were transduced with the HC-AdV FTC/HBVU6no.2 and FTC-hFIX-attB-(FRT)2 at an MOI of 300, 30, and 10. Control groups received pTHBV2 and pHBVU6no.2, the plasmid pTHBV2 only, or stuffer DNA. As an internal control and for normalization, all groups received the plasmid pRSV.hAAT.bpA, respectively. To analyze shRNA mediated knock-down during an established HBV infection, 2.2.15 cells (stably transduced with the HBV genome) were infected with FTC/HBVU6no.2 and FTC-hFIX-attB-(FRT)2 using an MOI 100 and MOI 500. HBsAg levels in the supernatant were measured three days post infection by enzyme immunoassay (Abbott Laboratories, Abbott Park, IL, USA).

2.1.4   Animal studies

C57Bl/6 mice (Jackson Laboratories) and HBV transgenic mice were kept under the Stanford rules and regulations (Yang *et al.,* 2002). Due to the fact that varying starting levels of serum HBsAg levels are present when using this HBV transgenic mouse line, each individual was pre-screened for HBsAg levels before treatment. For transient HBV studies C57Bl/6 mice (8 weeks old) were co-injected via high-pressure tail vein injection with 12 µg pTHBV2 and either 5 µg of pHBVU6no.2 or stuffer DNA. As an internal control for transduction efficiencies all individuals received pRSV.hAAT.bpA. This plasmid encodes the human α1-antitrypsin gene (hAAT), which can be monitored by ELISA in mouse serum.

Adenoviral vectors were diluted in Phosphate Buffered Saline (PBS) and a total volume of 200 µl per mouse was injected. Blood samples were obtained by retro-orbital bleeding. For bioluminescent images and measurements of emitted light units we used an *in vivo* imaging system (IVIS, Xenogen, Alemeda, CA).

Hepatitis B surface antigen (HBsAg) levels in mouse serum were monitored by enzyme immunoassay (Abbott Laboratories, Abbott Park, IL, USA). SGPT (alanine aminotransferase activity) assays were performed using a diagnostic kit for colorimetric determination of SGPT (Sigma procedure No. 505-OP). All animal experiments were performed by Anja Ehrhardt and Hui Xu in cooperation with Patricia L. Marion at the Stanford University.

2.1.5   Southern Blot analysis to measure HBV genome replication

For genomic DNA isolation, mouse liver was removed and used for DNA extraction as previously described (Ehrhardt and Kay 2002). Blots were hybridized with $[\alpha\text{-P}^{32}]$–deoxycytidine triphosphate (dCTP)–labeled cDNA lacZ probe (*Hind*III / *Stu*I fragment from pRSV/β-Gal) and a HBV probe (*EcoR*I / *Acc*I digested plasmid pTHBV2). To quantify the adenoviral vector genome copy number per cell and to generate a standard curve we digested the plasmid pHD28E4LacZ (Ehrhardt and Kay 2002) with the restriction enzyme *Hind*III.

2.1.6   Northern Blot to approve processing of short-hairpin RNAs

To test for small hairpin RNA expression and to verify processing into mature small inhibitory RNA molecules we performed a Northern blot analysis. These *in vitro* studies were performed in HEK293 cells (human embryonic kidney cells). HEK293 cells were seeded in 6-well plates and infected with the adenoviral vector FTC/HBVU6no.2 at an MOI of 20. As a positive control for HBVU6no.2 short hairpin RNA expression we transfected the previously described plasmid pHBVU6no.2 (McCaffrey *et al.,* 2003) and the plasmid pBS/hFIX/HBVU6no.2. The plasmid pBS/hFIX/HBVU6no.2 represents a subclone of the pFTC/HBVU6no.2. Both vectors contain the identical expression cassette for hFIX and HBVU6no.2. Other controls received either pBS/hFIX/lucRNAi expressing shRNA against luciferase and pBS/hFIX/empty without shRNA expression cassette. Forty-eight hours post-transfection and infection, cells were harvested and small RNAs isolated using a Trizol (Invitrogen) based procedure. Total RNA (20 µg) was separated on a 17% polyacrylamide gel containing 7 M urea in 0.5 x tris-borate-EDTA (TBE) buffer. As a positive control representing also the length marker we ran the reverse oligonucleotide of the first 21 nucleotides of the DNA oligo probe HBV-sense (see below) and the first 21 and 25

nucleotides of the DNA oligo probe Luc-antisense (see below). We performed a semi-dry transfer in 0.5 x TBE onto a Hybond-N+ membrane (GE Healthcare). Northern hybridizations were performed with the following radioactively end-labeled DNA oligonucleotide probes: HBV-sense (5' CTC AGT TTA CTA GTG CCA TTT GTT C 3'), HBV-antisense (5' GAA CAA ACG GCA CTA ATA AAC CGA G 3'), Luc-antisense (5' GGA TTC CAA CTC AGC GAG AGC CAC CCG AT 3'), and as an internal control the oligonucleotide 5.8 S-rRNA [34] (5' TTC ATC GAC GCA CGA GCC GAG TGA TCC 3'). Hybridization was performed in Denhardt's solution at 50ºC. Blots were washed two times for 10 min with 5X SSC/0.1%SDS and 1 time for 10 min with 1X SSC/0.1% SDS at 50 ˚C.

2.2 Results

2.2.1   Cloning of high-capacity adenoviral vectors

Several HC-AdV systems are available to insert a transgene of interest into the HC-AdV genome (Hillgenberg *et al.,* 2001; Shi *et al.,* 2006). Within these systems one has to consider the minimum packaging size of 27.7 kb, which in most cases requires insertion of stuffer sequences. The plasmid pAdFTC, the HC-AdV production plasmid used in our laboratory for instance contains DNA sequences derived from a centromere region on human chromosome 17 and a matrix attachment region, potentially stabilizing vector genomes in the nucleus (Ehrhardt and Kay 2002).

Our cloning system is based on two vectors. One vector is the shuttle vector pHM5 that contains a multiple cloning site (MCS) for easy insertion of the transgene expression cassette (Ehrhardt *et al.,* 2003). Furthermore, the pHM5 MCS is flanked by the rare restriction enzymes recognition sites I-*Ceu* and PI-*Sce*I and has a kanamycin selection marker. The second plasmid, the pAdFTC harbours the left and right ITR, stuffer sequences as mentioned before and near the 3´end the two rare restriction enzyme sites compatible to pHM5. The latter vector can be selected on ampicillin plates, which is of favour for the cloning procedure because there is a negative selection pressure for pHM5 plasmids. Notably, the pAdFTC plasmid is constructed, to keep inserts with a size ranging from 5 kb to 12 kb to reach an optimal packaging size. Therefore, if the transgene cassette of interest is too small, insertion of additional stuffer sequences is suggested.

The whole cloning procedure and helper virus amplification were performed by Martin Hausl. In brief, after insertion of the transgene of interest into the pHM5, this plasmid and pAdFTC were sequentially digested with I-*Ceu* and PI-*Sce* as recommended by the manufacturer's instruction. After each digestion step, a phenol-extraction is required, because both enzymes

change the performance of the DNA in an agarose gel. In order to prevent re-ligation, the pAdFTC is applied to a CIP reaction and on the basis of DNA amounts (calculated from an analytic agarose gel) both plasmids were ligated over night. The next day the ligation reaction has to be purified by phenol extraction and ethanol (EtOH) precipitation. Afterwards a *Swa*I digest of the purified ligation was performed, which destroys empty pAdFTC plasmids in the reaction, because it cuts between the two restriction enzymes used for cloning. Ligation samples were transformed into DH10B cells and selected on ampicillin containing plates. The colonies obtained from the cloning were tested for the correct fragment by I-*Ceu* and PI-*Sce* digest and large scale preparation was performed. For HC-AdV production 20 µg of the plasmid pAdFTC containing the trangene of interest has to be digested with *Not*I, purified using phenol extraction and precipitated with EtOH.

2.2.2 Helper virus amplification

High-capacity adenoviral vector production is dependent on a two-vector system, comprised of the HC-AdV pAdFTC and the helper virus, in our case AdNG163R-2 (Ng *et al.,* 2001; Palmer and Ng 2003), that provide all adenoviral proteins required for genome packaging. Amplification of the helper virus AdNG163R-2 was performed by infection of a 6 cm dish of HEK293 cells at a multiplicity of infection (MOI) of 5. Two days post infection cytopathic effect should be detectable and cell lysates were harvested, supplied to 4 consecutive freeze/thaw cycles performed with liquid nitrogen and a 37°C water bath and used to infect two 10 cm dishes of HEK293 cells each with one third of the lysate. For cesium chloride purification twenty 15 cm dishes are required which are prepared following the conditions used before. Detailed description of the purification of viruses is described in **section 2.2.4**. The viral titer was determined by optical density (**section 2.2.5**) and plaque forming assay described in (Curiel and Douglas 2002). Helper virus amplification and titration were performed by Lorenz Jäger and Martin Hausl, respectively.

2.2.3 Large scale production of high-capacity adenoviral vectors in a spinner flask system

Most of the present protocols for large-scale production of HC-AdV are based on adherent cell culture, which is cost and time intensive. Herein, a suspension culture system is used to produce high amounts of HC-AdV, which is less labour intensive.

Production of HC-AdV was performed in the special producer cell line 116. The 116 cells are HEK293 derived cells that stably express Cre-recombinase. Within the helper virus genome the packaging signal Ψ is flanked by loxP sites, which are recognized by the

Cre-recombinase. Upon infection, the helper virus expresses all viral proteins essential for HC-AdV amplification and packaging, whereby Cre-recombinase mediates the excision of the packaging signal from the helper virus genome, consequently inhibiting its packaging.

The amplification of HC-AdV starts with the transfection of 5 μg linearized pAdFTC, containing the respective transgene generated in section 2.2.1, using 30 μl of Superfect reagent (Qiagen) in a 6 cm dish of 116 cells at a confluency of 50-80%. Sixteen to eighteen hours post transfection the cells were infected with helper virus applying 5 transducing units (TUs) per cell. It is very important to make sure that the virus is distributed equally on the tissue culture dish. Forty-eight hours post transfection the cells were harvested and virus was released by four freeze/thaw cycles, resulting in passage PO. Afterwards, one 6 cm dish of 116 cells (80-90% confluency) was infected with one third of the lysate of P0 and co-transduced with 2 TUs of helper virus (P1). This step was repeated to reach passage P2. Of note, if cytopathic effect (CPE) is not observed from the 6 cm dish after two days an additional amplification step of one 6 cm dish should be performed to guarantee proper virus amplification. Two days post infection of P2, when CPE starts, the cells were harvested and virus was released from the cells following the infection of one 15 cm dish 116 cells with two thirds of the lysate and co-transduced with 2 TUs helper virus. Two days later the cell lysate was collected and stored at -80°C for further use.

For the spinner flask amplification, ten 15 cm dishes 116 cells were flushed off using 10 ml of fresh culture medium for each plate and cells were transferred to a 3 liter spinner flask containing 900 ml culture medium. Notably, 116 cells growing as adherent cells are relatively loosely attached to the tissue culture dishes, therefore no trypsin is required. In fact, trypsin may negatively affect growth of suspension cells. The spinner flask is incubated for 24 hours at 37°C on a magnetic stirrer adjusted to 70 rounds per minute (rpm). Twenty-four hrs and 48 hrs later 500 ml and 72 hours later 1 liter of fresh medium have to be added to grow the cells. In order to monitor health of 116 suspension cells, 3 ml of the spinner flask culture were transferred to a 6 cm dish and 2 hours later adherent cells can be obtained if cells are viable.

The infection of the 116 cells should be performed in a volume of 150 ml, therefore, the cells of the bioreactor were centrifuged at 500 g for 10 min and resuspended in 130 ml of fresh medium but supplemented with only 5% FBS (without hygromycin). The viral lysate (20 ml) from the 15 cm dish was subjected to 4 consecutive freeze and thaw cycles and added to the 130 ml fresh medium to reach the recommended volume of 150 ml. Assuming a density of 3×10^5 cells per ml, the total amount of cells in a 3 liter spinner flask is 9×10^8 cells. Thus, one needs to add 1.8×10^9 TU of the helper virus in order to reach 2 TU/cell. Infection was

incubated for 2 hrs at 37°C on a magnetic stirrer with 60 rpm. Afterwards, the whole infection lysate was transferred back to the spinner flask containing 2 liter of fresh culture medium (without hygromycin but 5% FBS) and maintained for two days at 37°C stirring at 70 rpm. Forty-eight hours later cells were harvested, centrifuged using 890 g for 10 min at room temperature and supernatant was removed carefully. For purification the cell pellet was resuspended in 28 ml sterile PBS and can be stored at -80°C for several weeks until purification.

2.2.4 Purification of HC-AdV by cesium chloride centrifugation and buffer exchange

Purification of the viral lysate was performed by a two-step cesium chloride centrifugation. An overview of the whole procedure is schematically shown in **Figure 2.2.** In order to release the virus from the cells, the PBS-virus solution was applied to 4 freeze and thaw cycles and cellular debris were centrifuged down at 500 g for 8 min. The remaining supernatant was then used for purification. The first centrifugation was performed using a step gradient, comprised of 0.5 ml 1.5 g/cm^3 cesium chloride (CsCl; 45.41 g CsCl, 54.50 ml H$_2$O) solution, 3 ml of 1.35 g/cm^3 (35.18 g CsCl, 64.22 ml H$_2$O) and 3.5 ml of 1.25 g/ cm^3 CsCl (26.99 g CsCl, 73.01 ml H$_2$O), which were carefully overlayed with 4.5 ml of cleared vector supernatant and approximately 0.5 ml PBS to reach the top of the ultra-clear centrifuge tube (Beckman Coulter; **Figure 2.2B**, left panel). The gradient was centrifuged at 12°C for 1.5 hours at 226.000 g using slow acceleration and deceleration in a ultra centrifuge to separate viral particles from remaining cellular fragments. A picture of the gradient after centrifugation is shown in **Figure 2.2B** (middle panel). The particular virus band was carefully removed and a second continuous gradient should concentrate the virus. Therefore the virus solution was filled up to 24 ml with 1.35 g/cm^3 CsCl solution, mixed and transferred to two centrifuge tubes. Of note, it is not recommended to use more than 3 ml of virus solution in one centrifuge tube because the viral band may be diffuse after centrifugation. The second centrifugation step was performed overnight for 18-20 hrs at 12°C and 226.000 g and results in a clear virus containing band appearing in the upper region of the tube (**Figure 2.2A** and **2.2B**, right pannel).

The virus solution was carefully removed and dialysis of the solution cleared the virus from cesium chloride, which is toxic for cells. Dialysis was performed in tubes (Spectra/Por Membrane, MWCO 50.000), which were first washed three times with sterile, deionised H$_2$O, then the tube was closed (Spectra/Por Closures) on one side to pipette the viral lysate inside and closed also on the other side. Dialyze solution contains 10 mM Tris-HCl (pH7.5), 10% glycerol, 1 mM MgCl$_2$ in deionised water. First buffer exchange was done after 2 hrs at 4°C

on a magnetic stirrer (32 rpm) in 1 liter of dialyze solution and was then extended in a new two liter dialyze solution for 24 hrs under the same conditions. The next day viral lysate was collected, multiple aliquots were made and stored at -80°C.
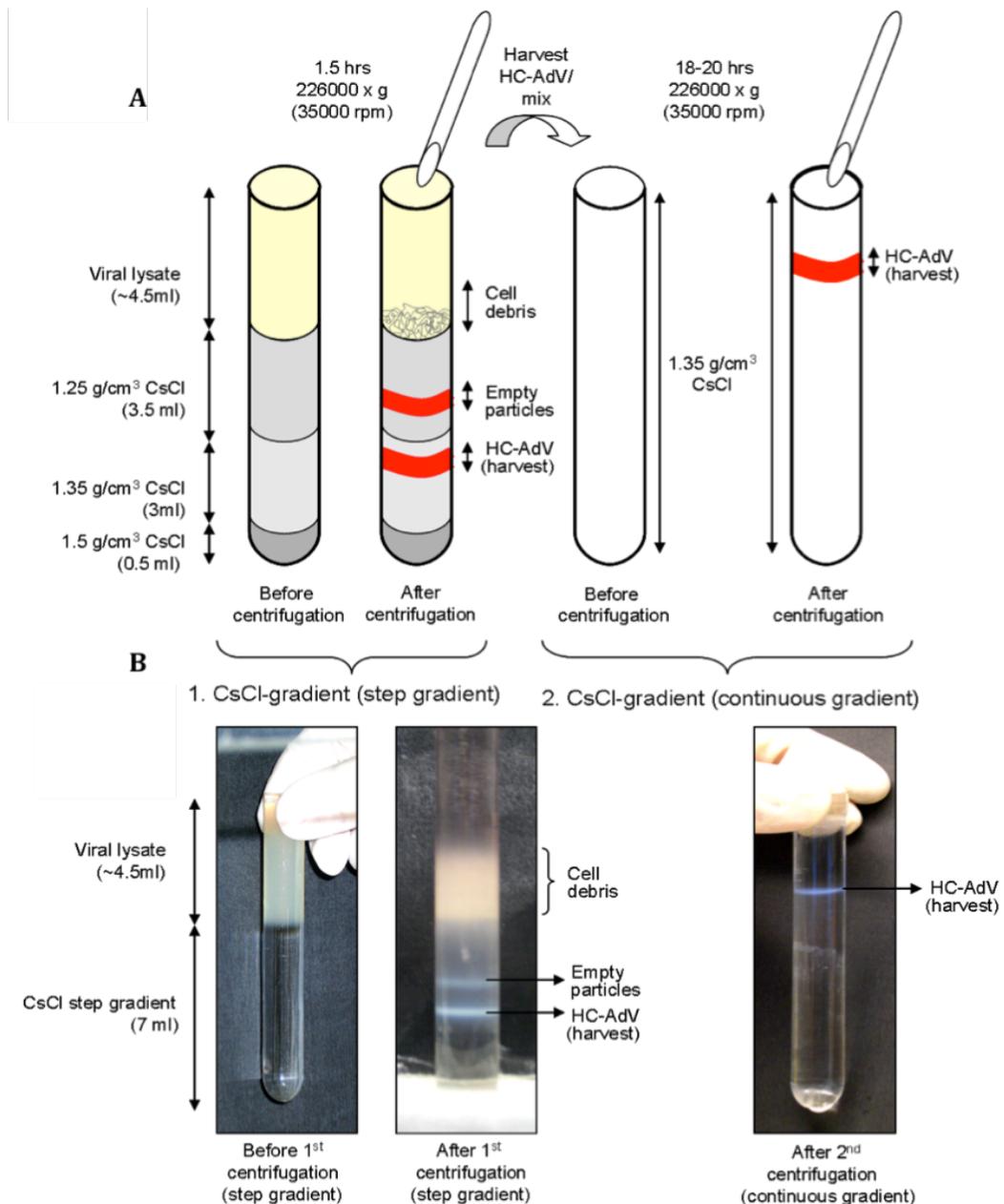
Figure 2.2: Flow chart of CsCl purification of HC-AdV. For both centrifugation steps centrifuge tubes are shown before and after centrifugation. The cesium chloride steps are indicated as well as the respective centrifugation parameters. (A) Schematic diagram of CsCl gradients. After three freeze and thaw cycles the viral lysate is carefully loaded onto the top of the CsCl gradient. After centrifugation at 226,000 x g (1.5 hrs) the band containing the HC-AdV is harvested from the top. Empty particles concentrate in the 1.25 g/cm^3 CsCl-phase complete HC vector particles concentrate in the 1.35 g/cm^3 CsCl-phase. In the continuous CsCl gradients, the HC-AdV particles concentrate in the upper part of the tube. Note, empty particles are concentrating above the complete particles. Be sure to harvest the complete particles in an as small as possible volume in order to concentrate them. **(B)** Photographs of the collection tubes before (left picture) and after the step gradient centrifugation (middle picture) and after the continuous gradient centrifugation (right picture). The particle bands (empty and complete) appear white with a light blue shadow.

2.2.5   Titration of HC-AdV by optical density and quantitative Real-Time PCR

Titration of purified virus can either be performed by measuring the physical titer in order to obtain all viral particles in your preparation or one can do quantitative Real-Time PCR (qRT-PCR) to calculate the actual TUs.

For the optical density (OD) 25 μl of purified virus was supplemented with 475 μl lysis buffer (10 mM Tris-HCl (pH 7.5), 10 mM EDTA (pH 8.0), 0.5% SDS) and shaked for 15 min at 37°C at 1000 rpm. After centrifugation of the virus solution at 15.000 g for one min., the OD was measured at 260 nm. The following formula was used to calculate optical particle units (OPU):

OPU/ml = (absorbance at 260nm) x (dilution factor) x (1.1×10^{12}) x (36) / (size of HC-AdV in kb).

In order to determine TUs of HC-AdV and to analyze helper virus contamination, qRT-PCR was performed. The helper virus contamination can be evaluated by treatment of 25 μl of purified virus with 200 μl Proteinase K solution (0.5 mg/ml proteinase K, 10mM Tris-HCl (pH 7.5), 0.5% SDS, 10mM EDTA (pH 8.0)) for 4 hours at 55°C. Afterwards the DNA was precipitated using 1 volume ethanol and 3 M Natrium acetat (pH 5.0) and was resuspended in 25 μl of sterile H_2O. Five μl were used for qRT-PCR. For the standard curve serial dilutions of purified wtAd5 DNA were generated and genome copy numbers were calculated by the formular:

$$10^{-12}/\text{plasmid size (bp)} * 6.02 * 10^{23}$$

QRT-PCR was carried out with the Taqman 7500 Fast Real-Time PCR System (Applied Biosystems) amplifying a 235 bp fragment of the adenoviral late gene 3 (L3), using the oligonucleotides L3 forward 5´AGA AGC TTA GCA TCC GTT ACT CGA GTT G and L3 reverse 5´ATA AGC TTG CAAT GTT GGT ATG CAG GAT GG together with an L3 specific probe 5´Fam CCA CCC GTG TGT ACC TGG TGG ACA-Tamra (Ella Biotech). The PCR was performed using the following program: AmpErase UNG reaction at 50°C for 2 min, pre-incubation/activation at 95°C for 10 min, amplification and data collection during 40 cycles (95°C for 15 sec and 60°C for 1 min). Universal PCR master mix (Roche) was used for Taqman qRT-PCR. On the basis of the standard curve, helper virus genomes were calculated in the final vector preparation.

For measuring TUs of the HC-AdV in the final virus preparation, HEK293 cells were seeded in a 6 cm culture dish to reach 90% confluence at the time point of infection. Two μl of purified virus was used to infect HEK293 cells. Two hours infected and non-infected cells

were harvested using trypsin to remove not internalized viral particles. Whole genomic DNA was isolated from the cells, ten-fold dilutions of the genomic DNA was prepared to perform qRT-PCR with the primer ITR Ad5ItRfw1-24 5´CAT CAT CAA TAA TAT ACC TTA TTT and 436Rev 5´ACG CCA CTT TGA CCC GGA ACG using LightCycler FastStart DNAMaster^{Plus} SYBR Green I kit (Roche) under the following conditions: Preincubation at 95°C for 10 min, amplification 45 cycles at 95°C for 10 sec, 55°C for 5 sec and 72°C for 30 sec. As described above, for the standard curve, purified wtAd5 DNA was used in serial dilutions. The primers used in this assay amplify the ITR/packaging signal region, which is in reverse orientation in the helper virus genome, and therefore only the ITR from the HC-AdV and not helper virus is amplified in this step.

Notably, for accurate measurements and production of clinical-grade HC-AdV the adenoviral reference material (ARM) could be used for titration. ARM is distributed by ATCC and is fully characterized regarding particle concentration and the amount of infectious units per volume. The advantage of this method is that adenoviral preparations produced in different laboratories can be directly compared also with respect to future clinical trials.

2.2.6 HC-AdVs for the delivery of short-hairpin RNAs to mediate inhibition of luciferase expression by RNAi *in vitro* and *in vivo*

After production of HC-AdVs utilizing our detailed protocol, we aimed at evaluating efficacy of our HC-AdVs in a clinically relevant animal model. Over the recent years various viral and non-viral vector systems have been studied for delivery of short hairpin RNA (shRNA) expression cassettes for instance to reduce hepatitis B virus transcripts. However, the *in vitro* and *in vivo* efficacy of HC-AdV lacking all viral coding sequences remains to be studied. In order to determine optimized conditions for shRNA delivery, we co-transduced HeLa cells with the HC-AdV FTC/lucRNAi expressing shRNA against luciferase (**Figure 2.3B**) and the first generation (fg) adenoviral vector fgAdluc expressing luciferase (**Figure 2.3A**). We observed a 77% reduction in luciferase expression at a 1:1 ratio (fgAdluc : FTC/lucRNAi). At a 1:5, 1:10, and 1:50 ratio (fgAdluc : FTC/lucRNAi) we measured up to 94% reduction in luciferase expression levels (**Figure 2.3F**). To demonstrate that this effect was specifically related to shRNA mediated transgene silencing, control cells received an adenoviral vector with an unrelated shRNA expression cassette (FTC/HBVU6no.2, **Figure 2.3C**). As showndemonstrated in **Figure 2.3B** there was no reduction of luciferase expression in control cells.
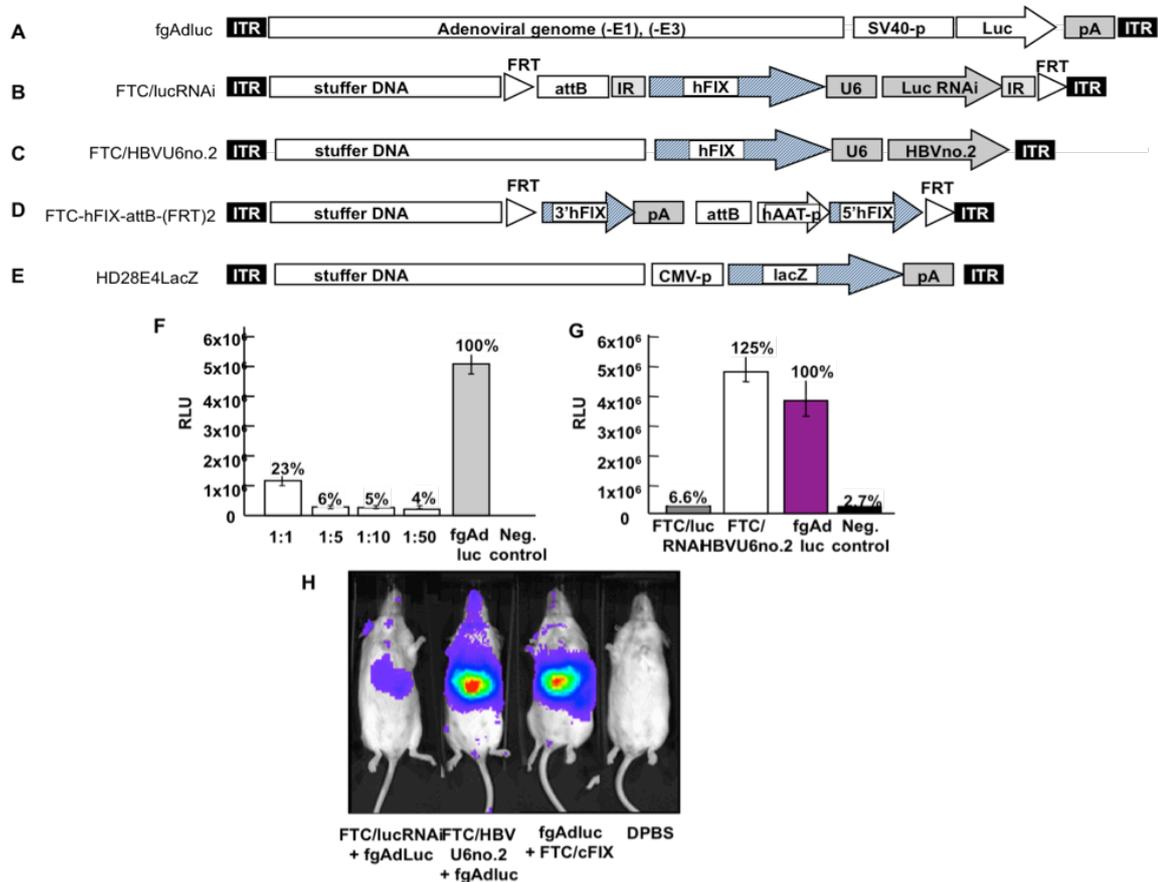
Figure 2.3: DNA sequences contained in the recombinant adenoviral vector genomes and inhibition of luciferase expression by luciferase RNAi-mediated RNA interference *in vitro* and *in vivo*. (A) The first generation adenoviral vector fgAdluc contained a luciferase expression cassette encoding luciferase (luc) under the control of Simian virus 40 promoter (SV40-p). pA: polyadenylation signal. (B) The adenoviral vector FTC/lucRNAi contained an expression cassette encoding a previously described small hairpin RNA (shRNA) against luciferase (Luc RNAi) under the control of the U6 promoter. The stuffer DNA contained in the high-capacity adenoviral vectors was based pAdFTC. In addition this vector contained a previously described human coagulation factor IX (hFIX) expression cassette[17] and the following DNA sequences: AttB: bacteriophage integrase phiC31 attachment site; IR: inverted repeats for Sleeping Beauty transposase; FRT: recognition sites for Flp mediated recombination. (C) The adenoviral vector FTC/HBVU6no.2 contained the shRNA expression cassette HBVU6no.2 and the identical hFIX expression cassette as described already for FTC/lucRNAi. (D) The control vector FTC-hFIX-attB-(FRT)2 without shRNA coding sequence contained a previously described split transgene expression cassette for hFIX under the control of the liver specific human α1-antitrypsin promoter (hAAT-p). (A)-(D) ITR: inverted terminal repeat. (E) The HC-AdV HD28E4LacZ was described previously (Palmer and Ng 2003) and contains the β-galactosidase cDNA (lacZ) under the control of the murine cytomegalovirus (CMV-p) promoter. (F) Optimization of RNA interference mediated post-transcriptional silencing by a high-capacity adenoviral vector (HC-AdV) with a shRNA expression cassette against luciferase. HeLa cells were co-transfected with the first generation adenoviral vector fgAdluc at an MOI of 10 and the shRNA expressing adenovirus FTC/lucRNAi at an MOI of 10, 50, 100, and 500 respectively. Mean ± SD is shown (n=3/group). Luciferase levels were measured 3 days post-infection. (G) Inhibition of luciferase expression by the HC-AdV FTC/lucRNAi. The negative control group received the adenoviral vector FTC/HBVU6no.2 with an irrelevant shRNA expression cassette. Mean ± SD is shown (n=3/group). (H) RNA interference in FVB mice (n=3/group). Shown are representative images of light emitted from mice, which received the luciferase expressing vector and a second adenoviral vector which expressed short hairpin RNA against luciferase (FTC/lucRNAi). Control groups received an adenoviral vector with an irrelevant shRNA (FTC/HBVU6no.2), no shRNA (AdFTC/cFIX/ChMAR[22]), or the vehicle control. Representative individuals of each group are shown. Cloning of the viral plasmids (A-D) and the animal experiment (H) were performed by A. Ehrhardt.

In order to demonstrate *in vivo* efficacy, FVB mice (n=3 per group) were co-injected with 1.2×10^{10} TUs of the adenoviral vector FTC/lucRNAi and 4×10^9 TUs of the fg adenoviral vector fgAdluc. Control mice were co-injected with 4×10^9 TUs fgAdluc and either 1.2×10^{10}.

TUs of the HC-AdV AdFTC/cFIX/ChMAR (Ehrhardt *et al.,* 2003) without shRNA coding sequence or the HC-AdV FTC/HBVU6no.2 (**Figure 2.3C**) with an irrelevant shRNA coding sequence. Negative control mice received the vehicle for adenoviral delivery (PBS). We found up to 96% reduction of luciferase expression seven days post-injection in mice, which received the adenoviral vectors FTC/lucRNAi and fgAdluc. **Figure 2.3H** shows representative images of light emitted from mice in all groups (this experiment was performed by Anja Ehrhardt). The effect of shRNA mediated post-transcriptional silencing of luciferase expression lasted for 2 weeks (data not shown). Long-term studies were not feasible because luciferase expression levels from the fg adenoviral vector fgAdluc decreased to undetectable levels 4 weeks post-injection. It was concluded that HC-AdVs are sufficient to mediate RNA interference mediated post-transcriptional gene silencing *in vitro* and *in vivo*.

2.2.7   Inhibition of hepatitis B virus infection *in vitro*

Using a non-viral gene therapy approach, it was demonstrated that a 25-mer shRNA against HBV (HBVU6no.2) driven by the polymerase III U6 promoter resulted in efficient knockdown of HBV infection *in vitro* (up to 94% reduction in hepatitis B virus surface antigen levels (HBsAgs)), a marker for progression of HBV infection (McCaffrey *et al.,* 2003). HBsAg of HBVU6no.2 treated mice was reduced by 84.5% in a transient animal model for HBV infection (McCaffrey *et al.,* 2003). Interestingly, another study reported that the identical shRNA, HBVU6no.2, was lethal at high dose in HBV transgenic mice and regular mice in the context of an AAV2/8 vector (Grimm *et al.,* 2006). It is speculated that this phenomenon was due to oversaturation of the micro RNA/shRNA pathways.

This study evaluated HC-AdV for delivery of HBVU6no.2. To verify expression and processing of the shRNA against HBV and luciferase contained in our shRNA expression plasmids and in the viral vector FTC/HBVU6no.2, we performed a Northern blot analysis. As depicted in **Figure 2.4** we detected expression and processing of the highly efficient shRNA against luciferase and the shRNA against HBV (**Figure 2.4B**). Notably, in contrast to the shRNA expression cassette against luciferase, we found that the ratio of hairpin to processed siRNA for HBVU6no.2 seems to be shifted towards the hairpin (**Figures 2.4A,B**).

This was in concordance with a previously described study showing efficacy of HBVU6no.2. In this study the identical hairpins were delivered by AAV2/8 vectors and analyzed by Northern blot analysis.
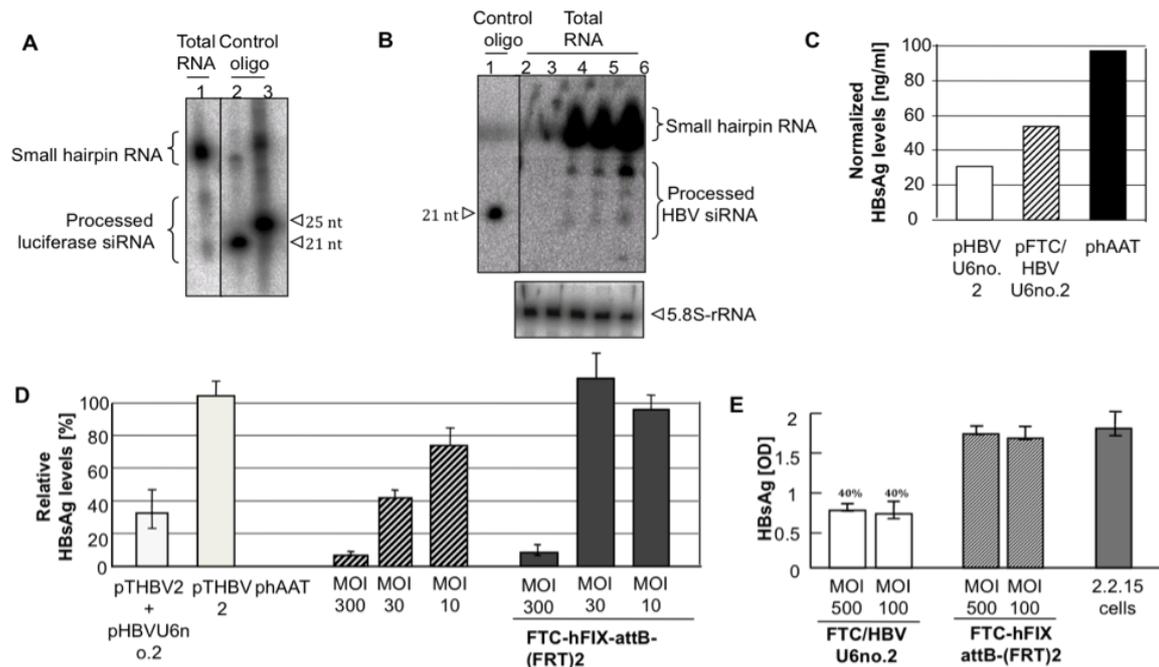
Figure 2.4: Expression of small hairpin RNA and inhibition of hepatitis B virus infection *in vitro*. (A) Small-hairpin expression and processing of the shRNA against luciferase. Cells were transfected with the luciferase shRNA expression plasmid pBS/hFIX/lucRNAi. As a standard we loaded the 21-mer and the 25-mer of the reverse sequence of the oligonucleotide Luc-antisense on the gel. The blotted membrane was probed with the radioactively labelled probe Luc-antisense. (B) Northern blot analysis to show expression and processing of short hairpin RNA (shRNA) against HBV. In order to show that equal amounts of total RNA were loaded on the gel, the membrane was subsequently hybridized with the 5.8S-rRNA oligonucleotide. As a standard we loaded the 21-mer of the reverse sequence of the oligonucleotide HBV-antisense. (C) DNA sequences contained in the HC-AdV FTC/HBVU6no.2 induce silencing of hepatitis B virus surface antigen (HBsAg). Huh7 cells were co-transfected with pTHBV2 and pHBVRNAno.2, or pFTC/HBVU6no.2 or stuffer DNA. HBsAg levels in the supernatant were measured two days post infection by enzyme immunoassay (n=2/group). (D) RNA interference induced silencing of HBsAg levels in the Huh 7 cells. Huh7 cells were transiently transfected with the plasmid pTHBV2 containing the HBV genome. Twenty-four hours post-transfection cells were transfected with the HC-AdV FTC/HBVU6no.2 or FTC-hFIX-attB-(FRT)2 at an MOI of 300, 30, and 10. Control groups were either co-transfected with the plasmids pTHBV2 and pHBVU6no.2, the plasmid pTHBV2 only or the negative control plasmid phAAT. HBsAg levels in the supernatant were measured two days post infection by enzyme immunoassay. Mean ± SD is shown (n=3/group). (E) RNA interference induced silencing of HBsAg from an adenoviral vector in 2.2.15 cells (stably transfected with the HBV genome). Control groups either were untreated or received the HC-AdV FTC-hFIX-attB-(FRT)2. HBsAg levels in the supernatant were measured three days post-infection by enzyme immunoassay. Mean ± SD is shown (n=3/group).

In order to demonstrate that the shRNA sequences against HBV contained in our adenoviral vector FTC/HBVU6no.2 (**Figure 2.4C**) are functional, an *in vitro* study solely based on plasmid transfection was performed. Human hepatoma cells (Huh7) were co-transfected with pTHBV2 (a plasmid that contained the complete HBV genome for establishment of transient HBV infection) and either the plasmid pHBVU6no.2 or pFTC/HBVU6no.2. A 68% and 47% drop in HBsAg levels was observed, respectively (**Figure 2.4C**).

In a further step we evaluated potency of the adenoviral vector FTC/HBVU6no.2 (**Figure 2.4C**). Huh7 cells were transiently transfected with the plasmid pTHBV2. This step was followed by infection with either the HC-AdV FTC/HBVU6no.2 or the control vector FTC-hFIX-attB-(FRT)2 (**Figure 2.4D**) at an MOI of 300, 30, and 10. For groups, which received the HC-AdV FTC/HBVU6no.2, we observed a 94%, 60%, and 30% reduction in HBsAg levels in the supernatant of Huh7 cells, respectively (**Figure 2.4D**). We observed vector related cellular toxicity at the highest adenoviral vector dose (MOI 300). This observation may explain reduction of HBsAg levels in the group, which received the highest dose of the control vector FTC-hFIX-attB-(FRT)2 (**Figure 2.4D**). The positive control group received the plasmids pTHBV2 and pHBVU6no.2 for RNA interference induced silencing of HBV transcripts. In concordance with results presented in **Figure 2.4C**, we observed a 75% reduction in HBsAg levels in the supernatant of Huh7 cells of this group (**Figure 2.4D**). All groups, including the negative control group, received the plasmid pRSV.hAAT.bpA encoding secreted human α1-antitrypsin (hAAT) for normalization of transfection efficiencies.

The 2.2.15 cells are stably transfected with the HBV genome and thus pre-existing HBV infection is present. In order to test susceptibility of 2.2.15 cells to super infection with adenovirus, we infected these cells at various MOIs with the HC-AdV expressing the marker gene β-gal. We found that an MOI of 100 was sufficient to transduce 100% of 2.2.15 cells (not shown). Thus, 2.2.15 cells were transduced at an MOI of 100 with the HC-AdV FTC/HBVno.2. We observed up to 60% reduction of secreted HBsAg levels in the supernatant (**Figure 2.4E**). This was in contrast to the control group which was transfected with the adenoviral vector FTC-hFIX-attB-(FRT)2 without shRNA expression cassette. HBsAg levels in this group were comparable to HBsAg levels in the supernatant of untransfected 2.2.15 cells.

2.2.8   HC-AdV results in reduction of hepatitis B surface antigen in small animal models for hepatitis B infection

In previous studies it was demonstrated, that hydrodynamic transfection of non-viral DNA containing the complete HBV genome represents a transient animal model for HBV infection

(Yang *et al.,* 2002; McCaffrey *et al.,* 2003). In this animal model blood antigen levels drop to undetectable concentrations as early as 7 days post-injection due to formation of neutralizing antibodies against HBV gene products (Yang *et al.,* 2002). McCaffrey *et al*. found that secreted HBsAg in mouse serum were significantly reduced after co-delivery of a plasmid containing the HBV genome (pTHBV2) and a second plasmid driving expression of the shRNA HBVU6no.2 (pHBVU6no.2) (McCaffrey *et al.,* 2003). To test efficacy of the HC-AdV FTC/HBVU6no.2 in this transient animal model, we sequentially injected pTHBV2 containing the HBV genome and the adenoviral vector FTC/HBVU6no.2 into C57Bl/6 mice (n=4 per group). The plasmid pTHBV2 was injected by high-pressure tail vein injection followed by injection of $5x10^9$ TUs of the HC-AdV FTC/HBVU6no.2. We measured HBsAg levels 2 and 4 days after adenoviral delivery and we observed a 68% drop in serum HBsAg levels (**Figure 2.5A**). Mice, which either received the HC-AdV HD28E4LacZ with a β-gal expression cassette (**Figure 2.3E)** (Palmer and Ng 2003) or pHBVU6no.2 showed a reduction of 73% and 66% in HBsAg levels, respectively (**Figure 2.5A)**. This finding may suggest that the transgene product β-gal itself may be responsible for reduction in HBsAg levels (experiments 2.5A and B were performed by A. Ehrhardt).

Recent studies by Uprichard *et al*. and Carmona *et al*. used fg adenoviral vectors (deleted for the adenoviral early genes E1 and E3) for delivery of HBV specific shRNAs (Uprichard *et al.,* 2005; Carmona *et al.,* 2006). After systemic application of the adenoviral vector into a transgenic mouse model for HBV infection, this approach resulted in reduced HBV infection levels for up to 26 days. Our goal was to evaluate HC-AdV lacking all adenoviral coding sequences in HBV transgenic mice. HBV transgenic mice (n=4 per group) were injected with $5x10^9$ TUs of the HC-AdV FTC/HBVU6no.2. After a transient increase in HBsAg levels, we observed an up to 68% reduction in serum HBsAg levels compared to the vehicle control group (**Figure 2.5B,** performed by A. Ehrhardt).

To analyze knockdown of HBV replication by other means, we performed a Southern blot analysis of HBV transgenic mouse liver genomic DNA. Compared to the control group, which received the vehicle (PBS), we found that HBV viral DNA is reduced in mice, which received FTC/HBVU6no.2 (**Figure 2.5C**).

In order to rule out unspecific effects of HC-AdV on HBV replication, we performed a second experiment in HBV transgenic mice. Individual mice were either transduced with $5x10^9$ transducing units of the HC-AdV FTC/HBVU6no.2 or $5x10^9$ transducing units of the HC-AdV FTC/lucRNAi (**Figure 2.3B**). The latter group functions as a control with an irrelevant shRNA expression cassette. We observed a transient decrease in HBsAg levels up to 7 days post-injection followed by an increase in HBsAg levels (data not shown, experiment was

performed by A. Ehrhardt). This finding was in contrast to our first experiment in HBV transgenic mice (**Figure 2.5B**). One fatality was accounted for in the group, which received FTC/HBVU6no.2, but the reason for this observation remains to be investigated. In contrast to FTC/HBVU6no.2 treated mice, only one mouse of the group, which received the HC-AdV FTC/lucRNAi showed a slight decrease in HBsAg levels. In concordance to our first experiment, we observed increased release of liver enzymes as demonstrated by SGPT levels (data not shown, experiment performed by A.Ehrhardt).
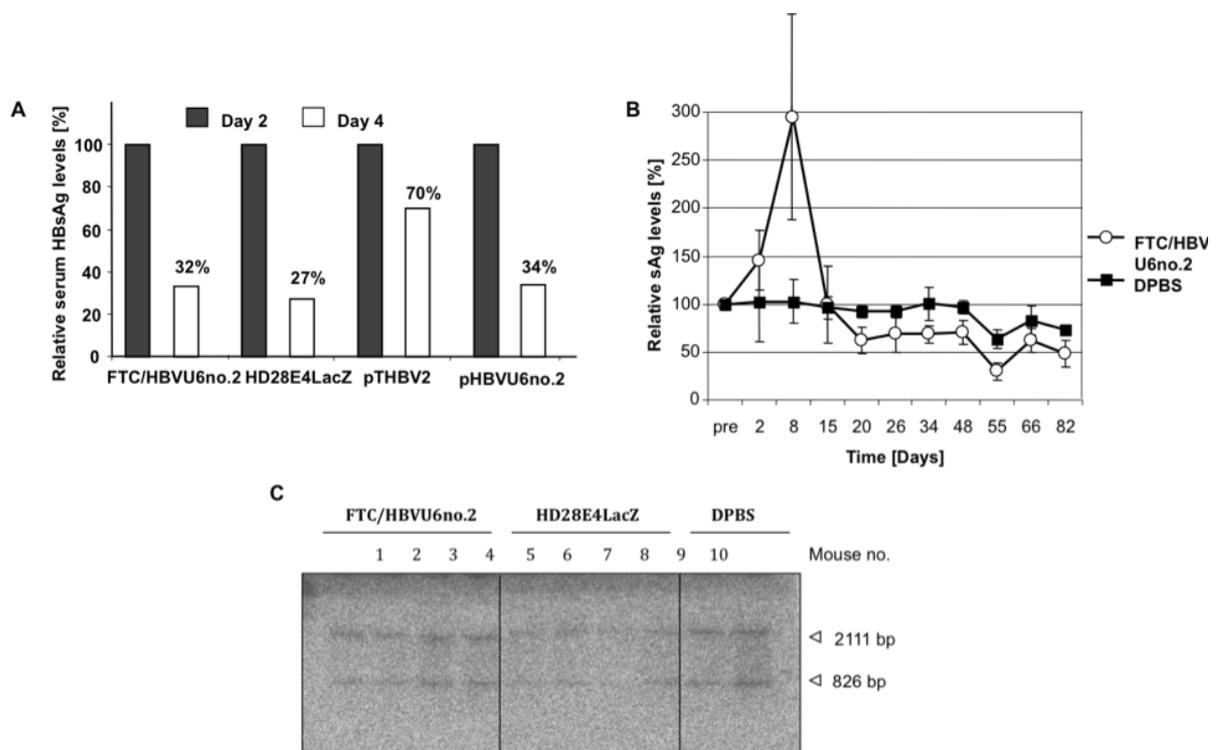
Figure 2.5: Reduction of hepatitis B virus surface antigen (HBsAg) levels *in vivo* by a high-capacity adenoviral vector (HC-AdV) in a transient and trangenic mouse model for hepatitis B virus infection. (A) Reduction of HBsAg levels in mouse serum. C57Bl/6 mice were injected with a plasmid containing the HBV genome (pTHBV2). This step was followed by injection of 5×10^9 transducing units of either the HC-AdV FTC/HBVU6no.2 or HD28E4LacZ. Control groups were injected with pTHBV2 or co-injected with pTHBV2 and pHBVRNAno.2. Serum HBsAg levels were measured two and four days after adenovirus injection by enzyme immunoassay. Mean is shown (n=4/group). (B) Relative hepatitis B virus surface antigen (HBsAg) levels after injection of the adenoviral vector FTC/HBVU6no.2 into HBV transgenic mice. Mean ± SD is shown (n=4). Control mice solely received the vehicle PBS. Mean ± SD is shown (n=3). Serum HBsAg levels were monitored by enzyme immunoassay. Mean ± SD is shown (n=4). (C) Analysis of HBV genome replication after injection of the HC-AdV FTC/HBVU6no.2 and HD28E4LacZ. We performed Southern blot analysis of mouse genomic DNA. Blots were hybridized with a [α-P[32]]–deoxycytidine triphosphate (dCTP)–labeled HBV probe. Experiments 5A and 5B were perfomed by Anja Ehrhardt.

2.3 Discussion

In conclusion, our in detail protocol for the fast and less labour intensive, large-scale production of HC-AdVs offers the opportunity to generate these vectors, even in non-experienced laboratories. The advanced cloning procedure, using rare restriction enzymes makes the insertion of the transgene cassette of interest independent of sophisticated and inefficient homologous recombination processes (**section 2.2.1**) (He *et al.,* 1998; Luo *et al.,* 2007). In addition, the helper virus AdNG163R-2 provided a pre-condition for a safe HC-AdV production, as it guarantees low helper virus contamination in the final vector preparation (Ng *et al.,* 2001).

The amplification procedure was adapted to HEK293 based cell line 116, which can be grown in suspension culture. Therefore, HC-AdVs production can be performed in a 3 liter spinner flask system, making the entire process less labour and cost intensive and allows amplification of multiple different HC-AdVs, as 5 pole magnetic stirrers (Belco) are already available (**Figure 2.1**). Moreover, the protocol for the cesium chloride gradient purification provides useful information about the composition of cesium chloride solutions, specifically optimized for Ad5 purification (**Figure 2.2**), and of course the ingredients of the dialyze buffer, which is in our case a glycerol based buffer. There are also sucrose-based buffers for dialysis available (Offringa *et al.,* 2005), as they should reduce the probability of precipitates within the final virus preparation; however the coherence of glycerol and precipitates has not been confirmed yet.

For calculation of transducing units a protocol for qRT-PCR is provided, whereby one can also perform Southern Blot analysis (experiment was performed by L. Jager within this study), but quantification of the infectious particles is faster and more precise. We used primer directed against the ITR and the packaging signal, which can be subjected to every generated HC-AdV, independent from the introduced transgene expression cassette. Thus, the calculation of different preparations is better comparable (**section 2.2.5**).

Furthermore, our study demonstrates that HC-AdV deleted for all viral coding sequences is suitable to deliver shRNAs. These shRNAs were recognized and processed by the RNAi enzymes, which render mature miRNAs (**Figure 2.4**) that have the potential to reduce transient and pre-existing HBV infection significantly. However, the present study also emphasizes that the design of DNA sequences contained in the vector and virus-host interactions during super infection need to be carefully considered.

The effect of shRNA mediated RNA interference against luciferase lasted for two weeks *in vivo* (data not shown, experiment done by A. Ehrhardt). A long-term study was not

applicable because luciferase expression levels from the first generation (fg) adenoviral vector fgAdluc decreased to undetectable levels 4 weeks post-injection. Persistence of transgene expression levels from fg adenoviral vectors depends on the promoter which controls transgene expression and the mouse strain (Schiedner *et al.,* 1998; Ehrhardt and Kay 2002). In the present work) luciferase expression was driven by the Simian virus 40 (SV40) promoter. However, tissue specific promoters may result in stabilized transgene expression levels with a reduced toxicity profile (Schiedner *et al.,* 1998; Ehrhardt and Kay 2002). Thus, future studies may investigate a HC-AdV with a liver specific promoter driving luciferase expression or transgenic mice for hepatic luciferase expression. With respect to long-term suppression of luciferase expression or therapeutically relevant target transcripts (e.g. viral transcription units or endogenous genes), shRNA may be delivered with recently developed HC-AdV for somatic integration (Ehrhardt *et al.,* 2007). These vectors were shown to result in stabilized transgene expression levels even during rapid cell cycling *in vivo* (Ehrhardt *et al.,* 2007).

We observed a transient increase in serum HBsAg levels shortly after HC-AdV administration the transgenic mouse model for HBV infection (**Figure 2.5B)**. This was in contrast to studies performed by Uprichard and Carmona (Uprichard *et al.,* 2005; Carmona *et al.,* 2006). After adenoviral injection there was no transient increase in HBsAg antigen levels. One explanation for these observed differences might be the fact that the two latter studies utilized fg adenoviral vectors. We speculate that the remaining adenoviral genes in fg adenoviral vectors and their gene products in contrast to HC-AdV may have an additional inhibitory effect on HBV infection. In fact, it was demonstrated that inflammatory cytokine induction after systemic administration of HBV transgenic mice with an fg adenoviral vector resulted in reduced HBV replication (Cavanaugh *et al.,* 1998). In contrast to fg adenoviral vectors, HC-AdV lack all viral coding sequences. Thus, immunomodulatory adenoviral gene products are not present after infection with HC-AdV. However, the host response against the incoming adenoviral viral capsid proteins and the subsequent change in the expression profile of the host cells may directly or indirectly result in increased HBsAg levels.

In our first experiment performed in HBV transgenic mice we found that HBsAg levels were transiently increased up to two weeks post-injection of the HC-AdV FTC/HBVU6no.2 (**Figure 2.5B**). This was in contrast to our second experiment in which we measured a decrease in HBsAg levels shortly post-injection (data not shown, experiment performed by A.Ehrhardt). We speculate that this difference may be related to the HBV viral load of each individual pre-injection of the adenoviral vector. At average HBV transgenic mice used in the first experiment had higher starting HBsAg levels (989 ng/ml, 548 ng/ml, 475 ng/ml, and 365

ng/ml) pre-injection compared to individuals used in the second experiment (103 ng/ml, 323 ng/ml, 276 ng/ml).

Very recently it was reported that injection of high dose of recombinant AAV vectors expressing various short hairpin RNAs caused lethality in mice (Grimm *et al.,* 2006). It was speculated that oversaturation of the shRNA/micro RNA pathways may be responsible. In contrast to superinfection with AAV2/8 vectors expressing the shRNA HBVU6no.2, we only observed one case of lethality in HBV transgenic mice after systemic administration of a high dose of a HC-AdV with the identical shRNA expression cassette (data not shown, experiment was performed by Anja Ehrhardt). However, it is important to point out that the reason for this fatality remains to be investigated and that further studies need to be performed. It was proposed that oversaturation of the micro/short hairpin RNA pathways may be responsible for lethality in AAV8 injected mice. Both, recombinant AAV2/8 and adenoviral vectors have the ability to infect 100% of mouse hepatocytes. However, for sufficient transduction of all mouse hepatocytes using single-stranded AAV2/8 vectors, a high vector dose (7.2×10^{12} viral genomes per mouse) is required. It was demonstrated by Nakai *et al*. that this dose resulted in up to 1000 vector genome copies per cell (Nakai *et al.,* 2005). Even for double-stranded AAV2/8 vectors with improved transduction efficiencies, 1×10^{12} AAV vector genomes per mouse are required to efficiently transduce all mouse hepatocytes (Grimm *et al.,* 2006). This feature of AAV vectors is in sharp contrast to adenoviral vectors. After transduction of 100% of mouse hepatocytes we only detected up to 12 adenoviral vector genomes per hepatocyte (data not shown, experiment performed by A. Ehrhardt). We believe that this vector genome copy number per cell and subsequent shRNA expression levels were not sufficient to oversaturate the micro RNA/shRNA pathways. To further shed light on the differences between AAV and adenoviral vectors for shRNA delivery against HBV, further studies remain to be performed. One may consider to analyze and to compare additional blood parameters or major factors of the innate immune response.

In summary, HC-AdV can be produced at high titers utilizing our detailed protocol. Since helper virus contamination is only negligible, final vector preparation can be used in small and large animal models and in the future potentially also in the clinics. We believe that HC-AdV have the potential to mediate potent shRNA mediated gene silencing *in vivo* but the design of DNA sequences including shRNAs contained in the vector need to be carefully considered. In addition, we believe that it will be essential to further elucidate biological virus-host interactions during super infection with HBV and adenovirus. Moreover, further understanding of the micro RNA/shRNA pathways will be required before pursuing these gene therapy approaches in a clinical setting.

3 Transcriptional activity of inverted terminal repeats of various human adenovirus serotypes

Recombinant adenoviral vectors (rAdVs) represent the most frequently used gene transfer system for preclinical and clinical approaches (Morral *et al.,* 1998; Brunetti-Pierri *et al.,* 2007). Different generations of rAdVs were developed by removing various viral coding regions, being replaced by foreign DNA. This largely expanded the potential of rAdV and to date rAdVs are extensively studied as oncolytics for the treatment of tumors and for treating genetic disorders.

To date 53 human wild type adenovirus (wtAds) serotypes have been identified, which are divided into the seven subgroups A, B1, B2, C, D, E and F. They differ by their tropism and their clinical manifestations. For instance, subgroups B1, C, and E cause respiratory infections, group B2 causes infections of the kidney and the urinary tract, group F viruses cause gastroenteritis, and subgroup D viruses are associated with epidemic keratoconjunctivitis. The most commonly used adenovirus serotype for generation of rAdVs is represented by the human adenovirus serotype 5 (Ad5) from subgroup C. However, over the recent years there was an increased interest in generation of other than Ad5-based rAdVs (Yang *et al.,* 1995a; Bromberg *et al.,* 1998) because Ad5 is restricted by its tropism and there is a high prevalence of neutralizing antibodies within the human population against Ad5 (Arnberg 2009). Therefore, by exploring the complete spectrum of all available human wtAds one could benefit from the diverse tissue tropism and one may circumvent pre-existing immunity.

All rAdVs used for genetic engineering of cells share the serotype-specific ITRs flanking both sides of the adenovirus genome as one common feature in their genomic composition. It is established that the ITRs play an important role in adenovirus DNA (Curiel and Douglas 2002). Dependent on the serotype the ITRs are approximately 160 base pairs (bp) in length and sequence comparisons revealed that in particular the first 50 bp from the ends contain sequences that have been well conserved in adenovirus evolution (Tolun *et al.,* 1979; Ishino *et al.,* 1987). There is evidence that transcriptional activity is located within the ITRs of Ad5 (bp 1-103) (Yamamoto *et al.,* 2003), nucleotide sequences 1 to 190 and 1 to 342 within the ITR (Yamamoto *et al.,* 2003), and downstream of the adenoviral ITR sequences within the packaging/enhancer region (bp 194-458) (Hearing *et al.,* 1987; Shi *et al.,* 1997; Rubinchik *et al.,* 2001). This feature is important because transcriptional activity derived from the ends of the adenovirus genome can influence the performance of a given transgene inserted into a rAdV genome. Towards this end it was shown that even highly tissue-specific promoters

delivered by rAdV display an altered transcriptional activity (Babiss *et al.,* 1986a; Hatfield and Hearing 1991; Imler *et al.,* 1996; Shi *et al.,* 1997). Additionally, in the relatively rare case of integration of the vector genome into the chromosomal host DNA (Harui *et al.,* 1999; Stephen *et al.,* 2008) a transcriptional active ITR may force or downregulate expression of nearby genes or even oncogenes. Although the left arm of Ad5 including the ITR and packaging/enhancer region were studied in the past, there is virtually no information about ITRs with respect to transcriptional activity from other than Ad5 human adenovirus serotypes. There are only studies based on Ad5 (Yamamoto *et al.,* 2003) and porcine adenovirus type 3 (Xing and Tikoo 2005; Xing and Tikoo 2006) indicating that promoter activity exists from the ITR itself.

Herein we investigated for the first time in a plasmid-based system whether ITRs from human adenovirus subgroups A, B1, B2, C, D, E and F show transcriptional activity in various cell lines.

3.1 Materials and Methods

3.1.1   Cell lines and viral lysates

HEK293, HeLa, Huh7 and ARPE-19 cells were obtained from the American Tissue Culture Collection (ATCC), A549 cells were a kind gift from Carsten Rudolph (Ludwig-Maximilians-University Munich, Germany) and HCT116 cells were obtained from Mark A. Kay (Stanford University, USA). All cell lines were cultivated at 37°C under a 5% CO_2 atmosphere. For HEK293, HeLa and A549 cells DMEM supplemented with 10% FBS and 1% Penicillin/Streptomycin (P/S) was used. The retinal cell line ARPE-19 was grown in a 1:1 mixture of F9: DMEM supplemented with 10% FBS and 1% P/S. The liver cell line Huh7 and the colon carcinoma cell line HCT116 were cultivated using DMEM supplemented with 1% non-essential amino acids, 10% FBS and 1% P/S.

Wild type Ad5 was obtained from ATCC. Genomic DNA of all other adenovirus serotypes Ad4, Ad7, Ad11, Ad12, Ad17 and Ad41 were a kind gift of the clinical virology of the Max von Pettenkofer-Institute (Ludwig-Maximilians-University Munich, Germany).

3.1.2   Plasmid constructs

All plasmid constructs were based on the pGL3-Control vector supplied by Promega. The control plasmid pGL3ΔSV40 was constructed by restriction enzyme digest of the plasmid pGL3-Control with *Hind*III and *Xho*I followed by religation. The forward orientated ITRs were constructed by direct cloning of the amplified PCR product digested with the restriction

enzymes *Kpn*I and *Sac*I (grey nucleotides in **Table 3.1**) into the *Kpn*I and *Sac*I sites of the plasmid pGL3ΔSV40, resulting into the plasmid pGL3ΔITR forward. For reverse orientation of the ITRs the *Kpn*I and the *Sac*I sites were exchanged and obtained PCR products were directly cloned blunt-ended into the blunted *Kpn*I and *Sac*I sites of the plasmid pGL3ΔSV40 resulting in pGL3ΔITR reverse. For the constructs containing the PGK promoter the plasmid pPGK (kindly provided by Martin Hausl, Max von Pettenkofer-Institute, Ludwig-Maximilians-University Munich, Germany was used to amplify the PGK promoter by PCR. The purified PCR product was then digested with *Mlu*I and *Nhe*I (grey nucleotides in Table 3.1) and directly cloned into the *Mlu*I and *Nhe*I site of pGL3-Control. For primer sequences please refer to **Table 3.1**.

Table 3.1 Oligonucleotides used in the present study.

Subgroup (Serotype)	Accession Number		Sequence	primer binding site
A (12)	# NC_001460	5´forw	GCATTC-GGTACC-CCTATCTAATAATATACCTTATAC	1bp-24bp
		3´rev	CCTAAG-GAGCTC-AACGTCACATCCGGCGCG	148bp-164bp
B1 (7)	# AC_000018	5´forw	GCATTC-GGTACC-CTCTCTATTTAATATACCTTATAGA	1bp-25bp
		3´rev	CCTAAG-GAGCTC-AGTCACGTCATTTTCCCACG	121bp-140bp
B2 (11)	# FJ_643676	5´forw	GCATTC-GGTACC- CATCATCAATAATATACCTTATAGA	1bp-24bp
		3´rev	CCTAAG-GAGCTC-AACGTCATTTTCCCACGGCC	118bp-137bp
C (5)	# AC_000008	5´forw	CCTAAG-GAGCTC-CATCATCAATAATATACCTTATTT	1bp-25bp
		3´rev	GCATTC-GGTACC-ACTACACGTCACCCGC	91bp-107bp
D (17)	# NC_002067	5´forw	GCATTC-GGTACC-CATCATCAATAATATACCCCAC	1bp-22bp
		3´rev	CCTAAG-GAGCTC-TCATCAGCCCCGCGACTT	163bp-180bp
E (4)	# NC_003266	5´forw	GCATTC-GGTACC-CATCATCAATAATATACCTTATTT	1bp-24bp
		3´rev	CCTAAG-GAGCTC-TGCCCCGCCCCTAACGAA	101bp-118bp
F (41)	# DQ_315364	5´forw	GCATTC-GGTACC-CATCATCAATAATATACCTTAAAAC	1bp-25bp
		3´rev	CCTAAG-GAGCTC-ACCGGATCCGTCACTTCCG	153bp-171bp
pPGK		5´forw	CCTAAG- ACGCGT- ATCTACCGGGTAGGGGAGG	
		3´rev	GCATTC- GCTAGC- GGTCGAAAGGCCCGGAGAT	
Luc rev		3´rev	TCCATCTTCCAGCGGATA	312bp
PCR Primer 1		5' forw	TCATACACATACGATTTAGGTGACACTATAGAGCGGCCGCCTGCAGGAAA	

3.1.3 Dual luciferase reporter assay to measure transcriptional activity of the ITRs

Potential transcriptional activity of the respective ITRs was determined by measuring firefly luciferase activity utilizing the dual luciferase reporter assay (Promega). Our experimental approach was based on seeding the respective cell lines in a 24-well dish and subsequently transfecting 250 ng of the different constructs displayed in **Figure 3.1A**. Two days post-transfection cells were harvested and prepared for luciferase assay. For normalization, 100 ng of the pRL-TK (Promega) plasmid were co-transfected and the ratio of firefly activity to

renilla luciferase activity was measured to determine the relative light units. A p-value < 0.05 demonstrated a significantly enhanced or reduced activity of the ITR in comparison to the negative control pGL3ΔSV40 lacking the SV40 promoter. An insignificant result means that the ITR has no influence on the transcription of the luciferase.

3.1.4   5´rapid amplification of cDNA ends

HEK293 cells were transfected with ITR constructs for Ad5 and Ad7 utilizing the same conditions as for luciferase assays shown in **Figure 3.2**. RNA was isolated based on Trizol reagent (Invitrogen) and samples were analyzed using a RACE Kit from Biozym according to the manufacturer's instructions (ExactSTART^{TM} Eukaryotic mRNA 5'-& 3'-RACE Kit, Cat. No. ES80910). In brief, total RNA was isolated, treated with Apex^{TM} Heat-Labile Alkaline Phosphatase, followed by Tobacco Acid Pyrophosphatase treatment to remove 5'CAPs. After T4 RNA ligase mediated tagging of the 5'end with the 5' RACE Acceptor Oligo we performed cDNA synthesis and amplified products with PCR primer 1 and PCR primer 2 provided with the Kit. This step was followed by a second PCR reaction utilizing the gene specific primer for luciferase (luc rev) in combination with PCR Primer 1 which binds to the 5'-RACE Acceptor Oligo. Sequences of these primers are shown in **Table 3.1.** PCR products were subcloned into the pCR-BluntII-Topo vector (Invitrogen) and sequenced. For Ad5 and Ad7 ITRs we analyzed 4 clones each.

3.2   Results

3.2.1   Constructs to analyze transcriptional activity of ITRs from different adenovirus serotypes

To cover the complete spectrum of all subgroups we have chosen one serotype from each group [Ad12(A), Ad7(B1), Ad11(B2), Ad5(C), Ad17(D), Ad4(E), Ad41(F)] and generated constructs, in which the luciferase expression is dependent on the transcriptional strength of the respective ITR. For amplification and cloning of the different ITRs, primers were designed to clone either the forward or the reverse orientation of the ITR. Respective primers and the accession number of the different adenovirus serotypes are provided in **Table 3.1**. All vector constructs tested in the present study were based on the pGL3-Control vector (Promega), in which the luciferase expression is under the control of the Simian virus 40 (SV40) promoter (**Figure 3.1A**). This vector served as a positive control for reporter gene expression. The negative control vector pGL3ΔSV40 (**Figure 3.1A**) was generated by deleting the SV40 promoter. In order to analyze all possible directions into which transcription can run, either into the transgene expression cassette or, in case of integration,

into the chromosomal DNA, the ITRs were cloned upstream of the reporter gene in forward and reverse orientation (**Table 3.1** and **section 3.1.2**).
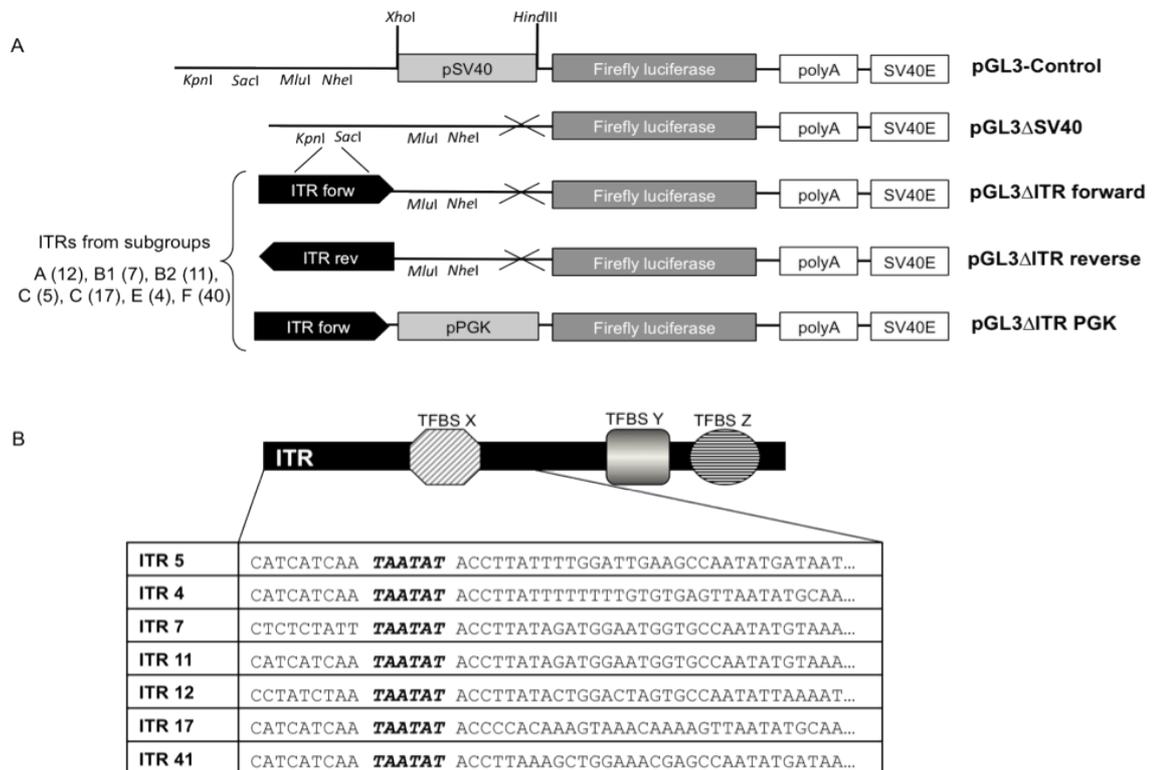
Figure 3.1: Vector constructs and TATA box predictions within the inverted terminal repeats (ITRs). (A) Final vector constructs for analysis of the transcriptional activity of adenoviral ITRs and the respective adenovirus subgroups. pSV40: promoter of the Simian virus 40; polyA: SV40 polyadenylation signal; pPGK: phosphoglycerate-kinase promoter; SV40E: Simian virus 40 enhancer. The respective restriction enzyme nucleases used for generation of the constructs are indicated. For cloning procedures please refer to the materials section. (B) Search for transcription factor binding sites in the ITRs utilizing a transcription element search system. As schematically shown as TFBS X, Y, and Z multiple transcription factor binding sites (TFBS) were identified. For all ITRs derived from different serotypes nucleotides 10 to 16 (TAATAT) could serve as a TATA box.

3.2.2 *In silico* analysis of transcriptional binding sites of ITRs

To search for potential transcription factor binding sites in the ITRs, which were used in our study, we used the "Transcription Element Search System" (TESS), a free online tool provided by the University of Pennsylvania (webpage: http://www.cbil.upenn.edu/cgi-bin/tess/tess?RQ=WELCOME (Schug 2008)). In all ITRs derived from different serotypes nucleotides 10 to 16 (TAATAT) could serve as a TATA box (**Figure 3.1B**) and multiple transcription factor binding sites (e.g. Oct-1, NFI, TBP, SP1, ATF) were predicted.

3.2.3   Transcriptional activity of ITRs derived from different adenoviral serotypes

In order to analyze if the transcriptional potential of the ITRs is cell-type dependent, different cell lines were used. First, we tested cells, which are permissive to adenovirus infection such as carcinoma and A549 cells originated from lung epithelia cells. Because of the natural liver tropism of Ad5, we also studied transcriptional activity in the hepatoma-derived human liver cell line Huh7. Adenovirus 41 displays a distinct tropism to the intestinal tract and therefore we analyzed transcription in the colon carcinoma cell line HCT116. Furthermore, the adult retinal pigment epithelia cell line ARPE-19 was studied because of the natural tropism of some adenoviral serotypes to the eye (Ad17 and Ad4).

Potential transcriptional activity of the respective ITRs based on the constructs displayed in **Figure 3.1A** was determined by measuring firefly luciferase activity utilizing a dual luciferase reporter assay. In the adenovirus permissive cell lines HEK293, HeLa and A549 we detected robust promoter activity of the ITRs from subgroup A, C and F if they appear in forward orientation (**Figure 3.2A, B, C**). Notably, expression levels were comparable or even higher compared to the strong SV40 promoter within the vector pGL3-Control. Most other forward orientated ITRs promote minor changes (ITRs 17) or background luciferase expression levels (ITRs 7 and 4). In contrast, in reverse orientation only serotypes 11 and 17 are transcriptional active in HEK293-, HeLa- and A549 cells, whereas all other ITRs seem to inhibit luciferase expression (ITR 4,5,7,12,41) emphasizing ITR 12 with even no detectable luciferase expression (**Figure 3.2A, B, C**). Similar results were obtained in the liver specific Huh7 cells and the colon carcinoma cell line HCT116 (**Figure 3.2D, E**). In forward orientation ITRs from adenovirus serotypes 12, 5 and 41 show strong luciferase expression. In reverse orientation ITRs 11 and 17 display slight promoter activity and the other ITRs negatively interfere with transcription.

We also investigated transcriptional activity in the retinal pigment epithelial cell line ARPE-19. Herein, the ITRs from subgroups A, C and F show the highest activity in comparison to the negative control lacking the SV40 promoter (**Figure 3.2F**). In concordance with results obtained in all other cell lines the reverse orientated ITRs from Ad serotypes 11 and 17 display robust activity and ITRs 5, 7, 12, 41 inhibiting function (**Figure 3.2F**). However, in contrast to results obtained in all other cells lines we measured slightly enhanced luciferase expression levels in ARPE-19 cells for the ITR from subgroup E (ITR 4) when cloned in reverse orientation (**Figure 3.2F**). The reason for this finding remains to be elucidated.
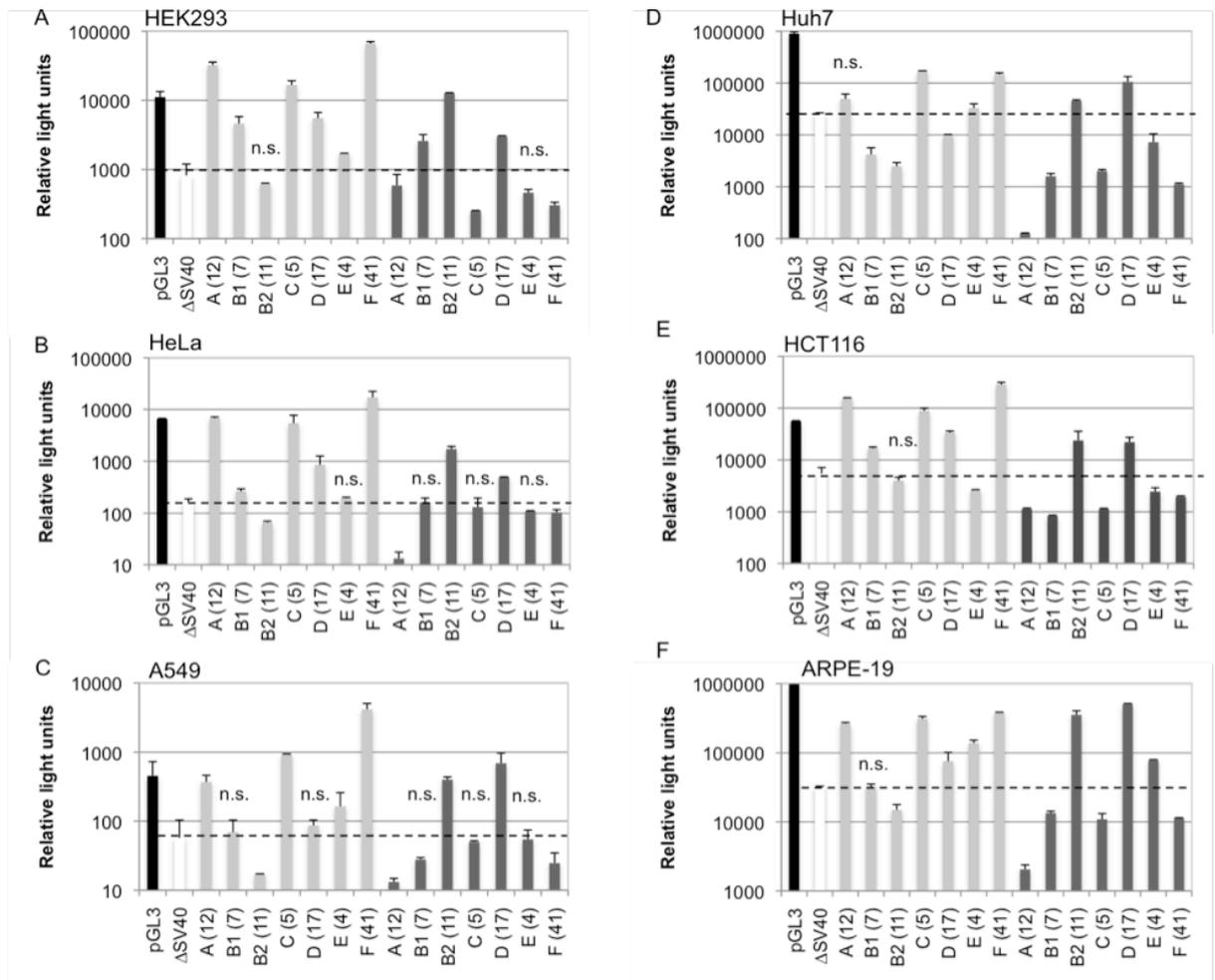
Figure 3.2: Analysis of the transcriptional activities of the ITRs from each adenoviral subgroup in various cell lines. Shown in light grey are pGL3-based constructs with the adenoviral ITRs in forward orientation, in dark grey constructs in reverse orientation. The nomenclature of the different groups mentions the subgroup as a capital and the respective serotype in parenthesis. Relative light units were calculated by determining the ratio of firefly luciferase activity to renilla luciferase activity. Relative light units in HEK293 cells (A), HeLa cells (B), A549 cells (C), Huh7 cells (D), Hep1a cells (E), and ARPE-19 cells (F) are displayed. The dashed line indicates the base line of luciferase expression after transfection of the promoter-less vector pGL3ΔSV40. pGL3: pGL3-Control; ΔSV40: pGL3 ΔSV40 lacking the SV40 promoter; n.s.: not significant, p-value >0.05.

3.2.4 Influence of ITR sequences upstream of the PGK promoter

To address the question whether ITRs from various adenovirus serotypes can influence a nearby promoter we analyzed the influence of the ITRs on the transcriptional activity of the ubiquitously expressed PGK promoter (pPGK). Towards this end the PGK promoter was cloned downstream of the forward orientated ITRs from each adenovirus subgroup (**Figure 3.1A,** lower panel). The experimental set up was identical to experiments shown in **Figure 3.2**. Unexpectedly, we detected that almost each ITR upstream of the pPGK significantly reduced luciferase expression to background level or even less (**Figure 3.3**). With the exception of results obtained in A549 cells, only the ITR 7 from subgroup B1 seems to have no or only minor influence on the activity of pPGK in the cell lines HEK293, HeLa, Huh7 and HCT116. This is in concert to results obtained for the ITR 7 without the pPGK. In all tested cell lines serotype 7 shows either no or only a minor influences on the
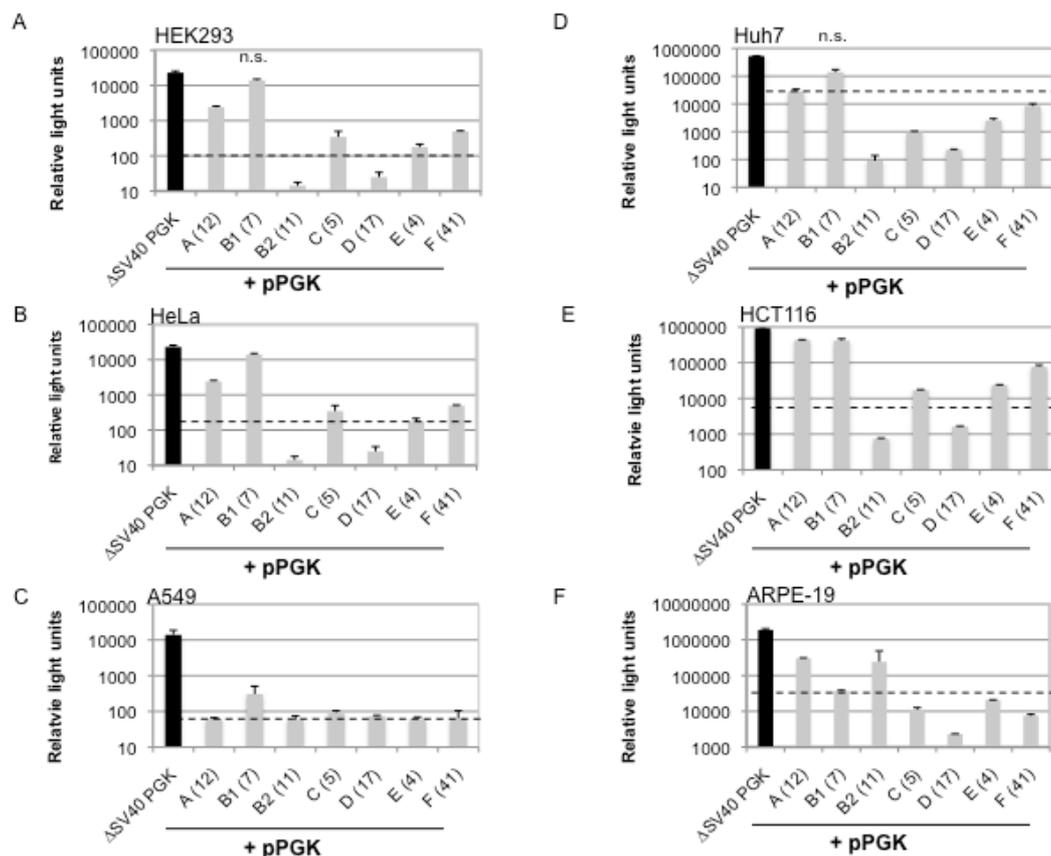
Figure 3.3: Influence of adenoviral ITRs on transcriptional activity of the PGK promoter. The nomenclature of the groups contains the ITR subgroup as capital and the respective serotype used in parenthesis. Additionally, each construct contains the phosphoglycerate kinase promoter (pPGK; see also **Fig.1**). Relative light units were calculated by determining the ratio of firefly luciferase activity to renilla luciferase activity. The dashed line indicates the base line of luciferase expression after transfection of the promoter-less vector pGL3ΔSV40. Relative light units in HEK293 cells (A), HeLa cells (B), A549 cells (C), Huh7 cells (D), Hep1a cells (E), and ARPE-19 cells (F) are shown. ΔSV40 PGK: pGL3 ΔSV40 with PGK promoter; n.s.: not significant, p-value >0.05.

transcriptional level in forward as well as in reverse orientation (**Figure 3.2**). This observation remains to be elucidated, but nevertheless this ITR seems to be a good candidate for the optimized design of rAdVs. However, it also remains to be elucidated whether this phenomenon is a special feature of the PGK promoter and whether another promoter may be differently influenced in its transcriptional activity by the ITRs.

3.3 Discussion

In summary, we show that solely the ITRs from several human adenovirus serotypes enhance or inhibit transcriptional activity in a tissue independent manner and that this activity can down regulate nearby promoters.

Our results may have important implications for the design of other than subgroup C based rAdVs. There is evidence that the position of the inserted transgene expression cassette within the rAdV genome has an impact on the expression level of the transgene. One may speculate that convergent promoter activity from an introduced, internal promoter and the ITR may occur. This would then lead to formation of double-stranded RNAs and may induce gene silencing due to RNA interference, influencing transgene expression (Hammond *et al.,* 2000; Hutvagner 2005) Furthermore, it was shown that the enhancer near the 5´end could lead to a leaky expression from the tissue-specific promoter even in non-target cells (Babiss *et al.,* 1986a; Shi *et al.,* 1997) and it has been reported that sequences around the ITR can reduce promoter activity up to 50-fold (Shi *et al.,* 1997). As these sequences can influence transgenes over large distances it is recommended to insert sequences preferentially at the 3´end, comparable to our present pAdFTC plasmid we use in our laboratory (Ehrhardt *et al.,* 2003). In addition, ITRs showing low or no inward transcriptional activity into the adenoviral genome may be advantageous for optimized vector design. To avoid interference between adjacent genes without termination signal (Proudfoot 1986) when inserting a transgene expression cassette into the rAdV genome, ITR sequences derived from an adenovirus serotype, which has no or less effect on transcription initiation could be beneficial especially when using tissue-specific or controllable promoters.

Moreover, the outward oriented transcriptional activity derived from ITRs could have a special importance for adenoviruses that show integration activity into the host genome of infected cells, such as Ad12 into hamster cells (Sutter *et al.,* 1978; Sawada *et al.,* 1979). In our experiments ITR 12 from subgroup A results into strongly inhibited luciferase expression when cloned in reverse orientation suggesting that this activity may result into inhibition of nearby genes. On the other hand, as we refer to a plasmid- based assay, ITR 12 may have insulator functions.

Notably, we used a plasmid based approach to investigate ITR transcriptional activity, in a viral background it could be, that transcriptional activity is further enhanced, due to viral proteins bound to the ends of the viral genome. The viral terminal protein for instance, that is attached to the ends of the viral DNA may serve as chaperon to guide transcription factors to the ITRs as shown by Yamamoto *et al.* (Yamamoto *et al.,* 2003). Therefore it would be of great interest to further investigate whether ITRs from other than subgroup C Ads in a viral context show the same expression pattern as in our plasmid based experiment. As the serotypes from subgroup B (7) and A (12) display the most advantageous transcriptional profile they might be possible alternatives to the standard Ad5 serotype in future studies.

4   The RNA interference pathway is responsible for silencing of transgene expression after Sleeping Beauty mediated transposition

Over the recent years various improved recombinases for somatic integration into the host genome were developed. Predominant integration systems currently being explored in mammalian cells are the transposable elements represented by the Sleeping Beauty (SB) transposase, the Frog Prince (FP) transposon, the piggyBac transposable element and the bacteriophage-derived integrase PhiC31 for targeted integration (Kuhstoss and Rao 1991; Ivics *et al.,* 1997; Groth *et al.,* 2000; Miskey *et al.,* 2003). All systems are widely being studied in multiple applications including gene therapeutic applications and functional genomics (Yant *et al.,* 2002; Ehrhardt *et al.,* 2005; Kaufman *et al.,* 2005; Patel and Yang 2010).

The SB transposase system represents one of the most prominent non-viral gene therapy vectors because it can efficiently and stably integrate therapeutic DNA into mammalian genomes. SB transposase is a synthetic transposable element derived from fish (Ivics *et al.,* 1997). For increased integration activities mutational analysis has been performed and hyperactive variants were developed (Ivics *et al.,* 2007; Mates *et al.,* 2009). The integration reaction is based on a cut-and-paste mechanism, which leads to genomic integration of the gene of interest, flanked by the SB inverted repeats (IRs) into a TA-dinucleotide. Multiple SB-based animal studies demonstrated efficacy in mice including stable correction of genetic disorders in clinically relevant animal models (Yant *et al.,* 2000; Yant *et al.,* 2002; Ehrhardt *et al.,* 2005).

There is accumulating evidence in invertebrates that DNA transposition is regulated by the endogenous RNA interference (RNAi) pathway (Vastenhouw *et al.,* 2003; Robert *et al.,* 2004; Vastenhouw and Plasterk 2004), a mechanism responsible for post-transcriptional gene silencing (Fire *et al.,* 1998; Elbashir *et al.,* 2001a; Elbashir *et al.,* 2001b). In these systems endogenously produced 21- to 25-nucleotide long non-coding micro RNAs (miRNAs) play a major role in downregulation of the transposase leading to inhibition of transposition in the respective cell (Hammond *et al.,* 2000; Vastenhouw and Plasterk 2004)..

However, only limited information is available regarding the potential influence of miRNA pathway on DNA transposons in mammalian cells. A recent study showed that the LINE-1 retrotransposition is suppressed by endogenous small interfering RNAs (Yang and Kazazian 2006). Hereby, bidirectional dsRNA transcripts from the transposon represent targets for the

RNAi machinery indicating that the RNAi pathway controls transposition in mammalian cells, too. Herein, we hypothesized that the SB transposase machinery may be regulated by the endogenous miRNA pathway as well, because recent data demonstrated that IRs display inward transcriptional activities in eukaryotic cells (Moldt *et al.,* 2007; Walisko *et al.,* 2008). This convergent transcription may lead to formation of double-stranded RNA templates for the endogenous RNAi machinery, thus silencing transgene expression.

Our experimental approach was based on generation and detailed characterization of RNAi knockdown cell lines based on the RNAi inhibitor protein P19 derived from the tomato bushy stunt virus (Voinnet *et al.,* 1999; Scholthof 2006), which inhibits 21 nt long small interfering RNAs (siRNAs) (Silhavy *et al.,* 2002; Dunoyer *et al.,* 2004a; Omarov *et al.,* 2006). After showing functionality of P19 in our RNAi knockdown cell lines, transposition events were quantified. We found that SB mediated transposition events were enhanced up to 4.2-fold in our RNAi knockdown cells indicating that transposition is regulated by the RNAi pathway in mammalian cells.

4.1 Materials and Methods

4.1.1   Plasmid construction

The plasmids used for the stable transfection of a P19 expression cassette were constructed with the gateway technology (Invitrogen). First the *p19* expression cassette was PCR amplified (without stop codon) with the primer Gp19forwK (5´AAAAAGCAGGCTCCGCCATGGAACGAGCTATACAAGGAA-3´) and the reverse primer Gp19rev (5´AGAAAGCTGGGTCGCTTTCTTTTTCGAAGGTTTGAG 3´) harboring a Kozak sequence for eukaryotic expression. To create homologous regions for recombination, attB specific primers were used for the nested PCR (One-for-all-forward: 5'-GGGGACAAGTTTGTACAAAAAAGCAGGCT-3' and One-for-all-reverse: 5'-GGGGACCACTTTGTACAAGAAAGCTGGGTC-3'). Using BP clonase the PCR fragment was introduced into the attP sites of pDonr207 and in the second LR clonase reaction p19 was cloned into the destination vector pCR3.1 N-His. All Gateway compatible vectors were kindly provided by A. Baiker (Uetz *et al.,* 2006; Vizoso Pinto *et al.,* 2010). These cloning steps resulted into the plasmid Kp19, which was used to generate a stable *p19* expressing cell line under G418 selection pressure (500 µg/ml) using *Superfect* transfection reagent (Qiagen). The *p19* encoding retroviral vector p19-MIE, for generation of the stable cell line G4 by retroviral transduction, was produced by triple transfection of plasmids providing all necessary factors for retrovirus production, the gag-pol proteins as well as the VSV glycoprotein (all plasmids were kindly provided by Charles Lecellier (Institut de Génétique

Humaine, Montpellier, France) and Olivier Voinnet (Institut de Biologie Moléculaire des Plantes, Strasbourg, France)).

The plasmids for the quantitative Real-Time PCR were constructed as follows. HoxB8 and GAPDH were amplified from human genomic DNA from HEK293 cells with the following primer, HoxB8forw_PD (5´-TGGAGCTGGAGAAGGAGTTC-3´), HoxB8rev_PD (5´-CTCCTCCTGCTCGCATTT-3´), hGAPDHforw (5´-TGCCTCCTGCACCACCAACT-3´) and hGAPDHrev (5´-CGCCTGCTTCACCACCTTC-3´) and either cloned into the *Eco*RI site of the the pBS P/P ΔNot vector (Yant *et al.,* 2002; Ehrhardt *et al.,* 2007) or into the commercial available pCR-Blunt II-TOPO (Invitrogen) vector, respectively, following the manufacturer instructions. Further plasmids used for luciferase assays in **Figure 4.1** were a kind gift from Olivier Voinnet and Charles Lecellier.

The plasmids pCMV-SB, pCMV-mSB, and pTnori (Yant *et al.* 2000) the plasmids pCI-Int, pCI-mInt and P7 were described elsewhere (Thorpe and Smith 1998; Ehrhardt *et al.,* 2005). The plasmids for Frog Prince transposition, pFV-FP, pFP-4a, pFP-neo, pFP-MCS and pT/neo-HS4 were kindly provided by Csaba Miskey and Zoltan Ivics (Max-Delbrück Center, Berlin, Germany). For construction of the plasmid pTMCS-IP, pIRESpuro2 (Clontech) was digested with *Xho*I, *Nru*I and *Nhe*I and the resulting 2678 bp fragment containing the puromycin resistance cassette was introduced into the *Bgl*II restriction site of pT-MCS (Yant *et al.,* 2000) by blunt end cloning. Moreover, the same 2678 bp fragment was inserted into the *Eco*RI site of pFP-MCS resulting into the plasmid pFP-IP. Finally the attB site was isolated from the P7 plasmid by *Eco*RI restriction enzyme digest and was inserted into the *Bgl*II site of pIRESpuro2. This resulted into the plasmid pIP-attB. The stuffer plasmid pBS P/PΔNot was described elsewhere (Yant *et al.,* 2002; Ehrhardt *et al.,* 2007). Transfection efficiencies in RNAi knockdown cell lines were determined using the plasmid pRL-TK expressing renilla luciferase (Promega).

4.1.2 Testing functionality of P19 in mammalian cells by luciferase assays

HEK293 cells were seeded in 24-well plates (DMEM supplemented with 10% FBS and 1% penecillin/streptomycin) and 24 hrs later (confluency of 60-70%) the *p19* expression plasmid or a plasmid expressing a non-functional version of *p19* (*p19m*) together with the pGL3-SV40 (Promega) vector or the pGL3-Control plasmid alone, harboring the luciferase expression cassette were transfected using lipofectamin 2000 (Invitrogen). The next day the GL3 siRNA (5´-CUUACGCUGAGUACUUCGATT-3´,) or an unspecific siRNA (5´-GAAGUUGGAUCUCUCAGAATT-3´) were transfected using lipofectamin 2000 (Elbashir *et*

al., 2001a). Twenty-four hrs after the latter step, cells were harvested and dual luciferase reporter assays were performed (Promega).

4.1.3 Generation of cell lines stably expressing P19

HEK293 cells were cultured in DMEM supplemented with 10% FBS and 1% penecillin/streptomycin. Stable transfection of HEK293 cells with plasmid Kp19 at 70% confluency was performed using Superfect (Qiagen) according to the manufacturer instructions. Two days post transfection cells were seeded in 10 cm dishes at two concentrations ($1x10^5$ and $1x10^4$ cells/dish) and 500 µg/ml medium G418 was added. After 14 days of selection, single cell clones were picked and amplified under G418 selection pressure.

For the production of the retrovirus harboring the *p19* cDNA, the plasmids p19-MIE, the gag-pol expressing plasmid and the VSV-glycoprotein expressing plasmid were triple transfected into HEK293T cells using calcium phosphate transfection following the protocol from Promega (ProFection @ mammalian cells, Promega). Two days post transfection cells were harvested and filtered through a 0,45 µm filter (Millipore) to remove the remaining cellular material. The viral lysate was then supplemented with the same volume of Polybrene (Invitrogen), which facilitates cellular entry of the virus. Subsequently a 95% confluent 10 cm dish of 293T cells was transduced with the prepared retroviral lysate. Two days post infection, cells were sorted by fluorescent activated cell sorting (FACS) and single cell clones exhibiting GFP expression were sorted in a 96-well plate. These cell clones were amplified. To check cells for GFP expression, several amplified cell clones were tested by flow cytometry using FACS-DIVA. In brief, stable GFP expressing cells as well as untreated HEK293 cells were harvested, washed once with PBS and centrifuged 3 min at 500 g. The cell pellet was then resuspended in PBS containing 0.1% FBS and supplied to the flow cytometer. Analysis was performed using FACS Diva software and the percentage of GFP positive cells within one population was calculated.

4.1.4 Western Blot analysis to investigate P19 protein expression

For Western Blot analysis a 6 cm tissue culture dish of the cell lines stably expressing a His-tagged version of P19, HEK293 control cells and transfected HEK293 cells with Kp19 were collected, washed once with PBS, treated with 300 µl NP-40 lysis buffer (150 mM NaCl, 1% NP-40, 50 mM Tris (pH 8.0)) and incubated for 30 min on ice. Protein lysates were separated on a 12% SDS-polyacrylamid gel and transferred to a PVDF membrane

(Millipore). Detection of P19 was carried out by a peroxidase labeled anti-His antibody (Invitrogen) and ECL reaction (Amersham).

4.1.5 P19 specific reverse transcription PCR to analyse expression from retrovirus transduced cells

The RNA of 3.2×10^6 cells was isolated using the RNeasy kit (Qiagen) following the manufacturer instructions. After determining the RNA amount by measuring the optical density, 1 μg RNA was used for reverse transcription using polydT primer supplied in the *First strand DNA synthesis kit* (NEB). As a control, a reaction without the reverse transcriptase enzyme was performed to exclude non-integrated plasmids. The generated cDNA was then subjected to a PCR reaction with *p19* specific primers or for quantification of HoxB8 expression with HoxB8 specific primers (for primer sequences see plasmid construction section).

4.1.6 Quantitative Real-Time PCR for quantification of HoxB8 expression levels

A quantitative Real-Time PCR (qRT-PCR) was performed using 4 μl of cDNA, 0.5 μM primer specific for HoxB8 and human GAPDH (see plasmid construction section) and the *LightCycler FastStart* DNA Master^{PLUS} SYBR *Green* I (Roche). The PCR reaction was run in the Light cycler 2.0 (Roche). For semi-quantitative analysis, the vectors pBSHoxB8 and pTopo-GAPDH were diluted and several 10-fold dilutions were used to create a standard curve. The fold increase in HoxB8 amount was determined in a semi-quantitative manner. *: p-value< 0.05.

4.1.7 Colony forming assays for quantification of integration events

For each colony forming assay HEK293 cells and the RNAi knockdown cell lines B6 and G4 were seeded in 6-well plates. At 60% confluency cells were transfected with a total of 1 μg plasmid DNA and 10 μl transfection reagent (Fugene 6, Roche). Experiments were performed in triplicates. Two days post transfection cells were split and cells of each 6-well were diluted (1:30) into three 10 cm dishes. Selection with either 500 μg/ml G418 or 600 ng/ml puromycin was started 72 hours post transfection and maintained for 2 weeks. The generated colonies were stained with methylene blue and counted.

The analysis of SB mediated transposition was performed by co-transfecting 50 ng pCMV-SB or 50 ng pCMV-mSB, 650 ng pBS P/P Δ Not (stuffer DNA) and either 300 ng pTMCS-IP if B6 cells and puromycin selection were used or 300 ng pTnori if G4 cells and G418 selection were used.

Frog Prince mediated transposition events were measured by transfection of 100 ng pFV-FP or 100 ng pFV-4a, 275ng pBS P/P Δ Not and either 625 ng pFP-IP in B6 cells or 625 ng pFPneo2 in G4 cells.

Integration events of the PhiC31 integrase were analyzed using 168 ng pCMV-Int or 168 ng pCMV-mInt, 682 ng pBS P/P Δ Not and 150 ng pIP-attB for selection in B6 cells or 150 ng P7 for selection with G418 in the G4 cell line.

To calculate the transposition events, the ratio of colony forming units between groups that received the functional transposase or integrase and groups that received a non-functional protein was determined. The fold increase in transposition or integration events could be identified by directly comparing this ratio in HEK293 cells and the RNAi knockdown cell lines. Significance of the data could be demonstrated by the p-value.

Finally, the transfection efficiency was determined in the context of the colony forming assay procedure by transfection of 100 ng pRL-TK plasmid instead of 100 ng of the stuffer plasmid pBS P/P Δ Not. Two days post transfection one sixth of the cell suspension was used to perform luciferase assays using the dual luciferase reporter assay (Promega).

4.2 Results

4.2.1 Analysis of the functionality of P19 in mammalian cells

There is clear evidence that SB transposase derived IRs display convergent transcriptional activities in eukaryotic cells (Moldt *et al.,* 2007; Walisko *et al.,* 2008). This inward transcription may lead to formation of double-stranded RNA templates for the endogenous RNAi machinery. These findings motivated us to investigate whether SB transposase mediated somatic integration in mammalian cells is influenced by these miRNAs. To address this question our experimental approach was to generate RNAi knockdown mammalian cell lines, which can then be used for evaluation of transposase activities.

To establish RNAi knockdown cell lines we took advantage of the P19 protein, which is derived from the tomato bushy stunt virus (Voinnet *et al.,* 1999; Scholthof 2006). It binds and inhibits 21 nucleotide (nt) long, small interfering RNAs (siRNAs) and was shown to sufficiently suppress RNAi (Silhavy *et al.,* 2002; Dunoyer *et al.,* 2004b; Omarov *et al.,* 2006). To check whether P19 is functional in a cell line typically used to study transposition, we performed reporter assays in the human embryonic kidney cell line HEK293. In this assay the abrogated effect of an established small inhibitor RNA (siRNA) against a reporter directly correlates with P19 activity. We transfected a luciferase expressing plasmid together with a

P19 expressing plasmid (p19Topo or p19HA) or a mutated and inactive version of P19 (p19mHA) in HEK293 cells via lipofectamin 2000 (Invitrogen) following the manufacturer instruction. Twenty-four hours later we transfected either a previously published siRNA against firefly luciferase (GL3) or an irrelevant siRNA also by the use of lipofectamin 2000 and 48 hours after the first transfection round we performed luciferase assays (Dunoyer *et al.,* 2004a). All plasmid constructs used were shown in **Figure 4.1A.** We found that P19 could restore the downregulation of firefly luciferase expression to up to 85% (**Figure 4.1B,** bars 4 and 6), whereas the mutated form of P19 (p19mHA) could not (**Figure 4.1B**, bar 8). Furthermore our data revealed, that the HA-tagged P19 molecules were not as sufficient in blocking activity of siRNAs as an untagged version of P19 (**Figure 4.1B**; compare bars 6 (tagged) and 4 (untagged)). Nevertheless, P19 was effective in suppressing siRNA-mediated silencing in HEK293 cells
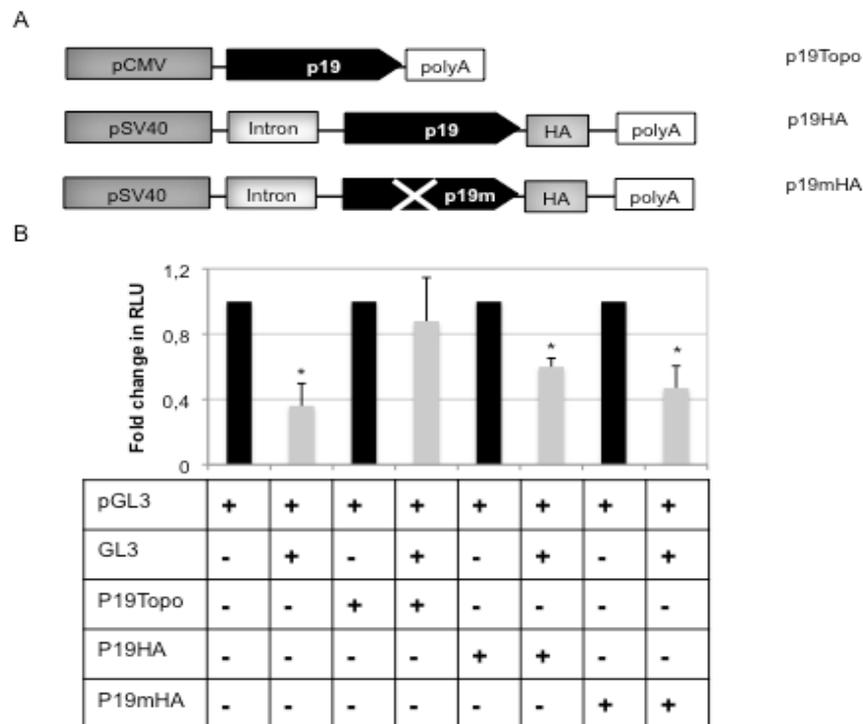
Figure 4.1: Functionality of P19 in mammalian HEK293 cells. (A) Plasmids used to analyze the functionality of P19 in mammalian HEK293 cells. pSV40: promoter of the simian virus-40; p19: p19 expression cassette; p19m: inactive p19 containing a Arg72 to Glycin exchange; polyA: polyadenylation signal of the simian virus-40, HA: hemaglutinin-tag. (B) Luficerase assay to check the functionality of p19. Each sample analyzed contains the pGL3-Control plasmid (Promega). In addition, for samples displayed in black bars either a non-specific stuffer plamsid, a functional p19 (p19Topo or p19HA) or the mutated version of p19 (p19mHA) was transfected together with a non-specific siRNA. In the samples referring to the grey bars, however, the GL3 specific siRNA was transfected together with the pGL3 alone or with a one of the plasmids displayed in **Figure 1A**. RLU: relative light units; GL3: luciferase specific siRNA; *:p-value > 0.5.

4.2.2 Generation and characterization of a stable p19 expressing cell line by retrovirus transduction and plasmid transfection

In order to analyze the effect of RNAi on SB transposition we established RNAi knockdown cell lines stably expressing P19. For this purpose we followed two different strategies. In a first approach we infected HEK293 cells with a retrovirus expressing P19 as an un-tagged version and with a green fluorescent protein (GFP) encoding cDNA (p19-MIE, **Figure 4.2A**). Using an un-tagged version of P19 could be advantageous because the tagged version of the P19 protein may be less biologically active compared to an un-tagged version (see also **Figure 4.1B**). Upon retrovirus transduction, single cell clones expressing GFP were isolated by fluorescence-activated cell sorting and individual cell clones expressing GFP were amplified without selection. By this method we could establish 6 cell clones (G3, G4, G5, G6 G14 and G16) of which 4 clones (G3, G4, G5, G16) expressed GFP as analyzed by flow cytometry (**Figure 4.2B** and **C**). Clones G4 and G16 showed highest amount of GFP expression and RT-PCR analysis of cDNA generated from the GFP positiv cell lines could demonstrate expression of the untagged *p19* mRNA (**Figure 4.2B** and **C)**.

The second approach was based on stably transfecting the *p19* and *neomycin* resistance gene encoding plasmid Kp19 into HEK293 cells (**Figure 4.2A,** upper panel). After plasmid transfection and subsequent G418 selection with 500 μg/ml, 15 single, neomycine resistant HEK293-based cell clones were isolated and amplified. To analyze *p19* expression, we performed Western Blot analysis using a peroxidase labeled anti-His antibody and found that cell clone B6 showed highest expression levels of both monomeric and dimeric P19 (**Figure 4.2E**) in comparison to two other cell clones (A1 and A2).

To investigate whether all generated cell lines express a functional P19 protein, we chose the HoxB8 gene as a marker. The HoxB8 gene encodes a homeobox protein, a transcription factor that is only active during development. In differentiated cells HoxB8 is permanently suppressed by the endogenous miRNA miR-196a (Kawasaki and Taira 2004b; personal communication, Charles H. Lecellier, Institut de Génétique Humaine, Montpellier, France).

Thus, if P19 is functional in our generated cell lines, HoxB8 expression should be upregulated, which can be measured by quantitative Real-Time PCR. By this approach we could show a 3.5 to 8-fold upregulation (p-value <0.05) of HoxB8 in the stable cell clones G4 and B6, respectively, clearly indicating that P19 is a sufficient inhibitor of the RNAi mechanism in this established cell lines (**Figure 4.2F**). However, all other clones showed only slight or no increase in HoxB8 amount (**Figure 4.2F**). Therefore, the following studies were performed using the RNAi knockdown cell lines B6 and G4.
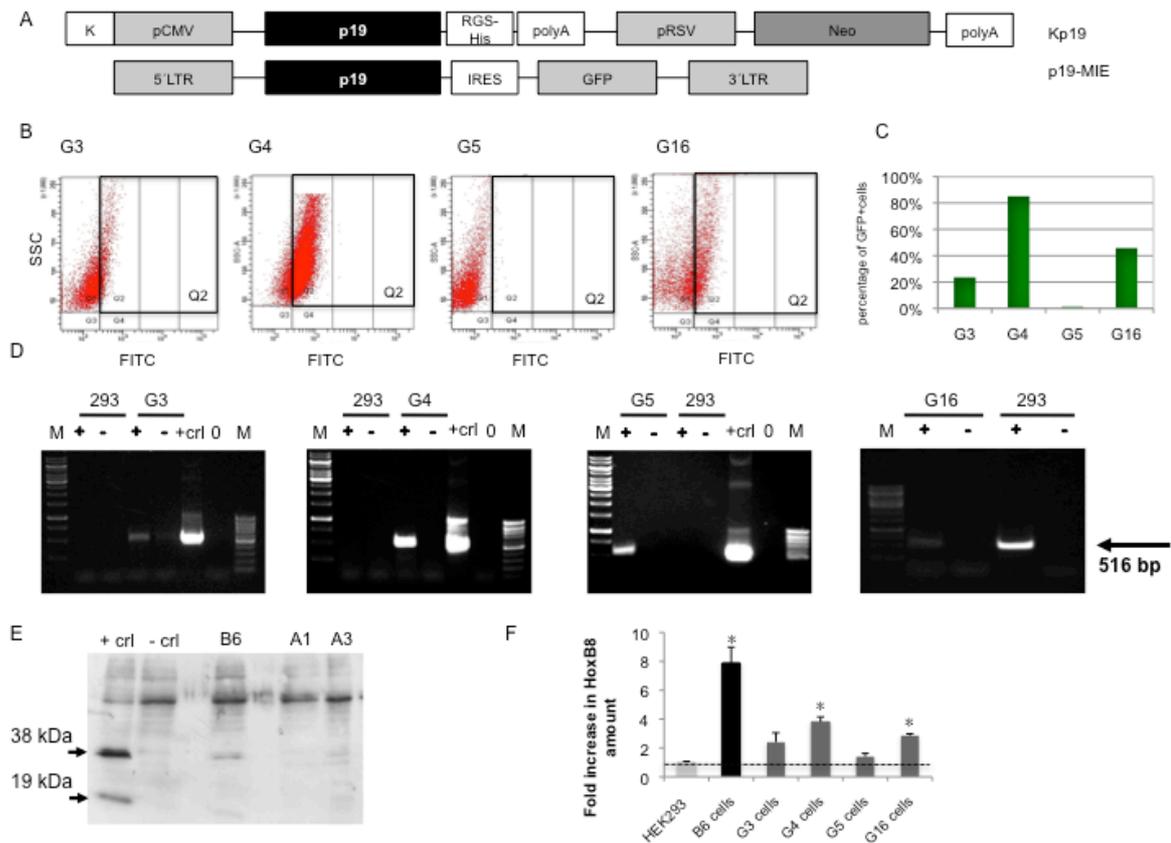
Figure 4.2: Generation and characterization of the RNAi knockdown cell lines. (A) DNA sequences used to generate stable *p19* expressing cell lines. Kp19 was used for stable plasmid transfection of HEK293 cells. The plasmid p19-MIE was used to produce a P19 expressing recombinant retrovirus for stable infection of HEK293 cells. K: Kozak sequence; pCMV: promoter of the cytomegalo virus; p19: *p19* expression cassette; pRSV: promoter of the rous sarcoma virus; RGS-His: 6 histidin residues connected to the P19 protein by an arginin-glycin-serin motive; Neo: neomycin resistance cassette that mediates G418 resistance; poly A: polyadenylation signal derived from the simian virus; GFP: green fluorescent protein expression cassette; LTR: long terminal repeats; IRES: internal ribosome entry site. (B) Flow cytometric analysis of cell clones generated by retroviral transduction. Single cell clones from cell sorting were amplified and analysed by flow cytometry. Cells appearing in quadrant Q2 refer to GFP+ cells. X-axis: Fluoresceinisothiocyanat (FITC) amount; Y-Axis: SSC : side scatter, to measure cell viability. (C) Quantitative analysis of GFP positive clones generated by cell sorting shown in **Figure 4.2B**. (D) Expression of *p19* mRNA in the stable cell lines G3, G4, G5 and G16. The generated cDNA was used for PCR amplification with *p19* specific primers. As positive control the *p19* expression cassette from the plasmid Kp19 (+ crl) was amplified. +: sample with RT; -: sample without RT; 0: untreated HEK293 cells; M: marker. (E) Detection of P19 expression by Western Blot analysis in cell lines, which expressed the His-tagged version of the P19 protein. Monomeric and dimeric P19 molecules were detected using a peroxidase labeled anti-His antibody. As a positive control HEK293 cells were transiently transfected with *p19* expressing plasmids (two left lanes). (F) Functionality of P19. RNA was isolated from HEK293, B6, G3, G4, G5, G16 cells and reverse transcribed. The cDNA was used for quantification of the HoxB8 mRNA amount by qRT-PCR. Normalization was performed by GAPDH measurement with GAPDH specific primers. The fold increase of the HoxB8 amount in the RNAi knockdown cell lines was determined in a semi-quantitative manner. *: p-value < 0.05.

4.2.3 Influence of the RNA interference pathway on different integration machineries

As a next step we analyzed the influence of the RNAi pathway on transposase and integrase mediated transposition events in our RNAi knockdown cell lines. As previously described (Ehrhardt, *et al.* 2005) we performed colony forming assays, which allow for selection and quantification of transposition events in eukaryotic cells. Importantly, in this particular experimental setup transgene expression most likely correlates with the transposition
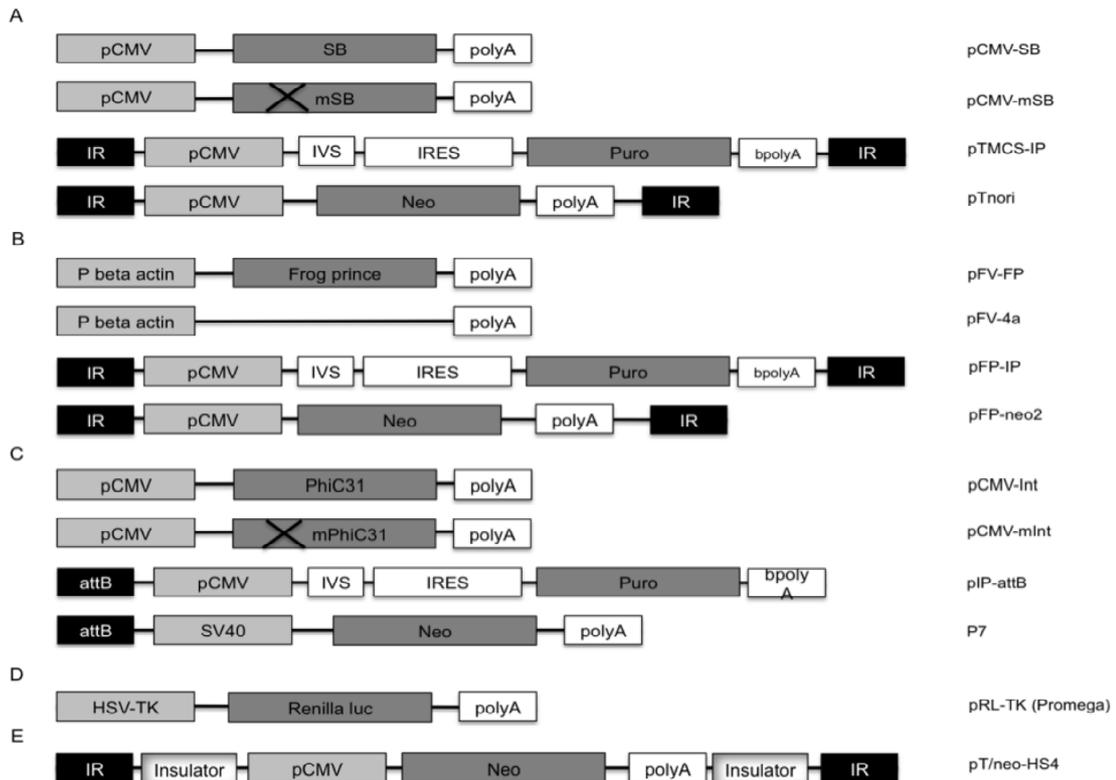
Figure 4.3: DNA constructs used in this study. Shown are all DNA constructs, which were used to test transfection efficiencies and to analyze the influence of the RNAi pathway on transposition and integration in HEK293 cells and the RNAi knockdown cell lines B6 and G4. Colony forming assays performed in G4 cells were performed with the respective substrate plasmids encoding neomycin (pTnori, pFP-neo2, and P7) and colony forming assays in B6 cells were performed using the respective substrate plasmids encoding puromycin (pTMCS-IP, pFP-IP, and pIP-attB). CMV: major immediate early promoter/enhancer; IRES: internal ribosome entry side of the encephalomyocarditis virus (ECMV); IVS: synthetic intron; Puro: puromycin-N-acetyl-transferase gene mediates puromycin resistance; bpolyA: bovine growth hormone A polyA signal; polyA: SV40 polyA signal; Neo: neomycin resistance cassette mediating G418 resistance; SV40: promoter of the simian virus. (A) Plasmids used to analyze Sleeping Beauty (SB) mediated transposition in HEK293 cells and the RNAi knockdown cell lines B6 and G4. SB: Sleeping Beauty transposase; mSB: mutated version of the Sleeping Beauty transposase; IR: Inverted repeats recognized by SB and mSB. (B) Vector constructs for Frog Prince mediated transposition. P beta actin: beta actin promoter; FP: Frog Prince transposase; IR: Inverted repeats and recognition sites for Frog Prince transposase. (C) Plasmids used for PhiC31 integrase mediated integration. PhiC31: PhiC31 integrase; mPhiC31: mutated version of the PhiC31 integrase; attB: attachment site B recognized by the PhiC31 integrase. (D) Plasmids for determination of the transfection efficiencies in HEK293 cells and the RNAi knockdown cell lines. HSV-TK: Herpes simplex virus thymidin kinase promoter; Renilla luc: renilla luciferase expression cassette. (E): Plasmid pTneo/HS4 containing insulator sequence in between the IR and the neomycin resistance cassette, used in combination with the SB machinery.

efficacy. Thus, increased integration events are speculated to be due to improved transgene expression in RNAi knockdown cells. All DNA constructs utilized in this study are schematically displayed in **Figure 4.3**.

Since these colony forming assays are based on plasmid transfection into eukaryotic cells, we initially analyzed plasmid transfection efficiencies in our RNAi knockdown cell lines and the parental cell line because the knockdown of the RNAi pathway potentially may have influenced the uptake of plasmid DNA. Therefore, we co-transfected a reporter plasmid expressing renilla luciferase (**Figure 4.3D**) to determine transfection efficiencies for each experiment performed in HEK293 cells, G4 cells and B6 cells,. We found that transfection efficiencies varied between the RNAi deficient cell lines B6/G4 and the parental cell line HEK293, but the ratios of functional protein (SB, Int, FP) compared to the mutated version
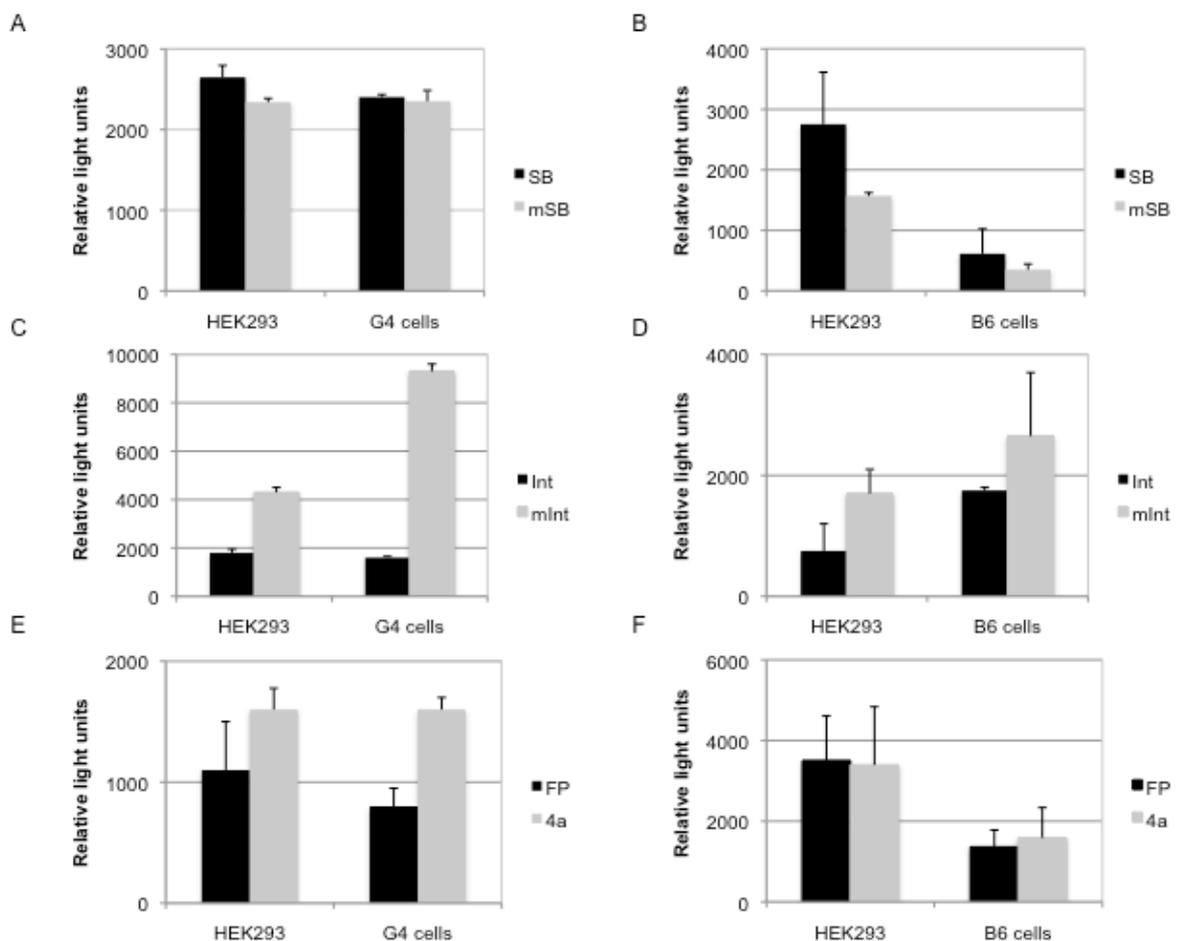
Figure 4.4: Luciferase assay to measure transfection efficiencies. Transfection efficiencies were measured as relative light units two days after transfection of plasmids to analyse either Sleeping Beauty transposase, Frog Prince transposase or PhiC31 integrase in HEK293 and G4 cells (A,C,E) or B6 cells (B,D,F). However, instead of 100 ng stuffer plasmid as used for integration assays, 100 ng of the renilla luciferase expressing plasmid pRL-TK were transfected into 6-well plates and 2 days post transfection one sixth of the respective volume was prepared to determine relative light units. For details please refer to the material and methods section. The amount of relative light units correlates with the transfection efficiency.

(mSB, mInt, 4a) were similar between the cell lines for each integration system tested (**Figure 4.4**). It is of note to mention that we also considered this in our transposition analysis. First we analyzed the transposition rate in the RNAi deficient cell lines and the parental cell line HEK293, independently. Therefore, we calculated the ratio of the functional transposase/integrase compared to the respective mutated version for each integration machinery. Afterwards, these data were used to compare transposition efficiencies in the RNAi knockdown cells and HEK293 cells. Importantly, this also takes into account the different cell states or alterations in the expression profile of one cell line within one experiment.

To analyze transposition efficiencies of the SB system, we co-transfected the RNAi knockdown cell lines G4 and B6 and the parental HEK293 cell line with the respective transposon donor vector and either a plasmid encoding wild type SB (pCMV-SB, **Figure 4.3A**) or the respective inactive version of the SB transposase (pCMV-mSB, **Figure 4.3A**) at a molar ratio of 1:4 (SB : transposon donor vector). For colony forming assays performed in neomycin resistant B6 cells we utilized the transposon donor vector pTMCS-IP with a puromycin resistance gene and for the G4 cell line we transfected the transposon donor plasmid pTnori (**Figure 4.3A**) encoding a neomycin resistance gene. After two weeks of G418 or puromycin selection the total number of colony forming units was determined. Transposition events for both cell lines and conditions (SB or mSB) were quantified by counting colony forming units and displayed as the fold increase of SB transposase mediated integration events compared to colony forming units in cells which received the inactive version of SB (mSB) (number above the bars). The same set up was used to detect transposition in the B6 cell line but instead of pTnori the plasmid pTMCS-IP containing a puromycin resistence was introduced. As shown in **Figures 4.5A** and **B,** a 4.2- and 2.6-fold increase in total transposition events in G4 (**Figure 4.5A**) and B6 cells (**Figure 4.5B**) in comparison to HEK293 cells was observed. To directly compare transposition events in HEK293, G4 and B6 cells this fold increase was set to 1 in the parental cell HEK293 and then directly compared to the respective ratio in G4 and B6 cells. All experiments regarding SB transposition were performed in triplicates and the average results of three independent experiments are shown in **Figure 4.5G** (left panel). We found that in sharp contrast to the parental cell line HEK293, SB-mediated integration showed at average an increase of 3.5-fold in the RNAi knockdown cell line G4 and an enhancement of 2.4-fold in the B6 cell line (p-value < 0.05) (**Figure 4.5G**). These data indicated that SB transposase-mediated integration is enhanced in RNAi knockdown cells. Hence, we concluded that the RNAi pathway interferes with transposition in mammalian cells.
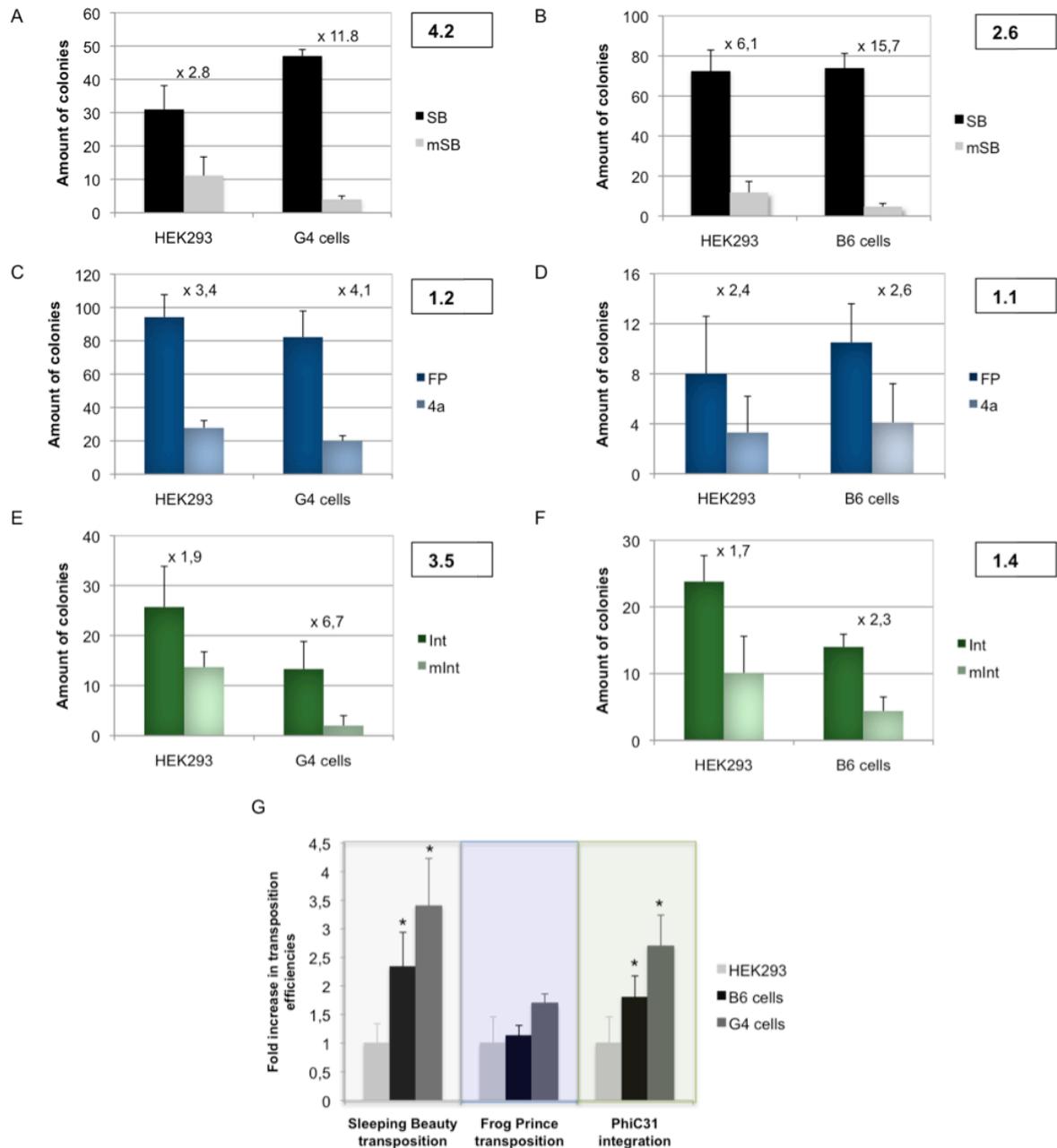
Figure 4.5: Influence of the RNA interference (RNAi) pathway on integration events mediated by Sleeping Beauty transposase, Frog Prince transposase and the PhiC31 integrase. (A) -(F) Total number of colony forming units after SB transposase mediated integration, Frog Prince mediated transposition and PhiC31 mediated integration in HEK293 cells and the RNAi knockdown cell lines G4 (A,C,E) or B6 (B,D,E) are shown. The fold increase in transposition events compared to the inactive protein is shown in numbers above the respective bars. The fold increase in integration events directly comparing the parental cell line HEK293 and the respective RNAi knockdown cell line is provided as a framed number. The data comparing the active integration protein with its inactive version within one cell line are statistically relevant (p-value < 0.05). (G) Fold increase of transposition/integration events of the functional transposase/integrase compared to the mutated version of the respective protein were determined for all cell lines and the respective transposase and integrase versions. This ratio in HEK293 cells was set to 1 and directly correlated to the fold increase in the RNAi knockdown cell lines G4 and B6. All experiments were performed in triplicates and the average results of three independent experiments are shown. * p-value < 0.05.

Previous studies suggested that the Frog Prince (FP) transposon does not display convergent transgene expression indicating that this transposon may not be influenced through the RNAi pathway (Moldt *et al.,* 2007). Therefore, we speculated that FP transposition could be potentially used as a negative control for transposition without impact of the RNAi pathway. FP is a reconstructed transposon from the Northern Leopard Frog *Rana pipiens* displaying high transpositional activity in vertebrate cells (Miskey *et al.,* 2003). It was originally recovered by correction of only two mutations and similar to SB it works by a cut-and-paste mechanism leading to somatic integration into TA dinucleotides (Miskey *et al.,* 2003). In concordance to our studies utilizing the SB transposase system, we performed colony forming assays with the FP transposase system in our RNAi knockdown cells and the parental HEK293 cell line. DNA constructs used for this study are schematically shown in **Figure 4.3B**. The experimental setup was identical to the one used for SB and the total number of colonies for all cell lines are shown in **Figures 4.5C** and **D. In Figure 4.5G** the relative fold increase of FP transposase mediated integration events compared to colony forming units in cells which received the inactive version of FP are displayed. As hypothesized we could not detect a significant difference in transposition events (up to 1.5-fold increase in the cell line G4; p-value > 0.05) in the RNAi knockdown cell lines in comparison to HEK293 cells after transfection of the FP expressing plasmid and the donor plasmids pFP-IP or pFP-neo2 (**Figure 4.3B**) at a molar ratio of 1:5 (pFV-FP: substrate plasmid) (**Figure 4.5C** and **D and 4.5G**, middle panel). We concluded that FP transposase mediated integration is not influenced by the RNAi machinery.

To investigate the influence of the RNAi machinery on integration of non-viral vectors in a more global manner, we also analyzed whether the integration reaction of the PhiC31 integrase system is influenced in our RNAi knockdown cells. PhiC31 integrase is derived from a bacteriophage (Kuhstoss and Rao 1991; Groth *et al.,* 2000; Groth and Calos 2004) and represents an attractive tool for site-directed recombination in mammalian cells (Groth *et al.,* 2000). Its integration reaction is based on recombination between the attachment site attB within an episomal substrate plasmid and pseudo attP attachment sites (attP') present in the mammalian genome (Thorpe and Smith 1998; Groth *et al.,* 2000; Thyagarajan *et al.,* 2001). PhiC31 integrase has successfully been applied in numerous preclinical *ex vivo* and *in vivo* gene therapy studies (Olivares *et al.,* 2002; Ortiz-Urda *et al.,* 2002; Ehrhardt and Kay 2005; Ehrhardt *et al.,* 2007) PhiC31 integrase methodology represents a platform for genetic engineering of eukaryotic genomes and transgenesis (Belteki *et al.,* 2003; Blaas *et al.,* 2007; Thyagarajan *et al.,* 2008; Allen and Weeks 2009).

In concordance with our transposition studies, we performed colony forming assays to quantify PhiC31 integrase mediated integration events in the RNAi knockdown cell lines B6 and G4 and the parental cell line with a functional RNAi pathway. We co-transfected a PhiC31 integrase expressing plasmid together with either the substrate plasmid pIP-attB in B6 cells or P7 in G4 cells (**Figure 4.3C**) at an equal molar ratio. Integration events in the respective cell line were expressed either in total numbers (**Figures 4.5E** and **F**) or as fold increase of colony forming units of the RNAi knockdown cell lines in relation to HEK293 cells (**Figure 4.5G**, right panel). After puromycin selection of transfected B6 cells or neomycin selection of the transfected G4 cells, we detected an up to 2-fold and up to 3-fold increase in integration events in the RNAi knockdown cell lines B6 and G4, respectively (**Figure 4.5G, right panel**). This finding indicated that PhiC31 may also be controlled by the RNAi interference pathways. However, further studies need to address whether convergent expression from hybrid attB and attP' sites (attR and attL) occurs or whether some other mechanisms are responsible for the increase in integration events.

In order to further characterize the effect we detected in our RNAi deficient cell lines, we tested the performance of SB mediated transposition from a substrate plasmid, containing two insulating sequences shielding the expression cassette from the influence of the IRs. The construct containing the insulating sequences used for this experiment were described elsewhere (Walisko *et al.,* 2008). Both insulating sequences prevent convergent transcription and therefore generation of dsRNA molecules. We hypothesized that the lack of trancriptional activity from the IRs would prevent the formation of dsRNA subsequently resulting in decreased RNAi-mediated reduction of transgene expression. We performed colony-forming assays transfecting the insulator containing plasmid (p/Tneo-HS4) either with functional SB or inactive version of SB (mSB) in HEK293 cells and G4 cells using the same conditions as described for experiments shown in **Figure 4.6**. After two weeks of G418 selection and in sharp contrast to results illustrated in **Figure 4.6A**, there was no significant difference in the ratio between HEK293 cells and the RNAi knockdown cell line G4 as shown in **Figure 4.6** (framed number), indicating no silencing of the transgene expression cassette mediated by the RNAi pathway. In addition this experiment confirmed the notion that the transcription of the region between the two IRs is responsible for the observed phenomenon and that the RNAi pathway drives downregulation of expression derived from integrated transposons.
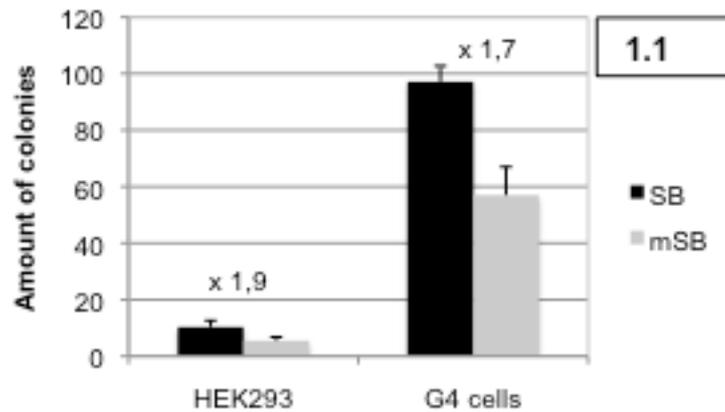
Figure 4.6: Influence of insulator sequences in HEK293 cells and the RNAi knockdown cell lines B6 and G4. The plasmid pT/neo-HS4 was transfected together with either the function Sleeping Beauty transposase (SB) or the inactive version of SB (mSB) in HEK293 or G4 cells. After 2 weeks of G418 selection, cells were stained and blue colonies were counted. Total numbers of colonies are displayed. The fold increase of SB to mSB is shown above the respective bars and the ratio between G4 cells and HEK293 cells is indicated in a black box. Comparing the data from the active SB transposase with the inactive mSB protein, within one cell line the results are statistically relevant (p-value < 0.05).

4.3 Discussion

In conclusion, our results indicate that SB-mediated transposition in human cells could be regulated through the RNAi pathway and that an evolutionary conserved self-regulatory mechanism for SB-mediated transposition may exist in eukaryotic cells. Components of the SB transposon system and the PhiC31 integrase system may either be directly or indirectly targeted by microRNAs. A model for the potential molecular mechanism is schematically shown in **Figure 4.7**. Herein, convergent transcription driven by the left and the right IRs (Moldt *et al*., 2007) leads to formation of double-stranded RNAs, which are exported out of the nucleus into the cytoplasm (Yi 2003; Zeng and Cullen 2004). In the cytoplasm these RNAs may serve as substrates for Dicer, an endonuclease, which cleaves the long dsRNAs into 21-23 nt long siRNAs (Hutvagner *et al.,* 2001; Ketting 2001). One strand of these siRNAs, the so-called guide strand can then be incorporated into the RNA-induced silencing complex (RISC) and direct siRNA mediated silencing of the transgene after somatic integration (Hutvagner *et al.,* 2001; Mourelatos 2002; Meister 2004). This hypothesis is also supported by other experiments performed in this study. Analysing the Frog Prince transposon system, for which no transcriptional activities derived from the IRs were demonstrated in the past, transposition efficiencies were similar in the RNAi knockdown cell line and the parental cell line HEK293 (Walisko *et al.,* 2008) (**Figure 4.4** and **4.5**). In
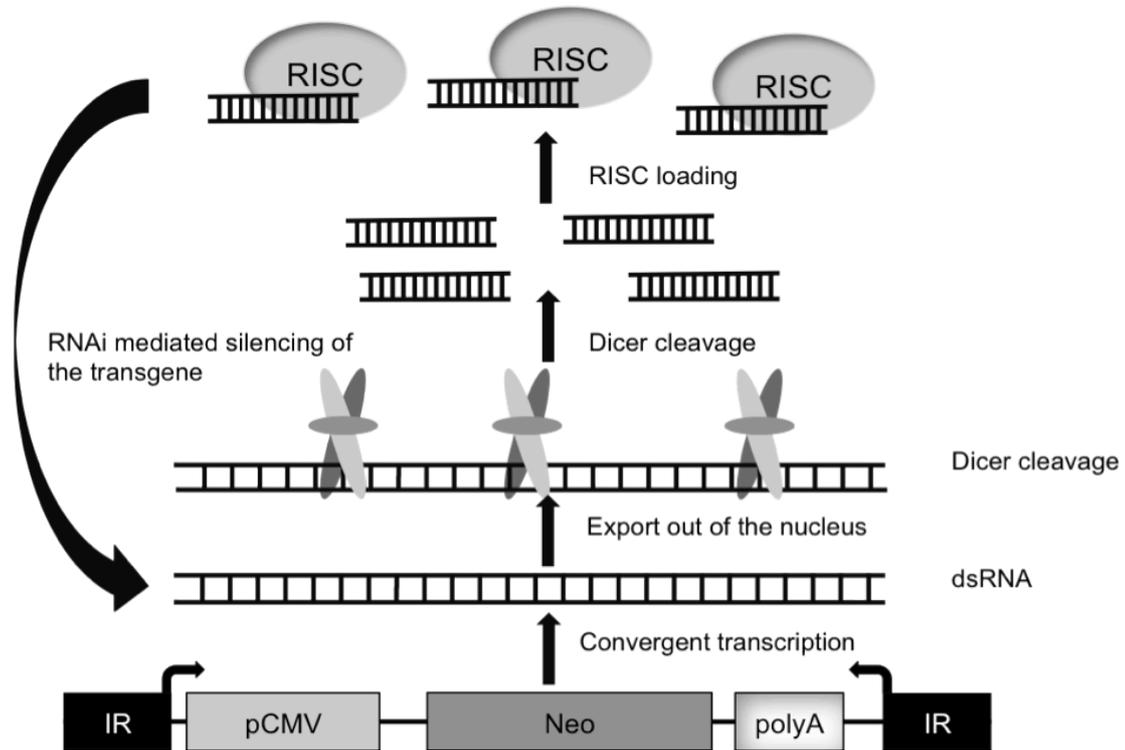
Figure 4.7: Model for the influence of the RNAi pathway on Sleeping Beauty mediated transposition. Convergent transcription driven by the left and the right inverted repeats (IRs) leads to formation of double-stranded RNA (dsRNA). These dsRNAs are exported out of the nucleus and in the cytoplasm they serve as substrates for DICER. This endonuclease cleaves the long dsRNA into 21-23nt long small interfering RNAs (siRNAs). One strand, the so-called guide strand can then be incorporated into the RNA induced silencing complex (RISC) and direct siRNA mediated silencing.

addition, the inhibition of the inward transcriptional activity by insulating sequences (cHS4-insulator), shielding the transgene cassette from the influence of the IRs (Walisko *et al*., 2008), did not show any differences in transposition efficacy in HEK293 cells and G4 cells (**Figure 4.6**). Finally, preliminary results, which were received after quantifying transposon-derived reporter gene mRNA levels (here puromycin) in HEK293 and B6 cells upon transposition indicated that transgene expression levels were significantly increased in B6 cells in comparison to HEK293 cells 10 days post transfection (data not presented). Thus, the obtained results confirm the assumption that transgene expression and not for instance increased transposase activities or levels contribute to the enhanced transposition efficacies.

Interestingly, although the inhibition of the RNAi pathway seems to be more pronounced in B6 cells compared to the G4 cells as indicated by the quantification of the HoxB8 expression levels (**Figure 4.2F**), we could not detect the same trend in the colony forming assays analyzing transposition events and PhiC31 mediated somatic integration. However, it is important to point out that different plasmid constructs were used to quantify transposition events in the G4 and B6 cells (**Figure 4.3**). All substrate plasmids used for colony forming

assays in B6 cells containing the puromycin expression cassette also harbour an intron as well as an IRES sequence (**Figure 4.3**). Since the transcriptional activity of the ITRs is quite low (Moldt *et al.,* 2007), these components may function as insulators or they may interfere with the convergent transcription levels from the IRs after somatic integration. Subsequently, only a small amount of dsRNA can be formed, which in turn may reduce the effect of the P19 protein in B6 cells.

Furthermore, when analyzing SB transposition in G4 cells in comparison to the parental cell line HEK293, total transposition events are comparable or even lower in the case of FP or PhiC31 integration processes, respectively (**Figure 4.5**). This discrepancy could be simply due to reduced transfection efficiencies or altered transgene expression levels in the different cell lines. However, to take this difference into account, the ratio of the transposition activities of the functional protein to the inactive version of the protein was calculated within one cell line. These data were then used to directly compare transposition efficiencies in the RNAi deficient cell lines and the parental cell line HEK293.

To further elucidate the molecular mechanism responsible for the influence of the endogenous RNAi machinery on transposition, future studies need to address which sequences of the integrated transposon are processed by the components of the cellular RNAi pathway. Pull-down assays for identification of transposon-derived sequences bound to the P19 protein in B6 cells or argonaute in normal cells may partially solve this question. Furthermore, it has to be clarified, which RNAi-mediated mechanism is responsible for gene silencing. If it is due to mRNA degradation, translational inhibition or if silencing is based on RNA-directed DNA methylation (Kawasaki and Taira 2004a). The latter mechanism is supported by a publication from 2007, where Garrison *et al*. could revert the silencing effect upon transposition by administration of a methyltransferase inhibitor (Garrison *et al.,* 2007). Notably, in the present study we analyzed the commonly used two-component vector system for SB-mediated integration and observed an up to 4.2-fold increase in transposition events (**Figure 4.5A**). However, effects may be increased when using the wild type SB transposase IRs with a 160 bp region between the left IR and the transposase translational start site with unknown function. This unknown region was recently shown to enhance transcriptional activities from the left IR (Walisko *et al.,* 2008), which in turn may lead to an increased amount of dsRNA and therefore, potentially a more pronounced silencing effect.

In conclusion, we believe that our findings may have important implementations for the design of improved non-viral vectors for somatic integration. Furthermore, the established RNAi knockdown cell lines G4 and B6 can also be explored to study not only non-viral vectors and their regulation by the RNAi machinery, but also the influence of RNAi on viral

vectors or viruses in general can be investigated. For instance herpesviruses and adenoviruses, which were shown to express siRNAs could be interesting candidates to address these questions (Pfeffer 2004; Andersson *et al.,* 2005; Aparicio *et al.,* 2006; Skalsky and Cullen 2010). Last but not least our experimental approach based on expression of P19 may also be applied to study the interference of the RNAi pathway with viral or non-viral systems *in vivo* in a tissue specific manner. P19 could be expressed from a viral vector under the control of a tissue specific promoter, which may lead to tissue specific block of 21 nt long small interfering RNAs and therefore also inhibition of RNAi pathway.

5   Adenovirus 5 replication is enhanced by RNAi knockdown

The understanding of basic virus host interactions is a key pre-condition to develop and improve viral vector systems for gene therapy. Within a virus life cycle several gene products can be modulated by host cell factors or mechanisms such as the RNA interference pathway that subsequently influence productive virus replication.

The RNA interference (RNAi) pathway is a well-conserved mechanism, which results in the post-transcriptional silencing of a target gene. Key players within the RNAi pathway are ≈ 22 nucleotid (nt) long, non-coding, double-strand RNA (dsRNA) molecules, the so-called micro RNAs (miRNAs). It is estimated that approximatly 75 % of all miRNA sequences are located within non-coding regions or intron sequences of genes (Lagos-Quintana 2001; Cai 2004; Lee *et al.,* 2004). In most cases the transcription is mediated by the RNA polymerase II, generating a 160 nt long primary miRNA, which is processed inside the nucleus by the RNaseIII enzyme Drosha and the RNA-binding protein DGCR8 (DiGeorge critical region-8) into 60 nt long, imperfectly pairing stem loop precursors, the pre-miRNAs (Pasquinelli and Ruvkun 2002; Lee *et al.,* 2004; Zeng and Cullen 2004; Zeng and Cullen 2005). By the energy-dependent Exportin5 pathway these molecules are transported into the cytoplasm, where further processing by Dicer renders mature ds-miRNAs with 21-23 nt in length (Yi 2003; Zeng and Cullen 2004). Afterwards one strand, the guide strand, is incorporated into the RNA induced silencing complex (RISC), which is composed of an argonaute protein, Dicer and TRBP (the human immunodeficiency virus transactivating response RNA-binding protein) of which only the argonaute protein covers the silencing function (Yi 2003; Meister 2004; Zeng and Cullen 2004). The single-stranded miRNA (ss-miRNA) then guides the RISC complex to the target mRNA. Finally, the interaction between the miRNA and the mRNA leads to mRNA degradation if there is 100% complementary between both molecules, otherwise and more likely in mammalian cells the interaction leads to a inhibition of translation and subsequently the downregulation of the protein level. Within the latter case, seed nucleotides 2-8 are crucial as they determine the contact to the target sequence (Chiu and Rana 2003; Haley and Zamore 2004).

During the past decade it became clear that the RNAi pathway is conserved throughout many organisms including viruses. The target mRNAs of the viral miRNAs and in consequence their biological functions are largely unknown but it is assumed that two main mechanisms are affected (Cullen 2010). On the one hand viral miRNAs inhibit cellular immune responses as it is shown for the polyomavirus SV40, which expresses a miRNA that

targets the large T-antigen and therefore reduces the cellular cytotoxic T-lymphocyte response (Sullivan *et al.,* 2005). On the other hand viral miRNAs seem to play a critical role in establishment and maintenance of latency, a mechanism predominantly important for herpes viruses, for which a large number of miRNAs have been identifed so far (Skalsky and Cullen 2010).

But also cellular miRNAs were shown to play a role in virus replication as Lecellier *et al.* demonstrated in 2005 when they identified the cellular miRNA miR32 as inhibitor of the replication of the primate foamy virus, based on experiments in an RNAi knockdown cell line (Lecellier *et al.,* 2005). Additionally, this and other viruses evolved RNAi suppressor proteins such as the primate foamy virus protein Tas, the human immunodeficiency virus Tat protein, or the adenovirus VA-RNAs to prevent degradation of its own RNAs (Andersson *et al.,* 2005; Bennasser *et al.,* 2005; Haasnoot *et al.,* 2007).

Adenoviruses (Ad) are non-enveloped viruses, which contain ds-DNA genome of 36 kb in length. The viral life cycle starts with the interaction of the Ad fiber protein with the cellular coxsackie and adenovirus receptor (CAR), whereas binding of penton to two members of the integrin family facilitates uptake of the virus. After internalization and escape from the endosome, the Ad is transported to the nuclear membrane, where the viral DNA is inserted into the nucleus through the nuclear pore complexes. Inside the nucleus the viral DNA exists as monomeric, episomal DNA (Jager and Ehrhardt 2009) and transcription of regulatory and structural viral proteins is performed in a time dependent manner. The entire life cycle takes about 24 hours and subsequently ends in lysis of the cell (Curiel and Douglas 2002).

Besides the coding regions spread on both strands of the adenoviral genome, two non-coding products, the virus-associated RNAs I and II (VAI-RNA and VAII-RNA) are transcribed, which are known RNAi inhibitors (Lu and Cullen 2004). VA-RNAs are 160 nucleotide long panhandle structured products transcribed by the RNA polymerase III (Thimmappaya 1982; Liao *et al.,* 1998). During a normal replication cycle about 10^8 VA-RNAs are produced and transported to the cytoplasm across the Exportin5/RanGTP pathway. Besides blockade of the RNAi pathway, another well established function of VAI-RNA is the blockade of the protein kinase R (PKR), an interferon-inducible serin threonin protein kinase that is activated by foreing dsRNA molecules and initiates apoptosis and release of cytokines as antiviral response (O'Malley 1986; Akusjarvi *et al.,* 1987).

However, the VA-RNAs also target several parts within the RNAi pathway. After transcription, VA-RNAs share the export machinery with endogenous miRNAs and mRNAs, which leads to a competitive inhibition of the cellular counterpart (Andersson *et al.,* 2005).

Furthermore Lu and colleagues showed that VA-RNAs bind to cytoplasmatic RNase III enzyme Dicer and the group of Aparicio discoverd that VA-RNAs can be cleaved by Dicer into 19-29 nucleotide long small-virus associated RNAs (svaRNAs) (Lu and Cullen 2004; Aparicio *et al.,* 2006; Sano *et al.,* 2006). These sva-RNAs were functional as they were able to enter the RISC complex and to inhibit expression of complementary reporter genes (Aparicio *et al.,* 2006; Sano *et al.,* 2006). In the beginning the naturural function of these svaRNAs remained unknown, since no cellular or viral target sequences could be identified. The inhibition of sva-RNAs by antagomir RNAs, however, revealed a severe attenuation of productive virus replication (Aparicio *et al.,* 2006). Very recently Aparicio *et al.* identified the TIA-1 protein as possible target of the sva-RNAs, a protein that is responsible for apoptosis induction (Aparicio *et al.,* 2010). In addition to these findings, it is hypothysized that in the early replication phase sva-RNAs were produced, which regulate cellular or viral target proteins and in later phases of infection VA-RNAs block the RNAi pathway in order to prevent silencing of own viral proteins.

In this study we aimed at investigating for the first time the influence of the RNAi pathway on the adenovirus life cycle in a more global manner and to apply the gained knowledge to improve adenovirus vector production systems. Therefore, we used our previously described RNAi knockdown cell line B6, expressing the RNAi suppressor protein P19, to analyze replication of wtAd5 (compare **section 3.2.1**). We found that adenovirus replicates up to 10-fold faster in an RNAi knockdown cell line, and up to 100-fold faster if an RNAi suppressor protein is expressed from an adenoviral genome, which generates 10-fold higher titers. This upregulation could be due to the higher expression of regulatory viral proteins such as E1B, DBP or the E4Orf6 proteins. Furthermore, we could demonstrate that sva-RNAs are bound to the dimeric P19 protein and that they were degraded after binding. Finally, we took advantage of our results to improve HC-AdV vector production by application of our novel established P19 system enhancing helper-adenovirus replication.

5.1 Materials and Methods

5.1.1 Plasmid constructs

The TopohB2m plasmid was kindly provided by Wenli Zhang (Max von Pettenkofer-Institut, Munich, Germany) and contains the hB2m expression cassette for normalization of B2m in quantitative Real-Time PCR (qRT-PCR). Standard curves for all adenoviral proteins were performed using DNA purified from wtAd5 viral particles.

The pCR2.1 BluntII-Topo based plasmid pFIPP is the main vector for BAC cloning containing the spacer, IRES, p19 and the poly A signal with the flanking homologous sequences to the adenovirus genome. The plasmid construct pNEB.PK.fiberIL supplied by Dirk Nettelbeck (German Cancer Research Center, Heidelberg, Germany), was basically used as main template for several overlapping PCR steps to generate the pFIPP construct. Primer sets were designed with 15-20 nt long overhangs if overlapping PCR products had to be generated. KOD Polymerase (Merck) was used for each step following the manufacturer instruction if not otherwise stated and primers are shown in **Table 5.1**. In detail to generate the 3′overlapping sequence to the adenovirus primer and the spacer together with the IRES sequence, first pNEB.PK.fiberIL was inserted into a PCR reaction with the primer set "5′fiber forw" and "IRES p19 rev" using an annealing temperature of 56°C and an elongation time of 40 seconds (sec.). Secondly, to generate the fragment containing the *p19* expression cassette and the poly A signal a KOD based PCR reaction with the primer pair "IRES-p19 forw" and the "polyA-3′fiber rev" using the pZacp19 plasmid was used. For pZacP19 the *p19* expression cassette was introduced by direct cloning of the PCR product into the *Xho*I and *Xba*I sites of the pZac expression vector. The latter PCR product was generated with the primer set "p19forw Xho" and "p19rev Xba". The PCR for the p19-polyA fragment was performed using an annealing temperature of 57°C and an elongation time of 40 sec. running for 35 cylces. Afterwards the 3′fiber fragment containing also homologous sequences to the adenovirus genome downstream of the *fiber* was generated with the primer "3′fiber-polyA forw" and "3′fiber rev" using the pNEB.PK.fiberIL as template and running 30 cycles with an annealing temperature of 56°C and 30 sec elongation time. The last two PCR products were purified by gel column purification (Promega) and subjected to a new PCR reaction with the outer primer "p19-IRES forw" and "3′fiber rev" using a two-fold excess of the long p19 polyA fragment. Conditions for this PCR were as follows: the primer annealing temperature was set to 56°C for 10 sec. and an elongation time of 30 seconds starting with 16 cycles without adding primer. After these cycles, 1.5 µl of each primer was added to the reaction followed by another 35 cycles under the same conditions. The gel fragment containing the PCR product was purified and cloned into the pCR-BluntII-TOPO vector following the manufacturer instructions resulting in the plasmid pTopop19big. At least, a PCR reaction of the PTopop19big plasmid was performed under the same conditions as before and the purified PCR product was inserted as a template into a PCR reaction together with the product of the first PCR containing the 5′fiber-spacer-IRES construct. For this reaction 12.5 µl of each purified product, an annealing temperature of 56°C, an elongation time of 50 sec and the primer "5′fiber forw" and "3′polyA rev" were used. All primer sequences used during these steps are displayed in **Table 5.1A**. The fragment was then gel purified and Topo cloned into the pCR-BluntII-Topo vector following the

manufacturer instructions, resulting in pFIPP. The right construct was confirmed by restriction enzyme digest using *Eco*RI and sequencing.

The Fiber-IRES-p19 construct within the pFIPP vector was incorporated into the genome of a first-generation adenoviral vector utilizing bacterial artificial chromosome (BAC) cloning methods as described elsewhere (Warming *et al.,* 2005). In brief, the galactokinase-kanamycin (galK-Kan) construct was amplified in two subsequent PCRs using the primer pair IRES-p19_IC_5 and IRES-p19_IC_3 and the primers IRES-p19_IC_5_ne and IRES-p19_IC_3_ne. The purified PCR product from the second PCR step was then transformed into SW102 *E.coli* containing BAC pB-FG (kindly provided by Zsolt Ruzsics, Max von Pettenkofer-Institute, Munich, Germany). After induction of homologous recombination and selection for kanamycin the intermediate clone pB-FG-fib-GK was isolated, which contains the the galK-Kan construct incorporated at the 3' end of the fiber encoding sequence. Subsequently, the construct IRES-p19 was PCR-amplified utilizing pFIPP as template and the primers IRES-p19_IC_5_ne and IRES-p19_IC_3_ne. After PCR amplification the generated product was purified and transformed into SW102 cells containing the intermediate BAC pB-FG-fib-GK. Final clone Bfgp19 was isolated after recombination and selection against galK.

Generation of the helper-virus BAC containing the *p19* encoding sequence coupled to the fiber gene (BHVp19) was performed analog to method described in Hausl et al., in preparation. Briefly, a construct containing a zeocin resistance cassette and the 5' end of the helper-virus AdNG163R-2 (Ng *et al.,* 2002) was PCR-amplified in two steps using the plasmid T-PacI-5'Hv-ΔKan as template for the first PCR and the primer pair Ng-Hv_Adv-pIX_3611 and wt/Hv-BAC-Zeo and the primers Ng-Hv_Adv-pIX_3611 wt/Hv-BAC-nested for the second PCR, respectively. The purified product was then transformed into SW102 bacteria containing the BAC Bfgp19. After induction of recombination and zeocin selection the BAC BHVp19 was isolated. Replication-competent adenovirus BAC with the *p19* expression cassette (Bwtp19ΔE3) was constructed analog but using plasmid T-PacI-5'wtAd5-ΔKan as PCR template. This plasmid contains the 5' end of the wild-type adenovirus 5 genome, which was generated analog to T-PacI-5'Hv-ΔKan but using isolated DNA from wild-type adenovirus 5 virus particles (Hausl et al., in preparation). Construction of negative controls pB-Hv and pB-wtAd5 were described elsewhere (Hausl et al., in preparation).

All PCRs were performed with high-fidelity KOD Hot Start DNA Polymerase (Novagen) with 95°C denaturation for 20 seconds, 60°C annealing temperature for 20 seconds and an

elongation of for 25 sec/kb at 70°C using 35 cycles. Primers used for generation of the BAC derived viruses are displayed in **Table 5.1B.**

Table 5.1: Oligonucleotides used within this study		
A		
5´fiber forw	5´forward	TATGCCTAACCTATCAGCTTATCC
IRES p19 rev	3´reverse	GTCGTTTCCTTGTATAGCTCGTTCCATGGTATCATCGTGTTTTTCAA
IRES p19 forw	5´forward	TTCCTTTGAAAAACACGATGATACCATGGAACGAGCTATACAAGGAA
poly 3´fiber rev	3´reverse	ACACAAACGATTACTCTACTAGTTACCACATTTGTAGAGGTTTTAC
p19 forw Xho	5´forward	ATTCTCGAGATGGAACGAGCT
p19 rev Xba	3´reverse	CGTCTAGATTACTCGCTTTCTTT
3´fiber polyA	5´forward	CAAGTAAAACCTCTACAAATGTGGTAACTAGTAGAGTAATCGTTTGTG
3´fiber rev	3´reverse	TGTCTGTTACCCATGATATGATG
B		
IRES-p19_IC_5	5´forward	CATGGGACTGGTCTGGCCACAACTACATCAAGCTTGGTACCGAGCTCGG
IRES-p19_IC_3	3´reverse	GCTATGTGGTGGTGGGGCTATACTACTGAGGGCGAATTGGGCCCTCTAG
IRES-p19_IC_5_ne	5´forward	ACAACTCCAAGTGCATACTCTATGTCATTTTCATGGGACTGGTCTGGCC
IRES-p19_IC_3_ne	3´reverse	GAGTTTGATTAAGGTACGGTGATCTGTATAAGCTATGTGGTGGTGGGGC
wt/Hv-BAC-Zeo	5´forward	ATGCAAGTGTGTCGCTGTCGAGTTTCGTGTCAGTCCTGCTCCTCGGCCAC
wt/Hv-BAC-nested	5´forward	CGGCACGTTAACCGGGCTGCATCCGATGCAAGTGTGTCGCTGTCGAGTTT
Ng-Hv_Adv-pIX_3611	3´reverse	CTTCCATCAAACGAGTTGGTGCTC
C		
human B2m	5´forward	TGCTGTCTCCATGTTTGATGTATCT
	3´reverse	TCTCTGCTCCCCACCTCTAAGT
DBP	5´forward	ACTTGCCGGAAAACTGATTG
	3´reverse	GCACGTGATTGAAATGGATG
E1B55K	5´forward	TAGTGAAAAGCGTGGCTGTG
	3´reverse	GGAACAGCGGGTCAGTATGT
E4 Orf6	5´forward	TTCAAAATCCCACAGTGCAA
	3´reverse	TACCGGGAGGTGGTGAATTA
Fiber	5´forward	CGTGCACGACTCCAAACTTA
	3´reverse	GGGCTCTTTCAAGTCAATGC
Hexon	5´forward	CTTACCCCCAACGAGTTTGA
	3´reverse	GGAGTACATGCGGTCCTTGT
D		
polydTTT adaptor		GCGAGCACAGAATTAATACGACTCACTATAGGTTTTTTTTTT
reverse primer		GCGAGCACAGAATTAATACGAC
E		
3´Van		AGGAGCGCTCCCCCGTTGT
3´Van-r		ACAACGGGGGAGCGCTCCT
3´VanII		CGCTCGTCCCTGTTTCCGGAG
3´VAII-r		CTCCGGAAACAGGGACGAGCG
5´VaII		AATAACCCTCCGGCTACAGGGAGCGAGCC

5.1.2   Cell lines and viruses

Human embryonal kidney cells (HEK293) were obtained from ATCC and used for construction of the *p19* expressing cell line B6 described in **section 4.2.2**. A549 cells were supplied by Carsten Rudolph (Ludwig-Maximilians-University Munich, Munich, Germany). The 116 cell line used for high-capacity adenovirus production was obtained from Philip Ng (Baylor College, Houston, Texas, USA). HEK293, A549 and B6 cell lines were cultured in DMEM medium, 116 cells in MEM, both supplemented with 10% FBS and 1% penicillin-streptomycin (P/S). As selection pressure for B6 cells 100 ng/ml G418 were added. Huh7 cells were cultured in DMEM supplemented with 1% non-essential amino acids, 10% FBS and 1% P/S. All cell lines were cultured at 37°C in a humidity atmosphere with 5%CO_2. The entire cell culture reagents were obtained from PAA.

Wildtype adenovirus 5 (Ad5) was obtained from ATCC, the adenovirus vector FG-Adluc was described in **section 2.2.6**. Wildtype adenovirus, first-generation adenoviruses and most bacterial artificial chromosome- (BAC-) based viruses (except AdfiberIL and dl705) were amplified in HEK293 cells. The VAII-deleted virus dl705 obtained from Göran Akjusjärvi (Department of Medical Biochemistry and Microbiology, Uppsala University, Sweden) and the AdΔfiberIL provided by Dirk Nettelbeck (German Cancer Research Center, Heidelberg, Germany) were amplified in A549 cells and described previously (Akusjarvi *et al.,* 1987; Rivera *et al.,* 2004). AdNG163R-2 was kindly provided by Philip Ng and the HC-AdV luc was generated by Lorenz Jager (Max von Pettenkofer-Institute, Munich, Germany) expressing luciferase under the control of the liver-specific human α1-antitrypsin promoter (hAAT). The first generation adenovirus fgAdluc was described in **section 2.1.2**.

For BHVp19 and Bwtp19ΔE3 virus reconstitution, 20 μg of the BAC vector was linearized by a *Pme*I digest and purified by phenol/ chlorophorm/ isoamylalcohol (25/24/1, Roth) extraction following a ethanol precipitation. The complete digest was then used for FuGene6 (Roche) transfection following the manufacturer instructions using 15 μl of FuGene 6 reagent for transfection of HEK293 cells (kindly provided by Zsolt Ruszicz, Max von Pettenkofer-Institute, Munich, Germany) at 40% confluency. Medium was changed every 5 days, until cytopathic effect (CPE) appeared. Whole cellular lysates were then harvested and virus was released from the cells by four consecutive freeze/thaw cycles. Afterwards, a 95% confluent 6 cm dish with HEK293 cell was infected using 2/3 of the lysate and 2 hours later the medium was aspirated and cells were overlayed with a 1:1 mixture of 1% autoclaved agarose (diluted in H_2O; Peqlab) and 2x DMEM (Invitrogen) supplemented with 20% FBS and 2% penicillin-streptomycin. The overlay was performed every 3 days (with 0.5 ml) until viral plaques were obtained. Single plaques were picked and stored in 500 μl of

culture medium. After the release of the virus from the cells a 24-well dish of HEK293 cells was infected with 400 µl of the lysate. Approximately two days later CPE starts, the cells were harvested and one half was subjected to DNA isolation and PCR analysis to confirm the correct viral construct. The other half was used to amplify the virus in 12 cm, 6 cm and 10 cm tissue culture dishes and subsequently in 15 cm dishes of HEK293. Twenty 15 cm tissue culture dishes were sufficient for purification.

Purification of all viruses used within this study was performed by double cesium chloride gradient ultra –centrifugation followed by an over-night dialysis step. The whole procedure of purification is described in **section 2.2.4**.

Titration of viruses was performed by agarose overlay as shown in Curiel and Douglas (Curiel and Douglas 2002). In brief, 100% confluent HEK293 cells were infected with serial dilutions of virus stocks. Two hours post infection medium was aspirated and cells were supplemented with 2.5 ml of a 1:1 dilution of 1% autoclaved agarose (Peqlab) and 2x DMEM (see above). The overlay was then performed every 3 days with 0.5 ml of the mixture. After approximately 10 days plaques obtained, which were counted and the titer determined.

5.1.3   Analysis of CAR expression of HEK293 and B6 cells

HEK293 and B6 cells were counted and $1*10^6$ cells were washed once with PBS supplemented with 1% BSA (PBS/BSA). After centrifugation of the cells at 500 g for 3 min they were resuspended in 100 µl PBS/BSA and 5 µl CAR antibody (Santa Cruz Biolaps) were added following an incubation step at 4°C for 1 hour. As controls each cell line was also incubated without supplementation of the primary antibody. Afterwards the cells were washed again with PBS/BSA, to remove unbound antibodies and resuspended in 100 µl PBS/BSA. To detect CAR expression using flow cytometry, 1 µl of an APC labeled anti-mouse secondary antibody (kindly provided by A. Baiker, Max von Pettenkofer-Institute, Munich, Germany) was supplied to the mixture and incubated for 1.5 hours at 4°C with continous shaking. Cells were again washed with PBS/BSA and finally resuspended in 400 µl PBS for flow cytometry using FACS DIVA (BD).

5.1.4   Isolation of wtAd DNA from purified particles

To isolate adenovirus DNA, 100 µl of purified virus stock was incubated with the same volume lysis buffer (10 mM Tris (pH 7.4), 10 mM EDTA, 0.5% SDS, 2 mg/ml Proteinase K) for four hours at 37°C. The DNA was then purified by adding 180 µl of phenol/ chlorophorm/ isoamylalcohol (25/24/1). After centrifugation for 2 min at 15.000 g the upper phase was

collected and DNA was precipitated using 60 μl of 3 M sodium acetat (pH 5) and 600 μl of 100% ethanol followed by a centrifugation step at 15.000 g for 10 min. Afterwards the DNA pellet was washed with 500 μl 70% ethanol and centrifuged for 5 min at 15.000 g. The pellet was dried and the DNA resuspended in 40 μl sterile H_2O.

5.1.5 Analysis of adenovirus replication in HEK293 and B6 cells

Either HEK293 and B6 or only HEK293 cells were seeded into 6 cm dishes to reach 80% confluency for infection. Notably, for infection B6 cells were cultivated without G418. Infection with wtAd5, FgAdluc (see also **section 2.1.2**) or BAC derived viruses were performed using a multiplicity of infection (MOI) of 0.05, 0.1 or 3 respectively. After two hours (hrs), 10 hrs, 24 hrs and 48 hrs DNA and RNA were isolated and cellular and protein lysates were collected, taking 3 independent samples at each time point. To ensure, that only internalized viral particles were analyzed, cells were treated with 5 % trypsin for 5 min, centrifugated at 500 g for 3 min and washed once with sterile PBS before preparing for different applications.

5.1.6 RNA isolation and reverse transcription

Cells of one 6 cm dish were resuspended in 500 μl TRIZOL (Invitrogen) reagent, homogenized with a 21-gauge needle and RNA was isolated following the manufacturer instruction. RNA was resuspended in 40 μl of RNA-H_2O and 4 μl were used for cDNA synthesis. Reverse transcription was performed using the cDNA synthesis kit from NEB following the manufacturer instruction (ProtoScript®First strand cDNA synthesis kit). For quantitative Real-Time PCR (qRT-PCR) 4 μl of the cDNA were used.

5.1.7 DNA isolation for analysing viral genome copy numbers

The cell pellet of one 6 cm dish or a 24-well was used to isolate whole genomic DNA, a method described elsewhere (Sambrook 2001). DNA amounts were quantified by measuring the optical density (OD) at 260 nm. For qRT-PCR, genomic DNA was diluted to 10 ng/μl and 5 μl were applied for qRT-PCR. Normal taq-polymerase (NEB) based PCR was performed with 100 ng of genomic DNA following the manufacturer instructions.

5.1.8 Quantitative Real-Time PCR (qRT-PCR)

Quantitative RT-PCR was performed using the Taq-man system (Applied Biosystems) and FastStart Universal SYBR Green Master (Roche) reagent following the manufacturer instruction. For qRT-PCR of genomic DNA, 50 ng of genomic DNA was used, for cDNA

analysis 5 μl of a reverse transcription was subjected to the reaction. Oligonucleotides were either designed with the Primer3 design program (Krawetz S, Misener S (eds) *Bioinformatics Methods and Protocols: Methods in Molecular Biology.* Humana Press, Totowa, NJ, pp 365-386) using a maximum template size of 150 bp or in case of human Beta-2 microglobulin (hB2m) a previous published primer pair was used (Vandesompele *et al.,* 2002). **Table 5.1C** shows all oligonucleotides, which were used for qRT-PCR. Each sample was normalized to either genomic B2m level (10 000 cells) or expression level of 10 000 RNA molecules of hB2m. Quantification was performed by calculating known hB2m levels from the plasmid pTopohB2m by the following term:

$$1 \text{ pg plasmid} = 10^{-12} / \text{plasmid size (bp)} * 6.02*10^{23} \text{ copies}$$

5.1.9 Western Blot analysis of adenoviral proteins

Protein lysates were generated from $3.2*10^6$ cells using 300 μl of NP-40 lysis buffer (50mM Tris-HCL pH 8.0, 150mM NaCl, 1% NP-40, storage at -20°C) supplemented with proteinase inhibitors without EDTA (Roche) following a 30 min incubation step on ice. To determine protein amounts, the Bradford test was applied following the manufacturer instructions (Roth). Equal protein amounts were separated on a 10% SDS polyacrylamid gel using a BioRad sytem. Afterwards proteins were blotted on a methanol treated PVDF membrane and incubated o/n in TBS buffer (10 mM Tris (pH 7.5), 150 mM NaCl) supplemented with 5% milk powder (Roth) at 4°C. After three washing steps with TBST (TBS + 0.01 % Tween20 (Roth)) blots were incubated with either first anti-adenovirus antibodies against DBP (1:250, mouse derived), E1B55K (1:1000; mouse derived), both supplied by Matthew Weitzman (Salk Insitute, San Diego, USA), E4Orf6 (1:10 anti mouse) obtained from Thomas Dobner (Heinrich-Pette-Insitut, Hamburg, Germany), Fiber (1:10 000 mouse derived; NeoMarkers), Hexon (1:1000 rabbit, Abcam) or GAPDH (1:1000, anti goat, R&D systems) as control for 1 hour at room temperature. This step was followed by another 3 washing steps with TBST and incubation with secondary peroxidase (POX) labeled antibodies specific to the first antibody. All secondary antibodies were obtained from Invitrogen. Finally, blots were washed 3 times with TBST and POX was activated by adding ECL reagent (GE Healthcare).

5.1.10 Isolation of small RNAs bound to P19 after His-tag purification

To investigate, if sva-RNAs from VAI-or VAII-RNA origin bind to P19, the His-tagged protein was purified from five 15 cm tissue culture dishes of B6 cells under native conditions after wtAd5 infection at an MOI of 3. Purification under native conditions was performed with magnetic beats (Qiagen) following the manufacturer instruction. For the destruction of the

cells, the lysate was either subjected to 3 consecutive freeze/thaw cycles or cells were sonificated at level 2 for 5 times on ice using a Branson 450 sonificator (Calabrese and Sharp 2006). For the isolation of siRNAs bound to P19 two methods were used. On the one hand Qiazol reagent (Qiagen) was supplied to the protein solution and standard RNA isolation was performed (see above). On the other hand protein lysates were incubated for 15 min with 2 x Proteinkinase K solution (200 mM Tris-Cl pH 7.4, 25 mM EDTA, 300 mM NaCl, 2% SDS, 2 mg/ml Proteinase K) and small RNAs were isolated by isopropanol precipitation over night at -20°C . Small RNA preparations were resuspended in 30 μl RNase free H_2O.

The purified small RNAs were polyadenylated using the polyAAA-tailing kit from Ambion. Reverse transcription was performed with polydT primer with an adaptor followed by a standard KOD (Novagen) based PCR with the reverse primer (**Table 5.1D**) 3′Van-r or the 5′VAII primer (**Table 5.1E**). The PCR products were either purified by gel extratction (Promega) and send for sequencing or they were subcloned in the pCR-Blunt II-Topo (Invitrogen) vector following the manufacturer instructions and send for sequencing (Eurofins, MWG).

5.1.11 Isolation of small RNAs and Northern Blot analysis

To confirm the VAII-RNA deletion in the mutant virus dl705, HEK293 cells were infected at an MOI of 3 with dl705 or wtAd5 and small RNA was isolated 2 days post transfection following a protocol obtained from Rebecca Schwab (University of Tuebingen, Tuebingen, Germany). In brief, cells were treated with Trizol reagent and cell lysates were homogenized using a 21-gauge needle. Afterwards, one third volume of chlorophorm was added and cells were centrifuged for 10 min at 5000 g at 4 °C. The upper phase was harvested and subjected to another phenol purification step using the same conditions as described before. Again the upper phase was collected and 1 volume of isopropanol was added to precipitate RNAs overnight at -20°C. The next day, RNA solution was precipitated by centrifugation for 30 min at 5000 g at 4°C and the RNA pellet was washed with 70% EtOH. After centrifugation the cell pellet was air-dried and resuspended in 40 μl of RNase-free water. Isolated RNAs were then separated on a 17% vertical polyacrylamid gel containing 7 M urea in 0.05x tris-borate-ethylenediaminetetracetic (TBE) buffer. As a positiv control for Northern Blot analysis also representing the length marker, we ran the reverse oligonucleotide of 3′Van (3′Van-r) or VAII-RNA (3′VanII and 3′VanII-r) oligonucleotide probe also published by Aparicio et al. (**Table 5.1E**) (Aparicio *et al.,* 2006). We performed a semi-dry transfer in 0.5x TBE onto a Hybond-N+ membrane (GE Healthcare) and detected the VAI-RNA and VAII-RNA, or sva-RNAs by radioactive end labelling of the oligonucleotides with gamma-P32

(Quick spin columns, Roche) and incubation in Denhardt´s solution at 50°C for 1 hour. Blots were washed twice for 10 min with 5x SSC/0.1% SDS and once for 10 min with 1 x SSC/ 0.1% SDS at 50°C. Afterwards blots were exposed to phospho-imager plates for 10 min and anaylsed in a phospho imager. The same procedure and oligonucleotides were used to track the fate of svaRNAs of VAI-RNA and VAII-RNA origin in the P19 expressing cell line B6.

5.1.12 Comparison of packaging efficiencies of standard helper virus and BHVp19

To compare the packaging efficiency of our new generated helper virus BHVp19 to the standard helper virus AdNG163R-2 (Ng *et al.,* 2001), 116 cells were seeded in two 15 cm dishes and grown to a confluency of 90%. The next day each dish was infected at an MOI of 10 with HC-AdV luc and co-infected either with BHVp19 or AdNG163R-2 at an MOI of 2. Two days post infection cells were harvested, viral particles were released by 4 consecutive freeze/thaw cycles and different amounts of the lysates were used to infect Huh7 cells at 90% confluency seeded in a 24-well plate. Twenty-four hours later, Huh7 cells were again harvested and prepared for luciferase assay using the dual luciferase reporter assay kit provided by Promega.

5.2 Results

5.2.1 The coxsackie and adenovirus receptor is expressed at similar rates on normal and RNAi knockdown cells

The uptake of adenovirus 5 (Ad5) in HEK293 cells is dependent on the interaction of viral fiber protein and the coxsackie and adenovirus receptor (CAR) on the cellular surface. Thus, we first asked the question, whether our previously described RNA interference (RNAi) knockdown cell line B6 (compare section 4.2.2), expressing the RNAi suppressor protein P19, exhibit similar amounts of CAR receptors on the cellular membrane. Therefore, CAR expression was measured from HEK293 and B6 cells by flow cytometry. Similar amounts of fluorescent signal in the B6 cells in comparison to HEK293 cells revealed no statistically relevant alteration of the CAR expression pattern in our RNAi deficient cell line (Figure 5.1). Subsequently, identical infection rates can be expected.
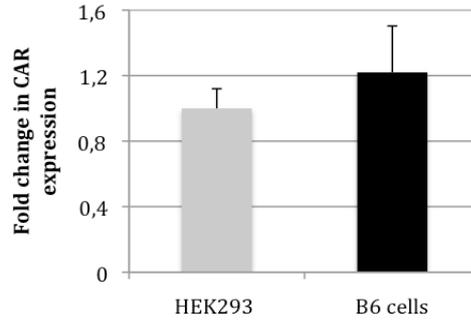
Figure 5.1: Quantification of CAR expression on HEK293 cells and the RNAi knockdown cell line B6 by flow cytometry. HEK293 and B6 cells were stained with an anti-CAR antibody labeled with FITC and measured by flow cytometry. The light emission of HEK293 cells after treatment was set to one and the emission of the B6 cells was caculated and expressed as fold change. p-value > 0.05.

5.2.2   Adenovirus replication is enhanced in the RNAi knockdown cell line B6

It was shown previously that viruses, for instance the primate foamy virus, display an enhanced replication profile in an RNAi knockdown cell line (Lecellier *et al.,* 2005). To test whether also Ad5 shows accelerated replication, either HEK293 or B6 cells were infected with Ad5 at a multiplicity of infection (MOI) of 0.05 and whole cellular DNA was isolated after 2 hours (hrs), 10 hrs, 24 hrs and 48 hrs. Relatively low MOIs were chosen for infection of stably expressing P19 cells to prevent an overload of the cells with viral proteins or RNAs, especially the VA-RNAs, which are usually produced in high amounts (Sano *et al.,* 2006). To analyze replication of Ad5, viral genome copy numbers were calculated from both cell lines by quantitative Real-Time PCR (qRT-PCR). Quantification revealed significantly increased viral genome copy numbers with up to 10-fold more genomes 24 hrs and 48 hrs after infection in the RNAi knockdown cell line B6 in comparison to the parental cell line HEK293 (**Figure 5.2A**). The initial amount of viral genome copies after 2 hrs and subsequently the infection efficiencies were comparable in both cell lines. It is of note that within our experimental set up a sufficient amount of P19 in the B6 cells during infection is crucial (Qiu *et al.,* 2002; Szittya *et al.,* 2002; Rawlings 2010). Therefore, we isolated RNA from infected cells and performed reverse transcription (RT). The cDNA was then analysed by qRT-PCR to track p19 mRNA molecules. Quantitative RT-PCR results demonstrated that the amount of p19 decreased to about 22% of basic value at later time points during infection, which may be due to the shut down of the host cell mRNA transport by viral encoded proteins (**Figure 5.2B**).
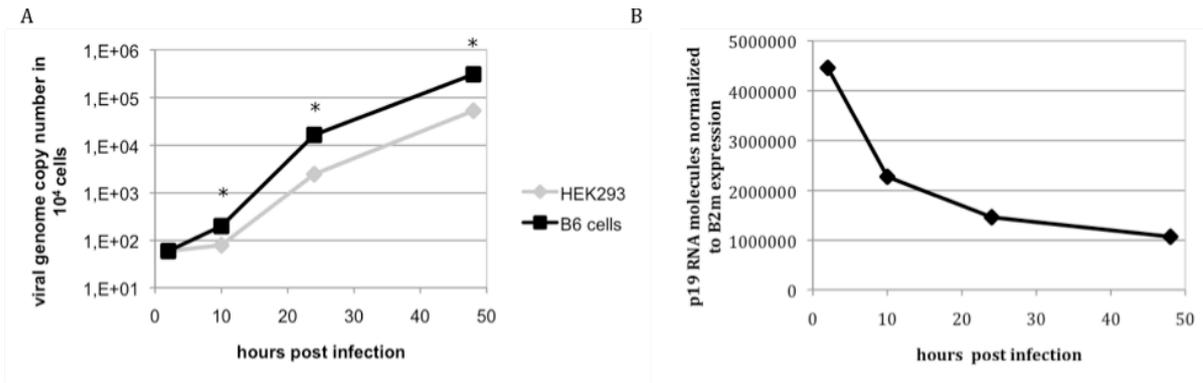
Figure 5.2: Quantification of adenoviral genome copy numbers derived from B6 cells in comparison to HEK293 and analysis of the p19 RNA status during infection. All results are statistically relevant with a p-value < 0.05. (A) Quantifiication of adenoviral genome copy numbers in B6 cells and HEK293 cells after infection. HEK293 and B6 cells were infected at an MOI of 0.05 and genomic DNA was isolated 2 hrs, 10 hrs, 24 hrs and 48 hrs post infection. Viral genome copy numbers were quantified using hexon specific primers for qRT-PCR and were normalized to expression levels of human B2m. (B) Analysis of p19 RNA molecules during infection of adenovirus at an MOI of 0.05. B6 cells were infected at an MOI of 0.05 and RNA was isolated at indicated time points. RNA was then subjected to reverse transcription and cDNA was normalized to endogenous human B2m expression levels of 10 000 molecules.

5.2.3 Replication of Bwtp19ΔE3 is significantly enhanced in comparison to wtAd and the control virus AdΔfiberIL

To further improve Ad5 replication, we attempted to increase P19 levels by introducing the *p19* cDNA into the adenovirus genome and couple its transcription to the adenovirus fiber protein. Therefore, an expression cassette containing parts of the flanking regions in the adenovirus genome (58 nt overlapping sequence to the 3´end of the fiber and 58 nt overlapping nucleotides to the sequence downstream of the fiber gene), the internal ribosomal entry site (IRES) of the encephalo myocarditis virus (EMCV), a spacer fragment, the p19 cDNA and a polyA signal was introduced into an E3-deleted Ad5 bacterial artifical chromosome (BAC) by homologous recombination (**Figure 5.3A**). We used an E3-deleted adenovirus BAC to ensure proper packaging of the adenoviral genome, because we introduced a DNA fragment of 1400 bp length, which may exceed the Ad packaging capacity. After reconstitution of single plaque forming viruses, respective lyates were used to re-infect HEK293 cells. After isolation of whole cellular DNA the specific 1700 bp fragment (including parts of the fiber) introduced into the Ad5 BAC could be confirmed by PCR (data not shown). Furthermore *p19* mRNA expression of two independent single plaques after reverse transcription (RT) and PCR with p19 specifiic primers confirmed functional viruses (**Figure 5.3B**). Hence, viral lysate of clone 2 was amplified, purified and titrated resulting in the virus Bwtp19ΔE3 (**Figure 5.3A**, upper panel). Viral titers obtained from Bwtp19ΔE3 were comparable to wtAd5 (data not shown).
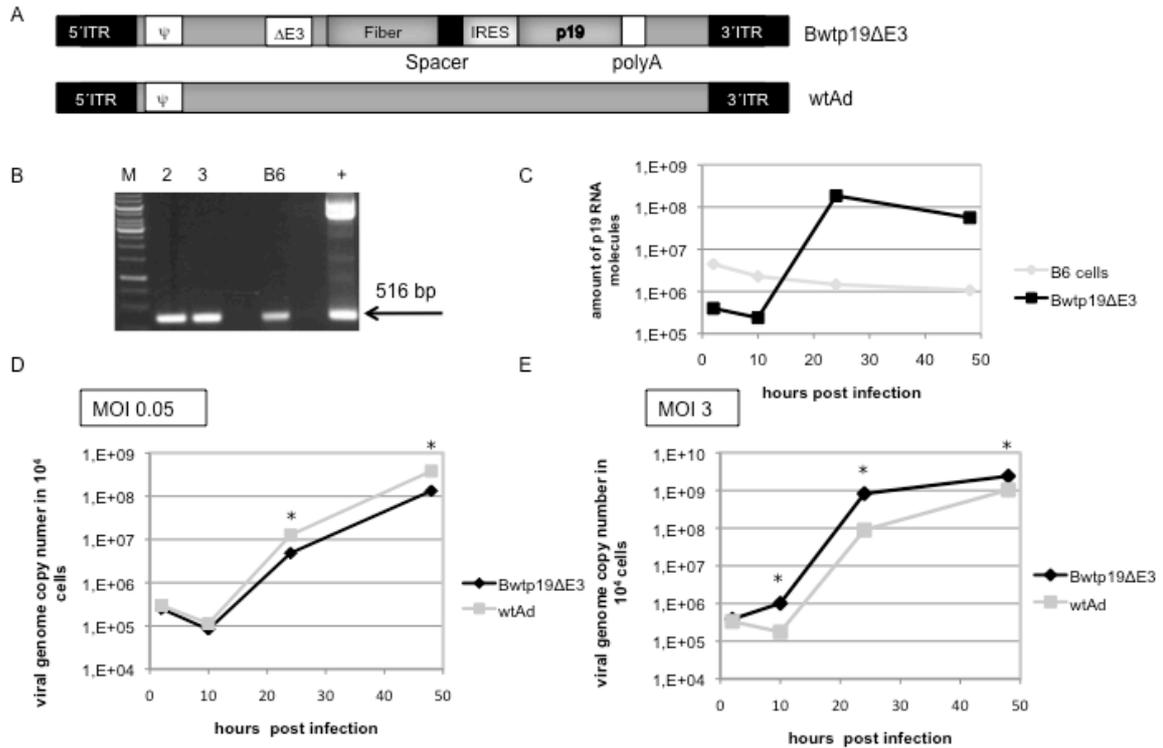
Figure 5.3: Design and characterization of a p19 expressing adenovirus deleted in E3 and analyzing its replication properties in comparison to wtAd5. (A) Constructs used to analyze replication efficiency of a *p19* expressing adenovirus. Upper panel: Bwtp19ΔE3: adenovirus containing a *p19* expression cassette expressed under the control of the fiber promoter. The spacer, the internal ribosomal entry site (IRES), P19 and a polyadenylation signal (polyA) containing fragment was inserted into the E3-deleted bacterial artificial chromosome (BAC) by homologous recombination and virus was reconstituted. Lower panel: wildtype adenovirus genome (wtAd5). (B) *P19* mRNA expression from the BAC-derived virus Bwtp19ΔE3 in comparison to stably *p19* expressing B6 cells. HEK293 cells were infected with the virus Bwtp19ΔE3 at a MOI of 1 and 24 hours post-infection RNA was isolated and reverse transcribed. The generated cDNA was then used as template for a PCR with *p19* specific primers. As control, reverse transcribed RNA from B6 cells and genomic DNA of Bwtp19ΔE3 infected cells are shown. (C) Quantification of p19 mRNA molecules during infection with Bwtp19ΔE3. HEK293 cells were infected with Bwtp19ΔE3 at an MOI of 3 and RNA was isolated and reverse transcribed. The cDNA was subjected to qRT-PCR reaction and normalized to 10,000 molecules of the internal control (human B2m). Quantification of viral genome copy numbers after infection of HEK293 cells at an MOI of 0.05 is displayed in (D) and at an MOI 3 in (E). After infection whole cellular DNA was isolated after given time points and DNA was quantified with hexon specific primers and normalized to human B2m. The amount of viral genomes was adopted to 10^4 cells. * indicates a statistically significant result; * p-value< 0.05.

To prove that enhanced virus replication in cells infected with the P19 expressing virus Bwtp19ΔE3 is due to enhanced P19 expression levels compared to the stably expressing cell line B6, *p19* mRNA levels were determined by qRT-PCR during virus infection. We infected HEK293 cells with the virus Bwtp19ΔE3 at an MOI of 3 and isolated RNA at the ndicated time points. After RT reaction, *p19* RNA molecules were quantified and the results confirmed a strong increase of p19 mRNA levels compared to B6 cells, reflecting the expression pattern of the fiber protein (**Figure 5.3C**). During infection with the virus

Bwtp19ΔE3, *p19* RNA expression levels were enhanced up to 100-fold 24 hrs and 48 hrs post infection when compared to the B6 cell line.

As the generated Bwtp19ΔE3 showed a high P19 expression level we hypothesized that there could also be a significant effect in virus replication. Subsequently, we investigated whether the newly designed virus Bwtp19ΔE3 displays an advanced replication profile in comparison to a control virus. As already mentioned before the amount of P19 protein is a major hurdle within the experimental set up and therefore, we first tested pre-conditions concerning the adenovirus transducing units required in our assay. We infected HEK293 cells with Bwtp19ΔE3 or wtAd5 (**Figure 5.3A**, lower panel) either at an MOI of 0.05 (**Figure 5.3D**) or 3 (**Figure 5.3E**), isolated whole genomic DNA and quantified viral genome copy numbers at the standard time points. QRT-PCR results confirmed our hypothesis that at an MOI of 3, and therefore higher P19 expression levels, produce sufficient amounts of P19 to enhance viral replication up to 10-fold 24 hours post infection, whereas an MOI of 0.05 was not sufficient (**Figure 5.3D** and **E**). In fact, we observed a slight increase in wtAd5 replication levels. This clearly indicated that the P19 effect on virus replication is controlled by the amount of P19 protein. Furthermore, we speculated that the slight decrease of Bwtp19ΔE3 replication compared to wtAd5 using an MOI of 0.05 could be due to an attenuation of virus replication because of the deletion of the E3 gene or introduction of a DNA sequence into the adenoviral genome, which may destabilize the viral DNA. Therefore, we explored another control virus, the virus AdΔfiberIL, harboring the same DNA fragment connected to the fiber but with a luciferase cDNA instead of the *p19* (**Figure 5.4A**, upper panel) (Rivera *et al.,* 2004). In addition, AdΔfiberIL contains a 24 bp deletion in the E1A gene, however, this has no effect on replication in the HEK293 cell line (data not shown). After infection of these viruses into HEK293 cells at an MOI of 3, quantification of viral genome copy numbers revealed significantly enhanced virus replication of Bwtp19ΔE3 compared to AdΔfiberIL, with up to 100-fold more viral genomes 24 hours post infection (**Figure 5.4B**). Furthermore, after titration of the viral lysates we obtained an up to 10-fold higher amount of viral particles from Bwtp19ΔE3 infection at 48 hours post infection, indicating a faster replication cycle in the presence of proper levels of P19 (**Figure 5.4C**).
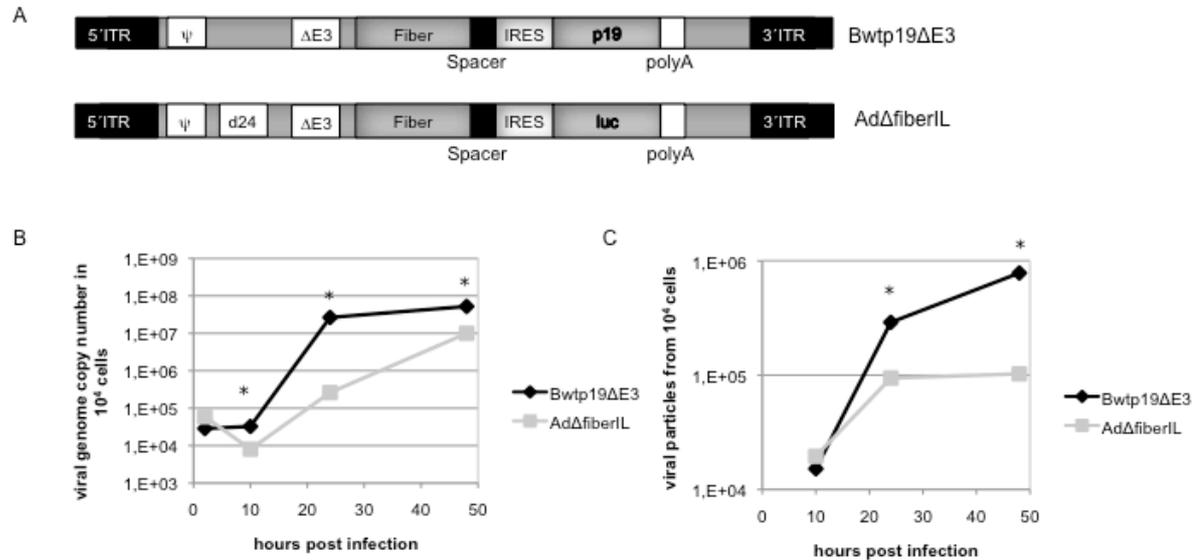
Figure 5.4: Bwtp19ΔE3 replication and virus production in HEK293 cells is enhanced in comparison to the control virus AdΔfiberIL. (A) Viruses used to analyze the influence of P19 on adenovirus replication. Upper panel: Bwtp19ΔE3, an adenovirus lacking E3 but containing the *p19* expression cassette (see also **Figure 5.3A**, upper panel). Lower panel: AdΔfiberIL, an E3-deleted adenovirus harbouring a luciferase expression cassette under control of the major late promoter (MLP) and a 24 bp deletion in the E1a gene (Rivera *et al.,* 2004). HEK293 cells were infected with Bwtp19ΔE3 and AdΔfiberIL at an MOI of 3. (B) A time course was performed and whole cellular DNA was isolated to quantify adenoviral genomes using hexon specific primers and normalized to B2m. (C) Lysates were harvested and viral particles were measured after reinfection of HEK293 cells with the lysates at the given time points. 2 hours post infection whole genomic DNA was isolated and viral genomes were quantified using hexon specific primers and normalized to hB2m. * indicates statistically significant results by calculating a p-value< 0.05.

5.2.4 Enhanced expression of adenovirus functional proteins

Adenoviral DNA appears in the nucleus approximately after 50 minutes, whereas replication starts around 3 hours post infection. Several viral proteins are involved in this process, thus we speculated that enhanced replication measured in the RNAi knockdown cell line B6 and with the p19 expressing adenovirus compared to controls may be due to increased expression levels of viral proteins. We have chosen 3 proteins encoded by the early transcription unit, encompassing the E1B55K protein, the ssDNA binding protein (DBP) and the E4Orf6 protein which all are responsible for either replication or mRNA stability and transport. Furthermore, also the structural proteins fiber and hexon were analyzed. As internal control GAPDH protein levels were detected, to demonstrate equal protein amounts.

In concordance with the experiment shown in **Figure 5.2A** we analyzed protein expression after infection of HEK293 and B6 cells with wtAd5 at an MOI of 0.05. Protein lysates were isolated at various time points post infection, equal amounts were separated on a 10% SDS polyacrylamid gel (SDS-PAGE) and blotted on a PVDF membrane. Proteins were analyzed using anti-DBP, anti-E1B55K, anti-E4Orf6, anti-Fiber and anti-Hexon and the respective peroxidase labeled secondary antibodies (**Figure 5.5**). We found that there was no difference in the overall expression levels between the two cell lines HEK293 and B6 as demonstrated by similar GAPDH expression leves (**Figure 5.5A**, GAPDH). Furthermore, the levels of the ssDNA-binding protein and hexon protein showed no changed profile in the B6 cell line (**Figure 5.5A**, DBP and Hexon), but E1B55K and the E4Orf6 were enhanced during
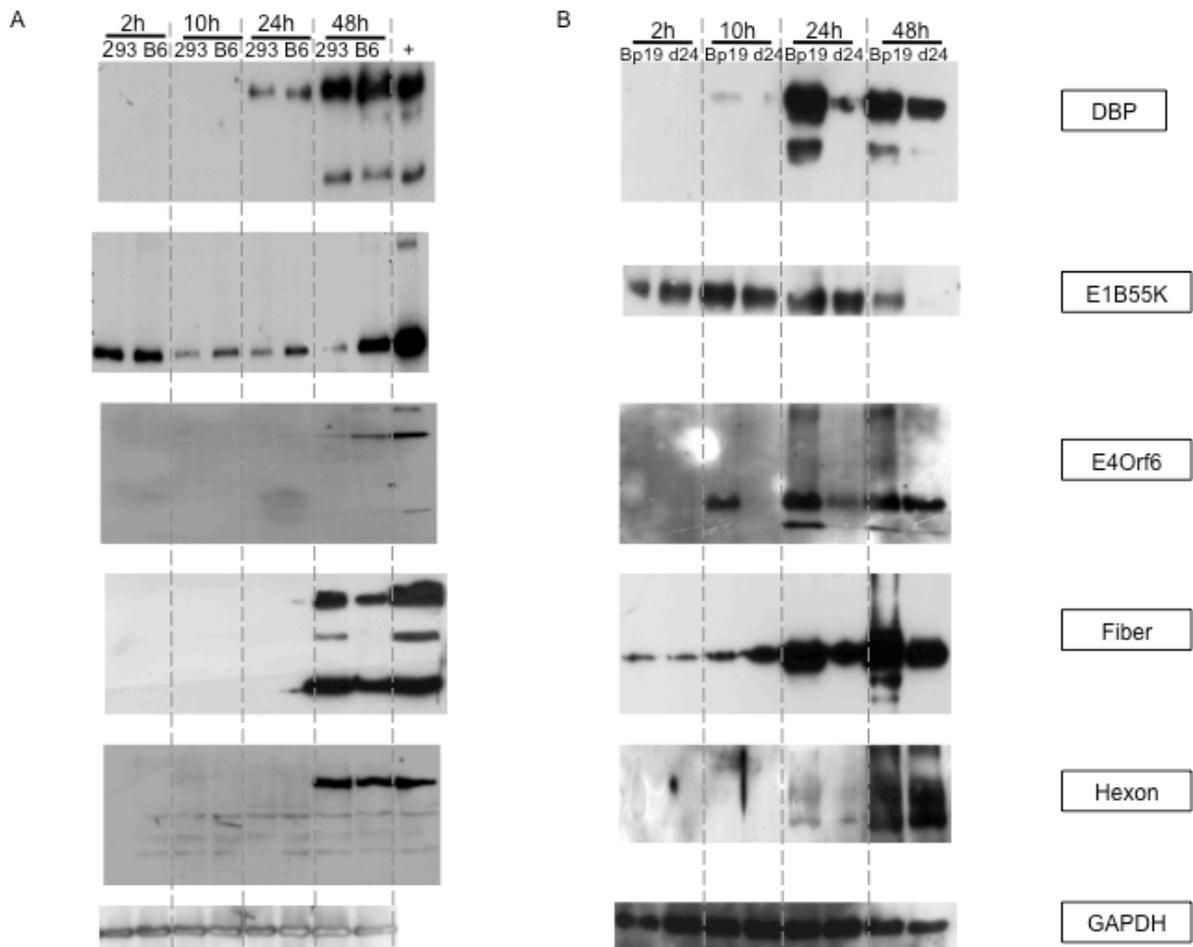
Figure 5.5: Viral protein expression measured by Western Blot analysis after adenovirus infection. HEK293 or B6 cell lysates from assays shown in **Figure 5.2A** (A) and lysates after infection with Bwtp19ΔE3 and AdΔfiberIL shown in **Figure 5.4B** (B) were used to isolate proteins at the given time points. Equal protein amounts were separated on a 10% SDS polyacrylamid gel and blotted on a PVDF membrane. Detection was carried out using primary antibodies against respective proteins (right panel). Secondary antibodies were peroxidase labelled. Detection was performed using ECL solution. Bp19: Bwtp19ΔE3; d24: AdΔfiberIL.

infection in the *p19* expressing cell line (**Figure 5.5A**, E1B55K and E4Orf6). Notably, E1B55K seems to accumulate during infection, since highest expression was detected 48 hrs post infection in comparsion to the parental cell line HEK293. In contrast, overall protein levels of fiber is decreased in B6 cells in comparison to HEK293 cells, wheras monomeric fiber molecules show similar expression at 48 hours post infection (**Figure 5.5A**, Fiber).

In contrast, the comparison of protein levels from the infection experiment performed with the Bwtp19ΔE3 and the control virus AdΔfiberIL (see also **Figure 5.4**) revealed strongly enhanced DBP, E4Orf6 and fiber levels of Bwtp19ΔE3. Nevertheless there was a prominent peak 24 hours post infection (**Figure 5.5B**, DBP, E4Orf6 and Fiber), which reflects the highest *p19* expression level at this time point (**Figure 5.3C**). However, E1B55K expression is only slightly increased 10 and 48 hours post infection and hexon levels are unaltered compared to the stably *p19* expressing cell line B6 (**Figure 5.5B**, E1B55K and Hexon). To investigate whether this effect is due to advanced translation, also the mRNA levels of the respective proteins (**Figure 5.5B)** were quantified. We obtained higher RNA expression levels for all tested viral proteins (**Figure 5.6**). The analysis of the structural proteins fiber and hexon revealed that the strongest effect could be observed 24 hours post infection (**Figure 5.6**, hexon and fiber). We speculate that this discrepancy in protein expression between the stably *p19* expressing cell line B6 and the *p19* expressing adenovirus is due to different P19 protein levels in the systems together with the higher MOIs we used with the Bwtp19ΔE3. Nevertheless, viral early proteins amount are enhanced in the presence of *p19* expression, which may be responsible for the increased virus production.
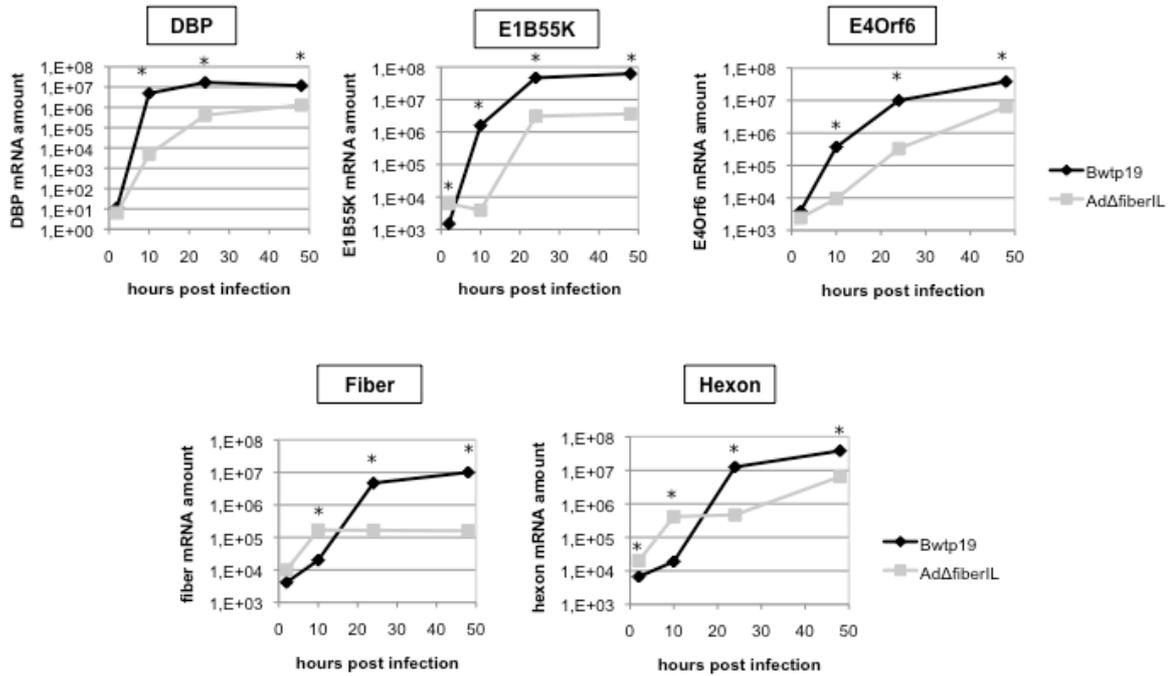
Figure 5.6: Quantification of viral RNA expression of the Bwtp19ΔE3 in comparison to AdΔfiberIL. HEK293 cells were infected with Bwtp19ΔE3 or AdΔfiberIL at a MOI of 3 and RNA was isolated at given time points post infection. RNAs were subjected to reverse transcription and viral mRNA amounts were quantified from cDNA using different adenovirus primers displayed in **Table 5.1**. Quantitative Real-Time PCR results were normalized to 10 000 molecules of hB2m as internal control. * indicates a p-value < 0.05.

5.2.5   Status of VA-RNAs and svaRNAs in the presence of P19

The wtAd5 VA-RNAs are known to interact with several parts of the RNAi pathway. After export into the cytoplasm, VA-RNAs were processed by Dicer into 19-29 nucleotide long small virus associated RNAs (sva-RNAs), which are able to enter the RNA induced silencing complex RISC. As VA-RNAs share structural features with cellular micro RNAs (miRNAs), we speculated that they could also be bound by P19 and may contribute to the observed effect on virus replication. Therefore, we isolated His-tagged P19 from infected B6 cells or as control infected HEK293 cells, using magnetic beads. After purifcation, small RNAs were purified from the protein fraction using different conditions and inserted into a polyA adding reaction followed by cDNA synthesis. In order to solely amplify sva-RNAs, specific primers for the VAI-RNA (3´VAn-r, **Table 5.1**) and the VAII-RNA (5´VAII, **Table 5.1**) were used and the generated fragments were subcloned and sequenced (**Figure 5.7A** and **5.7B**, upper panel). Using this method we could show that sva-RNAs from VAI-RNA as well as from VAII-RNA origin are bound to P19 and may be inhibited during infection.

It is estimated that miRNAs incorporated into the P19 dimer were translocated to the cellular processing bodies, where downstream processing of the RNA takes place (Beckham and Parker 2008; Eulalio *et al.,* 2008). Thus, we aimed at analyzing the fate of the sva-RNAs after interaction with the P19 dimer. HEK293 cells and the *p19* expressing cell line B6 were infected with wtAd5 at an MOI of 0.05 and small RNAs were isolated at different time points post infection (**Figure 5.7**, lower panel). After performing Northern Blot analysis using an sva-RNA specific probe either for VAI-RNA (3´Van probe) or VAII-RNA (3´VAII probe) (see
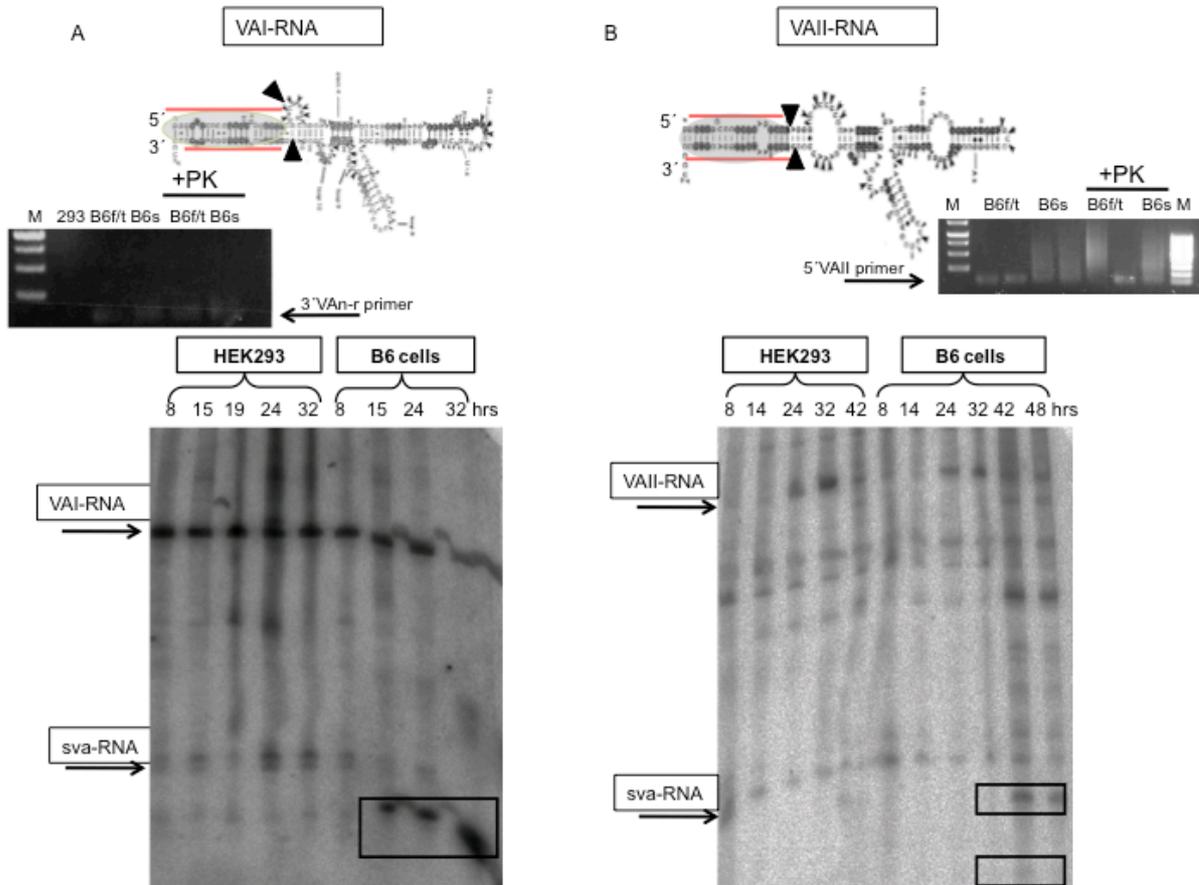
Figure 5.7: Binding of sva-RNAs to P19 and the fate of the svaRNAs during infection. Upper panel: structure of the VAI-RNA (A) and VAII- RNA (B). Highlighted by a grey circle are the predicted sva-RNAs generated from the mature VA-RNA by Dicer processing. Middle panel: PCR fragments of sva-RNAs. B6 cells were infected with wtAd5 at an MOI of 10 and P19 protein was purified 24 hours post infection. Small RNA molecules were isolated from the protein fraction and inserted into a polyA polymerase reaction followed by cDNA synthesis. PCR was then performed with an sva-RNA specific primer for 3´stem of VAI-RNA (3´Van-r) (A) or 5´stem of VAII-RNA (5´VAII) and a primer of the polydT adapter. M: Marker; 293: HEK293 cells; B6f/t: B6 cells were lysed by 4 consecutive freeze/thaw cycles; B6s: B6 cells were sonicated 5 times on ice; PK: Proteinkinase buffer was used to isolate miRNAs from P19. Other miRNAs were isolated using Qiazol reagent and following the manufacturer instructions. Lower panel: Northern Blot analysis to track the fate of sva-RNAs during adenovirus infection in HEK293 cells and B6 cells. HEK293 cells and the RNAi knockdown cell line B6 were infected at an MOI of 0.05 and small RNAs were isolated at time points displayed in the figure. Equal RNA amounts were loaded on a Northern gel, blotted to a NylonBond+ membrane and detected with a-P32 labbeled probe specific for either the stem of the VAI-RNA (3´Van) (A) or the VAII-RNA (5´VAII) (B). Degradation products observed in the B6 cell line were highlighted in boxes.

also **Table 5.1**) we observed VA-RNAs, sva-RNAs and also products of smaller size compared to sva-RNAs, which may refere to degraded sva-RNAs (black boxes in **Figure 5.7**, lower panel). Furthermore, svaRNAs from VAI-RNA origin (**Figure 5.7A**, lower panel) are degraded much earlier than the ones from VAII-RNA (3´VAII probe (**Figure 5.7B**, lower panel) as the small fragment appears at 15 hours post infection whereas the ones from VAII-RNA can be observed not until 42 hours post infection (**Figure 5.7B**. lower panel). The binding of the sva-RNAs to P19 suggests a contribution of the small VA-RNA derived fragments to the enhanced replication, however a direct proof is missing.

Therefore, we investigated a VAII-deleted adenovirus obtained from Göran Akusjärvi (Uppsala University, Uppsala, Sweden). The deletion was shown by Northern Blot analysis (data not shown). Replication was determined in HEK293 cells and the RNAi knockdown cell line B6 infected at an MOI of 0.5 (**Figure 5.8**). The quantification of viral genome copy numbers revealed a strong increase up to 100-fold in viral genome copies 10 hours post infection. However, replication adopted to slightly lower levels of viral genome copy numbers compared to virus derived from HEK293 cells 24 and 48 hours post infection (**Figure 5.8**). Thus, we speculated that VAII-RNA are rather important at later time points post infection as the lack of VAII-RNA leads to abrogation of the virus replication at later time points. This is in concordance with our Northern analysis, which showed that svaRNAs were processed only at late time points during infection.
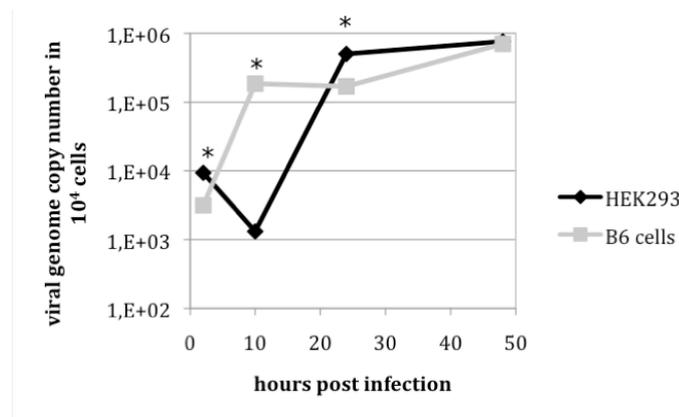
Figure 5.8: Replication of a VAII-deleted virus in HEK293 cells and the RNAi knockdown cell line B6. The VAII-deleted Virus dl705 was infected at an MOI of 0.1 into HEK293 cells and B6 cells. Whole cellular DNA was isolated at standard time points and viral genome copy numbers were quantified using gexon specific primers. Results were normalized to B2m as internal control and viral genome copies were calculated on the basis of 10^4 cells. * indicates a p-value < 0.05.

5.2.6 Application of *p19* expression to improve production of high-capacity adenoviral vectors

Recombinant adenoviral vectors are widely used in gene therapy. Especially the most advanced generation, the high-capacity adenoviral vectors (HC-AdV) hold great promise concerning safety and efficacy. With that respect it was shown that transgenes packaged in an HC-AdV introduced into several small and large animal models resulted into long-term transgene expression. However, the production of these HC-AdVs is sophisticated and only a few groups are able to produce these vectors in sufficient amounts. Therefore, we already generated a detailed protocol for their production (compare **chapter 2**) but we wanted to further improve the viral titers. Thus, we took advantage of our finding that Ad replication is
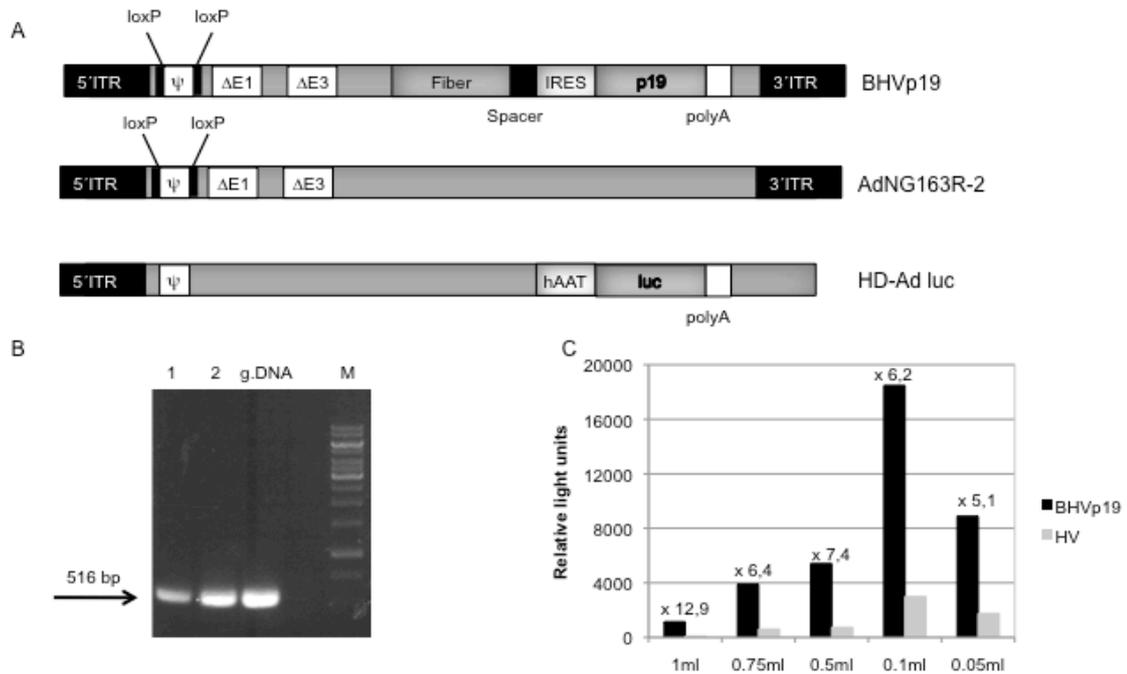
Figure 5.9: Comparison of the packaging efficiency of a luciferase expressing high-capacity adenovirus (HC-AdV) using a *p19* expressing helper virus (HV) or a conventionally used HV. (A) Viruses used to analyse packaging efficiency of HC-AdV by the two different helper viruses. Upper panel: BHVp19, an E3-, E1- deleted helper virus that contains the p19 expression cassette under the fiber promoter connected via a spacer and an IRES sequence. Additionally, the packaging signal is flanked by loxP sites. Middle panel: AdNG163R-2 standard helper virus deleted in E1 and E3 contains a loxP flanked packaging signal. Lower panel: HD-Ad luc, HC-AdV, lacking all viral coding sequences only containing the two ITRs and the packaging signal. This HC-AdV harbours a luciferase expression cassette driven by the human α1-antitrypsin promoter (hAAT) and the SV40 polyA signal (Jager and Ehrhardt 2007). (B) P19 mRNA expression from the helper virus BHVp19. HEK293 cells were infected with BHVp19 single clone lysates and RNA was isolated and reverse transcribed. The generated cDNA was then amplified using *p19* specific primers. M: Marker; g.DNA: genomic DNA from BHVp19 infection; 1, 2: two different single viral plaque lysates. (C) Luciferase expression after amplification of HD-Ad luc with either BHVp19 or standard AdNG163R-2. 116 cells (HC-AdV producer cell line) were co-infected with HD-Adluc and either BHVp19 or AdNG163-2. Forty-eight hours post infection cell lysates were harvested and Huh7 cells were reinfected with the generated lysates using different amounts. 24 hrs post infection cells were prepared for quantifying luciferase expression.

enhanced in the presence of P19. We introduced the *p19* expression cassette, also used for Bwtp19ΔE3, into a BAC containing a helper virus genome by homologous recombination resulting in BHVp19 (**Figure 5.9A**, upper panel). P19 expression on mRNA level was approved after RT by conventional PCR with *p19* specific primers. To test whether the newly generated helper virus BHVp19 displays advantagous features compared to a standard helper virus (**Figure 5.9A**, lower panel) we measured titers of a high-capacity adenoviral vector expressing luciferase (**Figure 5.9A**, middle panel). After reinfection of Huh7 cells with different amounts of the generated lysates, we could clearly observe increased viral titers with an average of 6-fold higher luciferase expression (**Figure 5.9B**). Notably, helper virus contamination remains at normal levels under 1%. These experiments clearly demonstrated that our novel BHVp19 is superior to the conventionally AdNG163R-2 for HC-AdV production

5.3 Discussion

In the present study we aimed at getting further insights into adenovirus-host interactions with a particular focus on the influence of the RNAi pathway on virus replication. Thus, we took advantage of the RNAi suppressor protein P19 in different set-ups to analyze its impact on the adenovirus life cycle. Our results showed, that Ad5 replicates significantly faster and grows to higher titers in the presence of P19, suggesting an important role of the RNAi pathway on the adenovirus life cycle.

Very recently, de Vries and his colleagues analyzed the influence of the RNAi pathway on HIV replication and obtained an upregulation of virus production in the presence of different RNAi supressor proteins including P19, which resulted in 50-fold enhanced Sindbis virus titers (de Vries *et al.,* 2008). In contrast to our data, they could not see any difference in the replication profile of an E1-deleted adenovirus using *p19* expressing cells in comparison to control cells. Notably, de Vries *et al*., investigated adenovirus titers 6 days post infection at an MOI of 0.05. We on the other hand observed 10-fold faster replication in the presence of the RNAi suppressor protein P19 in the B6 cell line (**Figure 5.2**). Concluding from our results, we speculate that *p19* expression in the cytoplasm is strongly decreased due to the shut down of the host RNA turnover initiated by adenovirus replication as we also observed significant decreased *p19* mRNA levels during the time course of infection (**Figure 5.2B**) (Curiel and Douglas 2002). Different groups already demonstrated that the dose of P19 in the cell is a crucial factor regarding its functional activities (Qiu *et al.,* 2002; Szittya *et al.,* 2002; Scholthof 2006). In the study by de Vries this point was not considered but instead it was discussed, that the inappropriate intracellular localization of P19 may have caused the

failure. In a recent dissertation from R. Rawlings, however, the strong interaction of P19 with ds-siRNAs was shown because an over 20-fold bias towards p19-siRNA complexes in comparison to Dicer-siRNA interactions was detected. Unexpectedly, P19 was also able to destroy siRNA-RISC complexes (Rawlings 2010). Furthermore, Renata Rawling disproved the existing model of a 1:1 stoichiometric binding of P19 to the siRNA (Scholthof 2006) and revealed that the binding follows a sub-stoichiometric process consisting of fast association and dissociation (Rawlings 2010). Although these facts would suggest independency of the P19 dose, the amount of protein still plays a critical role. Thus, we believe that it is more likely that the amount of P19, rather than the cellular localization causes the defect of the P19 protein to increase adenovirus replication.

In our experimental set-up we investigated two different strategies to express *p19* in HEK293 cells resulting into moderate and strong effects on upregulation of adenovirus genome replication. On the one hand, *p19* was stably expressed in a cell line comparable to the approach by de Vries and colleagues, which mediates a continuous but low-level *p19* expression (**Figure 5.2B**) (de Vries *et al.,* 2008). On the other hand P19 was inserted into the adenoviral genome under the control of the MLP promoter (Bwtp19ΔE3) resulting in high amounts of the RNAi suppressor protein at later time points after infection because *p19* expression is directly coupled to adenovirus genome replication (**Figure 5.3C**). Due to the higher P19 dose, adenovirus replication was significantly increased with up to 100-fold more genome copy numbers in the viral context (**Figure 5.4 B)**. With respect to the B6 cell line with less pronounce effects on adenovirus replication, there is evidence that infection of cells with an adenoviral vector blocks the host mRNA transport and transcription by several viral proteins encoded by the E1B and E4 transcription units (Curiel and Douglas 2002). Therefore, besides influencing the host mRNA metabolism the transcription of *p19* in our stable cell line B6 was also affected resulting in 80% decreased *p19* mRNA levels during infection compared to basic *p19* levels in uninfected cells (**Figure 5.2B**). We believe that this could be the reason for the less pronounced upregulation of viral genome replication in stably *p19* expressing cells.

The highest P19 protein level was observed 24 hours after Bwtp19ΔE3 infection, which reflects the expression profile of the fiber protein (**Figure 5.3C**). Transcription of the late transcription unit starts round 5 hrs post infection and shows the highest expression level approximately at this time point as concluded from the qRT-PCR data (**Figure 5.6**, fiber). Consequently, Bwtp19ΔE3 replication was strongly increased at this particular time point with a 100-fold more copy numbers and 8-fold higher titers in comparison to the control virus AdΔfiberIL (**Figure 5.4B** and **C**). Notably, Bwtp19ΔE3 titers were increased 10-fold after

48 hrs, thus, the enhanced number of adenovirus DNA molecules was maintained in the cells.

In order to ascertain the mechanism of up regulation of adenoviral replication, we analyzed expression levels of adenoviral proteins, which are important during adenoviral life cycle and may initiate a faster and more productive virus replication. In general, the adenovirus replication and virus production cycle is divided into two phases, the early transcription of predominantly regulatory proteins, responsible for transcription and replication and the expression of the late transcription unit, mainly encoding for structural proteins like the major capsid components hexon, fiber and penton (Curiel and Douglas 2002).

In the present study, proteins of the early transcription unit, in particular proteins E1B55K and E4Orf6 displayed an increased expression level in the presence of P19 in the B6 cell line (**Figure 5.5A**). The distinct regulatory functions of the E1B55K and E4Orf6 proteins during the adenovirus life cycle may thereby play a decisive role. A complex consisting of both proteins is required to bind p53 and initiate its proteasom-dependent degradation to prevent cell cycle arrest (Curiel and Douglas 2002). Furthermore, each protein alone is necessary to produce a cellular environment in favour of virus replication, for instance the E4Orf6 protein shuts down the host cell translation machinery but selectively stabilizes and transports viral mRNAs (Curiel and Douglas 2002). Thus, the accumulation of both proteins under RNAi knockdown conditions may prolong the production period of virus particles because E4Orf6 and E1B55K may stabilize selectively the adenovirus RNA turnover and lead to an effective down regulation of apoptosis induction.

We observed a different expression profile of viral proteins when we compared different sources of *p19* expression. As mentioned before *p19* expression was based on somatic integration of a *p19* expression cassette into the host genome or it was transduced into the cells utilizing a replicating adenovirus carrying a *p19* transcription unit. We speculate that this difference in viral protein expression is caused by the unequal time course and levels of *p19* expression (**Figures 5.3C**). P19 protein levels are clearly dependent on the experimental set-up and the varying virus loads used in the experiments. Furthermore, in case of the B6 cell line, the P19 may modulate the miRNA profile of the cell in advance of viral replication and therefore promote especially immediate early genes like E1B55K (**Figure 5.4**). In contrast, after Bwtp19ΔE3 infection P19 proteins are present at the earliest 3 hrs post infection. Thus, proteins, which were expressed later like the E4Orf6 and the DBP are affected to a greater extend (**Figure 5.5**).

Notably, E4Orf6 expression is significantly increased in both setups. However, the low infectious titer of only 0.05 transducing units used in the stable expressing cell line B6, led to low E4Orf6 levels even 48 hours post infection (**Figure 5.5**, E4Orf6). In contrast, in the viral context (Bwtp19ΔE3) we infected with an MOI of 3 leading to high E4Orf6 expression levels already 10 hours post infection. We speculate that the increased E4Orf6 protein levels enforce viral mRNA transport and stabilize the mRNA in the cytoplasm even at early time points. This hypothesis is supported by the strong increased viral mRNA levels observed after Bwtp19ΔE3 infection (**Figure 5.6**). In agreement to that, we also observed increased DBP protein amounts and RNA levels from Bwtp19ΔE3 infected cells another important protein for the initiation of adenovirus replication (**Figure 5.5B**, DBP).

The expression levels of the structural proteins, which would potentially indicate increased production of viral particles, remain almost unaltered. In the viral context, however, as shown in **Figure 5.6** we detected increased mRNA levels of hexon and fiber but protein levels appear unaltered. This is also in concert with the findings from the E1B55K protein and supports the notion that the increased E4Orf6 levels may enforce viral mRNA transport but coincidentally saturation of the translational machinery takes place, finally leading to an accumulation of viral mRNAs. This hypothesis is in agreement with observations of Renata Rawlings, as she detected increased mRNA levels after infection of plant cells with the *p19* expressing tomato bushy stunt virus (Rawlings 2010). Nevertheless, the increased viral titer of Bwtp19ΔE3 (**Figure 5.4C**) strengthens the suggestion that viral structural proteins are produced in excess as more infectious viral particles were produced from nearly the same amount of major capsid proteins present in the cell (**Figure 5.4**). We see this overproduction also in normal adenovirus production procedures, when we purify the virus by cesium chloride centrifugation (**Figure 2.2**). In the second, continuous centrifugation step, empty particles can be obtained, which separate from the complete particles due to the different density.

As already mentioned we observed that the potency of the P19-effect on adenovirus replication strongly depends on the time course and strength of *p19* expression. In our *p19* expressing virus Bwtp19ΔE3 we expressed *p19* under the control of a major late viral promoter. Therefore, it would be of great interest to analyze the replication profile of an adenovirus expressing *p19* under the control of an early viral promoter, for instance from the E1 region. With that strategy the time course and onset of *p19* expression and potentially the expression levels could be varied. However, the group of Dirk Nettelbeck already characterized reporter fusion proteins in the early viral coding regions. These adenoviral

vectors were attenuated in viral growth and particle production, which may be due to instable viral genomes or improper transcription efficiencies (Rivera *et al.,* 2004).

To further shed light on the mechanism involved in the advanced replication, either if its cellular or viral based, we investigated the only currently known products of adenovirus that interacts with the RNAi pathway, the virus associated RNAs I and II (VAI-RNA and VAII-RNA) and their processing products the small virus-associated RNAs (svaRNAs) (Andersson *et al.,* 2005; Aparicio *et al.,* 2006; Sano *et al.,* 2006; Xu *et al.,* 2007; Aparicio *et al.,* 2010). Renata Rawlings demonstrated that P19 acts in a complex consisting of Dicer, P19 and the ds-siRNA, therefore it is speculated that the loading of P19 is very efficient (Rawlings 2010). As svaRNAs share structural features with cellular miRNAs and are generated from Dicer (Aparicio *et al.,* 2006; Sano *et al.,* 2006) we indeed detected sva-RNAs originated from VAI-RNA and VAII-RNAs in the P19 fraction from B6 cells, but not control cells (**Figure 5.7**, middel panel). These svaRNAs are sequestered and degraded as detected by Northern Blot (**Figure 5.7,** lower panel). Notably, in our assay we detected VAI-RNA derived svaRNAs and their degradation fragments much earlier at 15 hrs post infection, whereas small products from VAII-RNA appear not until 42 hours after infection (**Figure 5.7**). This finding was supported by the investigation of a VAII-RNA deleted adenovirus. Up to 24 hrs post infection there was no impact on VAII-RNA-deleted adenovirus replication. However, 24 hrs post infection replication was stopped and converged to normal adenovirus copy numbers (**Figure 5.8**). Although VAI-RNAs are expressed at about 20-fold higher levels, around 2-fold more svaRNAs from VAII-RNA origin were detected within RISC complexes by Xu and colleagues (Xu *et al.,* 2007). Thus, Dicer exhibits a 40-fold higher substrate performance for VAII-RNA in comparison to VAI-RNA (Xu *et al.,* 2007). In addition, it was shown that RISC complexes are occupied at levels of up to 60% with sva-RNAs from VAII-RNA origin at late time points post infection. In conclusion, one can speculate that the tight binding of the VAII-RNA to Dicer, Dicer processing and loading of the RISC complex are highly efficient and svaRNAs are not as accessible to the P19 protein as svaRNAs from VAI-RNA. (**Figure 5.6**) (Xu *et al.,* 2007).

It is estimated that the generation of svaRNAs and subsequently silencing of complement mRNAs predominantly occurs during early times of infection, whereas the inhibition of RNAi is a relatively late event to prevent degradation of their own RNAs. However, one has to take into account, that cellular miRNAs have a relatively long half-life of 24 hrs, which therefore exceeds the adenovirus life cycle and may not be influenced by inhibition of the exportin pathway and Dicer. Solely the saturation of RISC complex by sva-RNAs could compete with

pre-existing cellular miRNAs, as it was demonstrated that 80% of RISC is occupied with svaRNAs at late infection phases (Xu *et al.,* 2007).

Assuming that svaRNAs play a role, several models on how P19 may influence viral replication at early and late time points of infection are possible. Starting with early time points (in particulare about 6 hours post infection) one could hypothesize that P19 binds to svaRNAs and other cellular or viral miRNAs. This lead to the increased production of E1B55K and E4Orf6 (**Figure 5.5**), which in turn stabilizes viral mRNAs in the cytoplasm and further boosts viral replication. However, during late phases of infection VA-RNAs are predominantly produced to inhibit the RNAi pathway to prevent down regulation of their own genes (Xu *et al.,* 2007). Although no further adenoviral miRNAs have been identified so far, the genome composition with convergent transcriptional units spread on both strands of the viral genome could lead to dsRNAs intermediates. These dsRNA molecules could be able to inhibit viral proteins. Besides this, also cellular miRNAs may inhibit viral proteins. Thus high P19 levels, present in late phase of infection in the case of Bwtp19ΔE3 may contribute to downregulate and sequester pre-existing cellular and viral miRNAs. This is in agreement with the lower replication of the VAII-deleted adenovirus dl705 at later time points of infection (**Figure 5.8**). As it was shown that svaRNAs from VAII-RNA origin occupy 60% of RISC it is assumed that the lack of these svaRNAs reduce the inhibition of the RNAi pathway significantly (Xu *et al*., 2007). In contrast, in the stable cell line B6, *p19* is diminished by the shut down of the host mRNA transport (**Figure 5.2**), therefore P19 proteins produced before infection may be already saturated and therefore inactive.

As we detected higher titers from an E3-deleted adenovirus we investigated whether this system can also be subjected to HC-AdV production. In fact, we detected increased luciferase expression levels from the helper virus BHVp19 expressing *p19* under the major late promoter (MLP), in comparison to the standard helper virus AdNG163R-2 (**Figure 5.9**). Importantly, helper virus contamination was similar in both virus preparations as measured by qRT-PCR (data not shown). To reach gene therapy relevant levels, however, we have to demonstrate increased HC-AdV titers also in large-scale production using the spinner flask system (compare to **chapter 2**). Furthermore the actual infectious titer has to be verified by qRT-PCR.

However, in order to unravel the whole mechanism and the real influence of svaRNAs on the enhanced replication in the *p19* expressing cell line one has to use an VAI- and VAII-RNA deleted virus. Furthermore RISC pulldowns to identify miRNAs that appear in P19 or in the argonaut complex in normal and in adenovirus infected cells are suggestable. Future

experiments should also include the analysis of cellular proteins involved in Ad replication, like the Oct1 protein or nuclear factor II (Curiel and Douglas 2002).

In conclusion, in the present study we generated a new system to improve adenovirus replication and the production of HC-AdV. Along this line, the significantly increased virus replication of the *p19* expressing adenovirus Bwtp19ΔE3 may be advantageous for the performance of oncolytic adenoviruses. Faster replication comes along with more efficient viral spread, better tumor penetration and consequently improved tumor regression. Furthermore, we started to investigate the complex interaction of the RNAi pathway with the adenovirus life cycle. However, more detailed information is required to understand the real importance of the silencing mechanism. Therefore, micro arrays to analyse the miRNA profile before and during infection as well as the identification of P19 and argonaute bound miRNAs may further uncover miRNAs that regulate adenovirus infection.

6   Discussion

To date, recombinant adenoviruses are amongst the most prominent viral vectors used in gene therapy (**Figure 1.1**). Their genomic and capsid composition and the life cycle offers great potential to a broad range of applications, including replication-deficient recombinant adenoviruses for the treatment of genetic diseases and replication-competent oncolytic viruses for the treatment of neoplastic diseases. Each indication has individual demands on the vector properties and faces predominantly the cellular response and defense mechanisms in the infected cell.

Monogenetic diseases are the third most frequently treated indication in gene therapy as demonstrated by a statistical analysis from "Gene Therapy Clinical Trials World Wide" (**Figure 1.4**) (Wiley 2010). These diseases are based on a defect of only a single gene, which is mainly due to mutations or deletions in the DNA sequence of the defective gene. Thus, the sufficient introduction of healthy copies of the affected gene by a viral vehicle to restore physiological protein production is a suitable method for the treatment of monogenetic diseases. Moreover, the vector system of choice should mediate lifelong transgene expression ultimately aiming at ameliorating the patient's clinical symptoms or completely rescuing the phenotype.

The treatment of monogenetic disease utilizing viral gene transfer vehicles is intended to be applied to human beings. Therefore, in comparison to initial *in vivo* experiments in mice and dogs either a 3500-fold or a 3.5-fold increase in body mass has to be considered for viral vector preparation. Thus, a prerequisite for performing small and large animal studies and finally clinical trials is the ability to up-scale viral vector production for production of clinical grade vector stocks preferentially with low costs. Using the advanced protocol for large-scale production of HC-AdV presented within this study (**chapter 2**) it is possible to produce up to $1*10^{13}$ viral particles with less than 1% helper virus contamination using 3 liters of producer cells grown in suspension in spinner flasks (**Figure 2.2**). In addition, since there are 5-point magnetic stirrers available to amplify producer cells in 5 spinner flasks at the same time, it is estimated that within one round of amplification the production up to $5*10^{13}$ particles is possible within two weeks. In comparison to other viral vectors currently used for the treatment of monogenetic diseases, for instance lentiviral and adeno-associated viral vectors this means a 100000- and 100- fold increased vector yield from one amplification round (Aucoin *et al.,* 2006; Tiscornia *et al.,* 2006; Smith *et al.,* 2009), respectively. Furthermore, for *in vivo* experiments the exact quantification of transducing units and the detailed characterization of the final viral vector stocks are required. In the case of HC-AdV the

simplified Real-Time PCR protocol provided within this study (**chapter 2**) offers the possibility to titrate different HC-AdV preparation independently of the introduced transgene expression cassette using only one primer pair. Thus, various vector preparations can be titrated comparably and the results obtained from experiments with these vectors are reliable.

Nearly all HC-AdVs available so far are based on the adenovirus serotype 5 (Ad5). It was shown by Waddington and colleagues that the Ad5 hexon could be efficiently recognized by the coagulation factor X in the blood stream. This mediates the liver tropism independently of the naturally interaction of the cellular coxsackie and adenovirus receptor (CAR) with the fiber protein (Waddington *et al.,* 2008). Therefore, AdVs were mainly used to treat liver associated diseases as this serotype has a strong tropism towards this organ. Within this work we demonstrated (**chapter 2**) that besides liver-derived monogenetic diseases such as hemophilia also liver-associated hepatitis B virus infection can be efficiently treated using HC-AdV vectors delivering shRNA sequences (**Figure 2.4 and 2.5**). Uprichard *et al*. already demonstrated the successful transfer of a shRNA incorporated into a first-generation adenoviral vector and detected down regulation of hepatitis B virus specific RNAs in a transgenic mouse model (Uprichard *et al.,* 2005). However, when using first generation adenovirus based vectors to deliver shRNAs, it is important to consider the strong expression of virus-associated RNAs. These double-stranded RNA molecules are produced in enormous amounts of around 10^8 molecules during infection and may compete with the introduced shRNAs for the RNAi enzymes (Akusjarvi *et al.,* 1987; Andersson *et al.,* 2005; Aparicio *et al.,* 2006; Xu *et al.,* 2007). Thus, taking advantage of the special features of adenoviral vectors, the use of HC-AdVs to deliver shRNA sequences into cells is superior because of the improved toxicity profile and the lack of VA-RNA expression.

Although Ad5 based vectors demonstrated efficacy for the treatment of liver associated diseases, there are several limitations when using this vector system for gene transfer. First of all, Ad5 displays a high serum prevalence in the human population and therefore also a high incidence of anti-adenovirus neutralizing antibodies, which in turn can mediate the clearance of the virus, just before reaching the target organ (Xu *et al.,* 2008; Arnberg 2009). Furthermore, the treatment of organs besides the liver is very inefficient and specific methods have to be used, for instance a tracheal catheter to target lung cells (Koehler *et al.,* 2005). In addition, HC-AdV harbours the inverted terminal repeats originated from Ad5, which are essential for proper replication. As shown in **chapter 3** of this work these ITRs however, displayed strong transcriptional activity in a plasmid-based assay (**Figure 3.2**). Transcriptional activity derived from the ITRs could either activate transgene expression in

an undesired tissue or could lead to changes in the promoter activity profile. Thus, serotypes other than Ad5 became of increasing interest in the research community. Regarding neutralizing antibodies, serotypes from subgroup B and D were advantageous as they only showed low serum prevalence (around 1-3% in subgroup B2 and 3-44% in subgroup D) in the Caucasian population (Arnberg 2009). In addition subgroup B adenoviruses and in particular serotypes 11 and 35 use mainly CD46 for cellular entry. Thus, on the one hand they can infect hematopoietic stem cells, escape from neutralizing antibodies and on the other hand they are not recognized by the clotting factor X, thereby omitting liver tropism (Waddington *et al.,* 2008; Arnberg 2009). Unfortunately, for ITRs derived from this preferred subgroup we detected high transcriptional activity and also strong inhibition of the ubiquitously expressed PGK promoter (**Figure 3.2** and **3.3**). Nevertheless, serotype 7 from the subgroup B1, which showed a moderate serum prevalence of around 35-70% and share most features with subgroup B2 Ads did neither alter transgene expression significantly nor influenced promoter activity **(Figure 3.2** and **3.3**). Therefore ITR 7 could be a model candidate for improved HC-AdVs (Arnberg 2009).

Our plasmid-based assay provides some hints about the performance of the ITRs, but expression from a viral vector is influenced by several other viral and cellular factors, too. Along this line it is estimated, that for instance the terminal protein, covalently bound to the ITRs of the adenoviral genome, recruits transcription factors that can bind to motifs located in the ITRs (Curiel and Douglas 2002; Yamamoto *et al.,* 2003). In concordance with these findings, Yamamoto *et al*. identified transcriptional start sites at the beginning of the ITRs at positions 15 and 25, located in close proximity to a TATA box (Yamamoto *et al.,* 2003). Also other motifs, like Oct-1 or NFIII binding sites were predicted for all serotypes, using the TESS program (**Figure 3.1**) (Schug 2008). The TATA box is conserved throughout all serotypes (**Figure 3.1**) and therefore one may speculate that the analyzed ITRs in our study can induce transcription in an adenoviral context, although we did not detect any activity in our plasmid based assays. In accordance with that finding, when we introduced a luciferase expression cassette under the control of the strong viral SV40 promoter in close proximity of the right ITR of an HC-AdV, transgene expression was normal after plasmid transfection. However, upon infection with the respective HC-AdV luciferase expression was completely abrogated (data not shown). Thus, the investigation of the ITR 7 within a viral context is required to demonstrate real improvements.

Although the construction of other than Ad5 serotype recombinant adenoviruses (rAdVs) including HC-AdV is recommended, the practical performance is still sophisticated. To date, the construction of rAdV is dependent on homologous recombination in eukaryotic producer

cells or bacteria, which is inefficient. Moreover, subcloned adenovirus genomes of the various serotypes for easy genetic manipulation are not available to many laboratories at the time (He *et al.,* 1998; Luo *et al.,* 2007). Up to now, most approaches aimed at exchanging one capsid element like the major capsid protein hexon, which is the main target for the neutralizing antibodies and clotting factor X (Waddington *et al.,* 2008; Xu *et al.,* 2008; Alba *et al.,* 2009; Seregin and Amalfitano 2009). But still, cloning of these vectors and virus reconstitution are inefficient because of instability of the capsid structure. Although Ad5/48, a chimeric adenoviral vector based on Ad5 carrying hexon regions from Ad48, could circumvent Ad5 based immunity, a complete exchange of the serotype may be more favourable in terms of immunity, tropism and transgene expression, as also other capsid components play a crucial role (Roberts *et al.,* 2006; Waddington *et al.,* 2008). Of note, there are upcoming strategies for subcloning and genetic manipulation of adenovirus genomes based on bacterial artificial chromosomes (BAC), which simplifies the cloning procedure extensively. This allows subcloning of any adenovirus genome and the introduction of arbitrary genetic manipulations (Hausl *et al.*, unpublished). Within the next few years a whole library of different rAdV could be available based on the complete biological reservoir of human adenoviruses. Thus, it would be possible to use vectors due to the specific demand of the specific therapeutic approach, for instance the serotype 7 we mentioned before, was shown recently to be advantageous for treatment of cancer cells (Wang *et al.,* 2010).

The treatment of monogenetic diseases and persistent chronic infections such as HBV requires a lifelong expression of the therapeutic DNA from the introduced vector. However, our group showed that HC-AdVs mainly persist as episomal linear double-stranded DNA molecules in the nucleus (Jager and Ehrhardt 2009) and thus, transgene expression diminishes over time in rapidly dividing tissues or upon induction of cell cycling due to natural degradation processes (Rauschhuber *et al.,* 2011). Consequently, in order to achieve long-term transgene expression, hybrid vector systems have been explored, which were designed to combine the high transduction efficiency of adenoviral vectors with integration systems that mediate the integration of the transgene into the chromosomal DNA. The most prominent non-viral integration system used in gene therapy is represented by the Sleeping Beauty (SB) transposase system, a DNA transposon from the Tc1/*mariner* group (Ivics *et al.,* 1997).

DNA transposons and other mobile genetic elements, such as retrotransposons are ancient remainings, which are estimated to account for around 40% of DNA sequences in the human genome (Lander *et al.,* 2001). The long interspersed element-1 (LINE-1) for example is a highly aboundant retrotransposon, which covers approximately 18% of the human

genome. Although most of the LINE-1s are inactive with respect to retrotransposition, 80-100 full length, replication-competent LINE-1s exist and their activation can be associated with several diseases including cancer (Kazazian *et al.,* 1988; Schwahn *et al.,* 1998; Brouha *et al.,* 2002; Cordaux and Batzer 2009). Since LINE-1s and DNA transposons encode for their own transposase protein, functional mobile elements are dependent on transcription from internal promoters to drive retro-transposition or transposition, respectively (Ostertag and Kazazian 2001). The transcription derived from two convergent promoters, however, can lead to formation of dsRNAs, which could present substrates for the RNAi machinery and subsequently target and inhibit protein expression required for transposition. Previously, this silencing mechanism was confirmed for the LINE-1 retrotransposons in human cells (Soifer *et al.,* 2005) and for the Tc1 element, another member of the Tc1/*mariner* group in the germ line of *Caenorhabditis elegans* (Sijen and Plasterk 2003). Notably, in the case of the Tc1 element dsRNAs derive from random external read-through from flanking genomic sequences as no transcriptional activity from the Tc1 inverted repeats were detected (Sijen and Plasterk 2003). In the present work we confirmed the influence of the RNAi pathway on SB transposition and in particular on transgene expression (**chapter 4**). DsRNAs derived from convergent transcription of the SB inverted repeats are thereby the effectors within the RNAi pathway (Moldt *et al*., 2007). Importantly, in contrast to the original DNA transposon, in which the transposase was embedded between the IRs in one DNA fragment, the current SB system consists of two components (**Figure 1.8**). In this two vector system the transgene cassette is flanked by the IRs, whereas the transposase is expressed from an independent vector. Thus, RNAi mediates silencing of the transgene and transposition itself remains unaltered.

Therefore, our finding strengthens the hypothesis that the RNA interference system is an evolutionary important mechanism that evolved to prevent the mobilization of transposable elements and consequently the damage of the chromosomal DNA (Gilbert *et al.,* 2002; Symer *et al.,* 2002). However, the Frog Prince transposable element, which belongs to the same group of transposable elements, did not show any inward transcriptional activity and therefore also no influence of the RNAi pathway could be detected (**Figure 4.4B** and **C**) (Moldt *et al.,* 2007; Walisko *et al.,* 2008). It is believed that during the reconstitution of the transposable elements, defects in the flanking sequences occurred, which now make the Frog Prince system less accessible to the RNAi mechanism (Moldt *et al.,* 2007).

The identification of transgene specific dsRNAs, derived from the transposon donor, mediating the silencing process may ultimately clarify the contribution of the RNAi pathway to transposition. However, this could be a difficult task, as transcriptional activties are quite

low in comparison to viral derived promoters (Moldt *et a*l., 2007). Furthermore it remains to be elucidated, how RNAi-mediated gene silencing upon transposition occurs. There are three possible mechanisms concievable. The DsRNAs generated by inward transcriptional activity could either result into degradation or translational inhibition of the complementary mRNA or gene expression may be inhibited on a transcriptional level by cystein methylation (Kawasaki and Taira 2004a). Methylation of cystein residues initiated by the RNAi pathway was already demonstrated to occur in mammalian cells by Kawasaki and Taira (Kawasaki and Taira 2004a). Notably, the transcriptional silencing mediated by methylation is also supported by a study of Garrison *et al*., in which the administration of a methyltransferase inhibitor could revert gene silencing upon SB transposition (Garrison *et al.,* 2007).

Moreover, we also identified an influence of the RNAi pathway on PhiC31 integrase (**Figure 4.3C** and **D**), but at the time the mechanism remains to be elucidated. Potentially, this phenomenon is a position dependent effect arising from the transgene promoter and a convergent promoter in the chromosomal DNA after somatic integration. Anyhow, PhiC31 is interesting as it mediates a unidirectional site-directed integration and there are already studies, in which targeted insertion of the transgene is performed by PhiC31-zinc-finger fusion proteins (Groth *et al.,* 2000) (Nadja Noske, unpublished results). Nevertheless, in contrast to the Sleeping Beauty system, for which already 100-fold improved versions (Mates *et al*., 2009) are available the activity of PhiC31 could be increased up to 5-fold (Liesner *et al.,* 2010).

In conclusion, transposable systems and potentially the PhiC31 integrase system seem to have an effective counter defense mechanism in mammalian cells. These mechanisms need to be carefully characterized for proper function and further improvements.

The database of "Clinical Trials World Wide" outlined the great potential of recombinant adenoviral vectors for a large variety of indications (**Figure 1.5**) (Wiley 2010). Herein, the majority of clinical trials face the treatment of cancer diseases. Thereby, the replication-competent adenoviral vectors seem to be superior to the replication defective ones as they showed an improved tumor penetration and regression (Hemminki and Alvarez 2002; Lichtenstein and Wold 2004). Replication-competent or oncolytic adenoviruses are based on deletions in either the E1A or E1B gene, in order to restrict virus replication specifically to tumor cells, which mostly lack the retinoblastoma protein or p53 mediated cell cycle control (Bischoff *et al.,* 1996; Fueyo *et al.,* 2000). Normal tissues, however, can inhibit virus replication due to an intact cell cycle control. But still the low replication rate of most oncolytic adenoviruses and the specific targeting of the aberrant tissues are major limitations. Within the present study (see also **chapter 5**) we demonstrated that an E3-

deleted adenovirus expressing the RNAi suppressor protein P19 under the control of the major late promoter (MLP), replicates 100-fold faster and produces 10-fold more infectious particles compared to the oncolytic adenovirus AdΔfiberIL virus in HEK293 cells (**Figure 5.4**) (Fueyo *et al.,* 2000). AdΔfiberIL has a 24 bp deletion in the E1A gene and usually shows a growth advantage in immortalized cell lines (Nettelbeck *et al.,* 2002; Gomez-Manzano *et al.,* 2004). Thus, the introduction of the P19 protein into an oncolytic adenovirus background may provide a faster replicating virus, which in turn may initiate a more efficient virus spread and tumor penetration. This subsequently can result into a faster tumor regression. Moreover, we demonstrated increased amounts of the viral E4Orf6 protein in Bwtp19ΔE3 infected cells in comparison to AdΔfiberIL (**Figure 5.5B**). Sufficient expression of E4Orf6 in combination with radiotherapy was shown very recently to improve the treatment of cancer cells significantly (Liikanen *et al.,* 2010). In addition, there were already efforts to improve oncolytic viruses by arming them with anti-tumoral genes. For instance the antiangiogenic vascular endothelial growth factor (VEGF) receptor can contribute to the inhibition of tumor growth (Zhang *et al.,* 2005; Guse *et al.,* 2009). Furthermore, it was already demonstrated, that in the human B cell lymphoma, oncogenic miRNAs are overexpressed (Cullen 2010). Thus, arming oncolytic Ads with *p19* may increase virus replication with additive effects on the downregulation of oncogenic miRNAs.

As mentioned above, there are E1B-deleted adenoviruses, like the well-established oncolytic virus Onyx-015 already used in many phase I and II clinical trials (Bischoff *et al.,* 1996; Heise *et al.,* 2000; Ries and Brandts 2004; Pesonen *et al.,* 2010). Thus, it would be interesting to analyse whether P19 can improve the productive virus replication of Onyx-015. This is of special interest, because the lack of the E1B55K protein impaired virus replication significantly due to the defective late virus mRNA transport (Pesonen *et al.*, 2010). Thus, P19 may provide a more stable environment for adenoviral mRNAs and therefore force virus replication. Moreover, it has to be elucidated if an adenovirus expressing P19 under an early promoter might further increase the virus particel production because of expected higher P19 amounts at early time points after infection.

Regarding the treatment of cancer it is also worth considering to introduce a *p19* expression cassette into an oncolytic adenovirus based on a serotype other than Ad5. Ad5 uses the CAR receptor for cellular entry, however on many malignant cell lines CAR is underrepresented and therefore resistant to Ad5 treatment (Hemmi *et al.,* 1998; Miller *et al.,* 1998; Cripe *et al.,* 2001; Breidenbach *et al.,* 2004; Rein *et al.,* 2004). Thus, it was demonstrated that chimeric viruses harbouring either fiber or hexon of the human adenovirus serotype 3 (Ad3), a member of subgroup B1, is superior when targeting cancer

cells (Krasnykh *et al.,* 1996; Short *et al.,* 2010). As mentioned before, most subgroup B adenoviruses use the CD46 receptor for cellular entry, a receptor that is present on many tumor cells (Krasnykh *et al.,* 1996). In addition, very recently the Desmoglein 2 receptor was identified to play a crucial role in internalization of Ad3 (Wang *et al.,* 2010). Desmoglein 2 is an epithelia tumor marker and would therefore be beneficial for the treatment of epithelia associated cancers. Ad3 displays only 30% serum prevalence in the human population and is not recognized by blood coagulation factor X, which diminishes the sequesteration of viral particles in the liver (Waddington *et al.,* 2008). Thus, considering the instability of capsid modified adenoviruses and the inefficient generation of theses viruses, a complete serotype switch to the Ad3 would be preferable for the treatment of different cancer variants.

It was already shown in the past by Lecellier and colleagues that virus replication such as the primate foamy virus can be enhanced in the presence of the RNAi suppressor protein P19 in a stable cell line (Lecellier *et al.,* 2005). Using the bacterial artificial chromosome (BAC) cloning procedure we therefore generated a functional P19 expressing helper virus and showed 6-fold increased HC-AdV production in comparison to the standard helper virus from Philip Ng (AdNG163R-2) in a small-scale experiment (**Figure 5.9**) (Ng *et al.*, 2001). This clearly indicated that the findings of this study can be used to improve virus production.

All RNA interference experiments within the present study were based on the RNAi suppressor protein P19, however, there are also other considerable systems available. Since the complete deletion of Dicer, the cytoplasmic endonuclease generating the miRNAs, is lethal in mouse embryogenesis, only Dicer knockdown cells (Dicer-/-) are available (Kanellopoulou *et al.,* 2005). However, most of these Dicer-/- cells are based on siRNA-mediated knockdown of the Dicer protein. Although this system is highly efficient and can be used to analyze miRNA expression profiles, we could not adjust this system to our long-term experiments in the colony forming assay or the infection with adenovirus. For instance colony forming assays last for 2 weeks and would exceed the activity span of the introduced siRNA, which is approximately maintained for one week within a cell (Bartlett and Davis 2006). In addition, Cummins *et al*. generated Dicer-/- cell lines by AAV mediated insertions into the Dicer gene, thereby disrupting the helicase function of Dicer (Cummins *et al.,* 2006). But within their study they still observed around 50% of normal miRNA expression levels, thus it is hypothesized that other mechanisms evolve upon Dicer knockdown, which compensate the defect.

Besides P19, there are several other RNAi suppressor proteins available targeting different steps of the RNAi pathway. The vaccinia virus-derived protein E3L or the Ebola virus VP35 protein are both RNA binding proteins with a known interferon antagonistic function (Li *et al.,*

2004; Haasnoot *et al.,* 2007). Therefore, they influence the innate immune response, which is potentially mediated by the miRNA arm of the RNAi pathway (Pedersen *et al.,* 2007). Previously, it was shown that both viral proteins (E3L and VP35) expressed in a stable cell line increased lentiviral titers (de Vries *et al*., 2008). In addition, there is evidence that RNA viruses and their virus-derived RNA intermediates, which occur during viral replication, may be recognized by helicases or intracellular receptors and activate the immune response (Baum and Garcia-Sastre 2010). Thus, it was concluded that both RNAi suppressor proteins are sufficient to increase lentivirus replication by disabling the immune response (de Vries *et al*., 2008). Since we were predominantly interested in the influence of the classical RNAi pathway in particular the influence of miRNAs on transgene expression and adenovirus performance, we have chosen the tomato bushy stunt virus P19 protein (Scholthof 2006). P19, as a miRNA inhibitory protein was already used to improve replication of the primate foamy virus (Lecellier *et al.,* 2005). However, a crucial factor within the experiments was the amount of the RNAi suppressor protein (Qiu *et al.,* 2002; Szittya *et al.,* 2002). Thus, with respect to P19 it is recommended to use highly efficient expression systems like strong viral promoters or in our case the expression of the protein in the viral context under the major late promoter linking *p19* expression to virus replication. Anyhow, it strongly depends on the experimental set up, which RNAi inhibitory system is most suitable. As shown by de Vries *et al*., the use of interferon antagonists may be very potent in terms of up-regulation of viral particle production, thus, it would be of great interest to introduce the VP35 protein into the adenoviral genome to further increase its replication (de Vries *et al.,* 2008).

Last but not least it is important to emphasize that the P19 system presented within this study can be also used to analyze the influence of the RNAi pathway on other viruses, like herpesviruses, for which most miRNAs have been identified so far (Skalsky and Cullen 2010). It could also help to identify to date unknown contributions of the RNAi pathway to viral life cycles, including many RNA viruses for which an interaction with the RNAi pathway was already demonstrated (Lecellier *et al*., 2005; Cullen 2010). In general, the P19 system is suitable to investigate different cellular processes under RNAi knockdown conditions *in vitro* and, for instance by introducing the *p19* expression cassette into an HC-AdV, also *in vivo* analyses are imaginable.

In conclusion, this work outlined the great perspectives of recombinant adenoviral vectors in gene therapy. Since the death of Jessie Gelsinger, adenoviral vectors were considered with scepticism; however, modifications and improvements of these vehicles during the past decade make them an attractive tool for different applications with a broad diversification potential. This trend is also reflected by newest publications, in which novel adenoviral

receptors were identified and the crystall structure of adenovirus solved at high resolution (Nilsson *et al.,* 2010; Reddy *et al.,* 2010; Wang *et al.,* 2010). In concert with upcoming advanced cloning strategies, adenoviral vectors will gain increasing attractivity for gene therapeutic applications. The results from this thesis add to the great potential of these viruses and provide novel insights into the complex interaction between adenovirus and the host cell.

7 Appendix

7.1 Abbrevations

°C	degree celsius
Amp	ampicillin
ATTC	American Tissue Culture Company
bp	basepair
cDNA	complementary DNA
CIP	calf intestinal phosphatase
CRE	Cre-recombinase
CsCl	cesium chloride
DGCR-8	DiGeorge critical region 8
DNA	desoxy ribonucleic acid
EDTA	Ethylene diamine tetra acedic acid
Fg	first generation
FIX	coagulation factor 9
FITC	Fluoresceinisothiocyanat
FP	Frog Prince
FX	coagulation factor 10
GAPDH	glycerinaldehyd3-phophat dehydrogenase
GFP	green fluorescent protein
HA	hemaglutinin
hAAT	human alpha-1-antitrypsin
HBV	hepatitis B virus
HC-AdV	high-capacity adenoviral vector
HCl	hydrogenchloride
HCR	hepatic control region
HEK	human embryonal kidney

His	histidin
Hox	homeobox
hrs	hours
IR	inverted repeat
ITR	inverted terminal repeat
LTR	long terminal repeat
Luc	firefly luciferase
MCS	multiple cloning site
miRNA	micro RNA
mg	milligram
ml	milliliter
MLP	major late promoter
mg	microgram
ml	microliter
moi	multiplicity of infection
mRNA	messenger RNA
Neo	neomycin
ng	nanogram
nM	nanomolar
nt	nucleotide
OD	optical density
OPU	optical particle units
ORF	open reading frame
PCR	polymerase chain reaction
PBS	phosphate buffered saline
PGK	phophoglycerinkinase promoter
polyA	polyadenylation signal
pRB	retino blastoma tumor suppressor protein

P/S	penicillin/streptomycin
qRT-PCR	quantitative Real-Time PCR
RISC	RNA induced silencing complex
RL	renilla luciferase
RNA	ribonucleicacid
RNAi	RNA interference
rpm	rounds per minute
RT	reverse transcription
SB	Sleeping Beauty
SDS	sodium dodecyl sulfate
siRNA	small interfering RNA
SSC	side scatter
SV40	simian virus 40
sva-RNA	small virus-associated RNA
TA	tyrosin and adenosin dinucleotide
TAE	tris-acetat-EDTA buffer
TBE	tris-borat-EDTA buffer
TESS	transcriptional element search system
Tris	tris-hydroymethyl ammonium methane
TSS	transcriptional start sites
TU	transducing units
VA-RNA	virus-associated RNA
wtAd5	wildtype adenovirus serotype 5

7.2 Publications and Awards

Parts of this thesis have already been published in Journals and were presented on meetings.

7.2.1 Publications in Journals

Christina Rauschhuber, Hui Xu, Felix H. Salazar, Patricia L. Marion, Anja Ehrhardt (2008). Exploring gene-deleted adenoviral vectors for delivery of short hairpin RNAs and reduction of hepatitis B virus infection in mice. *Journal of Gene Medicine*, 10:878-89.

Lorenz Jager*, Martin Haeusl*, **Christina Rauschhuber***, Nicola Wolf, and Anja Ehrhardt (2009). A rapid protocol for construction and production of high-capacity adenoviral vectors. *Nature Protocols,* 4: 547-64 (*these authors contributed equally to this work).

Martin A. Hausl, Wenli Zhang, Nadine Müther, **Christina Rauschhuber**, Helen G. Franck, Elizabeth P. Merricks, Timothy C. Nichols, Mark A. Kay and Anja Ehrhardt (2010). Hyperactive Sleeping Beauty transposase enables persistent phenotypic correction in mice and a canine model for hemophilia B. *Molecular therapy*, 18:1896-906.

Christina Rauschhuber, Armin Wolf and Anja Ehrhardt (2010). Transcriptional activity of inverted terminal repeats of various human adenovirus serotypes. *Journal of General Virology*, 17.

Christina Rauschhuber, Nadja Noske and Anja Ehrhardt (2010). New insights into stability of recombinant adenovirus vector genomes in mammalian cells. Review. *European Journal of cellular biology* (in revision)*.*

Martin Hausl, Wenli Zhang , Nadine Müther, Richard Voigtlander, **Christina Rauschhuber**, and Anja Ehrhardt (2011). Development of adenoviral hybrid vectors for Sleeping Beauty transposition in large mammals. Review. *Current Gene Therapy*. (submitted).

Christina Rauschhuber and Anja Ehrhardt. Sleeping Beauty mediated transposition in human cells is enhanced in RNA interference knockdown cells (Manuscript ready for submission).

Christina Rauschhuber, Martin Hausl, Matthew Weitzman, Dirk Nettelbeck and Anja Ehrhardt. Adenovirus Serotype 5 replication is enhanced in the presence of the RNA interference suppressor protein P19. (Manuscript in preparation).

7.2.2 Oral presentations

Christina Rauschhuber and Anja Ehrhardt (2008). *Adenovirus uptake and replication are enhanced in micro RNA knock-out cells.* SFB 455 Junior Faculty Meeting.

Christina Rauschhuber and Anja Ehrhardt (2009). *The micro RNA Machinery plays a prominent role in Adenovirus replication.* American Society of Gene Therapy Meeting, San Diego.

Christina Rauschhuber (2010). *Design of Recombinant Adenoviral Vectors for Gene Therapy: Improvements and Challenges.* Invited Speaker, Deutsche Gesellschaft für Gentherapie Meeting, Munich.

Christina Rauschhuber, Martin Hausl and Anja Ehrhardt (2010). *Micro RNA knockdown improves adenovirus replication and vector production.* European Society of Gene and Cell Therapy Meeting, Milano.

7.2.3   Poster presentations

Christina Rauschhuber and Anja Ehrhardt (2007). *Adenovirus uptake and replication are enhanced in micro RNA knock-out cells.* European Virology Kongress, Nürnberg.

Christina Rauschhuber and Anja Ehrhardt (2008). *Sleeping Beauty mediated transposition in human cells is influenced by the RNA interference machinery.* American Society of Gene Therapy Meeting, Boston.

Martin Hausl, **Christina Rauschhuber**, Zsolt Rusicz and Anja Ehrhardt (2010). *Method for Fast and Easy Adoption of First-Generation to High-Capacity Adenoviral Vectors.* American Society of Gene and Cell Therapy Meeting, Washington DC.

Christina Rauschhuber, Martin Hausl and Anja Ehrhardt (2010). *Micro RNA knockdown improves adenovirus replication and vector production.* SFB 455 Symposium, Munich.

Christina Rauschhuber and Anja Ehrhardt (2010). *Sleeping Beauty mediated transposition is enhanced in RNAi knockdown cell lines*. DGGT Meeting, Munich.

Christina Rauschhuber, Martin Hausl and Anja Ehrhardt (2010). *Micro RNA knockdown improves adenovirus replication and vector production.* DGGT Meeting, Munich.

7.2.4   Awards

Travel Grant award of the "American Society of Gene Therapy" in 2009 for the Abstract:

"*The micro RNA machinery plays a prominent role in Adenovirus replication.*"

7.3 Curriculum Vitae

Persönliche Daten

Name: Christina Rauschhuber

Geburtstag: 13.10.1982

Geburtsort: Eggenfelden

Nationalität: Deutsch

Schulausbildung

1988 – 1992:   Grundschule Gangkofen

1992 – 2001:   Karl-von-Closen Gymnasium Eggenfelden mit dem Abschluss Abitur

Hochschulausbildung

10 / 2001 – 5 / 2007   Studium der Biologie an der Ludwig-Maximilians Universität München, <u>Schwerpunkte</u>: Zellbiologie, Genetik, Medizinische Mikrobiologie, Pharmakologie und Toxikologie Mai 2007: Diplom mit der Note: sehr gut Thema: Der Einfluss von zellulären und viralen micro RNA Sequenzen auf den Lebenszyklus von Adenoviren

07 / 2006 – 2011   Doktorarbeit in der Abteilung für Virologie des Max von Pettenkofer-Instituts, der medizinischen Fakultät der Ludwig-Maximilians- Universität München. Betreuer: PD Dr. Anja Ehrhardt: Titel der Dissertation: "Analysis of adenovirus-host interactions to improve recombinant adenoviral vectors for gene therapy".

7.4 References

[1]   **Akusjarvi G., Svensson C. and Nygard O.** (1987). A mechanism by which adenovirus virus-associated RNAI controls translation in a transient expression assay. *Mol Cell Biol*, (**7**): 549-51

[2]   **Alba R., Bradshaw A. C., Parker A. L., Bhella D., Waddington S. N., Nicklin S. A., van Rooijen N., Custers J., Goudsmit J., Barouch D. H., McVey J. H. and Baker A. H.** (2009). Identification of coagulation factor (F)X binding sites on the adenovirus serotype 5 hexon: effect of mutagenesis on FX interactions and gene transfer. *Blood*, (**114**): 965-71

[3]   **Allen B. G. and Weeks D. L.** (2009). Bacteriophage phiC31 integrase mediated transgenesis in Xenopus laevis for protein expression at endogenous levels. *Methods Mol Biol*, (**518**): 113-22

[4]   **Andersson M. G., Haasnoot P. C., Xu N., Berenjian S., Berkhout B. and Akusjarvi G.** (2005). Suppression of RNA interference by adenovirus virus-associated RNA. *J Virol*, (**79**): 9556-65

[5]   **Aparicio O., Carnero E., Abad X., Razquin N., Guruceaga E., Segura V. and Fortes P.** (2010). Adenovirus VA RNA-derived miRNAs target cellular genes involved in cell growth, gene expression and DNA repair. *Nucleic Acids Res*, (**38**): 750-63

[6]   **Aparicio O., Razquin N., Zaratiegui M., Narvaiza I. and Fortes P.** (2006). Adenovirus virus-associated RNA is processed to functional interfering RNAs involved in virus production. *J Virol*, (**80**): 1376-84

[7]   **Arnberg N.** (2009). Adenovirus receptors: implications for tropism, treatment and targeting. *Rev Med Virol*, (**19**): 165-78

[8]   **Aucoin M. G., Perrier M. and Kamen A. A.** (2006). Production of adeno-associated viral vectors in insect cells using triple infection: optimization of baculovirus concentration ratios. *Biotechnol Bioeng*, (**95**): 1081-92

[9]   **Babiss L. E., Friedman J. M. and Darnell J. E., Jr.** (1986a). Cellular promoters incorporated into the adenovirus genome: effects of viral regulatory elements on transcription rates and cell specificity of albumin and beta-globin promoters. *Mol Cell Biol*, (**6**): 3798-806

[10]   **Babiss L. E., Liaw W. S., Zimmer S. G., Godman G. C., Ginsberg H. S. and Fisher P. B.** (1986b). Mutations in the E1a gene of adenovirus type 5 alter the tumorigenic properties of transformed cloned rat embryo fibroblast cells. *Proc Natl Acad Sci U S A*, (**83**): 2167-71

[11]   **Bainbridge J. W., Smith A. J., Barker S. S., Robbie S., Henderson R., Balaggan K., Viswanathan A., Holder G. E., Stockman A., Tyler N., Petersen-Jones S., Bhattacharya S. S., Thrasher A. J., Fitzke F. W., Carter B. J., Rubin G. S., Moore A. T. and Ali R. R.** (2008). Effect of gene therapy on visual function in Leber's congenital amaurosis. *N Engl J Med*, (**358**): 2231-9

[12] **Barouch D. H. and Nabel G. J.** (2005). Adenovirus vector-based vaccines for human immunodeficiency virus type 1. *Hum Gene Ther*, (**16**): 149-56

[13] **Bartlett D. W. and Davis M. E.** (2006). Insights into the kinetics of siRNA-mediated gene silencing from live-cell and live-animal bioluminescent imaging. *Nucleic Acids Res*, (**34**): 322-33

[14] **Baulcombe D. C.** (1999). Viruses and gene silencing in plants. *Arch Virol Suppl*, (**15**): 189-201

[15] **Baum A. and Garcia-Sastre A.** (2010). Induction of type I interferon by RNA viruses: cellular receptors and their substrates. *Amino Acids*, (**38**): 1283-99

[16] **Beck J. and Nassal M.** (1995). Efficient hammerhead ribozyme-mediated cleavage of the structured hepatitis B virus encapsidation signal in vitro and in cell extracts, but not in intact cells. *Nucleic Acids Res*, (**23**): 4954-62

[17] **Beckham C. J. and Parker R.** (2008). P bodies, stress granules, and viral life cycles. *Cell Host Microbe*, (**3**): 206-12

[18] **Belteki G., Gertsenstein M., Ow D. W. and Nagy A.** (2003). Site-specific cassette exchange and germline transmission with mouse ES cells expressing phiC31 integrase. *Nat Biotechnol*, (**21**): 321-4

[19] **Bennasser Y., Le S. Y., Benkirane M. and Jeang K. T.** (2005). Evidence that HIV-1 encodes an siRNA and a suppressor of RNA silencing. *Immunity*, (**22**): 607-19

[20] **Bergelson J. M., Cunningham J. A., Droguett G., Kurt-Jones E. A., Krithivas A., Hong J. S., Horwitz M. S., Crowell R. L. and Finberg R. W.** (1997). Isolation of a common receptor for Coxsackie B viruses and adenoviruses 2 and 5. *Science*, (**275**): 1320-3

[21] **Berkner K. L.** (1988). Development of adenovirus vectors for the expression of heterologous genes. *Biotechniques*, (**6**): 616-29

[22] **Bischoff J. R., Kirn D. H., Williams A., Heise C., Horn S., Muna M., Ng L., Nye J. A., Sampson-Johannes A., Fattaey A. and McCormick F.** (1996). An adenovirus mutant that replicates selectively in p53-deficient human tumor cells. *Science*, (**274**): 373-6

[23] **Blaas L., Musteanu M., Zenz R., Eferl R. and Casanova E.** (2007). PhiC31-mediated cassette exchange into a bacterial artificial chromosome. *Biotechniques*, (**43**): 659-60, 662, 664

[24] **Breidenbach M., Rein D. T., Wang M., Nettelbeck D. M., Hemminki A., Ulasov I., Rivera A. R., Everts M., Alvarez R. D., Douglas J. T. and Curiel D. T.** (2004). Genetic replacement of the adenovirus shaft fiber reduces liver tropism in ovarian cancer gene therapy. *Hum Gene Ther*, (**15**): 509-18

[25] **Brody S. L., Metzger M., Danel C., Rosenfeld M. A. and Crystal R. G.** (1994). Acute responses of non-human primates to airway delivery of an adenovirus vector containing the human cystic fibrosis transmembrane conductance regulator cDNA. *Hum Gene Ther*, (**5**): 821-36

[26]   **Bromberg J. S., Debruyne L. A. and Qin L.** (1998). Interactions between the immune system and gene therapy vectors: bidirectional regulation of response and expression. *Adv Immunol*, (**69**): 353-409

[27]   **Brouha B., Meischl C., Ostertag E., de Boer M., Zhang Y., Neijens H., Roos D. and Kazazian H. H., Jr.** (2002). Evidence consistent with human L1 retrotransposition in maternal meiosis I. *Am J Hum Genet*, (**71**): 327-36

[28]   **Brown B. D., Cantore A., Annoni A., Sergi L. S., Lombardo A., Della Valle P., D'Angelo A. and Naldini L.** (2007). A microRNA-regulated lentiviral vector mediates stable correction of hemophilia B mice. *Blood*, (**110**): 4144-52

[29]   **Brown B. D., Shi C. X., Powell S., Hurlbut D., Graham F. L. and Lillicrap D.** (2004). Helper-dependent adenoviral vectors mediate therapeutic factor VIII expression for several months with minimal accompanying toxicity in a canine model of severe hemophilia A. *Blood*, (**103**): 804-10

[30]   **Brunetti-Pierri N., Mendoza-Londono R., Shah M. R., Karaviti L. and Lee B.** (2004). von Voss-Cherstvoy syndrome with transient thrombocytopenia and normal psychomotor development. *Am J Med Genet A*, (**126A**): 299-302

[31]   **Brunetti-Pierri N., Nichols T. C., McCorquodale S., Merricks E., Palmer D. J., Beaudet A. L. and Ng P.** (2005). Sustained phenotypic correction of canine hemophilia B after systemic administration of helper-dependent adenoviral vector. *Hum Gene Ther*, (**16**): 811-20

[32]   **Brunetti-Pierri N., Stapleton G. E., Law M., Breinholt J., Palmer D. J., Zuo Y., Grove N. C., Finegold M. J., Rice K., Beaudet A. L., Mullins C. E. and Ng P.** (2009). Efficient, long-term hepatic gene transfer using clinically relevant HDAd doses by balloon occlusion catheter delivery in nonhuman primates. *Mol Ther*, (**17**): 327-33

[33]   **Brunetti-Pierri N., Stapleton G. E., Palmer D. J., Zuo Y., Mane V. P., Finegold M. J., Beaudet A. L., Leland M. M., Mullins C. E. and Ng P.** (2007). Pseudo-hydrodynamic delivery of helper-dependent adenoviral vectors into non-human primates for liver-directed gene therapy. *Mol Ther*, (**15**): 732-40

[34]   **Cai X., Hagedorn,X., and Cullen, B.** (2004). Human microRNAs are processed from capped, polyadenylated transcripts that can function as mRNAs. *RNA*, (**10**): 1957-1966

[35]   **Caplen N. J., Fleenor, J., Fire, A., Morgan, R:A.** (2000). dsRNA-mediated gene silencing in cultured Drosophila cells: a tissue culture model for the analysis of RNA interference. *Gene*, (**252**): 95-105

[36]   **Carmona S., Ely A., Crowther C., Moolla N., Salazar F. H., Marion P. L., Ferry N., Weinberg M. S. and Arbuthnot P.** (2006). Effective inhibition of HBV replication in vivo by anti-HBx short hairpin RNAs. *Mol Ther*, (**13**): 411-21

[37]   **Cartier N., Hacein-Bey-Abina S., Bartholomae C. C., Veres G., Schmidt M., Kutschera I., Vidaud M., Abel U., Dal-Cortivo L., Caccavelli L., Mahlaoui N., Kiermer V., Mittelstaedt D., Bellesme C., Lahlou N., Lefrere F., Blanche S., Audit M., Payen E., Leboulch P., l'Homme B., Bougneres P., Von Kalle C., Fischer A., Cavazzana-Calvo M. and Aubourg P.** (2009). Hematopoietic stem cell gene therapy with a lentiviral vector in X-linked adrenoleukodystrophy. *Science*, (**326**): 818-23

[38]   **Cavanaugh V. J., Guidotti L. G. and Chisari F. V.** (1998). Inhibition of hepatitis B virus replication during adenovirus and cytomegalovirus infections in transgenic mice. *J Virol*, (**72**): 2630-7

[39]   **Cavazzana-Calvo M., Payen E., Negre O., Wang G., Hehir K., Fusil F., Down J., Denaro M., Brady T., Westerman K., Cavallesco R., Gillet-Legrand B., Caccavelli L., Sgarra R., Maouche-Chretien L., Bernaudin F., Girot R., Dorazio R., Mulder G. J., Polack A., Bank A., Soulier J., Larghero J., Kabbara N., Dalle B., Gourmel B., Socie G., Chretien S., Cartier N., Aubourg P., Fischer A., Cornetta K., Galacteros F., Beuzard Y., Gluckman E., Bushman F., Hacein-Bey-Abina S. and Leboulch P.** (2010). Transfusion independence and HMGA2 activation after gene therapy of human beta-thalassaemia. *Nature*, (**467**): 318-22

[40]   **Cerullo V., Seiler M. P., Mane V., Cela R., Clarke C., Kaufman R. J., Pipe S. W. and Lee B.** (2007). Correction of murine hemophilia A and immunological differences of factor VIII variants delivered by helper-dependent adenoviral vectors. *Mol Ther*, (**15**): 2080-7

[41]   **Chen C. C., Ko T. M., Ma H. I., Wu H. L., Xiao X., Li J., Chang C. M., Wu P. Y., Chen C. H., Han J. M., Yu C. P., Jeng K. S., Hu C. P. and Tao M. H.** (2007). Long-term inhibition of hepatitis B virus in transgenic mice by double-stranded adeno-associated virus 8-delivered short hairpin RNA. *Gene Ther*, (**14**): 11-9

[42]   **Chirmule N., Propert K., Magosin S., Qian Y., Qian R. and Wilson J.** (1999). Immune responses to adenovirus and adeno-associated virus in humans. *Gene Ther*, (**6**): 1574-83

[43]   **Chiu Y. L. and Rana T. M.** (2003). siRNA function in RNAi: a chemical modification analysis. *Rna*, (**9**): 1034-48

[44]   **Cideciyan A. V., Hauswirth W. W., Aleman T. S., Kaushal S., Schwartz S. B., Boye S. L., Windsor E. A., Conlon T. J., Sumaroka A., Roman A. J., Byrne B. J. and Jacobson S. G.** (2009). Vision 1 year after gene therapy for Leber's congenital amaurosis. *N Engl J Med*, (**361**): 725-7

[45]   **Cordaux R. and Batzer M. A.** (2009). The impact of retrotransposons on human genome evolution. *Nat Rev Genet*, (**10**): 691-703

[46]   **Cripe T. P., Dunphy E. J., Holub A. D., Saini A., Vasi N. H., Mahller Y. Y., Collins M. H., Snyder J. D., Krasnykh V., Curiel D. T., Wickham T. J., DeGregori J., Bergelson J. M. and Currier M. A.** (2001). Fiber knob modifications overcome low, heterogeneous expression of the coxsackievirus-adenovirus receptor that limits adenovirus gene transfer and oncolysis for human rhabdomyosarcoma cells. *Cancer Res*, (**61**): 2953-60

[47]   **Cullen B. R.** (2010). Five questions about viruses and microRNAs. *PLoS Pathog*, (**6**): e1000787

[48]   **Cummins J. M., He Y., Leary R. J., Pagliarini R., Diaz L. A., Jr., Sjoblom T., Barad O., Bentwich Z., Szafranska A. E., Labourier E., Raymond C. K., Roberts B. S., Juhl H., Kinzler K. W., Vogelstein B. and Velculescu V. E.** (2006). The colorectal microRNAome. *Proc Natl Acad Sci U S A*, (**103**): 3687-92

[49]   Curiel D. and Douglas J. T. (2002). Adenoviral vectors for gene therapy.

[50]   **Davison E., Diaz R. M., Hart I. R., Santis G. and Marshall J. F.** (1997). Integrin alpha5beta1-mediated adenovirus infection is enhanced by the integrin-activating antibody TS2/16. *J Virol*, (**71**): 6204-7

[51]   **de Vries W., Haasnoot J., van der Velden J., van Montfort T., Zorgdrager F., Paxton W., Cornelissen M., van Kuppeveld F., de Haan P. and Berkhout B.** (2008). Increased virus replication in mammalian cells by blocking intracellular innate defense responses. *Gene Ther*, (**15**): 545-52

[52]   **Deol J. R., Danialou G., Larochelle N., Bourget M., Moon J. S., Liu A. B., Gilbert R., Petrof B. J., Nalbantoglu J. and Karpati G.** (2007). Successful compensation for dystrophin deficiency by a helper-dependent adenovirus expressing full-length utrophin. *Mol Ther*, (**15**): 1767-74

[53]   **Dunoyer P., Lecellier C. H., Parizotto E. A., Himber C. and Voinnet O.** (2004a). Probing the microRNA and small interfering RNA pathways with virus-encoded suppressors of RNA silencing. *Plant Cell*, (**16**): 1235-50

[54]   **Dunoyer P., Thomas C., Harrison S., Revers F. and Maule A.** (2004b). A cysteine-rich plant protein potentiates Potyvirus movement through an interaction with the virus genome-linked protein VPg. *J Virol*, (**78**): 2301-9

[55]   **Ehrhardt A. and Kay M. A.** (2002). A new adenoviral helper-dependent vector results in long-term therapeutic levels of human coagulation factor IX at low doses in vivo. *Blood*, (**99**): 3923-30

[56]   **Ehrhardt A. and Kay M. A.** (2005). Gutted adenovirus: a rising star on the horizon? *Gene Ther*, (**12**): 1540-1

[57]   **Ehrhardt A., Xu H., Dillow A. M., Bellinger D. A., Nichols T. C. and Kay M. A.** (2003). A gene-deleted adenoviral vector results in phenotypic correction of canine hemophilia B without liver toxicity or thrombocytopenia. *Blood*, (**102**): 2403-11

[58]   **Ehrhardt A., Xu H., Huang Z., Engler J. A. and Kay M. A.** (2005). A direct comparison of two nonviral gene therapy vectors for somatic integration: in vivo evaluation of the bacteriophage integrase phiC31 and the Sleeping Beauty transposase. *Mol Ther*, (**11**): 695-706

[59]   **Ehrhardt A., Yant S. R., Giering J. C., Xu H., Engler J. A. and Kay M. A.** (2007). Somatic integration from an adenoviral hybrid vector into a hot spot in mouse liver results in persistent transgene expression levels in vivo. *Mol Ther*, (**15**): 146-56

[60]   **Elbashir S. M., Harborth J., Lendeckel W., Yalcin A., Weber K. and Tuschl T.** (2001a). Duplexes of 21-nucleotide RNAs mediate RNA interference in cultured mammalian cells. *Nature*, (**411**): 494-8

[61]   **Elbashir S. M., Lendeckel W. and Tuschl T.** (2001b). RNA interference is mediated by 21- and 22-nucleotide RNAs. *Genes Dev*, (**15**): 188-200

[62]   **Eulalio A., Huntzinger E. and Izaurralde E.** (2008). Getting to the root of miRNA-mediated gene silencing. *Cell*, (**132**): 9-14

[63] **Fire A., Xu S., Montgomery M. K., Kostas S. A., Driver S. E. and Mello C. C.** (1998). Potent and specific genetic interference by double-stranded RNA in Caenorhabditis elegans. *Nature*, (**391**): 806-11

[64] **Freimuth P., Springer K., Berard C., Hainfeld J., Bewley M. and Flanagan J.** (1999). Coxsackievirus and adenovirus receptor amino-terminal immunoglobulin V-related domain binds adenovirus type 2 and fiber knob from adenovirus type 12. *J Virol*, (**73**): 1392-8

[65] **Fueyo J., Gomez-Manzano C., Alemany R., Lee P. S., McDonnell T. J., Mitlianga P., Shi Y. X., Levin V. A., Yung W. K. and Kyritsis A. P.** (2000). A mutant oncolytic adenovirus targeting the Rb pathway produces anti-glioma effect in vivo. *Oncogene*, (**19**): 2-12

[66] **Gao G. P., Yang Y. and Wilson J. M.** (1996). Biology of adenovirus vectors with E1 and E4 deletions for liver-directed gene therapy. *J Virol*, (**70**): 8934-43

[67] **Garber K.** (2006). China approves world's first oncolytic virus therapy for cancer treatment. *J Natl Cancer Inst*, (**98**): 298-300

[68] **Garrison B. S., Yant S. R., Mikkelsen J. G. and Kay M. A.** (2007). Postintegrative gene silencing within the Sleeping Beauty transposition system. *Mol Cell Biol*, (**27**): 8824-33

[69] **Gilbert N., Lutz-Prigge S. and Moran J. V.** (2002). Genomic deletions created upon LINE-1 retrotransposition. *Cell*, (**110**): 315-25

[70] **Gilbert R., Dudley R. W., Liu A. B., Petrof B. J., Nalbantoglu J. and Karpati G.** (2003). Prolonged dystrophin expression and functional correction of mdx mouse muscle following gene transfer with a helper-dependent (gutted) adenovirus-encoding murine dystrophin. *Hum Mol Genet*, (**12**): 1287-99

[71] **Gomez-Manzano C., Balague C., Alemany R., Lemoine M. G., Mitlianga P., Jiang H., Khan A., Alonso M., Lang F. F., Conrad C. A., Liu T. J., Bekele B. N., Yung W. K. and Fueyo J.** (2004). A novel E1A-E1B mutant adenovirus induces glioma regression in vivo. *Oncogene*, (**23**): 1821-8

[72] **Gorziglia M. I., Kadan M. J., Yei S., Lim J., Lee G. M., Luthra R. and Trapnell B. C.** (1996). Elimination of both E1 and E2 from adenovirus vectors further improves prospects for in vivo human gene therapy. *J Virol*, (**70**): 4173-8

[73] **Grimm D., Streetz K. L., Jopling C. L., Storm T. A., Pandey K., Davis C. R., Marion P., Salazar F. and Kay M. A.** (2006). Fatality in mice due to oversaturation of cellular microRNA/short hairpin RNA pathways. *Nature*, (**441**): 537-41

[74] **Groth A. C. and Calos M. P.** (2004). Phage integrases: biology and applications. *J Mol Biol*, (**335**): 667-78

[75] **Groth A. C., Olivares E. C., Thyagarajan B. and Calos M. P.** (2000). A phage integrase directs efficient site-specific integration in human cells. *Proc Natl Acad Sci U S A*, (**97**): 5995-6000

[76] **Guse K., Diaconu I., Rajecki M., Sloniecka M., Hakkarainen T., Ristimaki A., Kanerva A., Pesonen S. and Hemminki A.** (2009). Ad5/3-9HIF-Delta24-VEGFR-1-

Ig, an infectivity enhanced, dual-targeted and antiangiogenic oncolytic adenovirus for kidney cancer treatment. *Gene Ther*, (**16**): 1009-20

[77] **Haase R., Argyros O., Wong S. P., Harbottle R. P., Lipps H. J., Ogris M., Magnusson T., Vizoso Pinto M. G., Haas J. and Baiker A.** (2010). pEPito: a significantly improved non-viral episomal expression vector for mammalian cells. *BMC Biotechnol*, (**10**): 20

[78] **Haasnoot J., de Vries W., Geutjes E. J., Prins M., de Haan P. and Berkhout B.** (2007). The Ebola virus VP35 protein is a suppressor of RNA silencing. *PLoS Pathog*, (**3**): e86

[79] **Haley B. and Zamore P. D.** (2004). Kinetic analysis of the RNAi enzyme complex. *Nat Struct Mol Biol*, (**11**): 599-606

[80] **Hammond S. M., Bernstein E., Beach D. and Hannon G. J.** (2000). An RNA-directed nuclease mediates post-transcriptional gene silencing in Drosophila cells. *Nature*, (**404**): 293-6

[81] **Han J., Lee, y., Yeom,K.H., Kim,Y.K., Jin,H., and Kim,V.N.** (2004). The Drosha-DGCR8 complex in primary microRNA processing. *Genes & Development*, (**18**): 3016-3027

[82] **Hardy S., Kitamura M., Harris-Stansil T., Dai Y. and Phipps M. L.** (1997). Construction of adenovirus vectors through Cre-lox recombination. *J Virol*, (**71**): 1842-9

[83] **Harui A., Suzuki S., Kochanek S. and Mitani K.** (1999). Frequency and stability of chromosomal integration of adenovirus vectors. *J Virol*, (**73**): 6141-6

[84] **Hatfield L. and Hearing P.** (1991). Redundant elements in the adenovirus type 5 inverted terminal repeat promote bidirectional transcription in vitro and are important for virus growth in vivo. *Virology*, (**184**): 265-76

[85] **Hausl M. A., Zhang W., Muther N., Rauschhuber C., Franck H. G., Merricks E. P., Nichols T. C., Kay M. A. and Ehrhardt A.** (2010). Hyperactive sleeping beauty transposase enables persistent phenotypic correction in mice and a canine model for hemophilia B. *Mol Ther*, (**18**): 1896-906

[86] **Havenga M., Fisher R., Hoogerbrugge P., Valerio D. and van Es H. H.** (1996). Improved screening method for recombinant retrovirus producing clones. *Biotechniques*, (**21**): 1004-7

[87] **He T. C., Zhou S., da Costa L. T., Yu J., Kinzler K. W. and Vogelstein B.** (1998). A simplified system for generating recombinant adenoviruses. *Proc Natl Acad Sci U S A*, (**95**): 2509-14

[88] **Hearing P., Samulski R. J., Wishart W. L. and Shenk T.** (1987). Identification of a repeated sequence element required for efficient encapsidation of the adenovirus type 5 chromosome. *J Virol*, (**61**): 2555-8

[89] **Heise C., Hermiston T., Johnson L., Brooks G., Sampson-Johannes A., Williams A., Hawkins L. and Kirn D.** (2000). An adenovirus E1A mutant that demonstrates potent and selective systemic anti-tumoral efficacy. *Nat Med*, (**6**): 1134-9

[90] **Hemmi S., Geertsen R., Mezzacasa A., Peter I. and Dummer R.** (1998). The presence of human coxsackievirus and adenovirus receptor is associated with efficient adenovirus-mediated transgene expression in human melanoma cell cultures. *Hum Gene Ther*, (**9**): 2363-73

[91] **Hemminki A. and Alvarez R. D.** (2002). Adenoviruses in oncology: a viable option? *BioDrugs*, (**16**): 77-87

[92] **Hernando E., Nahle Z., Juan G., Diaz-Rodriguez E., Alaminos M., Hemann M., Michel L., Mittal V., Gerald W., Benezra R., Lowe S. W. and Cordon-Cardo C.** (2004). Rb inactivation promotes genomic instability by uncoupling cell cycle progression from mitotic control. *Nature*, (**430**): 797-802

[93] **Hillgenberg M., Schnieders F., Loser P. and Strauss M.** (2001). System for efficient helper-dependent minimal adenovirus construction and rescue. *Hum Gene Ther*, (**12**): 643-57

[94] **Hoelters J., Ciccarella M., Drechsel M., Geissler C., Gulkan H., Bocker W., Schieker M., Jochum M. and Neth P.** (2005). Nonviral genetic modification mediates effective transgene expression and functional RNA interference in human mesenchymal stem cells. *J Gene Med*, (**7**): 718-28

[95] **Hoffmann D., Jogler C. and Wildner O.** (2005). Effects of the Ad5 upstream E1 region and gene products on heterologous promoters. *J Gene Med*, (**7**): 1356-66

[96] **Hutvagner G.** (2005). Small RNA asymmetry in RNAi: function in RISC assembly and gene regulation. *FEBS Lett*, (**579**): 5850-7

[97] **Hutvagner G., McLachlan J., Pasquinelli A. E., Balint E., Tuschl T. and Zamore P. D.** (2001). A cellular function for the RNA-interference enzyme Dicer in the maturation of the let-7 small temporal RNA. *Science*, (**293**): 834-8

[98] **Imler J. L., Dupuit F., Chartier C., Accart N., Dieterle A., Schultz H., Puchelle E. and Pavirani A.** (1996). Targeting cell-specific gene expression with an adenovirus vector containing the lacZ gene under the control of the CFTR promoter. *Gene Ther*, (**3**): 49-58

[99] **Ishino M., Sawada Y., Yaegashi T., Demura M. and Fujinaga K.** (1987). Nucleotide sequence of the adenovirus type 40 inverted terminal repeat: close relation to that of adenovirus type 5. *Virology*, (**156**): 414-6

[100] **Ivics Z., Hackett P. B., Plasterk R. H. and Izsvak Z.** (1997). Molecular reconstruction of Sleeping Beauty, a Tc1-like transposon from fish, and its transposition in human cells. *Cell*, (**91**): 501-10

[101] **Ivics Z., Katzer A., Stuwe E. E., Fiedler D., Knespel S. and Izsvak Z.** (2007). Targeted Sleeping Beauty transposition in human cells. *Mol Ther*, (**15**): 1137-44

[102] **Ivics Z., Li M. A., Mates L., Boeke J. D., Nagy A., Bradley A. and Izsvak Z.** (2009). Transposon-mediated genome manipulation in vertebrates. *Nat Methods*, (**6**): 415-22

[103] **Jager L. and Ehrhardt A.** (2007). Emerging adenoviral vectors for stable correction of genetic disorders. *Curr Gene Ther*, (**7**): 272-83

[104] **Jager L. and Ehrhardt A.** (2009). Persistence of high-capacity adenoviral vectors as replication-defective monomeric genomes in vitro and in murine liver. *Hum Gene Ther*, (**20**): 883-96

[105] **Kanellopoulou C., Muljo S. A., Kung A. L., Ganesan S., Drapkin R., Jenuwein T., Livingston D. M. and Rajewsky K.** (2005). Dicer-deficient mouse embryonic stem cells are defective in differentiation and centromeric silencing. *Genes Dev*, (**19**): 489-501

[106] **Kaufman C. D., Izsvak Z., Katzer A. and Ivics Z.** (2005). Frog Prince transposon-based RNAi vectors mediate efficient gene knockdown in human cells. *J RNAi Gene Silencing*, (**1**): 97-104

[107] **Kawano R., Ishizaki M., Maeda Y., Uchida Y., Kimura E. and Uchino M.** (2008). Transduction of full-length dystrophin to multiple skeletal muscles improves motor performance and life span in utrophin/dystrophin double knockout mice. *Mol Ther*, (**16**): 825-31

[108] **Kawasaki H. and Taira K.** (2004a). Induction of DNA methylation and gene silencing by short interfering RNAs in human cells. *Nature*, (**431**): 211-7

[109] **Kawasaki H. and Taira K.** (2004b). MicroRNA-196 inhibits HOXB8 expression in myeloid differentiation of HL60 cells. *Nucleic Acids Symp Ser (Oxf)*, 211-2

[110] **Kay M. A., Glorioso J. C. and Naldini L.** (2001). Viral vectors for gene therapy: the art of turning infectious agents into vehicles of therapeutics. *Nat Med*, (**7**): 33-40

[111] **Kazazian H. H., Jr., Wong C., Youssoufian H., Scott A. F., Phillips D. G. and Antonarakis S. E.** (1988). Haemophilia A resulting from de novo insertion of L1 sequences represents a novel mechanism for mutation in man. *Nature*, (**332**): 164-6

[112] **Ketting R. F., Fischer, S.E.J. Bernstein,E., Sijen, T., Hannon,G.J., and Plasterk, R.H.A** (2001). Dicer functions in RNA interference and in synthesis of small RNA involved in developmental timing in C.elegans. *Genes Dev*, (**15**): 2654-2659

[113] **Kim D. H., Behlke M. A., Rose S. D., Chang M. S., Choi S. and Rossi J. J.** (2005). Synthetic dsRNA Dicer substrates enhance RNAi potency and efficacy. *Nat Biotechnol*, (**23**): 222-6

[114] **Kloosterman W. P. and Plasterk R. H.** (2006). The diverse functions of microRNAs in animal development and disease. *Dev Cell*, (**11**): 441-50

[115] **Koehler D. R., Frndova H., Leung K., Louca E., Palmer D., Ng P., McKerlie C., Cox P., Coates A. L. and Hu J.** (2005). Aerosol delivery of an enhanced helper-dependent adenovirus formulation to rabbit lung using an intratracheal catheter. *J Gene Med*, (**7**): 1409-20

[116] **Krasnykh V. N., Mikheeva G. V., Douglas J. T. and Curiel D. T.** (1996). Generation of recombinant adenovirus vectors with modified fibers for altering viral tropism. *J Virol*, (**70**): 6839-46

[117] **Krutzfeldt J. and Stoffel M.** (2006). MicroRNAs: a new class of regulatory genes affecting metabolism. *Cell Metab*, (**4**): 9-12

[118] **Kuhstoss S. and Rao R. N.** (1991). Analysis of the integration function of the streptomycete bacteriophage phi C31. *J Mol Biol*, (**222**): 897-908

[119] **Lagos-Quintana M., Rauhut,R., Lendeckel, W., and Tuschl,T.** (2001). Indentification of novel genes coding for small expressed RNAs. *Science*, (**294**): 853-858

[120] **Lakatos L., Szittya G., Silhavy D. and Burgyan J.** (2004). Molecular mechanism of RNA silencing suppression mediated by p19 protein of tombusviruses. *EMBO J*, (**23**): 876-84

[121] **Lander E. S., Linton L. M., Birren B., Nusbaum C., Zody M. C., Baldwin J., Devon K., Dewar K., Doyle M., FitzHugh W., Funke R., Gage D., Harris K., Heaford A., Howland J., Kann L., Lehoczky J., LeVine R., McEwan P., McKernan K., Meldrim J., Mesirov J. P., Miranda C., Morris W., Naylor J., Raymond C., Rosetti M., Santos R., Sheridan A., Sougnez C., Stange-Thomann N., Stojanovic N., Subramanian A., Wyman D., Rogers J., Sulston J., Ainscough R., Beck S., Bentley D., Burton J., Clee C., Carter N., Coulson A., Deadman R., Deloukas P., Dunham A., Dunham I., Durbin R., French L., Grafham D., Gregory S., Hubbard T., Humphray S., Hunt A., Jones M., Lloyd C., McMurray A., Matthews L., Mercer S., Milne S., Mullikin J. C., Mungall A., Plumb R., Ross M., Shownkeen R., Sims S., Waterston R. H., Wilson R. K., Hillier L. W., McPherson J. D., Marra M. A., Mardis E. R., Fulton L. A., Chinwalla A. T., Pepin K. H., Gish W. R., Chissoe S. L., Wendl M. C., Delehaunty K. D., Miner T. L., Delehaunty A., Kramer J. B., Cook L. L., Fulton R. S., Johnson D. L., Minx P. J., Clifton S. W., Hawkins T., Branscomb E., Predki P., Richardson P., Wenning S., Slezak T., Doggett N., Cheng J. F., Olsen A., Lucas S., Elkin C., Uberbacher E., Frazier M., Gibbs R. A., Muzny D. M., Scherer S. E., Bouck J. B., Sodergren E. J., Worley K. C., Rives C. M., Gorrell J. H., Metzker M. L., Naylor S. L., Kucherlapati R. S., Nelson D. L., Weinstock G. M., Sakaki Y., Fujiyama A., Hattori M., Yada T., Toyoda A., Itoh T., Kawagoe C., Watanabe H., Totoki Y., Taylor T., Weissenbach J., Heilig R., Saurin W., Artiguenave F., Brottier P., Bruls T., Pelletier E., Robert C., Wincker P., Smith D. R., Doucette-Stamm L., Rubenfield M., Weinstock K., Lee H. M., Dubois J., Rosenthal A., Platzer M., Nyakatura G., Taudien S., Rump A., Yang H., Yu J., Wang J., Huang G., Gu J., Hood L., Rowen L., Madan A., Qin S., Davis R. W., Federspiel N. A., Abola A. P., Proctor M. J., Myers R. M., Schmutz J., Dickson M., Grimwood J., Cox D. R., Olson M. V., Kaul R., Shimizu N., Kawasaki K., Minoshima S., Evans G. A., Athanasiou M., Schultz R., Roe B. A., Chen F., Pan H., Ramser J., Lehrach H., Reinhardt R., McCombie W. R., de la Bastide M., Dedhia N., Blocker H., Hornischer K., Nordsiek G., Agarwala R., Aravind L., Bailey J. A., Bateman A., Batzoglou S., Birney E., Bork P., Brown D. G., Burge C. B., Cerutti L., Chen H. C., Church D., Clamp M., Copley R. R., Doerks T., Eddy S. R., Eichler E. E., Furey T. S., Galagan J., Gilbert J. G., Harmon C., Hayashizaki Y., Haussler D., Hermjakob H., Hokamp K., Jang W., Johnson L. S., Jones T. A., Kasif S., Kaspryzk A., Kennedy S., Kent W. J., Kitts P., Koonin E. V., Korf I., Kulp D., Lancet D., Lowe T. M., McLysaght A., Mikkelsen T., Moran J. V., Mulder N., Pollara V. J., Ponting C. P., Schuler G., Schultz J., Slater G., Smit A. F., Stupka E., Szustakowski J., Thierry-Mieg D., Thierry-Mieg J., Wagner L., Wallis J., Wheeler R., Williams A., Wolf Y. I., Wolfe K. H., Yang S. P., Yeh R. F., Collins F., Guyer M. S., Peterson J., Felsenfeld A., Wetterstrand K. A., Patrinos A., Morgan M. J., de Jong P., Catanese J. J., Osoegawa K., Shizuya H., Choi S. and Chen Y. J.** (2001). Initial sequencing and analysis of the human genome. *Nature*, (**409**): 860-921

[122] **Lecellier C. H., Dunoyer P., Arar K., Lehmann-Che J., Eyquem S., Himber C., Saib A. and Voinnet O.** (2005). A cellular microRNA mediates antiviral defense in human cells. *Science*, (**308**): 557-60

[123] **Lee Y., Kim M., Han J., Yeom K. H., Lee S., Baek S. H. and Kim V. N.** (2004). MicroRNA genes are transcribed by RNA polymerase II. *Embo J*, (**23**): 4051-60

[124] **Li W. X., Li H., Lu R., Li F., Dus M., Atkinson P., Brydon E. W., Johnson K. L., Garcia-Sastre A., Ball L. A., Palese P. and Ding S. W.** (2004). Interferon antagonist proteins of influenza and vaccinia viruses are suppressors of RNA silencing. *Proc Natl Acad Sci U S A*, (**101**): 1350-5

[125] **Liao H. J., Kobayashi R. and Mathews M. B.** (1998). Activities of adenovirus virus-associated RNAs: purification and characterization of RNA binding proteins. *Proc Natl Acad Sci U S A*, (**95**): 8514-9

[126] **Lichtenstein D. L. and Wold W. S.** (2004). Experimental infections of humans with wild-type adenoviruses and with replication-competent adenovirus vectors: replication, safety, and transmission. *Cancer Gene Ther*, (**11**): 819-29

[127] **Liesner R., Zhang W., Noske N. and Ehrhardt A.** (2010). Critical amino acid residues within the phiC31 integrase DNA-binding domain affect recombination activities in mammalian cells. *Hum Gene Ther*, (**21**): 1104-18

[128] **Liikanen I., Dias J. D., Nokisalmi P., Sloniecka M., Kangasniemi L., Rajecki M., Dobner T., Tenhunen M., Kanerva A., Pesonen S., Ahtiainen L. and Hemminki A.** (2010). Adenoviral E4orf3 and E4orf6 proteins, but not E1B55K, increase killing of cancer cells by radiotherapy in vivo. *Int J Radiat Oncol Biol Phys*, (**78**): 1201-9

[129] **Lindow M. and Gorodkin J.** (2007). Principles and limitations of computational microRNA gene and target finding. *DNA Cell Biol*, (**26**): 339-51

[130] **Liu T. C., Galanis E. and Kirn D.** (2007). Clinical trial results with oncolytic virotherapy: a century of promise, a decade of progress. *Nat Clin Pract Oncol*, (**4**): 101-17

[131] **Lu S. and Cullen B. R.** (2004). Adenovirus VA1 noncoding RNA can inhibit small interfering RNA and MicroRNA biogenesis. *J Virol*, (**78**): 12868-76

[132] **Luo J., Deng Z. L., Luo X., Tang N., Song W. X., Chen J., Sharff K. A., Luu H. H., Haydon R. C., Kinzler K. W., Vogelstein B. and He T. C.** (2007). A protocol for rapid generation of recombinant adenoviruses using the AdEasy system. *Nat Protoc*, (**2**): 1236-47

[133] **Lusky M., Christ M., Rittner K., Dieterle A., Dreyer D., Mourot B., Schultz H., Stoeckel F., Pavirani A. and Mehtali M.** (1998). In vitro and in vivo biology of recombinant adenovirus vectors with E1, E1/E2A, or E1/E4 deleted. *J Virol*, (**72**): 2022-32

[134] **Ma Y., and Mathews.M. B.** (1996). Structure, function, and evolution of adenovirus-associated RNA: a phylogenetic approach. *J Virol*, (**70**): 5083-5099

[135] **Madon J. and Blum H. E.** (1996). Receptor-mediated delivery of hepatitis B virus DNA and antisense oligodeoxynucleotides to avian liver cells. *Hepatology*, (**24**): 474-81

[136] **Mates L., Chuah M. K., Belay E., Jerchow B., Manoj N., Acosta-Sanchez A., Grzela D. P., Schmitt A., Becker K., Matrai J., Ma L., Samara-Kuko E., Gysemans C., Pryputniewicz D., Miskey C., Fletcher B., Vandendriessche T., Ivics Z. and Izsvak Z.** (2009). Molecular evolution of a novel hyperactive Sleeping Beauty transposase enables robust stable gene transfer in vertebrates. *Nat Genet*, (**41**): 753-61

[137] **McCaffrey A. P., Meuse L., Pham T. T., Conklin D. S., Hannon G. J. and Kay M. A.** (2002). RNA interference in adult mice. *Nature*, (**418**): 38-9

[138] **McCaffrey A. P., Nakai H., Pandey K., Huang Z., Salazar F. H., Xu H., Wieland S. F., Marion P. L. and Kay M. A.** (2003). Inhibition of hepatitis B virus in mice by RNA interference. *Nat Biotechnol*, (**21**): 639-44

[139] **McCormack W. M., Jr., Seiler M. P., Bertin T. K., Ubhayakar K., Palmer D. J., Ng P., Nichols T. C. and Lee B.** (2006). Helper-dependent adenoviral gene therapy mediates long-term correction of the clotting defect in the canine hemophilia A model. *J Thromb Haemost*, (**4**): 1218-25

[140] **Meister G.** (2004). Human Argonaute2 mediates RNA cleavage targeted by miRNAs and siRNAs. *Mol Cell*, (**15**): 185-197

[141] **Mellits K. H., Kostura M. and Mathews M. B.** (1990). Interaction of adenovirus VA RNAI with the protein kinase DAI: nonequivalence of binding and function. *Cell*, (**61**): 843-52

[142] **Mellits K. H. and Mathews M. B.** (1988). Effects of mutations in stem and loop regions on the structure and function of adenovirus VA RNAI. *Embo J*, (**7**): 2849-59

[143] **Miller C. R., Buchsbaum D. J., Reynolds P. N., Douglas J. T., Gillespie G. Y., Mayo M. S., Raben D. and Curiel D. T.** (1998). Differential susceptibility of primary and established human glioma cells to adenovirus infection: targeting via the epidermal growth factor receptor achieves fiber receptor-independent gene transfer. *Cancer Res*, (**58**): 5738-48

[144] **Miskey C., Izsvak Z., Plasterk R. H. and Ivics Z.** (2003). The Frog Prince: a reconstructed transposon from Rana pipiens with high transpositional activity in vertebrate cells. *Nucleic Acids Res*, (**31**): 6873-81

[145] **Mizuguchi H. and Kay M. A.** (1998). Efficient construction of a recombinant adenovirus vector by an improved in vitro ligation method. *Hum Gene Ther*, (**9**): 2577-83

[146] **Moldt B., Yant S. R., Andersen P. R., Kay M. A. and Mikkelsen J. G.** (2007). Cis-acting gene regulatory activities in the terminal regions of sleeping beauty DNA transposon-based vectors. *Hum Gene Ther*, (**18**): 1193-204

[147] **Moore M. D., McGarvey M. J., Russell R. A., Cullen B. R. and McClure M. O.** (2005). Stable inhibition of hepatitis B virus proteins by small interfering RNA expressed from viral vectors. *J Gene Med*, (**7**): 918-25

[148] **Morral N., Parks R. J., Zhou H., Langston C., Schiedner G., Quinones J., Graham F. L., Kochanek S. and Beaudet A. L.** (1998). High doses of a helper-

dependent adenoviral vector yield supraphysiological levels of alpha1-antitrypsin with negligible toxicity. *Hum Gene Ther*, (**9**): 2709-16

[149] **Mourelatos Z., Dostie,J., Paushkin, S., Sharma, A.K., Charroux, B., Abel, L., Rappsilber, J., Mann, M., and Dreyfuss, G.** (2002). miRNPs: A novel class of ribonucleoproteins containing numerous microRNAs. *Genes & Development*, (**16**): 720-728

[150] **Murphy S. J., Chong H., Bell S., Diaz R. M. and Vile R. G.** (2002). Novel integrating adenoviral/retroviral hybrid vector for gene therapy. *Hum Gene Ther*, (**13**): 745-60

[151] **Nakai H., Fuess S., Storm T. A., Muramatsu S., Nara Y. and Kay M. A.** (2005). Unrestricted hepatocyte transduction with adeno-associated virus serotype 8 vectors in mice. *J Virol*, (**79**): 214-24

[152] **Nakano H., Amemiya S., Shiokawa K. and Taira M.** (2000). RNA interference for the organizer-specific gene Xlim-1 in Xenopus embryos. *Biochem Biophys Res Commun*, (**274**): 434-9

[153] **Nettelbeck D. M., Rivera A. A., Balague C., Alemany R. and Curiel D. T.** (2002). Novel oncolytic adenoviruses targeted to melanoma: specific viral replication and cytolysis by expression of E1A mutants from the tyrosinase enhancer/promoter. *Cancer Res*, (**62**): 4663-70

[154] **Ng P., Beauchamp C., Evelegh C., Parks R. and Graham F. L.** (2001). Development of a FLP/frt system for generating helper-dependent adenoviral vectors. *Mol Ther*, (**3**): 809-15

[155] **Ng P., Parks R. J. and Graham F. L.** (2002). Preparation of helper-dependent adenoviral vectors. *Methods Mol Med*, (**69**): 371-88

[156] **Nilsson E. C., Storm R. J., Bauer J., Johansson S. M., Lookene A., Angstrom J., Hedenstrom M., Eriksson T. L., Frangsmyr L., Rinaldi S., Willison H. J., Domellof F. P., Stehle T. and Arnberg N.** (2010). The GD1a glycan is a cellular receptor for adenoviruses causing epidemic keratoconjunctivitis. *Nat Med*,

[157] **O'Neal W. K., Zhou H., Morral N., Aguilar-Cordova E., Pestaner J., Langston C., Mull B., Wang Y., Beaudet A. L. and Lee B.** (1998). Toxicological comparison of E2a-deleted and first-generation adenoviral vectors expressing alpha1-antitrypsin after systemic delivery. *Hum Gene Ther*, (**9**): 1587-98

[158] **O'Malley R. P., T. M. Mariano, J. Siekierka, and M. B. Mathews.** (1986). A mechanism for the control of protein synthesis by adenovirus VA RNAI. *Cell*, (**44**): 391-400

[159] **Offringa R., Kwappenberg K., Rabelink M., Rea D. and Hoeben R.** (2005). Adenoviral transduction of dendritic cells. *Methods Mol Med*, (**109**): 83-96

[160] **Ogata N., Ostberg L., Ehrlich P. H., Wong D. C., Miller R. H. and Purcell R. H.** (1993). Markedly prolonged incubation period of hepatitis B in a chimpanzee passively immunized with a human monoclonal antibody to the a determinant of hepatitis B surface antigen. *Proc Natl Acad Sci U S A*, (**90**): 3014-8

[161] **Oka K., Belalcazar L. M., Dieker C., Nour E. A., Nuno-Gonzalez P., Paul A., Cormier S., Shin J. K., Finegold M. and Chan L.** (2007). Sustained phenotypic correction in a mouse model of hypoalphalipoproteinemia with a helper-dependent adenovirus vector. *Gene Ther*, (**14**): 191-202

[162] **Olivares E. C., Hollis R. P., Chalberg T. W., Meuse L., Kay M. A. and Calos M. P.** (2002). Site-specific genomic integration produces therapeutic Factor IX levels in mice. *Nat Biotechnol*, (**20**): 1124-8

[163] **Omarov R., Sparks K., Smith L., Zindovic J. and Scholthof H. B.** (2006). Biological relevance of a stable biochemical interaction between the tombusvirus-encoded P19 and short interfering RNAs. *J Virol*, (**80**): 3000-8

[164] **Ortiz-Urda S., Thyagarajan B., Keene D. R., Lin Q., Fang M., Calos M. P. and Khavari P. A.** (2002). Stable nonviral genetic correction of inherited human skin disease. *Nat Med*, (**8**): 1166-70

[165] **Ostertag E. M. and Kazazian H. H., Jr.** (2001). Biology of mammalian L1 retrotransposons. *Annu Rev Genet*, (**35**): 501-38

[166] **Paddison P. J., Caudy A. A., Bernstein E., Hannon G. J. and Conklin D. S.** (2002). Short hairpin RNAs (shRNAs) induce sequence-specific silencing in mammalian cells. *Genes Dev*, (**16**): 948-58

[167] **Palmer D. and Ng P.** (2003). Improved system for helper-dependent adenoviral vector production. *Mol Ther*, (**8**): 846-52

[168] **Parks R. J., Bramson J. L., Wan Y., Addison C. L. and Graham F. L.** (1999). Effects of stuffer DNA on transgene expression from helper-dependent adenovirus vectors. *J Virol*, (**73**): 8027-34

[169] **Parks R. J., Chen L., Anton M., Sankar U., Rudnicki M. A. and Graham F. L.** (1996). A helper-dependent adenovirus vector system: removal of helper virus by Cre-mediated excision of the viral packaging signal. *Proc Natl Acad Sci U S A*, (**93**): 13565-70

[170] **Pasquinelli A. E. and Ruvkun G.** (2002). Control of developmental timing by micrornas and their targets. *Annu Rev Cell Dev Biol*, (**18**): 495-513

[171] **Patel M. and Yang S.** (2010). Advances in Reprogramming Somatic Cells to Induced Pluripotent Stem Cells. *Stem Cell Rev*,

[172] **Pedersen I. M., Cheng G., Wieland S., Volinia S., Croce C. M., Chisari F. V. and David M.** (2007). Interferon modulation of cellular microRNAs as an antiviral mechanism. *Nature*, (**449**): 919-22

[173] **Peng Z.** (2005). Current status of gendicine in China: recombinant human Ad-p53 agent for treatment of cancers. *Hum Gene Ther*, (**16**): 1016-27

[174] **Pesonen S., Kangasniemi L. and Hemminki A.** (2010). Oncolytic Adenoviruses for the Treatment of Human Cancer: Focus on Translational and Clinical Data. *Mol Pharm*,

[175] **Pfeffer S., Zavolan, M., Grässer, F.A., Chien, M., Russo, J.J., Ju, J., John, B., Enright, A.J., Marks, D., Sander, C. and Tuschl, T.** (2004). Identification of Virus-Encoded MicroRNAs. *Science*, (**304**): 734-736

[176] **Picard-Maureau M., Kreppel F., Lindemann D., Juretzek T., Herchenroder O., Rethwilm A., Kochanek S. and Heinkelein M.** (2004). Foamy virus--adenovirus hybrid vectors. *Gene Ther*, (**11**): 722-8

[177] **Priddy F. H., Brown D., Kublin J., Monahan K., Wright D. P., Lalezari J., Santiago S., Marmor M., Lally M., Novak R. M., Brown S. J., Kulkarni P., Dubey S. A., Kierstead L. S., Casimiro D. R., Mogg R., DiNubile M. J., Shiver J. W., Leavitt R. Y., Robertson M. N., Mehrotra D. V. and Quirk E.** (2008). Safety and immunogenicity of a replication-incompetent adenovirus type 5 HIV-1 clade B gag/pol/nef vaccine in healthy adults. *Clin Infect Dis*, (**46**): 1769-81

[178] **Proudfoot N. J.** (1986). Transcriptional interference and termination between duplicated alpha-globin gene constructs suggests a novel mechanism for gene regulation. *Nature*, (**322**): 562-5

[179] **Qiu W., Park J. W. and Scholthof H. B.** (2002). Tombusvirus P19-mediated suppression of virus-induced gene silencing is controlled by genetic and dosage features that influence pathogenicity. *Mol Plant Microbe Interact*, (**15**): 269-80

[180] **Qu F. a. M., T.J.** (2002). Efficient infection of Nicotiana bentthamiana by Tomato bushy stunt virus is facilitated by the coat protein and maintained by p19 through suppression of gene silencing. *Mol Plant Microbe Interact*, (**15**): 193-202

[181] **Raper S. E., Chirmule N., Lee F. S., Wivel N. A., Bagg A., Gao G. P., Wilson J. M. and Batshaw M. L.** (2003). Fatal systemic inflammatory response syndrome in a ornithine transcarbamylase deficient patient following adenoviral gene transfer. *Mol Genet Metab*, (**80**): 148-58

[182] **Rauschhuber C., Noske N. and Ehrhardt A.** (2011). New insights into stability of recombinant adenovirus genomes in mammalian cells. *European Journal of Cell Biology*

[183] Rawlings R. A. (2010). An in Vitro and in Silico Kinetic Study of a Viral RNA Silencing Suppressor.

[184] **Reddy V. S., Natchiar S. K., Stewart P. L. and Nemerow G. R.** (2010). Crystal structure of human adenovirus at 3.5 A resolution. *Science*, (**329**): 1071-5

[185] **Rehermann B. and Nascimbeni M.** (2005). Immunology of hepatitis B virus and hepatitis C virus infection. *Nat Rev Immunol*, (**5**): 215-29

[186] **Rein D. T., Breidenbach M., Wu H., Han T., Haviv Y. S., Wang M., Kirby T. O., Kawakami Y., Dall P., Alvarez R. D. and Curiel D. T.** (2004). Gene transfer to cervical cancer with fiber-modified adenoviruses. *Int J Cancer*, (**111**): 698-704

[187] **Ries S. J. and Brandts C. H.** (2004). Oncolytic viruses for the treatment of cancer: current strategies and clinical trials. *Drug Discov Today*, (**9**): 759-68

[188] **Rivera A. A., Wang M., Suzuki K., Uil T. G., Krasnykh V., Curiel D. T. and Nettelbeck D. M.** (2004). Mode of transgene expression after fusion to early or late

viral genes of a conditionally replicating adenovirus via an optimized internal ribosome entry site in vitro and in vivo. *Virology*, (**320**): 121-34

[189] **Robert V. J., Vastenhouw N. L. and Plasterk R. H.** (2004). RNA interference, transposon silencing, and cosuppression in the Caenorhabditis elegans germ line: similarities and differences. *Cold Spring Harb Symp Quant Biol*, (**69**): 397-402

[190] **Roberts D. M., Nanda A., Havenga M. J., Abbink P., Lynch D. M., Ewald B. A., Liu J., Thorner A. R., Swanson P. E., Gorgone D. A., Lifton M. A., Lemckert A. A., Holterman L., Chen B., Dilraj A., Carville A., Mansfield K. G., Goudsmit J. and Barouch D. H.** (2006). Hexon-chimaeric adenovirus serotype 5 vectors circumvent pre-existing anti-vector immunity. *Nature*, (**441**): 239-43

[191] **Roy S., Shirley P. S., McClelland A. and Kaleko M.** (1998). Circumvention of immunity to the adenovirus major coat protein hexon. *J Virol*, (**72**): 6875-9

[192] **Rubinchik S., Lowe S., Jia Z., Norris J. and Dong J.** (2001). Creation of a new transgene cloning site near the right ITR of Ad5 results in reduced enhancer interference with tissue-specific and regulatable promoters. *Gene Ther*, (**8**): 247-53

[193] Sambrook J. a. R., D.W. (2001). Molecular Cloning: A Laboratory Manual.

[194] **Sandig V., Youil R., Bett A. J., Franlin L. L., Oshima M., Maione D., Wang F., Metzker M. L., Savino R. and Caskey C. T.** (2000). Optimization of the helper-dependent adenovirus system for production and potency in vivo. *Proc Natl Acad Sci U S A*, (**97**): 1002-7

[195] **Sano M., Kato Y. and Taira K.** (2006). Sequence-specific interference by small RNAs derived from adenovirus VAI RNA. *FEBS Lett*, (**580**): 1553-64

[196] **Saphire A. C., Guan T., Schirmer E. C., Nemerow G. R. and Gerace L.** (2000). Nuclear import of adenovirus DNA in vitro involves the nuclear protein import pathway and hsc70. *J Biol Chem*, (**275**): 4298-304

[197] **Sawada Y., Ojima S., Shimojo H., Shiroki K. and Fujinaga K.** (1979). Transforming DNA sequences in rat cells transformed by DNA fragments of highly oncogenic human adenovirus type 12. *J Virol*, (**32**): 379-85

[198] **Scaglioni P., Melegari M., Takahashi M., Chowdhury J. R. and Wands J.** (1996). Use of dominant negative mutants of the hepadnaviral core protein as antiviral agents. *Hepatology*, (**24**): 1010-7

[199] **Schiedner G., Morral N., Parks R. J., Wu Y., Koopmans S. C., Langston C., Graham F. L., Beaudet A. L. and Kochanek S.** (1998). Genomic DNA transfer with a high-capacity adenovirus vector results in improved in vivo gene expression and decreased toxicity. *Nat Genet*, (**18**): 180-3

[200] **Schmitz H., Wigand R. and Heinrich W.** (1983). Worldwide epidemiology of human adenovirus infections. *Am J Epidemiol*, (**117**): 455-66

[201] **Scholthof H. B.** (2006). The Tombusvirus-encoded P19: from irrelevance to elegance. *Nat Rev Microbiol*, (**4**): 405-11

[202] **Schug J.** (2008). Using TESS to predict transcription factor binding sites in DNA sequence. *Curr Protoc Bioinformatics*, (**Chapter 2**): Unit 2 6

[203] **Schwahn U., Lenzner S., Dong J., Feil S., Hinzmann B., van Duijnhoven G., Kirschner R., Hemberger M., Bergen A. A., Rosenberg T., Pinckers A. J., Fundele R., Rosenthal A., Cremers F. P., Ropers H. H. and Berger W.** (1998). Positional cloning of the gene for X-linked retinitis pigmentosa 2. *Nat Genet*, (**19**): 327-32

[204] **Seregin S. S. and Amalfitano A.** (2009). Overcoming pre-existing adenovirus immunity by genetic engineering of adenovirus-based vectors. *Expert Opin Biol Ther*, (**9**): 1521-31

[205] **Sherr C. J.** (1996). Cancer cell cycles. *Science*, (**274**): 1672-7

[206] **Shi C. X., Graham F. L. and Hitt M. M.** (2006). A convenient plasmid system for construction of helper-dependent adenoviral vectors and its application for analysis of the breast-cancer-specific mammaglobin promoter. *J Gene Med*, (**8**): 442-51

[207] **Shi Q., Wang Y. and Worton R.** (1997). Modulation of the specificity and activity of a cellular promoter in an adenoviral vector. *Hum Gene Ther*, (**8**): 403-10

[208] **Short J. J., Rivera A. A., Wu H., Walter M. R., Yamamoto M., Mathis J. M. and Curiel D. T.** (2010). Substitution of adenovirus serotype 3 hexon onto a serotype 5 oncolytic adenovirus reduces factor X binding, decreases liver tropism, and improves antitumor efficacy. *Mol Cancer Ther*, (**9**): 2536-44

[209] **Sijen T. and Plasterk R. H.** (2003). Transposon silencing in the Caenorhabditis elegans germ line by natural RNAi. *Nature*, (**426**): 310-4

[210] **Silhavy D., Molnar A., Lucioli A., Szittya G., Hornyik C., Tavazza M. and Burgyan J.** (2002). A viral protein suppresses RNA silencing and binds silencing-generated, 21- to 25-nucleotide double-stranded RNAs. *EMBO J*, (**21**): 3070-80

[211] **Skalsky R. L. and Cullen B. R.** (2010). Viruses, microRNAs, and host interactions. *Annu Rev Microbiol*, (**64**): 123-41

[212] **Smith R. H., Levy J. R. and Kotin R. M.** (2009). A simplified baculovirus-AAV expression vector system coupled with one-step affinity purification yields high-titer rAAV stocks from insect cells. *Mol Ther*, (**17**): 1888-96

[213] **Soifer H. S., Zaragoza A., Peyvan M., Behlke M. A. and Rossi J. J.** (2005). A potential role for RNA interference in controlling the activity of the human LINE-1 retrotransposon. *Nucleic Acids Res*, (**33**): 846-56

[214] **Stephen S. L., Sivanandam V. G. and Kochanek S.** (2008). Homologous and heterologous recombination between adenovirus vector DNA and chromosomal DNA. *J Gene Med*, (**10**): 1176-89

[215] **Stewart P. L., Burnett R. M., Cyrklaff M. and Fuller S. D.** (1991). Image reconstruction reveals the complex molecular organization of adenovirus. *Cell*, (**67**): 145-54

[216] **Stewart S. A., Dykxhoorn D. M., Palliser D., Mizuno H., Yu E. Y., An D. S., Sabatini D. M., Chen I. S., Hahn W. C., Sharp P. A., Weinberg R. A. and Novina C. D.** (2003). Lentivirus-delivered stable gene silencing by RNAi in primary cells. *RNA*, (**9**): 493-501

[217] **Sullivan C. S., Grundhoff A. T., Tevethia S., Pipas J. M. and Ganem D.** (2005). SV40-encoded microRNAs regulate viral gene expression and reduce susceptibility to cytotoxic T cells. *Nature*, (**435**): 682-6

[218] **Sutter D., Westphal M. and Doerfler W.** (1978). Patterns of integration of viral DNA sequences in the genomes of adenovirus type 12-transformed hamster cells. *Cell*, (**14**): 569-85

[219] **Symer D. E., Connelly C., Szak S. T., Caputo E. M., Cost G. J., Parmigiani G. and Boeke J. D.** (2002). Human l1 retrotransposition is associated with genetic instability in vivo. *Cell*, (**110**): 327-38

[220] **Szittya G., Molnar A., Silhavy D., Hornyik C. and Burgyan J.** (2002). Short defective interfering RNAs of tombusviruses are not targeted but trigger post-transcriptional gene silencing against their helper virus. *Plant Cell*, (**14**): 359-72

[221] **Taylor P. A., Lees C. J., Wilson J. M., Ehrhardt M. J., Campbell M. T., Noelle R. J. and Blazar B. R.** (2002). Combined effects of calcineurin inhibitors or sirolimus with anti-CD40L mAb on alloengraftment under nonmyeloablative conditions. *Blood*, (**100**): 3400-7

[222] **Thimmappaya B., C. Weinberger, R. J. Schneider, andShenk, T.** (1982). Adenovirus VAI RNA is required for efficient translation of viral mRNAs at late times after infection. *Cell*, (**31**): 543-551

[223] **Thomas C. E., Ehrhardt A. and Kay M. A.** (2003). Progress and problems with the use of viral vectors for gene therapy. *Nat Rev Genet*, (**4**): 346-58

[224] **Thorpe H. M. and Smith M. C.** (1998). In vitro site-specific integration of bacteriophage DNA catalyzed by a recombinase of the resolvase/invertase family. *Proc Natl Acad Sci U S A*, (**95**): 5505-10

[225] **Thyagarajan B., Liu Y., Shin S., Lakshmipathy U., Scheyhing K., Xue H., Ellerstrom C., Strehl R., Hyllner J., Rao M. S. and Chesnut J. D.** (2008). Creation of engineered human embryonic stem cell lines using phiC31 integrase. *Stem Cells*, (**26**): 119-26

[226] **Thyagarajan B., Olivares E. C., Hollis R. P., Ginsburg D. S. and Calos M. P.** (2001). Site-specific genomic integration in mammalian cells mediated by phage phiC31 integrase. *Mol Cell Biol*, (**21**): 3926-34

[227] **Tillmann H. L.** (2007). Antiviral therapy and resistance with hepatitis B virus infection. *World J Gastroenterol*, (**13**): 125-40

[228] **Tiscornia G., Singer O. and Verma I. M.** (2006). Production and purification of lentiviral vectors. *Nat Protoc*, (**1**): 241-5

[229] **Toietta G., Mane V. P., Norona W. S., Finegold M. J., Ng P., McDonagh A. F., Beaudet A. L. and Lee B.** (2005). Lifelong elimination of hyperbilirubinemia in the Gunn rat with a single injection of helper-dependent adenoviral vector. *Proc Natl Acad Sci U S A*, (**102**): 3930-5

[230] **Tolun A., Alestrom P. and Pettersson U.** (1979). Sequence of inverted terminal repetitions from different adenoviruses: demonstration of conserved sequences and homology between SA7 termini and SV40 DNA. *Cell*, (**17**): 705-13

[231] **Tomko R. P., Xu R. and Philipson L.** (1997). HCAR and MCAR: the human and mouse cellular receptors for subgroup C adenoviruses and group B coxsackieviruses. *Proc Natl Acad Sci U S A*, (**94**): 3352-6

[232] **Uetz P., Dong Y. A., Zeretzke C., Atzler C., Baiker A., Berger B., Rajagopala S. V., Roupelieva M., Rose D., Fossum E. and Haas J.** (2006). Herpesviral protein networks and their interaction with the human proteome. *Science*, (**311**): 239-42

[233] **Uprichard S. L., Boyd B., Althage A. and Chisari F. V.** (2005). Clearance of hepatitis B virus from the liver of transgenic mice by short hairpin RNAs. *Proc Natl Acad Sci U S A*, (**102**): 773-8

[234] **Vandesompele J., De Preter K., Pattyn F., Poppe B., Van Roy N., De Paepe A. and Speleman F.** (2002). Accurate normalization of real-time quantitative RT-PCR data by geometric averaging of multiple internal control genes. *Genome Biol*, (**3**): RESEARCH0034

[235] **Vargason J. M., Szittya G., Burgyan J. and Tanaka Hall T. M.** (2003). Size selective recognition of siRNA by an RNA silencing suppressor. *Cell*, (**115**): 799-811

[236] **Vastenhouw N. L., Fischer S. E., Robert V. J., Thijssen K. L., Fraser A. G., Kamath R. S., Ahringer J. and Plasterk R. H.** (2003). A genome-wide screen identifies 27 genes involved in transposon silencing in C. elegans. *Curr Biol*, (**13**): 1311-6

[237] **Vastenhouw N. L. and Plasterk R. H.** (2004). RNAi protects the Caenorhabditis elegans germline against transposition. *Trends Genet*, (**20**): 314-9

[238] **Vizoso Pinto M. G., Pfrepper K. I., Janke T., Noelting C., Sander M., Lueking A., Haas J., Nitschko H., Jaeger G. and Baiker A.** (2010). A systematic approach for the identification of novel, serologically reactive recombinant Varicella-Zoster Virus (VZV) antigens. *Virol J*, (**7**): 165

[239] **Voinnet O.** (2001). RNA silencing as a plant immune system against viruses. *Trends Genet*, (**17**): 449-59

[240] **Voinnet O., Pinto Y. M. and Baulcombe D. C.** (1999). Suppression of gene silencing: a general strategy used by diverse DNA and RNA viruses of plants. *Proc Natl Acad Sci U S A*, (**96**): 14147-52

[241] **Voinnet O., Pinto, Y.M. and Baulcombe, D.C.** (2003). An enhanced transient expression system in plants based on suppression of gene silencing by the p19 protein of tomato bushy stunt virus. *Plant J*, (**33**): 949-956

[242] **Waddington S. N., McVey J. H., Bhella D., Parker A. L., Barker K., Atoda H., Pink R., Buckley S. M., Greig J. A., Denby L., Custers J., Morita T., Francischetti I. M., Monteiro R. Q., Barouch D. H., van Rooijen N., Napoli C., Havenga M. J., Nicklin S. A. and Baker A. H.** (2008). Adenovirus serotype 5 hexon mediates liver gene transfer. *Cell*, (**132**): 397-409

[243] **Walisko O., Schorn A., Rolfs F., Devaraj A., Miskey C., Izsvak Z. and Ivics Z.** (2008). Transcriptional activities of the Sleeping Beauty transposon and shielding its genetic cargo with insulators. *Mol Ther*, (**16**): 359-69

[244] **Wang H., Li Z. Y., Liu Y., Persson J., Beyer I., Moller T., Koyuncu D., Drescher M. R., Strauss R., Zhang X. B., Wahl J. K., 3rd, Urban N., Drescher C., Hemminki A., Fender P. and Lieber A.** (2010). Desmoglein 2 is a receptor for adenovirus serotypes 3, 7, 11 and 14. *Nat Med*,

[245] **Wang H. and Lieber A.** (2006). A helper-dependent capsid-modified adenovirus vector expressing adeno-associated virus rep78 mediates site-specific integration of a 27-kilobase transgene cassette. *J Virol*, (**80**): 11699-709

[246] **Warming S., Costantino N., Court D. L., Jenkins N. A. and Copeland N. G.** (2005). Simple and highly efficient BAC recombineering using galK selection. *Nucleic Acids Res*, (**33**): e36

[247] **Weinberg D. H. and Ketner G.** (1983). A cell line that supports the growth of a defective early region 4 deletion mutant of human adenovirus type 2. *Proc Natl Acad Sci U S A*, (**80**): 5383-6

[248] **Welch P. J., Tritz R., Yei S., Barber J. and Yu M.** (1997). Intracellular application of hairpin ribozyme genes against hepatitis B virus. *Gene Ther*, (**4**): 736-43

[249] **Wickham T. J., Mathias P., Cheresh D. A. and Nemerow G. R.** (1993). Integrins alpha v beta 3 and alpha v beta 5 promote adenovirus internalization but not virus attachment. *Cell*, (**73**): 309-19

[250] **Wiley** (2010). Gene Therapy Clinical Trials Worldwide. *J of Gene Med*. URL: www.abedia.com/wiley.

[251] **Wright J. F., Wellman J. and Hig K. A.** (2010). Manufacturing and regulatory strategies for clinical AAV2-hRPE65. *Curr Gene Ther*, (**10**): 341-9

[252] **Wright T. L.** (2006). Introduction to chronic hepatitis B infection. *Am J Gastroenterol*, (**101 Suppl 1**): S1-6

[253] **Wu J. and Gerber M. A.** (1997). The inhibitory effects of antisense RNA on hepatitis B virus surface antigen synthesis. *J Gen Virol*, (**78 (Pt 3)**): 641-7

[254] **Xing L. and Tikoo S. K.** (2004). cis-Acting packaging motifs of porcine adenovirus type 3. *Virus Res*, (**104**): 207-14

[255] **Xing L. and Tikoo S. K.** (2005). Promoter activity of left inverted terminal repeat and downstream sequences of porcine adenovirus type 3. *Virus Res*, (**109**): 51-8

[256] **Xing L. and Tikoo S. K.** (2006). E1A promoter of bovine adenovirus type 3. *J Gen Virol*, (**87**): 3539-44

[257] **Xu N., Segerman B., Zhou X. and Akusjarvi G.** (2007). Adenovirus virus-associated RNAII-derived small RNAs are efficiently incorporated into the rna-induced silencing complex and associate with polyribosomes. *J Virol*, (**81**): 10540-9

[258] **Xu Z., Tian J., Smith J. S. and Byrnes A. P.** (2008). Clearance of adenovirus by Kupffer cells is mediated by scavenger receptors, natural antibodies, and complement. *J Virol*, (**82**): 11705-13

[259] **Xu Z. L., Mizuguchi H., Mayumi T. and Hayakawa T.** (2003a). Regulated gene expression from adenovirus vectors: a systematic comparison of various inducible systems. *Gene*, (**309**): 145-51

[260] **Xu Z. L., Mizuguchi H., Mayumi T. and Hayakawa T.** (2003b). Woodchuck hepatitis virus post-transcriptional regulation element enhances transgene expression from adenovirus vectors. *Biochim Biophys Acta*, (**1621**): 266-71

[261] **Yamamoto M., Davydova J., Takayama K., Alemany R. and Curiel D. T.** (2003). Transcription initiation activity of adenovirus left-end sequence in adenovirus vectors with e1 deleted. *J Virol*, (**77**): 1633-7

[262] **Yang N. and Kazazian H. H., Jr.** (2006). L1 retrotransposition is suppressed by endogenously encoded small interfering RNAs in human cultured cells. *Nat Struct Mol Biol*, (**13**): 763-71

[263] **Yang P. L., Althage A., Chung J. and Chisari F. V.** (2002). Hydrodynamic injection of viral DNA: a mouse model of acute hepatitis B virus infection. *Proc Natl Acad Sci U S A*, (**99**): 13825-30

[264] **Yang Y., Ertl H. C. and Wilson J. M.** (1994). MHC class I-restricted cytotoxic T lymphocytes to viral antigens destroy hepatocytes in mice infected with E1-deleted recombinant adenoviruses. *Immunity*, (**1**): 433-42

[265] **Yang Y., Li Q., Ertl H. C. and Wilson J. M.** (1995a). Cellular and humoral immune responses to viral antigens create barriers to lung-directed gene therapy with recombinant adenoviruses. *J Virol*, (**69**): 2004-15

[266] **Yang Y., Xiang Z., Ertl H. C. and Wilson J. M.** (1995b). Upregulation of class I major histocompatibility complex antigens by interferon gamma is necessary for T-cell-mediated elimination of recombinant adenovirus-infected hepatocytes in vivo. *Proc Natl Acad Sci U S A*, (**92**): 7257-61

[267] **Yant S. R., Ehrhardt A., Mikkelsen J. G., Meuse L., Pham T. and Kay M. A.** (2002). Transposition from a gutless adeno-transposon vector stabilizes transgene expression in vivo. *Nat Biotechnol*, (**20**): 999-1005

[268] **Yant S. R. and Kay M. A.** (2003). Nonhomologous-end-joining factors regulate DNA repair fidelity during Sleeping Beauty element transposition in mammalian cells. *Mol Cell Biol*, (**23**): 8505-18

[269] **Yant S. R., Meuse L., Chiu W., Ivics Z., Izsvak Z. and Kay M. A.** (2000). Somatic integration and long-term transgene expression in normal and haemophilic mice using a DNA transposon system. *Nat Genet*, (**25**): 35-41

[270] **Yi R., Qin,Y., Macara, I.G., and Cullen,B.R.** (2003). Expotin-5 mediates the nuclear exprot of pre-miRNAs and short hairpin RNAs. *Genes Dev*, (**17**): 3011-3016

[271] **Ylosmaki E., Hakkarainen T., Hemminki A., Visakorpi T., Andino R. and Saksela K.** (2008). Generation of a conditionally replicating adenovirus based on targeted destruction of E1A mRNA by a cell type-specific MicroRNA. *J Virol*, (**82**): 11009-15

[272] **Yu W. and Fang H.** (2007). Clinical trials with oncolytic adenovirus in China. *Curr Cancer Drug Targets*, (**7**): 141-8

[273] **Zeng Y. and Cullen B. R.** (2004). Structural requirements for pre-microRNA binding and nuclear export by Exportin 5. *Nucleic Acids Res*, (**32**): 4776-85

[274] **Zeng Y. and Cullen B. R.** (2005). Efficient processing of primary microRNA hairpins by Drosha requires flanking nonstructured RNA sequences. *J Biol Chem*, (**280**): 27595-603

[275] **Zhang Y. and Bergelson J. M.** (2005). Adenovirus receptors. *J Virol*, (**79**): 12125-31

[276] **Zhang Z., Zou W., Wang J., Gu J., Dang Y., Li B., Zhao L., Qian C., Qian Q. and Liu X.** (2005). Suppression of tumor growth by oncolytic adenovirus-mediated delivery of an antiangiogenic gene, soluble Flt-1. *Mol Ther*, (**11**): 553-62

[277] **Zheng C., Baum B. J., Iadarola M. J. and O'Connell B. C.** (2000). Genomic integration and gene expression by a modified adenoviral vector. *Nat Biotechnol*, (**18**): 176-80

[278] **Zoulim F.** (2006). Assessment of treatment efficacy in HBV infection and disease. *J Hepatol*, (**44**): S95-9

7.5 Acknowledgment